

Contents

Abbreviations	v
1 Introduction	1
2 Theoretical background	5
2.1 Chemical synthesis of RNA	5
2.2 The Sonogashira coupling reaction	10
2.3 The Heck coupling reaction	14
2.4 Labeling methods for oligonucleotides	20
2.5 Methods for RNA structural elucidation	24
2.6 MALDI-TOF mass spectrometry of oligonucleotides	26
3 Results and discussion	28
3.1 Synthesis of modified uridine, adenosine and guanosine building blocks by the Sonogashira coupling reaction	28
3.1.1 Retrosynthesis of the modified building blocks by the Sonogashira coupling reaction	28
3.1.2 Synthesis of <i>N</i> -propargyltrifluoroacetamide L3	29
3.1.3 Synthesis of 5'- <i>O</i> -(4,4'-dimethoxytrityl)-2'- <i>O</i> - <i>tert</i> -butyldimethylsilyl-5-(3-trifluoroacetamidoprop-1-ynyl)uridine	30
3.1.4 Synthesis of 8-(3-trifluoroacetamidoprop-1-ynyl)adenosine	33
3.1.5 Synthesis of 2-(3-trifluoroacetamido-1-prop-1-ynyl)adenosine	38
3.1.6 Synthesis of 8-(3-trifluoroacetamidoprop-1-ynyl)guanosine	39
3.2 Synthesis of modified uridine and adenosine building blocks by the Heck coupling reaction	42
3.2.1 Retrosynthesis of the modified building blocks by the Heck coupling reaction	42
3.2.2 Synthesis of <i>N</i> -allyltrifluoroacetamide L1	43
3.2.3 Synthesis of <i>N</i> -allyl-6-(<i>N</i> -trifluoroacetylamino)hexanamide L2	44
3.2.4 Synthesis of 5-(3-trifluoroacetamidoprop-1-enyl)uridine	45
3.2.5 Synthesis of 5-(3-[6-trifluoroacetylaminohexanamido]prop-1-enyl)uridine	48

3.2.6	The Heck coupling reaction of 8-bromo-, 8-iodoadenosine and its derivatives with L1	49
3.2.6.1	The Heck coupling reaction of 8-bromoadenosine in non-aqueous solvents	49
3.2.6.2	The Heck reaction of 8-bromoadenosine and L1 in aqueous organic solvents	51
3.2.6.3	Synthesis of 8-iodoadenosine and its derivatives	55
3.2.6.4	The Heck coupling reaction of 2',3',5'-tri(<i>tert</i> -butyldimethylsilyl)-8-iodoadenosine and L1	57
3.2.6.5	The Heck coupling reaction of 8-iodoadenosine and L1	58
3.2.6.6	The Heck coupling reaction of <i>N</i> -isobutyryl-8-iodoadenosine and <i>N,N'</i> -diisobutyryl-8-iodoadenosine with L1	59
3.2.7	The Heck coupling reaction of 8-bromoadenosine and L2	60
3.2.8	The Heck cross-coupling reaction of 2-iodoadenosine and L1	61
3.2.9	The Heck coupling reaction of 2-iodoadenosine and L2	64
3.3	Amino linker modified nucleosides for further protection and phosphitylation	64
3.4	The protection of the exo-cyclic amino functions of adenosine and guanosine derivatives	65
3.5	The protection of the 5'-OH group by dimethoxytritylation	69
3.6	The protection of the 2'-OH group by <i>tert</i> -butyldimethylsilylation	71
3.7	Synthesis of amino linker modified phosphoramidite building blocks	74
3.8	RNA: chemical synthesis, purification, labeling, analysis and hybridization	77
3.8.1	Chemical synthesis and purification of modified RNAs	80
3.8.2	Labeling of amino linker modified RNAs	82
3.8.3	Analysis of modified and dye-labeled RNAs by MALDI-TOF-MS	86
3.8.4	Treatment of the oligonucleotide D1L2 with calf intestinal alkaline phosphatase (CIAP) and snake venom phosphodiesterase (SVP)	88
3.8.5	Hybridization of single-stranded RNAs	91
3.8.6	Influences of linker length and rigidity on the quantitative FRET experiments of dye-labeled RNAs	92
4	Summary	93
5	Experimental	96
5.1	Materials	96
5.1.1	General remarks	96
5.1.2	Buffers	96
5.1.3	Enzymes	97
5.1.4	Apparatus	97

5.2	Methods for purification and analysis of the samples	98
5.2.1	Chromatographic methods	98
5.2.2	NMR	100
5.2.3	MALDI-TOF	100
5.2.4	Chemical synthesis and purification of RNAs	101
5.3	Synthesis of linkers	107
5.3.1	<i>N</i> -Allyltrifluoroacetamide L1	107
5.3.2	<i>N</i> -Allyl-6-(<i>N</i> -trifluoroacetyl amino)hexanamide L2	108
5.3.3	<i>N</i> -Propargyltrifluoroacetamide L3	109
5.4	5'- <i>O</i> -(4,4'-Dimethoxytrityl)-2'- <i>O</i> - <i>tert</i> -butyldimethylsilyl-3'-(2-cyanoethyl- <i>N,N'</i> -diisopropylamino phosphoramidite)-5-(3-trifluoroacetamidoprop-1-ynyl)uridine	109
5.5	5'- <i>O</i> -(4,4'-Dimethoxytrityl)-2'- <i>O</i> - <i>tert</i> -butyldimethylsilyl-3'-(2-cyanoethyl- <i>N,N'</i> -diisopropylamino phosphoramidite)-5-(3-trifluoroacetamidoprop-1-enyl)uridine	113
5.6	5'- <i>O</i> -(4,4'-Dimethoxytrityl)-2'- <i>O</i> - <i>tert</i> -butyldimethylsilyl-3'-(2-cyanoethyl- <i>N,N'</i> -diisopropylamino phosphoramidite)-5-(3-[6-trifluoroacetylaminohexanamido]-prop-1-enyl)uridine	115
5.7	5'- <i>O</i> -(4,4'-Dimethoxytrityl)- <i>N</i> -6-isobutyryl-8-(3-trifluoroacetamidoprop-1-ynyl)-adenosine	118
5.8	5'- <i>O</i> -(4,4'-Dimethoxytrityl)-2'-(<i>tert</i> -butyldimethylsilyl)-3'-(2-cyanoethyl- <i>N,N'</i> -diisopropylaminophosphoramidite)- <i>N</i> -6-isobutyryl-2-(3-trifluoroacetamidoprop-1-ynyl)adenosine	122
5.9	5'- <i>O</i> -(4,4'-Dimethoxytrityl)-2'-(<i>tert</i> -butyldimethylsilyl)- <i>N</i> -2-isobutyryl-8-(3-trifluoroacetamidoprop-1-ynyl)guanosine	125
5.10	5'- <i>O</i> -(4,4'-Dimethoxytrityl)-2'-(<i>tert</i> -butyldimethylsilyl)-3'-(2-cyanoethyl- <i>N,N'</i> -diisopropylaminophosphoramidite)- <i>N</i> -6-isobutyryl-8-(3-trifluoroacetamidoprop-2-en-1-yl)adenosine	128
5.11	8-(3-[6-Trifluoroacetylaminohexanamido]prop-2-en-1-yl)adenosine	131
5.12	2-(3-Trifluoroacetamidoprop-1-enyl)adenosine and 2-(3-trifluoroacetamidoprop-2-en-1-yl)adenosine	131
5.13	8-Iodoadenosine	133
5.14	Post-synthetic labeling of the modified oligonucleotides	136
5.15	Preparation of hybrids	137
5.16	Analyses of D1L2 with enzymes	137
	List of Tables	139
	List of Figures	141
	Literatures	145

Appendix	157
Acknowledgments	160
Curriculum vitae	162
Publications	163

Abbreviations

A	Adenosine
Ac	Acetyl
ACE	Bis(2-acetoxyethoxy)methyl
AsPh ₃	Triphenylarsine
br	broad
Bu ₃ N	Tributylamine
CDI	Carbonyl Diimidazole
CIAP	Calf Intestinal Alkaline Phosphatase
CPG	<i>controlled pore glass</i>
d	Doublet
dba	Dibenzylideneacetone
DCE	Dichloroethane
DCM	Dichloromethane
DIPEA	<i>N,N</i> -Ethyl-diisopropylamine
DMA	<i>N,N</i> -Dimethylacetamide
DMAP	<i>N,N</i> -Dimethylaminopyridine
DMF	<i>N,N</i> -Dimethylformamide
DMSO	Dimethyl sulfoxide
DMT	Dimethoxytrityl
dppf	1,1'-Bis(diphenylphosphino)ferrocene
dppp	1,3-Bis(diphenylphosphino)propane
EDTA	Ethylenediaminetetraacetic Acid
ENDOR	Electron Nuclear Double Resonance
EPR	Electron Paramagnetic Resonance
eq.	equivalent
Et ₃ N	Triethylamine
FRET	Fluorescence Resonance Energy Transfer

G	Guanosine
hc	Herrmann's catalyst
HOBT	1-Hydroxybenzotriazole
HPA	3-Hydroxy Picolinic Acid
HPLC	High Performance Liquid Chromatography
Hz	Hertz
Ibu	Isobutyryl
lcaa	<i>long chain alkylamine</i>
LDA	Lithium Diisopropyl Amide
m	Multiplet
MALDI	Matrix Assisted Laser Desorption/Ionization
MeCN	Acetonitril
MeOH	Methanol
MS	Mass Spectrometry
NaOAc	Sodium Acetate
NHS	<i>N</i> -Hydroxysuccinimidyl
NMP	<i>N</i> -Methylpyrrolidole
NMR	Nuclear Magnetic Resonance
ns	Nanosecond
<i>o</i> -tol	<i>o</i> -Tolyl
<i>p</i> -tol	<i>p</i> -Tolyl
PAA	Polyacrylamide
PAC	Phenoxyacetyl
PAGE	Polyacrylamide Gel Electrophoresis
PCR	Polymerase Chain Reaction
PELDOR	Pulsed Electron Double Resonance
ppm	parts per million
q	Quartet
RNA	Ribonucleic Acid
RT	Room Temperature

s	Singlet
SD	Shine-Dalgarno
sept	Septet
SMD	Single Molecule Detection
smFRET	Single-molecule FRET
SVP	Snake Venom Phosphodiesterase
t	Triplet
TBAF	Tetrabutylammonium Fluoride
tBoc	<i>tert</i> -Butyloxycarbonyl
TCSPC	Time Correlated Single Photon Counting
TEAAc	Triethylammmonium Acetate
TFA	Trifluoroacetyl
TFP	Tetrafluorophenyl
THF	Tetrahydrofurane
TMS	Trimethylsilyl
TOF	Time-Of-Flight
TOM	Tris(isopropylsilyl)oxymethyl
Tris	Tris(hydroxymethyl)aminomethane
tRNA	transfer RNA
U	Uridine

1 Introduction

RNA is a ubiquitous biopolymer with complex functions in the maintenance, transfer, processing and regulation of genetic information. A fundamental basis for these biological functions is the ability of RNA to adopt complex three-dimensional structures and to interconvert rapidly between multiple functional states. Since the discovery of RNA enzymes, so called ribozymes, at the beginning of the 80s by Cech and co-workers (Kruger *et al.* 1982) followed by Altman and co-workers (Guerrier-Takada *et al.* 1983), many catalytic RNAs have been found and led to an even more increasing interest in RNA structures. Nevertheless, at a molecular level, the current understanding of conformational change mechanisms and RNA folding pathways is rather limited. Extensive biochemical and biophysical studies have been dedicated to get better pictures of RNA structures and dynamic folding events. These studies have led to an increased demand for site-specifically modified RNA samples.

Two strategies have been applied in parallel for the production of RNA: The enzymatic synthesis of RNA using run off transcription with T7 RNA polymerase from linearized plasmid templates or chemically synthesized DNA templates and the chemical synthesis of RNA.

The enzymatic synthesis of RNA has been extensively used to synthesize multi-milligram quantities of RNA but is accompanied by experimental difficulties. *In vitro* transcribed RNAs often possess 5'- and/or 3'-heterogeneities (Milligan *et al.* 1987; Pleiss *et al.* 1998; Helm *et al.* 1999). Basically, this problem can be resolved by the use of ribozymes to excise the full-length transcript from the flanking sequences (Ferré-D'Amaré & Doudna 1996). This approach, however, may suffer from alternative secondary structure formation or from the generation of the 2', 3'-cyclic phosphate group at the 3'-end. Moreover, an inevitable limitation of transcription is that modified nucleotides are not often recognized as the substrates of the enzymes. Even when an enzyme accepts a modified nucleotide as its substrate, site-specific modification is hardly achieved as the enzyme will randomly incorporate this modified nucleotide into the growing sequence. In this context, chemical synthesis is a promising alternative to enzymatic RNA preparation.

After the first synthesis of a thymidine dinucleotide with a 5', 3'-internucleotide linkage identical to natural DNA (Michelson & Todd 1955), oligonucleotide synthesis has been developed to be one of the most important areas in nucleic acid chemistry. Nowadays, the common procedure for the synthesis of RNA is based on the phosphoramidite chemistry conducted on solid support (Beaucage & Caruthers 1981). The chemical synthesis of RNA by the phosphoramidite approach enables the introduction of diverse modified nucleotides, labels and biomolecular structures at precise positions within RNA sequences. Various modifications have been made for the phosphodiester backbone, the purine and pyrimidine heterocyclic bases and the sugar

moiety.

Modifications of the phosphodiester backbone can be achieved by a number of ways. For example, the non-bridging oxygen atom can be exchanged with a sulfur or a selenium atom (Figure 1). The resulting phosphorothioate and phosphoroselenoate oligonucleotides have been used for the determination of the stereochemical courses of the reactions occurring at the chiral phosphorus center (Eckstein 1985), the identification of metal-ion binding sites (Waring 1989) and structural studies by X-ray crystallography (Pallan & Egli 2007).

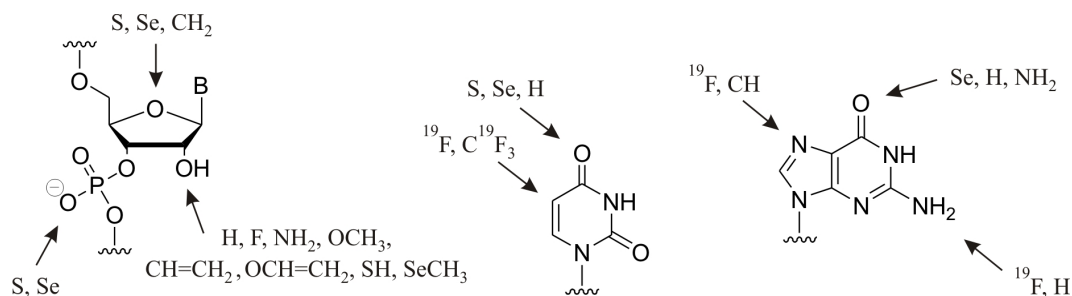


Figure 1 – Selected examples of modifications that can be incorporated at the phosphodiester backbone (left), sugar (left) and base moieties (middle and right) of RNA using the chemical synthesis of oligonucleotides.

The heterocyclic rings of the purine and pyrimidine bases provide hydrogen-bonding groups in nucleic acids. Carefully designed base analogs, when introduced into RNA, can provide information on the importance of the specific functional groups in nucleobases (Figure 1). Purine and modified purine derivatives such as 7-deazapurine, inosine, 2-aminopurine and 2,6-diaminopurine have been used in studies of protein-DNA interaction (Duggan *et al.* 1995) or for the identification of the purine nucleosides essential for RNA catalysis (Liu *et al.* 1997). Modified pyrimidine analogs such as 4-thio-, 4-selenouridine and 2-pyrimidinone have been used to identify the conserved pyrimidines in the central core of the hammerhead ribozyme (Murray *et al.* 1995) and to investigate base-pairing and stacking interactions by X-ray experiments (Salon *et al.* 2007; Salon *et al.* 2008).

The modifications at the 2'-position of the sugar moiety such as deoxy, fluoro, amino, methoxy, allyl, allyloxy, mercapto and methylseleno groups (Figure 1) have been utilized to investigate the catalytic activity of hammerhead ribozymes (Pieken *et al.* 1991; Paoletta *et al.* 1992), hairpin ribozymes (Chowrira *et al.* 1993), *Tetrahymena* ribozymes (Pyle & Cech 1991) and Diels-Alder ribozymes (Serganov *et al.* 2005). In addition, selective labeling with stable isotopes of C, N and H allows the investigation of RNA structure and dynamics by high-resolution nuclear magnetic resonance (NMR) spectroscopy (Kreutz *et al.* 2005; Wenter *et al.* 2006; Lu *et al.* 2009).

Another approach to modify oligonucleotides for application in molecular biology is to functionalize them with reporter groups. Conjugates are designed to furnish the oligonucleotides

with new properties, either physical or chemical, while keeping their natural characters intact. Reporter groups combined with oligonucleotides can be subdivided into the following major categories: Chemically reactive groups, groups promoting intermolecular interactions, fluorescent and spin-labels and radioactive groups. Chemically reactive groups such as thiols have been used to study interactions between nucleic acids and proteins (Erlanson *et al.* 1993) and non-canonical DNA structures (Wolfe *et al.* 1995) via site-specific cross-linking. Biotin-labeled RNAs that bind to streptavidin are typical examples of conjugates that support intermolecular interactions (Goodchild 1990). Spin-labeled RNAs have been widely used in studying dynamic properties of RNA by electron paramagnetic resonance (EPR) spectroscopy (Zhang *et al.* 2009).

Besides these modifications, fluorescently labeled RNAs have been extensively applied for fluorescence spectroscopy, especially in fluorescence resonance energy transfer (FRET) experiments (Wachowius & Höbartner 2010). Since fluorescent signals are sensitive to changes of molecular surroundings, they can be monitored in real time to reveal kinetic information and structural dynamics of RNA molecules which are related to a number of tertiary interactions being formed and broken at various rates and levels.

To conduct fluorescence-based experiments, dye-labeled oligonucleotide samples are indispensable. Nevertheless, apart from the amino linkers for 3'- and 5'-labeling, only a few of building blocks for internal labeling are commercially available as the deoxynucleoside analogs of thymidine with amino linkers at the C-5 position of the heterocyclic base. Such building blocks derived from ribonucleosides are more or less missing. For the functionalization of RNA, modified deoxyribonucleosides are, however, not always sufficient. The replacement of a ribonucleotide in RNA against a deoxyribonucleotide in cases of physical studies like FRET may potentially cause systematic errors, since the furanose rings of ribo- and deoxyribonucleotides adopt distinctive sugar conformations. The 2'-deoxyfuranose ring prefers C2'-*endo* (Figure 2, left), whereas the C3'-*endo* sugar puckering is generally favored by ribonucleotides (Figure 2, right).

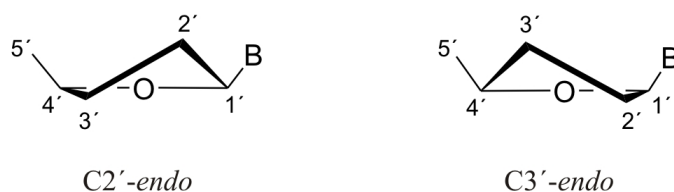


Figure 2 – Preferred conformations of pentose sugars: C2'-*endo* (left) and C3'-*endo* (right).

These two conformations cause variations in relative orientations of the base (with respect to the sugar) and in the distance between 3'- and 5'- phosphate groups. Consequently, the overall conformation of the oligonucleotide is thoroughly affected. In this context, the synthesis of modified ribonucleoside phosphoramidite building blocks for RNA synthesis and functionalization is an urgent demand.

For internal labeling of RNA, in addition to the C-5 position of uridine and cytidine, the C-8 position of purine nucleosides is also suitable for linker attachment. In RNA helical duplexes, protons at the C-8 position of purine bases point into the major groove which is deep and narrow. On the contrary, protons at the C-2 position of adenosine nucleotides reach into the minor groove which is shallow and wide. Therefore, in the case of adenosine, it may be more reasonable to attach reporter groups to the C2 in order to increase accessibility for their counterparts. Linker modifications at the C-5 position of pyrimidine bases, the C-8 position of purine bases as well as at the C-2 position of adenosine's nucleobase will not intervene in the hydrogen-bond formation of the nucleobases.

Within a collaborative project with Prof. Dr. Claus Seidel at the University of Düsseldorf, a series of functional RNAs are studied by fluorescence spectroscopy. For this purpose, modified phosphoramidite building blocks bearing amino linkers of varying length and flexibility were to be synthesized. The linkers should be attached to the nucleobases as explained above and illustrated in Figure 3. Linker modified building blocks should be incorporated into RNAs of specific sequences followed by post-synthetic labeling with dyes to be used in FRET studies.

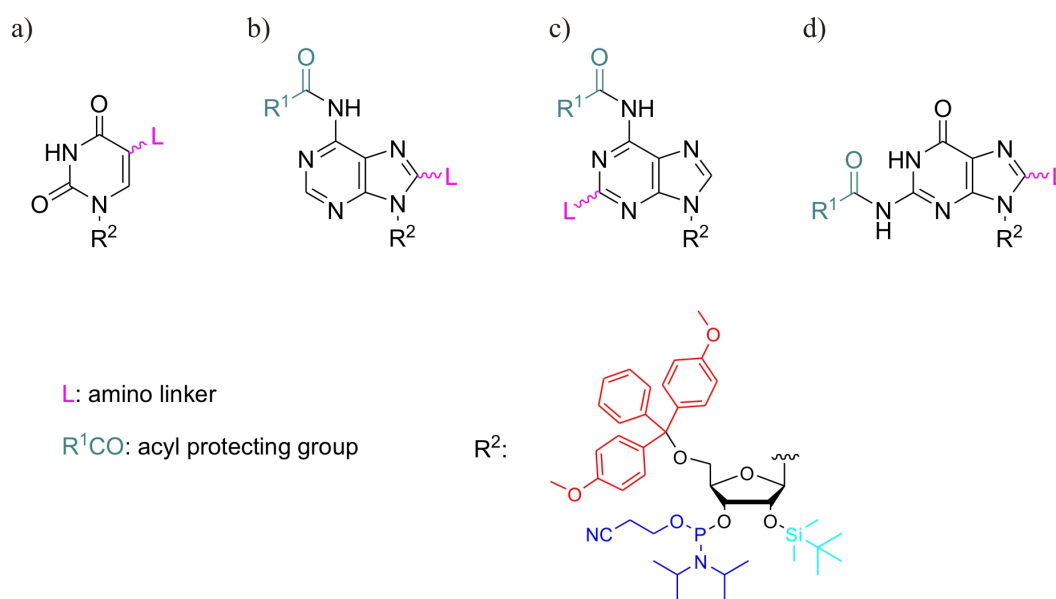


Figure 3 – The structures of the building blocks to be prepared for RNA synthesis based on the 2'-O-TBDMS-3'-O-phosphoramidite chemistry: a) C-5 amino modified uridine phosphoramidite; b) C-8 amino modified adenosine phosphoramidite; c) C-2 amino modified adenosine phosphoramidite; d) C-8 amino modified guanosine phosphoramidite.

2 Theoretical background

2.1 Chemical synthesis of RNA

At the early age of the chemical synthesis of oligonucleotides, the "phosphodiester" (Khonara *et al.* 1956; Khonara *et al.* 1957) followed by the "phosphotriester" approach (Letsinger & Ogilvie 1967) has been applied. This important field of nucleic chemistry was then revolutionized by the breakthrough of Letsinger and co-workers, the "phosphite triester" approach (Letsinger & Lunsford 1976). The phosphite triester approach was then modified to the phosphoramidite method by Beaucage and Caruthers (Figure 4) (Beaucage & Caruthers 1981).

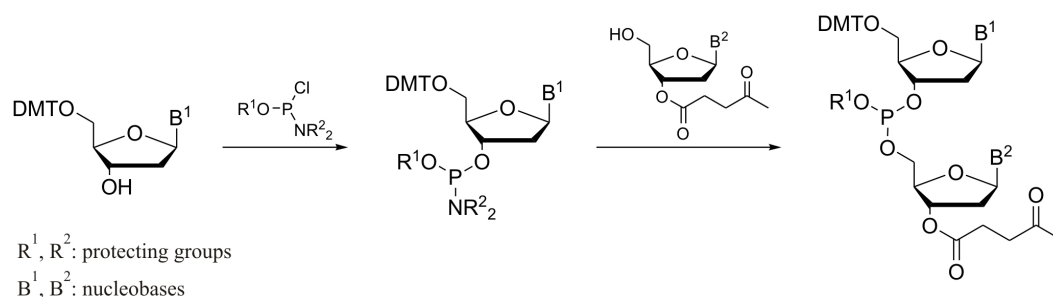


Figure 4 – Phosphoramidite approach established by Beaucage and Caruthers (Beaucage & Caruthers 1981).

This phosphorylation methodology allows high coupling efficiencies and fast coupling rates of monomer building blocks and became a powerful tool for the chemical synthesis of oligonucleotides. The current method for the chemical synthesis of oligoribonucleotides is still based on the phosphite triester chemistry.

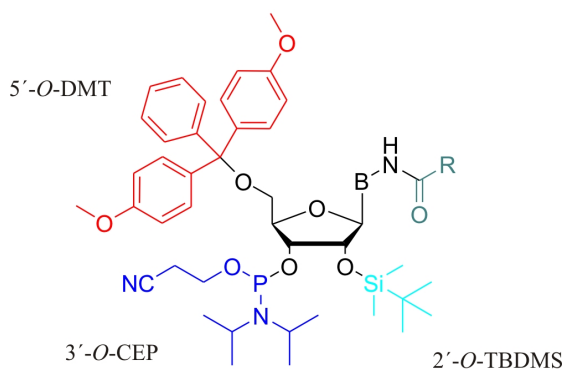


Figure 5 – Structure of building blocks for automated RNA synthesis based on 2'-O-TBDMS-3'-O-phosphoramidite chemistry. The 2'- and 5'-OH groups are protected with the *tert*-butyldimethylsilyl (TBDMS) and 4,4'-dimethoxytrityl (DMT) groups, respectively. The amino functions of adenosine, guanosine and cytidine (B) are protected with acyl groups and the *N,N*-diisopropylphosphoramidite with the β -cyanoethyl group (3'-O-CEP).

In a typical phosphoramidite building block (Figure 5), the 2' and 5'-OH groups are protected with the *tert*-butyldimethylsilyl (TBDMS) and 4,4'-dimethoxytrityl (DMT) groups, respectively. The exocyclic amino functions of the nucleobases are protected with acyl groups and the *O,N,N*-diisopropylphosphoramidites are protected with the β -cyanoethyl group.

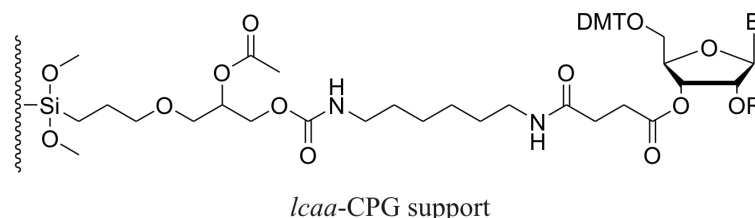


Figure 6 – *Lcaa*-CPG used as solid support used for RNA synthesis. The starting nucleoside is anchored on the support at its 3'-hydroxyl group via a succinate linker arm. B: nucleobase.

The chemical synthesis of an oligonucleotide proceeds by automated chain elongation on a controlled pore glass (CPG) solid support (Figure 6), facilitating fast building up of the growing chain without requirement for the separation of the intermediates (Gough *et al.* 1981). The CPG support has been extensively applied for the solid-phase synthesis due to its rigid and non-swellable texture.

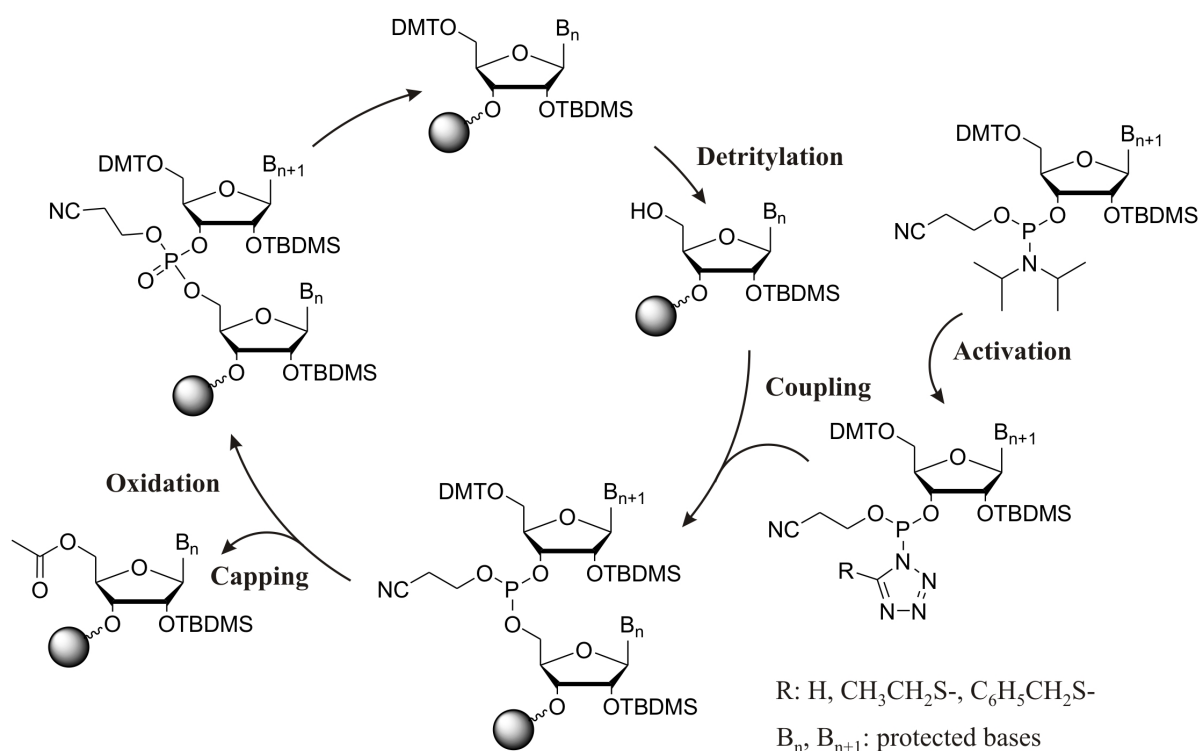


Figure 7 – Synthesis cycle of the 2'-*O*-TBDMS-3'-*O*-phosphoramidite method.

In contrast to the RNA synthesis in biological systems, the chemical synthesis of oligonucleotides progresses from the 3'- to the 5'- end (Figure 7). The first nucleotide of the 3'-end is anchored on the CPG support via a succinimidyl linker. After the detritylation of the support, the incoming phosphoramidite is activated *in situ* by a tetrazole derivative and couples to the

free 5'-OH group. The 5'-OH groups that fail to condense with the activated phosphoramidite are blocked with acetyl groups, rendering them inert towards further chain extension. This capping step ensures that the subsequent reactions proceed only by the growing chains of the desired sequence. Therefore, it gives a higher yield of the product and easier purification at the end of the synthesis. The unstable phosphite triester is then oxidized to the phosphate triester by a basic solution of iodine in aqueous MeCN. After detritylated, the growing oligomer again has a free 5'-OH group which is ready for the next coupling round. The cycle is repeated until the oligonucleotide of desired length is assembled.

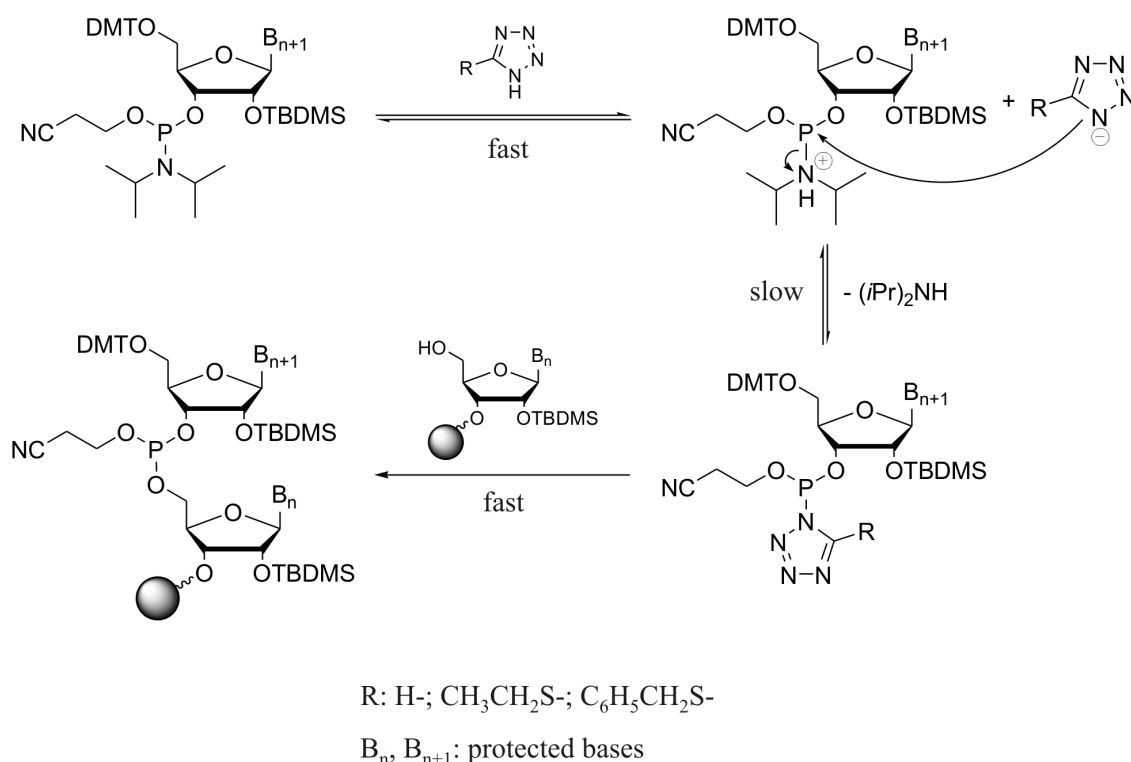


Figure 8 – Activation mechanism of 1*H*-tetrazole and derivatives (Dahl *et al.* 1987; Welz & Müller 2002).

The coupling reaction between a phosphoramidite and a hydroxyl group involves the acidic and nucleophilic catalyses by 1*H*-tetrazole derivatives (Figure 8). The activator protonates the nitrogen of the *N,N*-diisopropyl moiety and supports for the nucleophilic substitution of the *N,N*-diisopropylamino group by tetrazolide to give the activated intermediate. This intermediate can quickly couple with any free hydroxyl group present in the reaction mixture. The catalytic activities of activators increase with the increase of their acidities: tetrazole (pK_a= 4.89) < EMT (pK_a= 4.28) < BMT (pK_a= 4.08) (Lieber & Enkoji 1961), as stronger acidic activators can better activate the phosphoramidite at the protonation step. DCI (pK_a= 5.5) has a lower acidity than that of 1*H*-tetrazole, but its catalysis capacity is higher, as its conjugated base possesses a higher nucleophilicity. The presence of the benzyl group makes BMT more hydrophobic, reducing its affinity to water, hence allowing it to stay dry when stored or in acetonitrile solution.

The protection of different functionalities of the nucleosides in the chemical synthesis of oligonucleotides is a central issue. Protecting groups help to control the growing chain in a defined direction. Moreover, they also have complex effects on the coupling efficiency and the purification of the synthetic oligonucleotides. These protecting groups should satisfy at least three criteria: i) they can be easily and selectively introduced, ii) they should be stable under the reaction conditions and iii) they can be easily and completely removed at the end of the synthesis under the conditions under which the desired product stays intact. In addition, protecting groups used in oligonucleotide synthesis must be orthogonal, so that they can be selectively removed during the synthesis and purification. During the chemical synthesis, the *O*-phosphoramidite and the 2'-OH groups are permanently protected, while the 5'-OH groups are periodically released for coupling reactions with the incoming phosphoramidites after every cycle of the chain assembly.

The 5'-OH group is the only primary hydroxyl of the three hydroxyl groups of ribonucleosides which can be selectively protected with the DMT group (Andersen *et al.* 1954; Smith *et al.* 1962). Under mild acidic conditions, DMT groups are easily cleaved off to release free hydroxyl groups, but sufficiently stable to tetrazoles, which are used as activators in chain extension steps. Especially in the automated synthesis of oligonucleotides, the concentrations of the dimethoxytrityl cations released after every coupling determined by means of spectrophotometry or conductometry can be used to qualitatively evaluate the efficiency of each coupling step. Furthermore, in a "DMT-on" synthesis, the terminal 5'-*O*-DMT group makes the oligonucleotide product more hydrophobic what facilitates the isolation of the target oligonucleotide from the mixture of truncated fragments. Base-labile groups such as 9-fluorenylmethoxycarbonyl (Fmoc) (Lehmann *et al.* 1989), 2-dansylethoxycarbonyl (Dnsec) (Bergmann & Pfeleiderer 1994) and levuliny (Lev) (Iwai & Ohtsuka 1988) have also been tested for their potential as 5'-*O*-protecting group. Recently, Scaringe and co-workers have introduced a novel protecting approach for the 5'-OH function based on silylation chemistry (Figure 9b) (Scaringe 2001).

The acyl amino protecting approach established by Khorana and co-workers (Agarwal *et al.* 1972) applied for oligodeoxynucleotides have been proved to be unsuitable for RNA synthesis as they require strong basic deprotection conditions. Therefore, new exocyclic amino protecting groups were searched for, among which phenoxyacetyl- (PAC) and 4-isopropylphenoxyacetyl (*i*Pr-PAC) (Schulhof *et al.* 1987) are the most suitable. They can be fast and completely removed under rather mild alkaline conditions (concentrated ammonia/ethanolic methylamine (AMA) at 65 °C in 1 hour (the standard condition in our working group). The protection of the amino functions is based on the transient protection method described by Ti and co-workers (Ti *et al.* 1982).

Among different amidites which have been tested (Beaucage & Caruthers 1981; McBride & Caruthers 1983), *N,N*-diisopropylamino phosphoramidites are the reagents of choice for the

synthesis of oligodeoxyribonucleotides, as they are sufficiently stable in acetonitrile solution that is a key character for the success in oligonucleotide synthesis. The internucleotide linkages are protected with β -cyanoethyl groups (Sinha *et al.* 1983) which can be cleaved by a β -elimination under alkaline conditions.

The presence of the 2'-OH group makes the chemical synthesis of oligoribonucleotides more challenging. The protection of this functional group requires a selective reaction of the two secondary 2'- and 3'-OH groups. In addition, the 2'-O-protecting group may cause steric hindrance which restricts the coupling reactions of the phosphoramidites. The presence of 2'-OH groups also leads to the requirement of more elegant protecting groups for other functional groups that can be cleaved off under mild conditions, as the internucleotide linkages of oligoribonucleotides are sensitive to alkaline hydrolysis (Kuusela & Lönnberg 1994) as well as cleavage and migration in acidic medium (Griffin *et al.* 1968). Among the 2'-O-protecting groups having been investigated, the 2'-O-*tert*-butyldimethylsilyl (TBDMS) group, introduced by Ogilvie (Ogilvie *et al.* 1974), has been extensively applied in solid-phase synthesis, as it is relatively stable under both acidic and basic conditions. The TBDMS group can remain intact through the synthesis but can be easily removed when the synthetic oligonucleotide is treated with fluorides (Westman & Stromberg 1994). The phosphoramidites relying on this protecting group, however, have only modest coupling efficiencies when 1*H*-tetrazole is used as activator. This disadvantage can be assigned to the bulkiness of the TBDMS group, which may sterically hinder the reaction center and reduce the rate of the reaction. Regarding this problem, studies have been carried out to evaluate the potential of the hitherto known activators for RNA synthesis based on 2'-O-TBDMS method (Welz & Müller 2002). In the working group of Prof. Müller, 2'-O-TBDMS-3'-O-phosphoramidite approach in combination with the activator BMT has been successfully applied and developed to a higher level of coupling yields.

In order to achieve adequate coupling yields, only reagents and solvents of the highest quality are admitted because the phosphitylating reagents and the phosphoramidites involved in the coupling reaction are extremely moisture sensitive. The presence of traces of water in the reaction system leads to the hydrolysis of the reaction components to unactive substances such as phosphonates (Atkinson & Smith 1990). After the synthesis, the nucleobases and phosphate esters are deprotected by alkaline treatment during which the synthetic oligonucleotide is detached from the support. The deprotection is followed by the treatment with fluorides to cleave off 2'-O-TBDMS protecting groups (Westman & Stromberg 1994). The completely deprotected oligonucleotide is then purified by HPLC or denaturing PAGE.

In 2001, new classes of 2'-O-protecting groups for chemical synthesis of oligoribonucleotides have been reported by Pitsch (Pitsch *et al.* 2001) and Scaringe (Scaringe 2001). The first method developed by Pitsch and co-workers involves the protection of the 2'-OH group with the tris(isopropylsilyl)oxy)methyl group (2'-O-TOM) (Figure 9a). The second strategy intro-

duced by Scaringe is based on the protection of the 2'-OH group with bis(2-acetoxyethoxy)-methylorthoester (2'-O-ACE), while the 5'-OH group is protected with bis(trimethylsiloxy)-cyclododecyloxysilyl group (Figure 9b). Phosphoramidite building blocks based on these new 2'-O-protection chemistry can afford high coupling yields when activated by the powerful activator 5-ethylthio-1*H*-tetrazole. Importantly, the 2'-O-TOM and -ACE protecting groups can not be rearranged, which is a priority required for the synthesis of oligonucleotides of high purity.

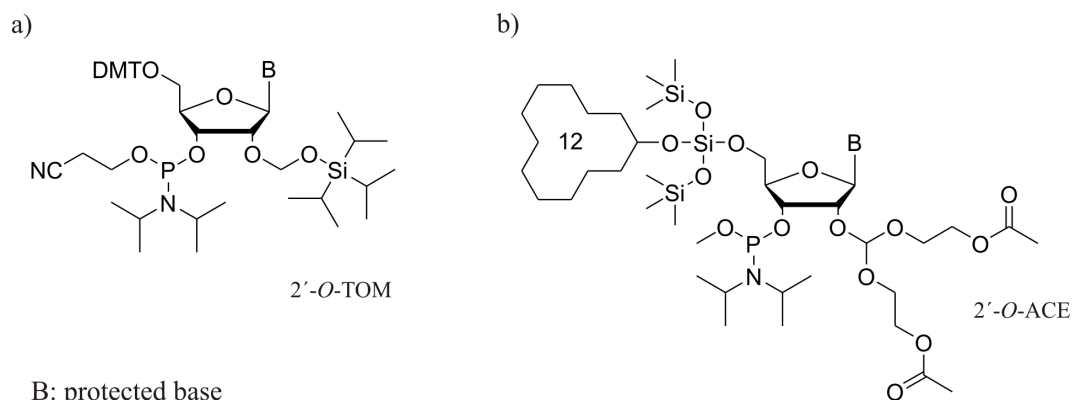


Figure 9 – Phosphoramidite building blocks based on a) "ACE" and b) "TOM" chemistry (adapted from Pitsch *et al.* 2001; Scaringe 2001).

Nevertheless, the synthesis of these building blocks requires rather complicated procedures. In addition, the 2'-O-ACE chemistry is not compatible to that established for TBDMS chemistry and will need adjustment of the existing synthesizers.

Very recently, new building blocks for RNA synthesis using 2'-O-thiomorpholine-4-carbothioate (2'-O-TC) protection (Figure 10) have been introduced by Link chemistry. However, their designated superiority has not yet been proved.

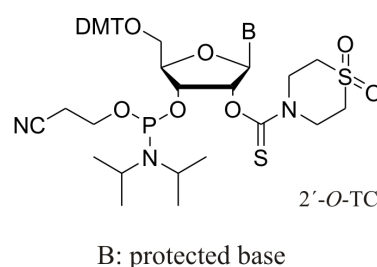


Figure 10 – New phosphoramidite building blocks for RNA synthesis using 2'-O-thiomorpholine-4-carbothioate (2'-O-TC) protection (Link technologies).

2.2 The Sonogashira coupling reaction

The Sonogashira coupling reaction can be generally defined as the palladium-catalyzed Csp²-Csp coupling of aryl and vinyl halides or triflates with terminal alkynes in the presence of a

copper(I) co-catalyst and a base (Figure 11). This kind of reactions has first been reported in 1975 by Heck (Diek & Heck 1975) and Cassar (Cassar 1975). Shortly after that, Sonogashira and co-workers have modified the coupling conditions by the addition of catalytic amounts of copper(I) iodide (Sonogashira *et al.* 1975). The presence of the copper(I) co-catalyst has significantly accelerated the reaction rate, allowing the alkynylation to take place at ambient or slightly elevated temperatures.

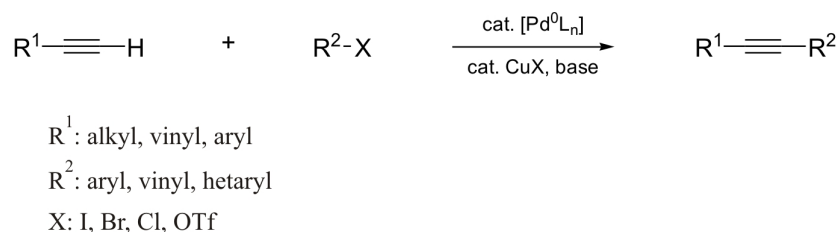


Figure 11 – The Sonogashira coupling reaction.

The copper co-catalyzed Sonogashira reaction involves two related catalytic cycles, namely the Pd-cycle and the Cu-cycle (Figure 12).

Generally, the Pd-cycle involves the catalytically active Pd(0) which was previously postulated to be the neutral 14-electron Pd^0L_2 (Sonogashira *et al.* 1975). This species is generated from Pd^0L_4 by the endergonic dissociation of two neutral phosphine ligands or from the reduction of different Pd(II) pre-catalysts by reductive reagents present in the reaction mixture. These reducing reagents are normally n -electron donors such as phosphines and amines or the terminal alkynes which reduce Pd(II) species typically via a σ -complexation-dehydropalladation-reductive elimination (Sonogashira 2002; Negishi & de Meijere 2002). More recently, some studies have indicated the formation of anionic palladium species $[\text{Pd}^0\text{L}_2\text{X}]^-$ (X: halides or AcO^-), which can be the actual catalysts instead of the neutral coordinatively unsaturated Pd^0L_2 (Amatore & Jutand 2000). The catalytic cycle starts with the oxidative insertion of the active Pd(0) to $\text{R}^1\text{—X}$ (R^1 = aryl, hetaryl, vinyl; X= I, Br, Cl, OTf) (Pd-cycle, Figure 12). The characteristics of the $\text{R}^1\text{—X}$ substrates have a thorough influence on the oxidative addition step. The reactivity order of the $\text{Csp}^2\text{—X}$ substrates has been reported as: aryl iodide > aryl triflate \geq aryl bromide \gg aryl chloride which corresponds to the bond strength order: $\text{Csp}^2\text{—Cl}$ ($E = 96$ kcal/mol) > $\text{Csp}^2\text{—Br}$ ($E = 81$ kcal/mol) > $\text{Csp}^2\text{—I}$ ($E = 65$ kcal/mol) (Grushin & Alper 1994). The presence of electron-withdrawing groups on the $\text{Csp}^2\text{—X}$ moiety and electron-pushing groups on the ligands can enhance the oxidative addition (Hundertmark *et al.* 2000; Böhm & Herrmann 2000). The terminal alkyne can retard the oxidative addition, as it forms the complex $[(\eta^2\text{—RC}\equiv\text{CH})\text{Pd}^0\text{L}_2]$ with the reactive zero-valence palladium species and reduces its concentration (Amatore *et al.* 2004).

The next step in the Pd-cycle is connected with the cycle of the copper(I) co-catalyst, the Cu-cycle (Figure 12). The Pd(II) complex resulted from the oxidative insertion is reacted with the terminal acetylene via a transient copper(I) acetylide species, leading to the formation of an

alkynylpalladium(II) $R^1Pd(-C\equiv CR^2)L_2$ intermediate. This intermediate undergoes a *trans/cis* isomerization and reductive elimination to give the cross-coupled product and to regenerate the active Pd(0) for the next catalysis round.

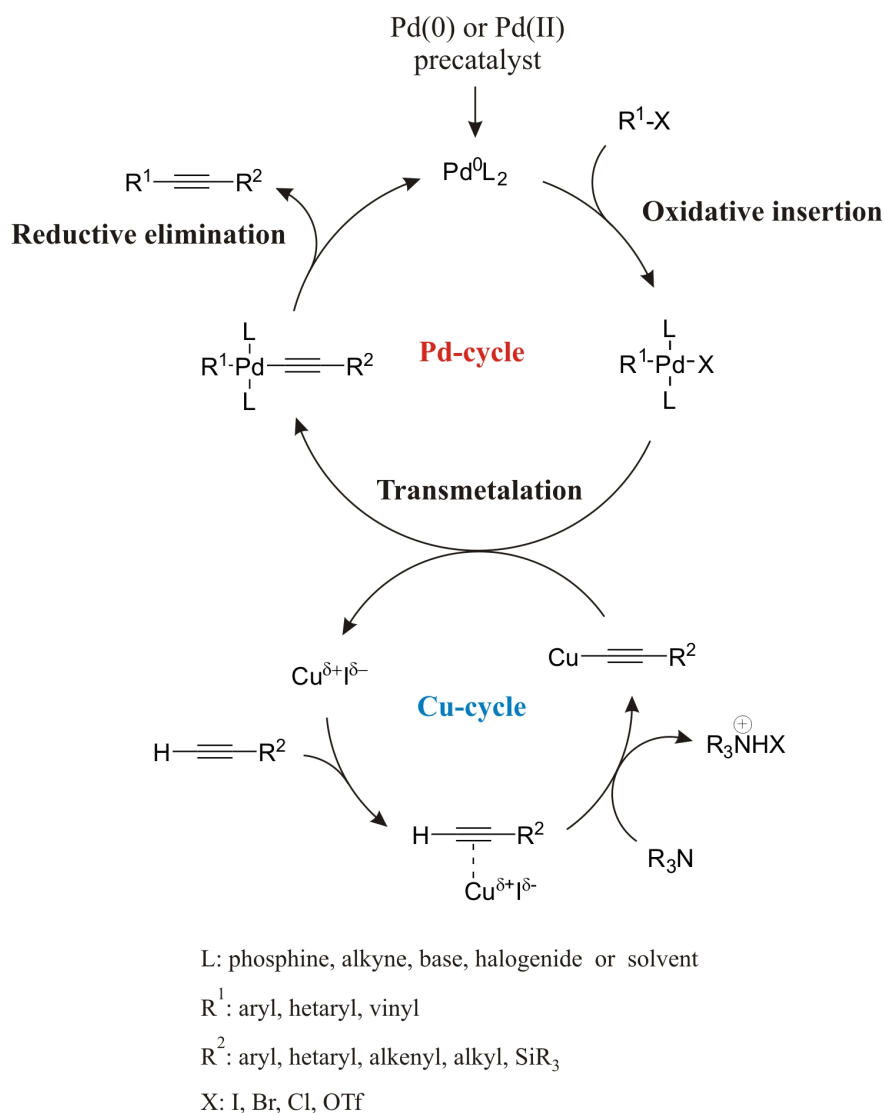


Figure 12 – The mechanism of the Sonogashira coupling reaction. The reaction can be formerly considered to consist of two related catalytic cycles: the Pd-cycle and the Cu-cycle (adapted from Sonogashira 2002 and Chinchilla & Nájera 2007).

The copper(I) salt is supposed to coordinate to the triple bond of the alkyne as a Lewis acid (Figure 12, Cu-cycle) (Bertus *et al.* 2004; Létinois-Halbes *et al.* 2005). This coordination affects the electron distribution over the triple bond, altering the electron density of the acetylenic C-H bond and making it more polar. Therefore, the terminal alkyne could easily be deprotonated even by simple amines, leading to the formation of copper(I) acetylide. In fact, in the absence of copper(I) co-catalyst, the Sonogashira coupling requires much higher temperatures (Diek & Heck 1975; Cassar 1975). The copper acetylide can also react with palladium(II) complexes to form the $Pd(-C\equiv CR^2)_2L_2$ complexes which generate the active Pd^0L_2 and diacetylene side-products via reductive elimination (Sonogashira 2002; Liu & Burton 1997). Although the dry reagents for the Sonogashira coupling reaction are relatively stable, they

become more sensitive to oxygen once in solution. A complex mixture of products can be formed if dissolved oxygen is not completely removed from the system at this point. The *in situ* generation of copper acetylides under the reaction conditions often gives rise to the homocoupling of the terminal alkyne (Glaser 1869).

The traditional Sonogashira reaction is normally catalyzed by a palladium-phosphine ligand complex in the presence of copper(I) iodide and an amine in aprotic polar solvents such as DMF under homogeneous conditions. Studies with different alkynylation reactions have shown that it is not always possible to predict which palladium reagent will work most effectively. The most commonly used catalysts are triphenylphosphine-based complexes such as $\text{Pd}(\text{PPh}_3)_2\text{Cl}_2$ and $\text{Pd}(\text{PPh}_3)_4$. $\text{Pd}(\text{dba})_2$, $\text{Pd}_2(\text{dba})_3$ and $(\text{CH}_3\text{CN})_2\text{PdCl}_2$ in combination with tertiary phosphines or palladium complexes with bidentate ligands such as $\text{Pd}(\text{dppe})\text{Cl}_2$, $\text{Pd}(\text{dppp})\text{Cl}_2$ and $\text{Pd}(\text{dppf})\text{Cl}_2$ have also been used as sources of the catalytic palladium(0).

Sonogashira coupling reaction is highly stereospecific as well as regioselective. A *cis*-olefine is alkynylated under the Sonogashira reaction condition to give the cross-coupled product having *cis*-conformation, while under the same conditions, its *trans*-isomer is transformed to the *trans* cross-coupled product (Schreiber & Kiessling 1988). The regioselective Sonogashira coupling reaction can also be achieved with multi-halogenated derivatives by fine-tuning the reaction conditions (Figure 13) (Comins *et al.* 2005).

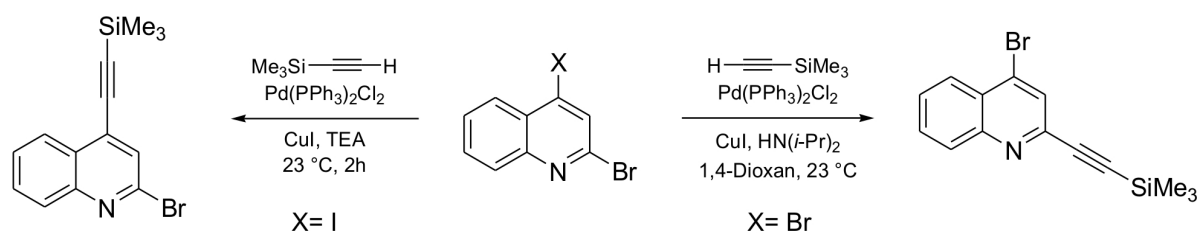


Figure 13 – Regioselective Pd(0)-catalyzed alkynylation.

Because of its mild conditions, the Sonogashira coupling reaction has become the method of choice for the alkynylation of aryl and alkenyl halides. Recently, primary alkyl bromides or iodides (Eckhardt & Fu 2003) and secondary alkyl bromides (Altenhoff *et al.* 2006) have also been used as substrates for Sonogashira coupling reactions. The final products of the Sonogashira coupling reactions can be used to produce building blocks for electrooptical devices and material sciences (Nagy *et al.* 2005), non-nucleoside reverse transcriptase inhibitors (Deng *et al.* 2005), pharmacologically active cyclic peptides (Balraju *et al.* 2005) and ligands in coordination chemistry (Zoppellaro & Baumgarten 2005). Particularly, the traditional Sonogashira coupling procedures have been extensively applied in the total synthesis of natural compounds (Nicolaou *et al.* 2005).

In the field of nucleic acid chemistry, the Sonogashira coupling reaction has proved to be a powerful and versatile approach for the C-C bond formation. Importantly, protecting groups

are not necessary in almost all cases, making this method widely applicable. Thus, amphiphilic nucleosides with lipophilic alkynyl substituents attached to the *N*-heterocyclic ring were synthesized by Sonogashira coupling reactions of C-5 and C-8 halogenated pyrimidine and purine nucleosides (Flasche *et al.* 2004). C-4 substituted pyrimidines with alkynyl tethers obtained by Sonogashira coupling reactions have been incorporated into antisense oligonucleotides (Acevedo *et al.* 1994). Various 5-alkynyl pyrimidine and 7-alkynyl-7-deazapurine nucleosides have been extensively applied in the production of antiviral reagents (Crisp & Flynn 1993), artificial dinucleotide duplexes (Sessler & Wang 1998), fluorescent labeled 2',3'-dideoxynucleotides in DNA sequencing techniques (Prober *et al.* 1987), transitional metal containing DNA for multicolor redox DNA labeling and DNA minisequencing (Vrábel *et al.* 2009) and substrates in studies of PCR reactions (Jäger *et al.* 2005; Kuwahara *et al.* 2006; Hock & Fojta 2008; Ikonen *et al.* 2010). In other studies, Sonogashira cross-coupled products of 2-iodoadenosine have been used for the investigations of adenosine receptors (Matsuda *et al.* 1992) or pyrene intercalation in RNA duplexes (Förster *et al.* 2010). Recently, site-directed spin-labeling of oligonucleotides being used in PELDOR (pulsed EPR) experiments of conformational rearrangement of riboswitch upon ligand binding have been synthesized via Sonogashira cross-coupling reactions of 5-iodouridine and 2-iodoadenosine derivatives (Krstić *et al.* 2010). 6-Iodo pyrimidine nucleosides have been coupled with terminal alkynes to give the anti-HIV-1 agent HEPT (Tanaka *et al.* 1991). A number of C-8 substituted purines were synthesized by Sonogashira coupling reaction and tested for their potential anti-HIV activity (Lang *et al.* 2000) or adenosine receptors (Volpini *et al.* 2001). Sonogashira coupling reactions have also been applied to introduce modifications into sugar moieties of the nucleosides for the studies of anti-HIV agents (Haraguchi *et al.* 1991) and enzyme activities (Wnuk *et al.* 2004).

In conclusion, there is no doubt that nowadays the Sonogashira alkylation reaction is a versatile cross-coupling methodology with growing applications in diverse areas of chemistry, biochemistry and material sciences. Especially, modified building blocks synthesized by the Sonogashira coupling reactions can be incorporated into oligonucleotides during the chemical synthesis, allowing for post-synthetic modifications. The development of this field in nucleic acid chemistry gives rise to various types of substrates for studies in molecular biology.

2.3 The Heck coupling reaction

The Heck reaction can be generally defined as the palladium-catalyzed Csp^2 - Csp^2 cross-coupling between alkenyl and aryl halides or triflates and alkenes (but not applicable with double-bonds in aromatic rings) (Figure 14). This kind of palladium-catalyzed coupling reaction was independently mentioned by Mizoroki (Mizoroki *et al.* 1971) and Heck (Heck &

Nolley 1972) and then developed by Heck to a widely applicable method in organic synthesis.

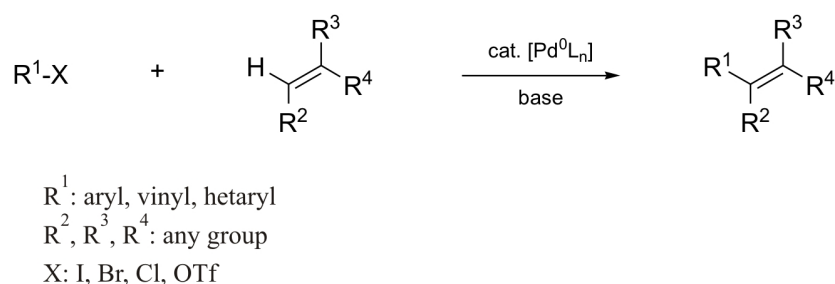


Figure 14 – The Heck coupling reaction.

Mechanistic studies carried out in different systems have revealed that the mechanism of the coupling reaction can not be adequately depicted by a single diagram. In each individual case, the reaction intermediates and their transformations are intimately associated with the chosen catalysts, substrates, ligands, additives, solvents and the conditions under which the reaction is conducted. Concerning the narrow scope of our work, a simplified scheme illustrating the main steps of the Heck catalytic cycle is shown in Figure 15.

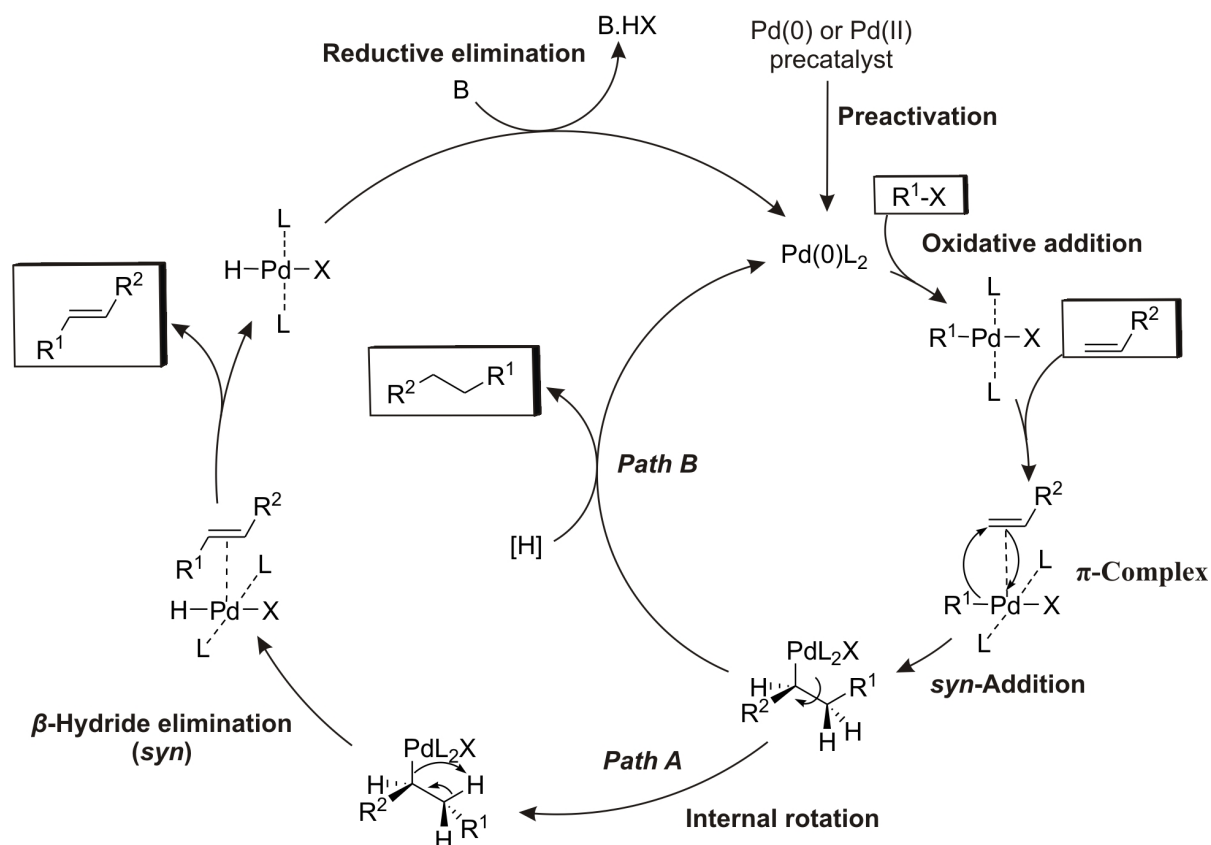


Figure 15 – The general mechanism of Heck coupling reaction (adapted from de Meijere & Meyer 1994; Amatore & Jutand 2000; Whitcombe *et al.* 2001).

The Heck coupling reaction can be catalyzed by palladium complexes with or without phosphine ligands (Quadir *et al.* 2000). Palladium salts such as $PdCl_2$, $Pd(OAc)_2$ alone or other palladium(0) and palladium(II) complexes such as $Pd(MeCN)_2Cl_2$, $Pd(dba)_2$ and $Na_2[PdCl_4]$

can be utilized as sources of the catalytic palladium species. The catalytic cycle starts with the reduction of the palladium(II) complexes to palladium(0) and multiple ligand exchange equilibria through which the active catalytic palladium species are generated. The primary reduction of Pd(II) to Pd(0) is most likely performed by the phosphine in phosphine-assisted systems (Figure 16) (Amatore *et al.* 1995). In phosphine-free reactions, the reduction of Pd(II) can be taken over by amines or olefins (Clayden *et al.* 2006).

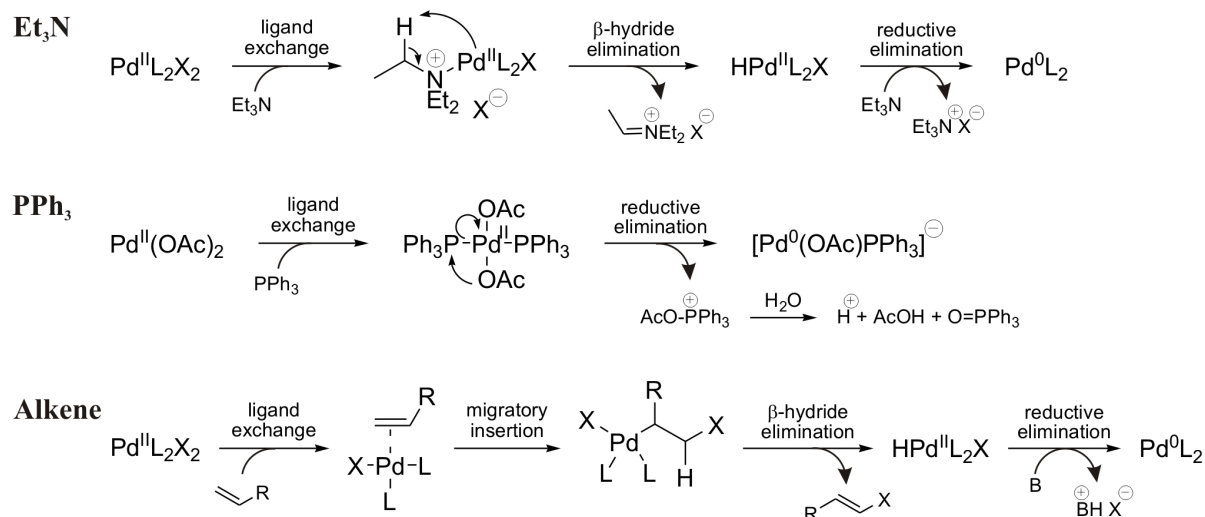


Figure 16 – The *in situ* formation of Pd(0) by the reduction of Pd(II) in the presence of amines, phosphine, organometallics or alkenes (adapted from Clayden *et al.* 2006; Amatore *et al.* 1995).

The palladium catalytic precursor was previously postulated to be a neutral coordinatively unsaturated 14-electron species Pd⁰L₂. In the presence of halides or other anions, the actual active catalytic species have been proved to be the anionic [Pd⁰L₂X]⁻ complex (Amatore & Jutand 2000). The oxidative addition occurs through a concerted process in which Csp²-X rupture happens almost simultaneously with the formation of Pd-C and Pd-X bonds to give a *cis*-R¹Pd^{II}XL₂ species. Subsequently, this intermediate isomerizes to the thermodynamically more stable *trans* isomer (Casado & Espinet 1998). Amatore and coworkers have also reported the formation of the pentacoordinated anionic complex [R¹Pd^{II}XX'L₂]⁻ (X': halogenides or other anions) as the main intermediate of the oxidative addition (Amatore & Jutand 2000). The order of reactivity of aryl halides and triflates toward oxidative addition is: R¹-I > R¹-OTf > R¹-Br ≫ R¹-Cl, which is consistent to the order of bond strengths: Ar-Cl (96 kcal/mol) > Ar-Br (81 kcal/mol) > Ar-I (65 kcal/mol) (Grushin & Alper 1994). Ligands can have different effects on the oxidative addition of different aryl and alkenyl halides: phosphine ligands accelerate the transformation of bromo substrates, while slowing down that of the iodo analogues (Quadir *et al.* 2000). Electron-withdrawing substituents on the halogen substrates can facilitate the oxidative addition, while the electron-pushing ones have the opposite effect.

Coordinatory insertion is the product-forming step in which the new C-C bond is formed. It is this step that is most likely responsible for the regio- and stereoselectivity of the coupling.

The insertion process requires a coplanar assembly of the metal, the aryl or alkenyl moiety R^1 and the olefin (Figure 15). Therefore, the insertion process proceeds stereoselectively in a *syn* manner. The insertion of the olefin into the palladium(II) complex demands a free coordination site on the palladium(II) complex that can be achieved by deligation of one of the bound ligands. Results of catalytic and stoichiometric investigations of this step in phosphine-assisted systems revealed a coordination process involving two possible pathways (Figure 17) (Cabri & Candiani 1995).

Path 1 is initiated with the dissociation of a neutral ligand to give the neutral intermediate 2, while path 2 involves deligation of an anionic ligand to generate the cationic species 3'. Therefore, the regioselectivity of the Heck coupling reaction depends heavily on the structures of the ligands, as they can define the mechanism of the coordination-insertion pathway. The coordination of the π -system with cationic complex 3' results in an increase in the polarization of the double-bond, favoring the selective attack of the aryl moiety (formally considered as an anion) to the carbon which has a higher positive charge density (Cabri *et al.* 1992). Though there is no experimental data available, the non-polar route is hardly conceivable in phosphine-free systems. This is based on the fact that almost all phosphine-free coupling reactions are performed in polar solvents or in the presence of additives that support the exchange of the anionic ligands. Interestingly, the reaction can easily be switched from one mechanism to the other by fine-tuning the reaction conditions (Larock *et al.* 1989; Cabri *et al.* 1991; Cabri *et al.* 1992).

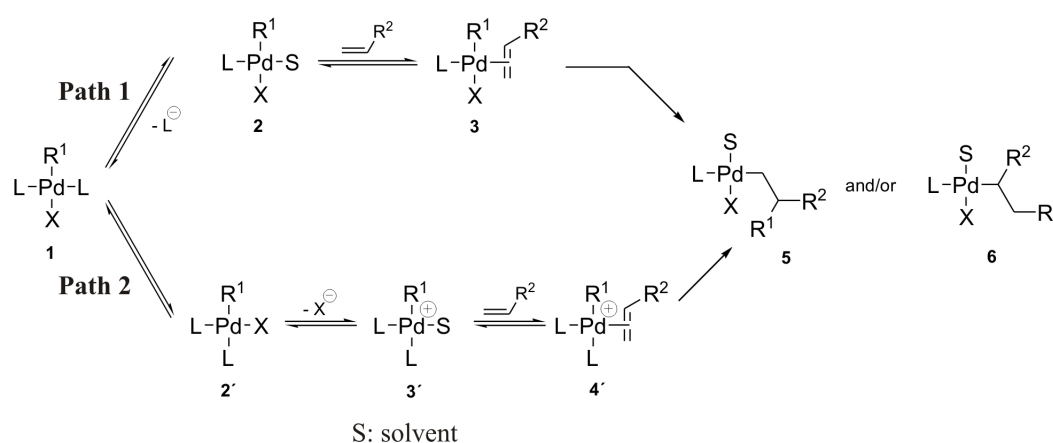


Figure 17 – The coordination-insertion process (adapted from Cabri & Candiani 1995).

The insertion step can follow three possible pathways: i) R^1PdX acts as a carbanion and the migratory insertion can be considered as a nucleophilic addition; ii) R^1PdX and especially R^1Pd^+ species electrophilically attack the double bonds in the way of an electrophilic addition and iii) R^1PdX and R^1Pd^+ intermediates are added to the double bond via a concerted process. In this case, the steric factors are predominant (Beletskaya & Cheprakov 2000). Steric factors favor the insertion of the R^1 group in complexes 3 and 4' to the less substituted carbon through which the linear coupling product is formed (Davis & Hallberg 1989).

The intermediate alkylpalladium species of the insertion step can undergo a *syn* β -hydride elimination (path A, Figure 15) or a protolytical cleavage (path B, Figure 15) (Chu *et al.* 1992).

For the β -hydride elimination, the palladium and the β -proton being eliminated with it must become *syn* and co-planar via an internal rotation (Heck 1969). The elimination goes through a rather strong agostic interaction between palladium and the β -hydrogen atom, thus taking place in a concerted process without the involvement of bases. The β -hydride elimination is essentially a reversible process in which HPdL_2X stays coordinated with the double-bond of the olefin product. Dissociation and readdition of the palladium(II)-hydride complex to the double-bond can lead to the isomerization of the product which can be avoided by adding agents to trap hydrohalic acids such as Ag(I) (Larock *et al.* 1989) or Ti(I) salts (Grigg *et al.* 1991). HPdL_2X may also complex with the starting alkene, isomerizing it and leading to the formation of isomeric Heck products (Spencer 1982; Hii *et al.* 1997). The β -hydride elimination follows the Curtin-Hammett kinetic control principle. Thus, the (*E*)-isomer is normally dominant and the Heck coupling reaction is highly stereospecific even for simple systems. Post-reaction isomerization of the products can also lead to a thermodynamically controlled mixture of isomers (Beletskaya & Cheprakov 2000). The presence of a stoichiometric amount of a base is required to transform the $\text{HPd}^{II}\text{L}_2\text{X}$ into the catalytically active $\text{Pd}^0\text{L}_2\text{X}$ complex via reductive elimination. Typical organic bases are trialkylamines such as Et_3N , $i\text{Pr}_2\text{NEt}$ or inorganic salts like NaOAc , NaHCO_3 and K_2CO_3 .

According to kinetic studies, the rate-determining step can be any element step of the catalysis cycle such as the β -hydride elimination (Schmidt & Smirnov 2001), the coordination/insertion of the olefin (Buback *et al.* 2003) or the halide dissociation (Albert *et al.* 1998) depending on the substrates and the conditions being used.

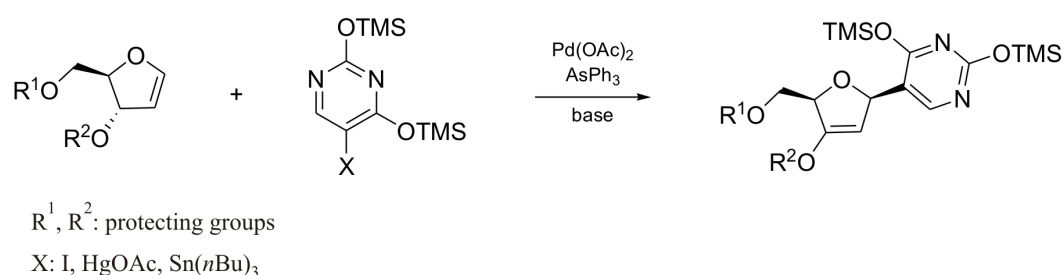


Figure 18 – Regio- and stereoselectivity in Heck coupling reaction.

The Heck coupling reactions are highly enantioselective (Dounay & Overman 2003) as well as regio- and stereoselective (Štambaský *et al.* 2009). When applied to glycals whose double bond is electron-rich, the new C-glycosidic bond is formed selectively at the anomeric carbon and the attack occurs at the less sterically hindered face of the glycal ring (Figure 18). In addition, under Heck coupling reaction conditions, the *cis*- and *trans*-configurations of the alkenyl halogen substrates are conserved without isomerization of the double-bond (Brückner

2004).

In order to optimize the reaction conditions, many efforts have been made, i.e. by variation of catalysts and ligands (Spencer 1984; Littke & Fu 1999), solvents (Chandrasekhar 2002; Cacchi *et al.* 1999), the use of phase-transfer reagents (Jeffery 1996) and recyclable systems (Bergbreiter *et al.* 2000). The discovery of the dimeric complex $\text{Pd}_2(\text{P}(o\text{-tol})_3)_2(\mu\text{-OAc})_2$ (Figure 19) has set a milestone in the development of palladium-catalyzed cross-coupling reactions (Herrmann *et al.* 1995). Herrmann's catalyst (*hc*) and its analogues exhibit a number of distinctive characters: they are easily available, not air- and moisture-sensitive, thermally stable but very active under Heck coupling conditions.

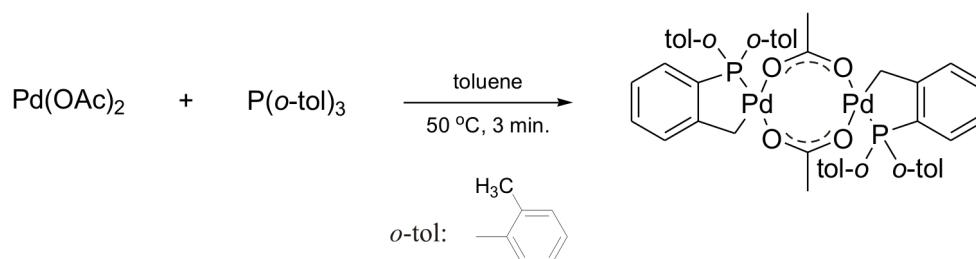


Figure 19 – The preparation of Palladacycle (Herrmann *et al.* 1995).

Besides phosphine-assisted systems, phosphine-free coupling reactions have also gained interest (Spencer 1983). As can be noticed from the catalytic cycle, none of the individual steps demands the support of a phosphine nor any other strongly bound ligands in the coordination shell of the catalytic palladium species. The inherent reactivity of non-ligated palladium is sufficient for the oxidative addition of most kinds of $\text{Csp}^2\text{-X}$ bonds. Moreover, non-ligated palladium catalytic species may possess high catalytic capacity, allowing for reactions involving bulky substrates. The disadvantage of phosphine-free systems is the instability of catalytic species which must often be compensated by high loading of the palladium catalysts.

Polar aprotic solvents such as DMF and DMA are commonly used in Heck coupling reactions. They can dissolve various substrates and catalysts and tolerate hard Heck coupling conditions. Additionally, they are able to support palladium complexes by extra weak coordinations. Apart from these organic solvents, water has been proved to be a promising candidate. Due to its high polarity, the cationic migratory insertion of underligated complexes may be accelerated (path 2, Figure 17). Water has also been demonstrated to be a good ligand for palladium-strongly bonded but kinetically labile. Therefore, it can serve as a place-holder, particularly effective in the absence of phosphine ligands. Moreover, water can literally wash iodide and other interfering ligands out of the coordination shell. Aqueous phosphine-free procedures have also been reported to be milder, more selective than phosphine-related reactions in anhydrous solvents and allow coupling reactions of hydrophilic substrates without complicated protection (Zhang & Daves 1993; Demik *et al.* 1995). Thus, many Heck coupling reactions catalyzed by simple palladium salts have been carried out in aqueous organic solvents (Jeffery 1994; Zhang

& Daves 1993; DeVasher *et al.* 2004) or neat water (Bumagin *et al.* 1989). Noticeably, many Heck coupling reactions, especially those involving complex nitrogen heterocycles which do not occur in anhydrous solutions give satisfactory yields in aqueous organic solvents in the presence of phase-transfer reagents (Zhang & Daves 1993).

Although the Heck cross-coupling reaction was discovered in the late 1960s, it was not until the 1980s, when the asymmetric Heck chemistry was developed, that its potential application in organic synthesis was realized and further investigated. Nowadays, the Heck coupling reaction is one of the most straightforward methods to synthesize substituted olefins which are tremendously useful in both industrial and basic research areas such as the production of fine chemicals (de Vries 2001), pharmaceuticals (Larsen 1999; Pastre & Correia 2006) and especially in the total synthesis of natural compounds (Nicolaou 2005).

In molecular biology, the Heck reaction has been used for the stereospecific synthesis of C-nucleosides used in gene therapy (Wellington & Benner 2006; Štambaský *et al.* 2009). The Heck reaction was first applied in the synthesis of modified nucleosides by Bergstrom and Ogawa (Bergstrom & Ogawa 1978) basing on the organomercury nucleoside chemistry. Later, the reaction was modified for halopyrimidine nucleosides and extensively applied for the synthesis of C-5 modified uridine analogs (Dey & Sheppard 2001). C-5 modified pyrimidine nucleosides have been used in the production of antiviral agents (Whale *et al.* 1991). Particularly, C-5 modified pyrimidine nucleoside triphosphates have been extensively applied in the enzymatic synthesis of modified DNAs for *in vitro* selections (Sakthivel & Barbas 1998), photo- and fluorescent labeling (Kolpashchikov *et al.* 2000; Giller *et al.* 2003) and in the studies of PCR reactions (Kuwahara *et al.* 2006). Recently, the Heck reactions of 2- and 6-halopurines with alkenes bearing electron-withdrawing substituents have been reported (Tobman & Dvořák 2008). In a novel strategy, Pd-catalyzed direct C-H arylation with aryl halides allows a straightforward single-step for the introduction of diverse aryl groups into the C-8 position of purine nucleosides (Čerňa *et al.* 2007).

2.4 Labeling methods for oligonucleotides

Modified oligonucleotides containing reporter groups have been extensively applied as probes for biochemical and biophysical structure-function analyses. With the progresses in the chemical synthesis of RNA over the last two decades, modified nucleosides can now be readily site-specifically incorporated into RNA at specific positions. It is important to notice that the modifications should not interfere with the hybridization of the single-stranded RNAs or destabilize the overall structure.

Reporter groups can be introduced either during or after the synthesis of the oligonucleotides. In the first approach, a modified phosphoramidite building block carrying reporter groups is

incorporated into the RNA during its chemical synthesis. On the contrary, in the post-synthetic labeling approach, reporter groups are attached to the oligonucleotide after its synthesis via linkers specifically designed for the purpose.

From a synthetic point of view, the incorporation of reporter groups during the synthesis of an oligonucleotide allows the highest control over the number and position of the modifications. Side-reactions are minimized because all nucleotides are still protected. Additionally, work-up and purification of the modified oligonucleotides are facilitated by the solid-support based synthesis. In most cases, however, the preparation of reporter-modified phosphoramidites requires costly and multiple-step synthetic routes. Moreover, the reporter group must be stable under the conditions used in the chemical synthesis as well as deprotection. This will restrict the choice of modifications.

The post-synthetic introduction of the reporter groups circumvents possible stability problems of the modification. This is also an efficient strategy when the aim is to create a library of modified oligonucleotides without having to synthesize the corresponding library of reporter-modified phosphoramidites. Once modified oligonucleotides with designed ports have been synthesized, they can be conveniently labeled with a large number of reporter groups (Dey & Shepard 2001; Erdwards & Sigurdsson 2005; Gramlich *et al.* 2008). In another approach, modifications have been introduced "on-column" during the chain assembly of oligonucleotides via halogenated nucleotides (Khan & Grinstaff 1999; Schieman *et al.* 2007).

Basing on the chemical synthesis of RNA, reporter groups can be post-synthetically attached to RNA at terminal or internal positions (Quin & Pyle 1999). For example, amino linkers can be introduced into the 5'-end via a special phosphoramidite (Figure 20a) or into the 3'-end via a specifically functionalized CPG support (Figure 20b).

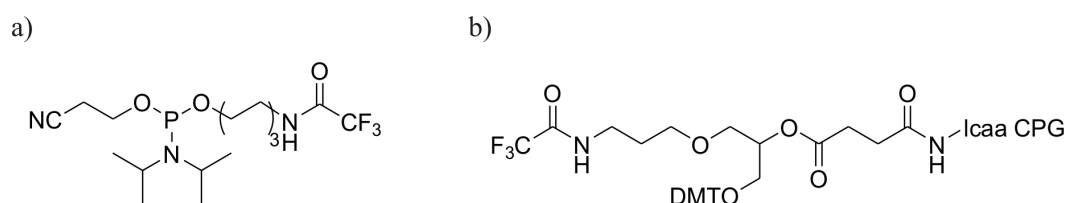


Figure 20 – Amino linkers for post-synthetic 3'- and 5'-end labeling: a) C6-Amino linker phosphoramidite for 5'-end labeling (ChemGens), b) C6-Amino linker CPG for 3'-end labeling (ChemGenes).

The selective periodate-mediated oxidation of the RNA 3'-terminal ribose *cis*-diol gives another possibility for 3'-labeling (Proudnikov & Mirzabekov 1996). The oxidation reaction results in a dialdehyde which can readily react with an alkyldiamine under reductive conditions to yield a primary aliphatic amine. The resulting primary amino function can then be further derivatized with desired labels which are functionalized with amine-reactive groups such as the isothiocyanate group (Figure 21, 2a). Alternatively, labels bearing amino components such as hydrazine derivatives can be introduced into the 3'-end by the direct reaction

with the dialdehyde under reductive conditions (Figure 21, 2b).

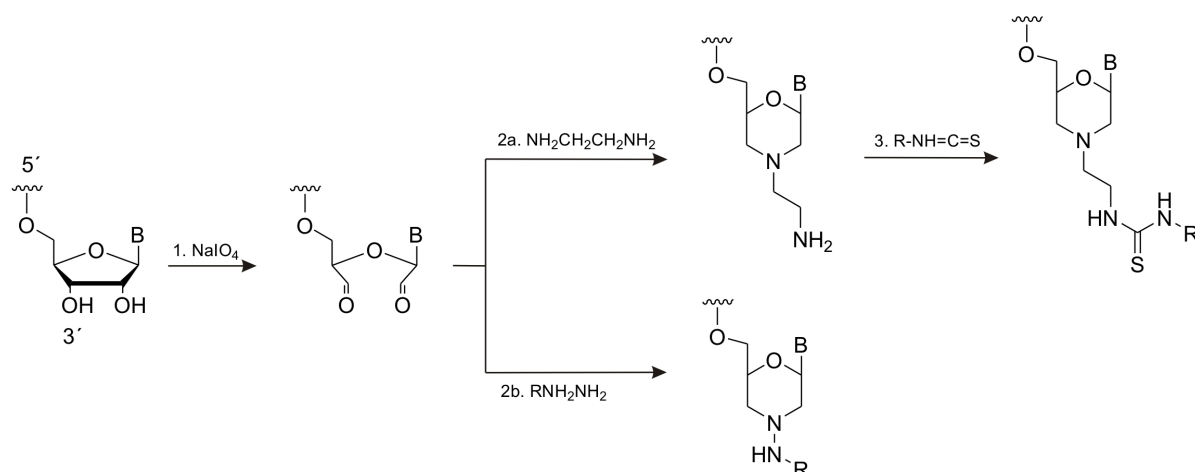


Figure 21 – Post-synthetic 3'-label chemistry based on the selective periodate-mediated oxidation: 1. Oxidation of the ribose 2',3'-diol with sodium periodate results in a dialdehyde; 2a. Reaction of the dialdehyde with an alkyldiamine under reductive conditions to give a primary amine; 2b. Reaction of the dialdehyde with a hydrazine derivative; 3. Reaction of the primary amine with a isothiocyanate derivative. R: reporter group, B: base.

For internal labeling, 2'-amino or 2'-O-(2-aminoethyl) uridine phosphoramidite (Figure 22a) (Smalley & Silverman 2006) and a modified uridine phosphoramidite carrying a C6 amino linker at the C-5 position (Figure 22b) can be used. The primary amino groups are protected by the trifluoroacetyl (TFA) group which can be cleaved off under basic conditions. Amino linkers can be introduced into the C-5 position of the pyrimidine (Cruickshank & Stockwell 1988; Dey & Sheppard 2001) or the C-2 and C-8 positions of purine nucleosides (Saito *et al.* 2005; Matsuda *et al.* 1992) basing on the Heck or Sonogashira cross coupling reaction.

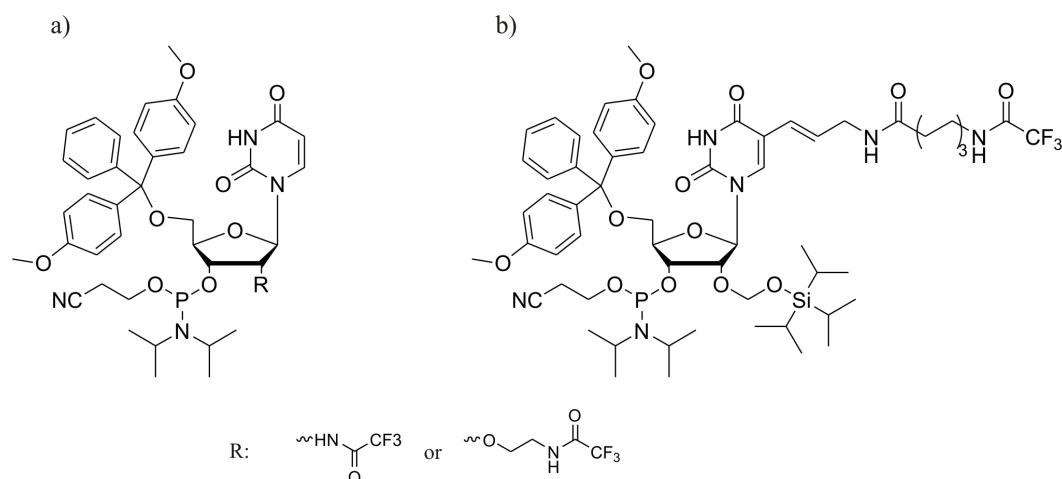


Figure 22 – Phosphoramidite building blocks for internal labeling: a) 2'-Amino or 2'-O-(2-aminoethyl) uridine phosphoramidite (ChemGenes); b) C-5 modified uridine phosphoramidite with C6 amino linker.

Among the functionalized linkers that can be attached to oligonucleotides, amino linkers are the most commonly used as their length and rigidity can be customarily designed. Moreover, the primary aliphatic amine of the linkers is much more reactive, i.e. more nucleophilic than

the aromatic amines of the nucleobases and the hydroxyl groups of the sugars, making the post-synthetic labeling method highly selective. Thus, different kinds of reporter groups containing amine-reactive functions can be coupled to amino modified oligonucleotides. There are three commonly applied types of labeling reagents functionalized with amine-reactive groups: a) active esters including succinimidyl esters (SE), tetrafluorophenyl esters (TFP) and sulphodichlorophenyl esters (SDP), b) sulfonyl chlorides and c) isothiocyanates (ITC) (Figure 23). These amine-reactive labeling reagents are nowadays commercially available.

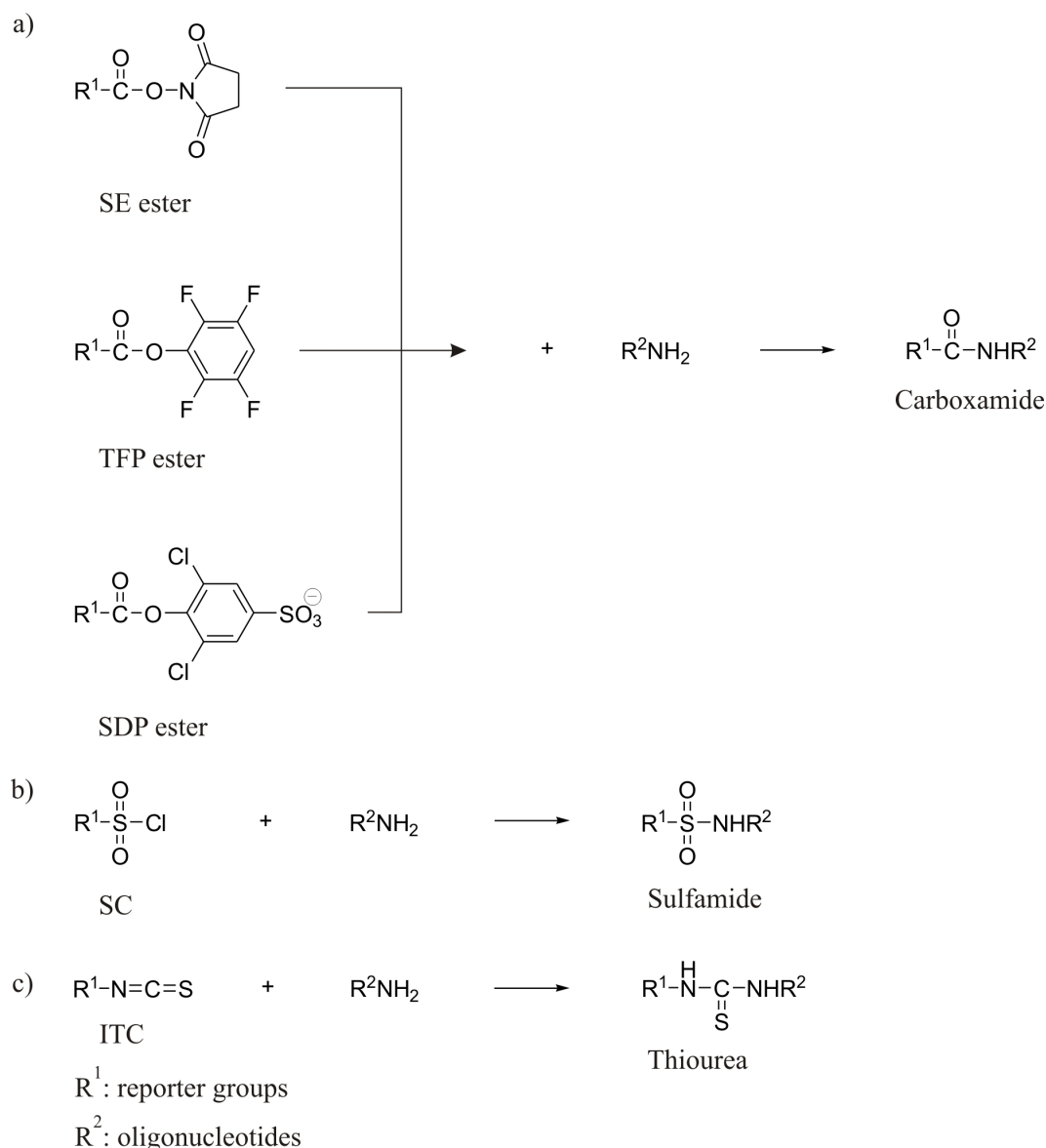


Figure 23 – Reactions of primary amines with amino-reactive reporter groups.

Of the three major classes, active esters are preferred for conjugation as they form with primary amines the stable carboxamide bond. Isothiocyanates also react with amino groups to produce thioureas which are in general less stable and deteriorate over time. Sulfonyl chlorides belong to another group of amine-reactive compounds forming very stable sulfoamides, yet are more difficult to work with. Of the three active esters, SDP esters are significantly less susceptible

to hydrolysis. Therefore, SDP ester based labeling reagents can provide greater control and tolerate longer reaction times in aqueous reaction solutions required for sufficient solubility of oligonucleotides.

Since the amino function must stay nonprotonated to be reactive, pHs of the reaction solutions have to be adjusted sufficiently high. With all active esters, unavoidable hydrolysis takes place and competes with the desired labeling reaction. Therefore, the solution has to be carefully buffered. It is also important to avoid buffers that contain primary amines like Tris, as they will compete for conjugation with the amine-reactive labeling reagents. Generally, reactive dyes are hydrophobic and should be dissolved in amine-free aprotic solvents such as DMF, DMSO or MeCN just before each labeling reaction.

The combination of amino linkers with orthogonal ports such as those based on the Click chemistry (Gramlich *et al.* 2008) allows the selective labeling of the oligonucleotides with different reporter groups. The amino function can also be replaced by a thiol group via an "adapter" which offers the possibility to couple the oligonucleotide with labels containing thiol-reactive groups (Li *et al.* 1987; Cohen & Cech 1997).

2.5 Methods for RNA structural elucidation

In order to understand the relationship between structure and function of RNAs as well as to improve the functions which they inherently have, different biophysical techniques for RNA structural elucidation have been developed.

Structures of small and large RNAs have recently been elucidated by high-resolution X-ray crystallography (Serganov *et al.* 2009). Determination of 3D RNA structures requires derivatization of the RNA with heavy atom by soaking crystals in salt solutions or by chemical modification of nucleosides with halogen or selenium atoms (Mooers 2009). The incorporation of 2'-methylseleno (Puffer *et al.* 2008) and 4'-selenium (Watts *et al.* 2008) modified phosphoramidites into RNA by solid-phase synthesis has been reported.

NMR spectroscopy has proven to be a powerful tool for determining structures of small RNAs (Martadinata & Phan 2009). Recent developments to directly detect hydrogen-bonding interactions in combination with time-resolved techniques have been used to identify secondary structures and to study mechanisms of ligand-binding events in RNA (Latham *et al.* 2009; Puffer *et al.* 2009). RNA dynamics in solution as well as long-range structural interactions and orientations of helical domains can be investigated by NMR relaxation and residual dipolar coupling techniques (Zhang *et al.* 2007). For these experiments, RNA labeled with stable isotopes such as ^{13}C , ^{15}N and especially ^{19}F have been used to suppress the effects of signal degeneracy (Lu *et al.* 2009). ^{13}C - (Wenter *et al.* 2006), ^{15}N - (Wenter *et al.* 2006) and ^{19}F -modified RNAs (Kreutz *et al.* 2005) have been prepared by solid-phase synthesis.

EPR spectroscopy can provide information on local and global dynamic properties as well as metal binding sites of RNA. This technique can precisely determine distances up to 80 Å, can be applied for biomolecules in buffer solutions or membranes and is not size-limited (Zhang *et al.* 2009; Sowa & Quin 2008). Geometry of the binding sites of RNA have been elucidated by ENDOR, an advanced EPR method (DeRose 2003). Long-range structural restraints have been obtained by measuring the distance between two spin-labels by PELDOR, a pulsed EPR technique (Schiemann & Prisner 2007). Halogenated nucleosides have been derivatized with spin-labels basing on Pd-catalyzed Sonogashira coupling reactions and incorporated into RNA by solid-phase synthesis (Piton *et al.* 2007).

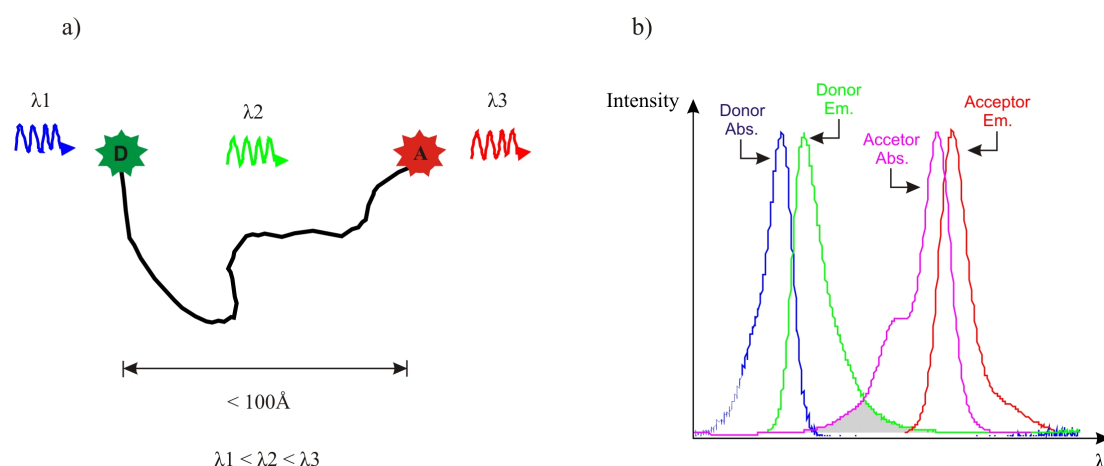


Figure 24 – The principles of FRET spectroscopy: a) The donor, in an electronically excited state, transfers its excitation energy to a neighbor molecule, the acceptor by non-radiative dipole-dipole interaction. The distance between the donor the acceptor groups ranges within the distance of up to 100 Å; b) The donor molecule emits at shorter wavelength which overlaps with the absorption spectrum of the acceptor.

Besides the above mentioned techniques, fluorescence spectroscopy is also an effective biophysical method for monitoring global structure and conformational dynamics of RNA. The applications of fluorescently labeled RNA range from measurement of fluorescence emission quenching, fluorescence anisotropy, fluorescence lifetime to fluorescence resonance energy transfer (FRET). FRET is a process by which a molecule in an electronically excited state (donor) transfers its excitation energy to another molecule (acceptor) by nonradiative dipole-dipole interaction, provided that the pair fulfills the following conditions: i) The energy donor must be luminescent; ii) the emission spectrum of the donor must have some overlap with the absorption spectrum of the acceptor and iii) the distance between the donor and acceptor must be within the range of up to 100 Å (Figure 24) (Förster 1948), typically 30-80 Å for most fluorophore-pairs (Karunatilaka & Rueda 2009). FRET signals are sensitive to the changes of the donor-acceptor distance. Therefore, FRET spectroscopy can serve as a quantitative tool to explore structures and dynamics in biological systems.

Recently, time-resolved (Zhao & Xia 2009) and advanced single-molecule FRET (smFRET) (Hengesbach *et al.* 2008) have been developed to be a powerful tool for probing global con-

formations of RNA. smFRET offers an insight into subpopulations of a system and has the capacity to identify conformational heterogeneity or the presence of intermediates that would otherwise be hidden in ensemble-averaged populations. smFRET experiments have been extensively applied in studies of complex folding mechanisms of functional RNAs (Karunatilaka & Rueda 2009; Alemán *et al.* 2008), protein-mediated assembly of telomerase RNP complex (Stone *et al.* 2007), folding path-way of a self-splicing ribozyme (Steiner *et al.* 2008) and dynamic equilibria of RNA conformations in a protein-free U2-U6 snRNA model complex (Guo *et al.* 2009). These fluorescence-based assays always depend on the modification of RNA with fluorescent labels.

2.6 MALDI-TOF mass spectrometry of oligonucleotides

MALDI (Matrix Assisted Laser Desorption/Ionization) is a soft ionization technique which allows sensitive detection of large, non-volatile and labile molecules by mass spectrometry. The ionization is supported by matrix molecules which typically are small aromatic acids having high molar absorptivities at the radiation wavelength. The sample is co-crystallized with an excess amount of a suitable matrix. UV radiation leads to the photoionization of the matrix via proton transfer processes and subsequently to the ionization of the molecules to be measured. The excitation energy in UV radiation is stored in the π -electron system of the aromatic matrix molecules and relaxes in extremely short time periods into the solid-state lattices. Under high vacuum, this process results in an explosively vaporization of the solid-state surface during which matrix and sample molecules are released into the gas phase (desorption) with minimal thermal fragmentation. The released ions are accelerated towards the detector by an electrostatic field. The masses of the ions are calculated based on the time periods from the point they are accelerated to their arrival on the detector (Time-Of-Flight, TOF). Integrating a reflector into the system help to compensate energy distributions, leading to higher resolution. When measuring a sample with molecular weight M in negative-ion mode, $[M-zH]^{z-}$ (typically, $z = 1; 2$) or dimer $[2M-H]^-$ ion can be detected. Thus, m/z peaks corresponding to the masses of $(M-z)/z$ or $2M$ can be observed.

Nowadays, MALDI-TOF-MS has become a powerful tool for the analysis of oligonucleotides due to its high accuracy, sensitivity, speed and simplicity. Normally, singly charged molecule ions of oligonucleotides are observed, facilitating the interpretation of MALDI-MS spectra. MALDI-MS analyses of oligonucleotides are often performed in negative-ion mode due to its higher sensitivity, higher resolution and lower fragmentation compared to positive mode (Stemmler *et al.* 1995). The most important problem in molecular weight measurement of oligonucleotides is the presence of salt adducts. They shift the signals to higher m/z values and complicate the determination of the molecular weight. Therefore, both of the sample and the

matrix solutions must be treated with cation-exchange beads before the measurement (Roskey *et al.* 1996).

A number of matrices have been tested but only some are suitable for MALDI-MS analyses of oligonucleotides (Figure 25). Among them, 3-hydroxypicolinic acid (3-HPA) showed significant improvement in terms of mass range available and signal-to-noise ratio (Wu *et al.* 1993). Nevertheless, trials are required in order to find out a suitable matrix or a mixture of matrices for individual oligonucleotide samples (Chou & Limbach 2000).

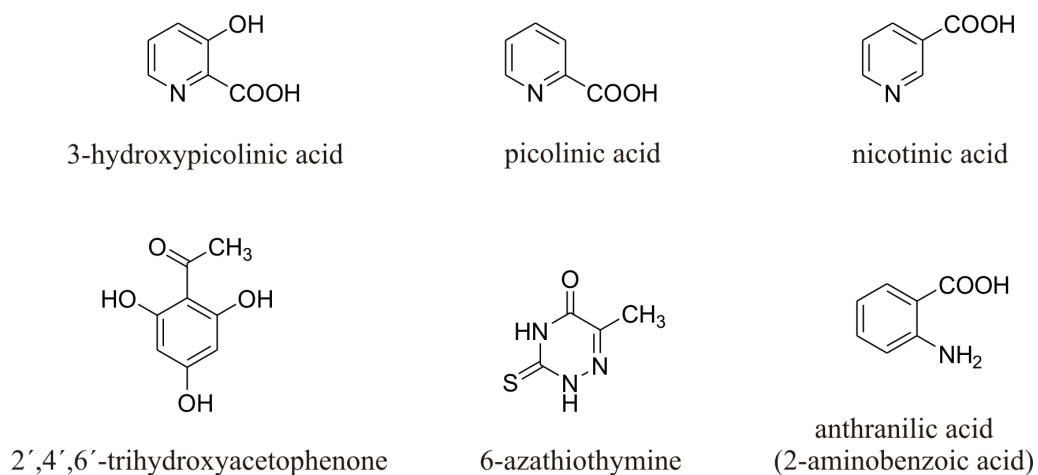


Figure 25 – Structures of matrices commonly used for MALDI-MS analysis of oligonucleotides.

3 Results and discussion

3.1 Synthesis of modified uridine, adenosine and guanosine building blocks by the Sonogashira coupling reaction

For FRET experiments, fluorescently labeled RNAs have been chemically synthesized. Linker length and flexibility are critical parameters for optimal performance. Short and rigid triple-bond linkers are advantageous for accurate distance measurements and allow the assessment of the molecular motion independently of the motion of the labels. They have been introduced into the C-5 position of uridine, C-2 and C-8 positions of adenosine and C-8 position of guanosine by the Sonogashira coupling reactions of the corresponding halogenated nucleosides.

3.1.1 Retrosynthesis of the modified building blocks by the Sonogashira coupling reaction

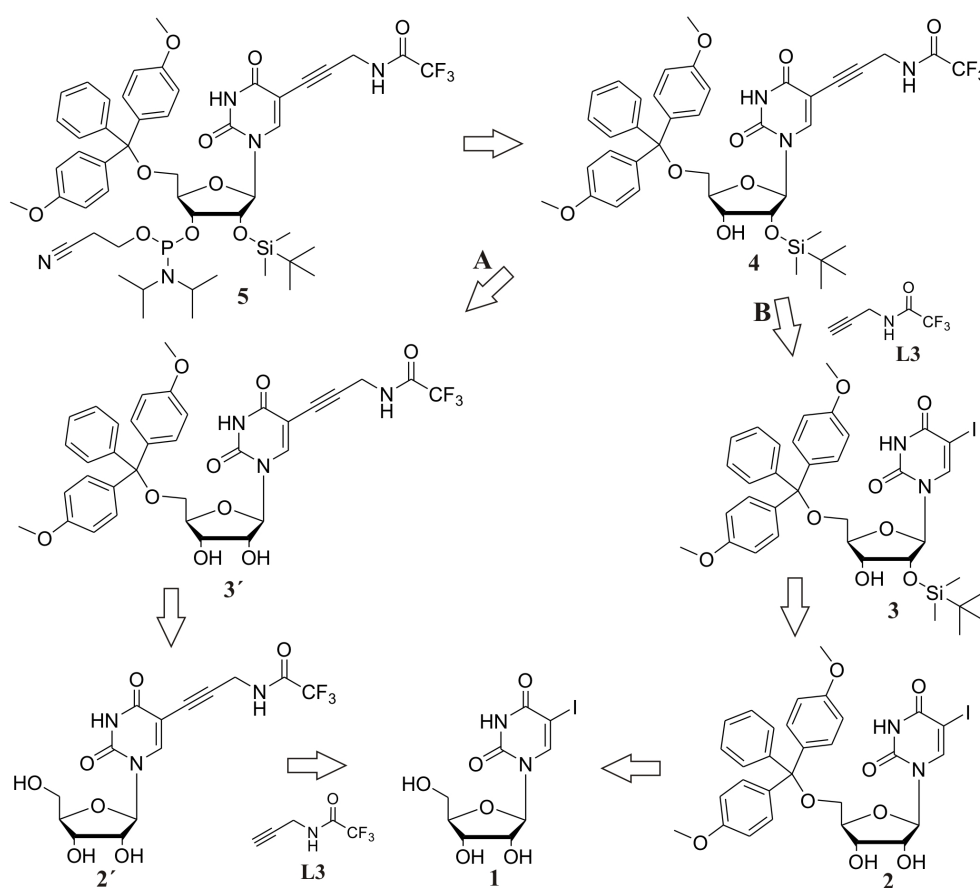


Figure 26 – Retrosynthesis of the modified uridine building block by the Sonogashira cross-coupling reaction.

The modified uridine phosphoramidite building block **5** can be synthesized by the 3'-*O*-phosphitylation of the protected 5-amino linker (**L3**) modified uridine **4**. **4** can be synthesized by the tritylation and silylation of the 5-L3 modified uridine **2'** (path A, Figure 26) or by the Sonogashira coupling reaction of the linker **L3** with the 5'-*O*-DMT-2'-*O*-TBDMS uridine **3** (path B). Both synthesis routes can start from 5-iodouridine **1**.

Similarly, the 8-L3 modified adenosine building block can be synthesized by the tritylation and silylation of the 8-L3 Sonogashira cross-coupled adenosine **20** or **21a** (Figure 27). The amino protecting group can be introduced before (path A) or after (path B) the Sonogashira coupling reaction of 8-bromoadenosine **19** and **L3**. 2-L3 modified adenosine building blocks can be prepared by the same synthetic route starting from 2-iodoadenosine **27**.

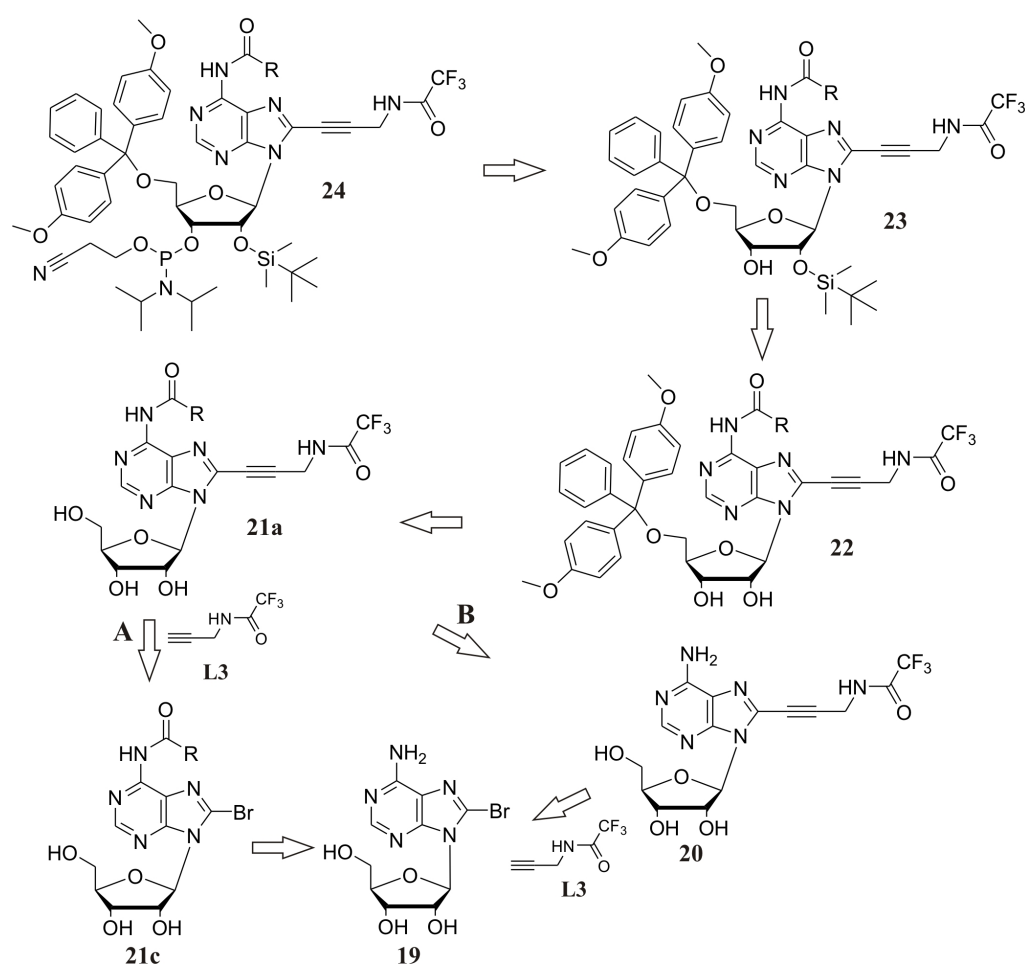


Figure 27 – Retrosynthesis of adenosine building blocks by the Sonogashira coupling reaction. R: $\text{CH}(\text{CH}_3)_2$ or $\text{CH}_2\text{OC}_6\text{H}_5$.

3.1.2 Synthesis of *N*-propargyltrifluoroacetamide **L3**

For the Sonogashira coupling reaction, the triple-bond amino linker **L3** was synthesized from propargylamine and ethyl trifluoroacetate (Figure 28). The amino function of the linker must be protected before the building block can be introduced into the oligonucleotides during the

solid-phase synthesis, as it is a nucleophile and can disturb the activation of the phosphoramidites by BMT or be coupled with the activated phosphoramidites, causing unwanted side-reactions and reducing the coupling efficiencies.

The *tert*-butyloxycarbonyl (*t*Boc) (Haralambidis *et al.* 1987) or trifluoroacetyl (TFA) (Cruickshank & Stockwell 1988) protecting group can be used to protect the propargylic amine. The *t*Boc group requires a post-synthetic treatment of the oligonucleotide with ethanedithiol - trifluoroacetic acid to be completely removed, while trifluoroacetyl can be cleaved off by the ammonia treatment under the same deprotection conditions used for the oligonucleotide. The trifluoroacetyl protecting group is also stable under the Sonogashira coupling reaction (Section 3.1.3) as well as the conditions in the chemical synthesis of RNA.

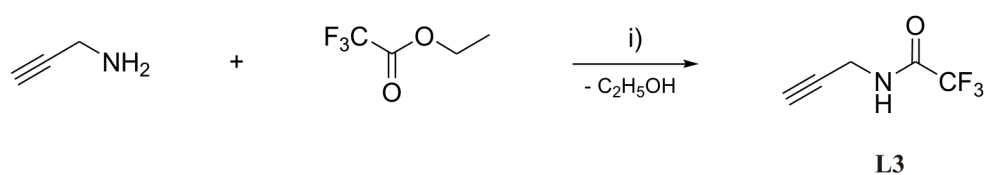


Figure 28 – Synthesis of *N*-propargyltrifluoroacetamide **L3**: i) propargylamine, 1.3 eq. ethyl trifluoroacetate, dry MeOH, RT, overnight, 65%.

Primary amines are most commonly converted to their corresponding trifluoroacetyl derivatives by treatment with fluoroacetic anhydride in the presence of a tertiary amine or with the ethyl ester of the corresponding acid. Ethyl trifluoroacetate was chosen, as it was more easily available, easier to handle and allowed the acylation reaction to proceed under mild conditions. The ester was used in a slight excess in order to completely consume propargylamine and to facilitate the purification of the product. In fact, both the starting material, ethyl trifluoroacetate, and the by-product, ethanol, can be readily evaporated under vacuum. Thus, 1.3 eq. ethyl trifluoroacetate were added dropwise to the ice-cold solution of propargylamine in dry methanol. The reaction was stirred overnight at room temperature. The linker **L3** was separated from the reaction mixture in 65% yield by distillation under vacuum to give a colorless liquid which solidified when stored at -20 °C. Structural analysis of **L3** by NMR indicated that the separated compound had the desired structure.

3.1.3 Synthesis of 5'-*O*-(4,4'-dimethoxytrityl)-2'-*O*-*tert*-butyldimethylsilyl-5-(3-trifluoroacetamidoprop-1-ynyl)uridine

It has been reported that the Sonogashira coupling reaction of a halogen nucleoside derivative in which methanol was present in equimolar concentration to the nucleoside substrate could successfully be carried out (Cruickshank & Stockwell 1988). Therefore, the protection of the hydroxyl groups of the nucleoside in the Sonogashira coupling reaction is not essential. In addition, the DMT and TBDMS protecting groups are stable under the Sonogashira coupling

condition (slightly basic, room temperature for several hours). Due to these reasons, the linker can be introduced into the C-5 position of the pyrimidine ring either before or after the protection of the hydroxyl groups (path A and B, Figure 26).

The second synthetic route was chosen, as the DMT and TBDMS protecting groups could tolerate the Sonogashira coupling condition. Moreover, it is easier to work up and chromatography the protected nucleoside, as it becomes more hydrophobic and is better soluble in organic solvents. Therefore, the synthesis of the building block **4** from 5-iodoadenosine **1** based on the Sonogashira coupling reaction can be planned as shown in Figure 29.

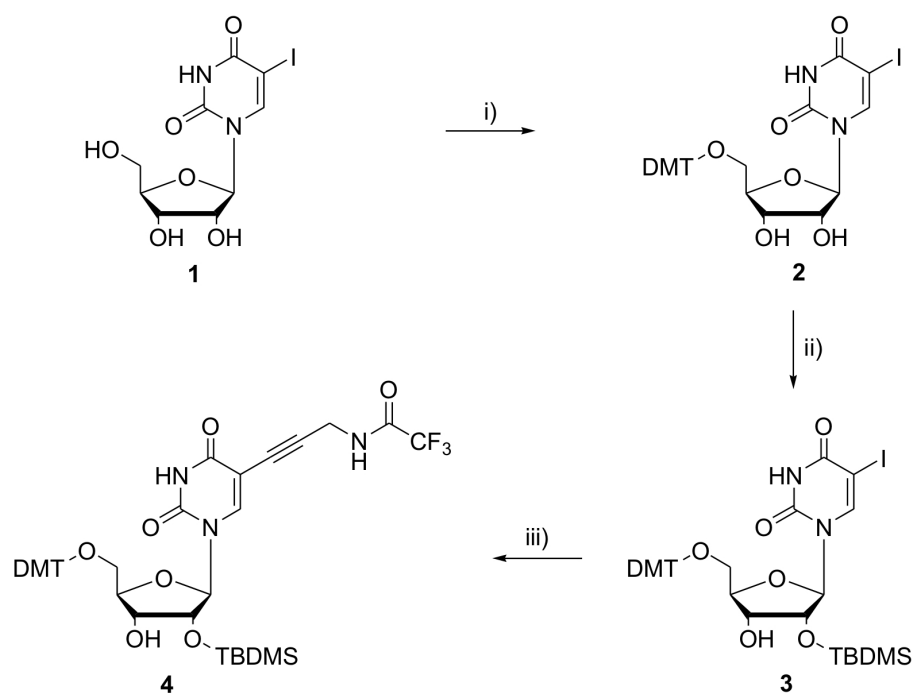


Figure 29 – Synthesis of 5'-O-(4,4'-dimethoxytrityl)-2'-O-*tert*-butyldimethylsilyl-5-(3-trifluoroacetamidoprop-1-ynyl)uridine **4**: i) **1**, 1.2 eq. DMT-Cl, pyridine, RT, overnight, 59%; ii) **2**, 1.3 eq. TBDMS-Cl, 1.2 eq. AgNO₃, 5.0 eq. pyridine, THF, RT, 2.5 h, 71%; iii) **3**, 3.0 eq. *N*-propargyltrifluoroacetamide **L3**, 0.1 eq. Pd(PPh₃)₄, 0.2 eq. CuI, 4.3 eq. Et₃N, DMF, RT, 8 h, 69%.

Depending on the substrates, the ratio of palladium(0) to copper(I) is decisive to the success of the coupling reaction. An unsuitable scale of the catalyst and the co-catalyst can lead to no transformation or to the formation of by-products and the black palladium precipitate. When the alkynylamine was unprotected, the coupling reactions with a 2:1 ratio of copper to palladium were rather slow (Hobbs 1989). In these cases, a 5:1 ratio worked better. It was speculated that the coupling reactions were supported when copper(I) removed two triphenylphosphine ligands from Pd(PPh₃)₄. Therefore, when a large excess of unprotected alkynylamine linker was present, a higher amount of copper(I) was required due to the competition between the phosphine ligand and the free amino group of the linker. Pd(PPh₃)₂Cl₂ has also been used in the Sonogashira coupling reaction of 5-iodouridine derivatives (Robins & Barr 1981), but in some cases, the coupling reaction could succeed only when Pd(PPh₃)₄ was applied (Hobbs

1989). When $\text{Pd}(\text{PPh}_3)_2\text{Cl}_2$ salt is used as the palladium(0) source, only two strong transition-metal ligands are introduced with each palladium, while four strong ligands are introduced with each palladium in case of $\text{Pd}(\text{PPh}_3)_4$. The ligand stoichiometry, rather than the initial palladium oxidation state, probably accounts for the difference in catalytic activity between these two systems (Hobbs 1989). Regarding these facts, we have chosen the 2:1 ratio of $\text{Pd}(\text{PPh}_3)_4$ to CuI for the Sonogashira coupling reaction between the TFA-protected propargylamine **L3** and the protected 5-iodouridine **3**.

The Sonogashira cross-coupling reaction of the linker **L3** and **3** was implemented following the $\text{Pd}(\text{PPh}_3)_4$ -assisted procedures described in the literature (Ahmadian *et al.* 2000; Ruparel *et al.* 2005). The tritylation and silylation steps will be described in more detail in Sections 3.5 and 3.6, respectively. For the Sonogashira coupling reaction with **L3**, a solution of the protected 5-iodouridine **3** in dry DMF was degased and saturated with argon by exchanging several times between vacuum and the introduction of argon. To the degased solution, 0.1 eq. $\text{Pd}(\text{PPh}_3)_4$ and 0.2 eq. co-catalyst CuI were added. Although the dry reagents can be handled in the open air, they become more sensitive to oxygen when in solution. Side-reactions may occur if the dissolved oxygen in the reaction mixture is not completely eliminated at this point (Glaser 1869). In this coupling reaction, the polar aprotic DMF was preferred over other organic solvents, as it allows the homogenization of all the components of the coupling reaction. More importantly, it can suppress the secondary cyclization reactions (Robins *et al.* 1990) to form pyrrolo-C derivatives (Figure 30) first reported by Robins and Barr (Robins & Barr 1981; Berry *et al.* 2004).

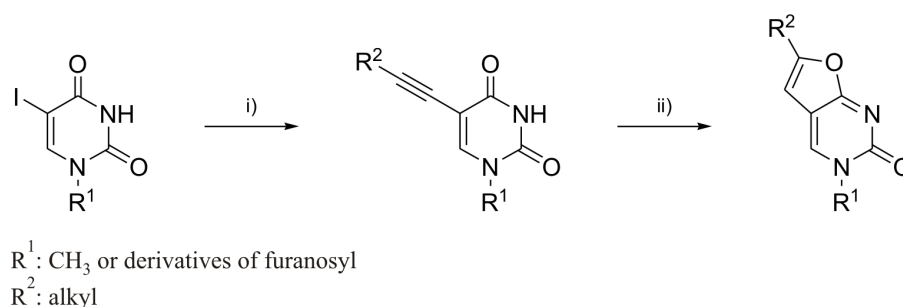


Figure 30 – Cyclization of 5-alkynyl uracine derivatives: i) $\text{R}^2\text{C}\equiv\text{CH}$, $(\text{Ph}_3\text{P})_2\text{PdCl}_2$, CuI , Et_3N ; ii) Et_3N , CuI , MeOH , reflux.

After the addition of the catalysts, the resulting solution was yellowish and became brownish yellow after several hours, but remained homogeneous without the formation of the precipitated black palladium element. This indicated that the catalyst was well recycled during the coupling reaction without loss of the catalytic activity. After about 8 hours at room temperature, TLC showed that almost all of the starting material was consumed with no detectable degradation of the DMT and TBDMS protecting groups. In order to remove traces of copper(I), the reaction mixture was treated with a dilute solution of EDTA until the aqueous phase was colorless. The organic phase was concentrated and purified by silica gel column chro-

matography with a gradient of ethyl acetate in hexane. Only one main cross-coupled product was obtained in relatively good yield (69%). ^1H and ^{13}C NMR analyses confirmed the structure of the cross-coupled product **4**. The ^1H and ^{13}C NMR spectra of the product are nearly the same as those of the compound **3**, except that the product's proton NMR spectrum contains new signals of the newly introduced linker arm (see Section 5.4). In addition, the signal of Csp²-I of **3** undergoes a significant downfield shift, from 70.23 ppm to 98.08 ppm due to the replacement of iodine by the triple-bond linker. Furthermore, no side-products were generated by cyclization of the triple-bond moiety of the linker and O-4 of the pyrimidine heterocycle as has been reported (Robins & Barr 1981).

3.1.4 Synthesis of 8-(3-trifluoroacetamidoprop-1-ynyl)adenosine

The introduction of the triple-bond linker *N*-propargyltrifluoroacetamide **L3** into the C-8 position of adenosine by the Sonogashira coupling reaction of the commercially available 8-bromoadenosine **19** is outlined in Figure 31.

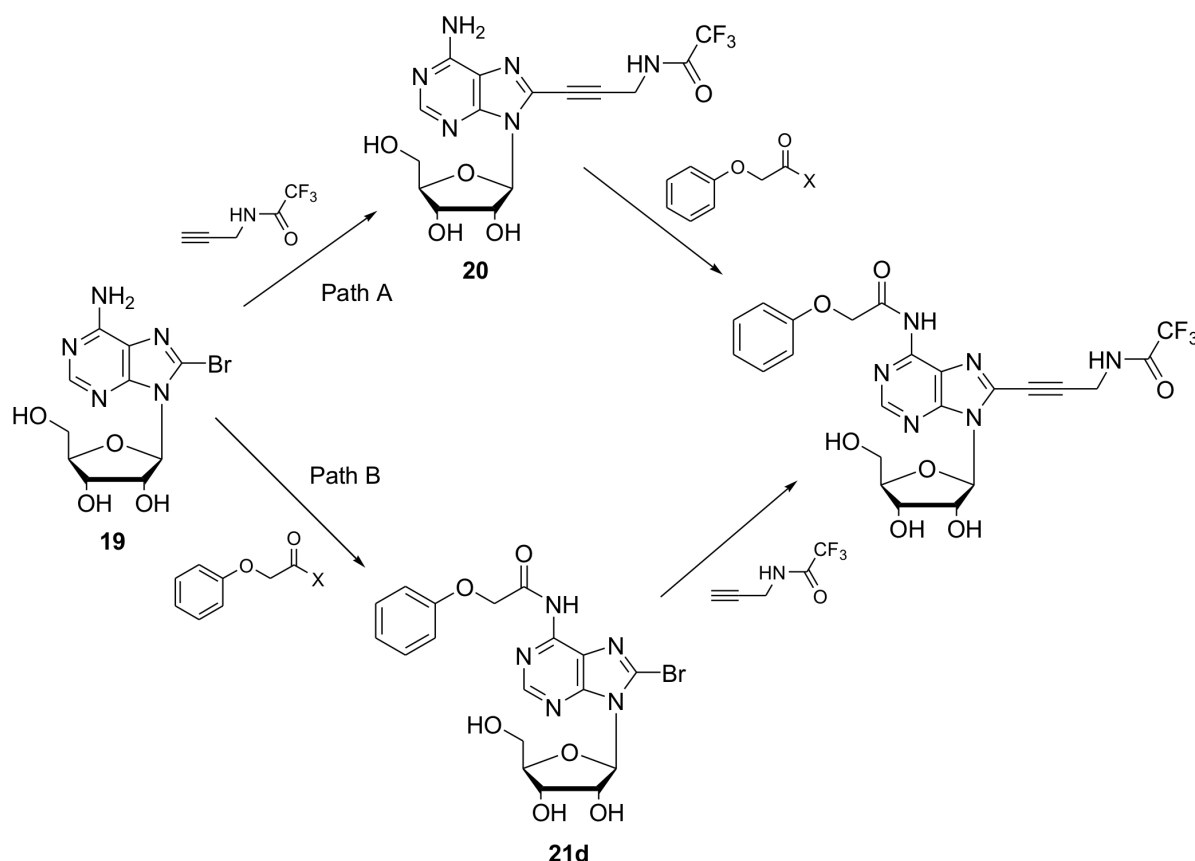


Figure 31 – Two strategies to introduce the amino linker **L3** into the C-8 position of adenosine by the Sonogashira coupling reaction.

It has been reported that bromo substrates are less active than the corresponding iodo analogues in the Sonogashira coupling reaction. Therefore, their coupling reactions normally require elevated temperatures. Under these conditions, the DMT and TBDMS protecting groups can be

cleaved off, because they are thermally unstable. Originally, the phenoxyacetyl group (PAC) was chosen to protect the exo-cyclic amino function of adenosine, as this protecting group could be readily removed under mild basic conditions after the chemical synthesis of RNA. This group should then be introduced into the amino group after the linker has been coupled to the C-8 position of adenosine, as it may not be able to tolerate the Sonogashira coupling reaction at elevated temperatures. Thus, the first strategy was the Sonogashira coupling reaction of the unprotected 8-bromoadenosine **19** with the linker **L3** and then phenoxyacetylation of its amino function (path A, Figure 31).

In many procedures reported for the Sonogashira coupling reactions of 8-bromoadenosine and its derivatives with different kinds of linkers, the catalyst $\text{Pd}(\text{PPh}_3)_2\text{Cl}_2$ and the co-catalyst copper(I) iodide were used in the presence of triethylamine as base (Volpini *et al.* 2001; Flasche *et al.* 2004; Firth *et al.* 2006), except that described by Saito and co-workers (Saito *et al.* 2005). In this procedure, $\text{Pd}(\text{PPh}_3)_2\text{Cl}_2$ was replaced by $\text{Pd}(\text{PPh}_3)_4$. In the experiments using $\text{Ph}(\text{PPh}_3)_2\text{Cl}_2$, the catalyst has been shown to be able to effect the transformation of 8-bromodeoxyadenosine and its analogues. Therefore, different reaction conditions for the Sonogashira coupling reaction between 8-bromoadenosine **19** and the linker **L3** have been investigated following the $(\text{PPh}_3)_2\text{PdCl}_2$ -based protocols (Table 1).

Table 1 – Sonogashira coupling reactions of 8-bromoadenosine and **L3** catalyzed by $\text{Pd}(\text{PPh}_3)_2\text{Cl}_2$ ^a.

Entry	L3 (eq.)	Pd(II) (eq.)	Cu(I) (eq.)	Et ₃ N (eq.)	Temp. (°C)	Time (h)	Result ^b
1	6.0	0.024	0.005	30.0	RT	overnight	No reaction
2	12.0	0.024	0.006	60.0	RT	44.0	No reaction
3	12.0	0.024	0.006	60.0	56	2.0	P/SP 1:5
					67	1.5	
4	1.1	0.02	0.08	40.0	70	1.5	P/SP 1:5

^aAll the reactions were carried out in DMF with $\text{Pd}(\text{PPh}_3)_2\text{Cl}_2$, CuI as catalysts and Et₃N as base. The amount of 8-bromoadenosine is 1.0 eq. ^bP: product, SP: side-product.

In the coupling reactions of **L3** and **19**, however, the reagents which have been reported to work effectively did not support any conversion of the substrates at room temperature (entries 1-2). At elevated temperatures, transformations were observed, but with the formation of a side-product (Figure 32A) which was impossible to be separated from the main product by silica gel column chromatography (entries 3-4). Therefore, other coupling reaction conditions were tried in order to reduce the amount of the side-product. Unfortunately, all of these attempts were unsuccessful. Under these conditions, the formation of the side-product was

not avoidable. According to reversed-phase HPLC (Figure 32A), this side-product (retention-time: 9.5 minutes) was always formed simultaneously with the main product (retention-time: 7.6 minutes) from the beginning of the reaction and became dominant when the reaction time was prolonged (entry 3) or was the only compound formed if the reaction temperature was significantly increased (entry 4). From the ^1H NMR spectrum of the side-product, its structure could not be elucidated, but it could be noticed that the proton of the amide group NHCOCF_3 of the linker was missing.

The Sonogashira coupling reaction between **19** and **L3** was investigated again, but $\text{Pd}(\text{PPh}_3)_4$ was used as catalyst instead of $\text{Pd}(\text{PPh}_3)_2\text{Cl}_2$. These conditions are based on the condition successfully applied for the Sonogashira coupling of 5-iodouridine and **L3** (Section 3.1.3). The conditions having been tried are summarized in Table 2.

Table 2 – Sonogashira coupling reactions of 8-bromoadenosine and **L3** catalyzed by $\text{Pd}(\text{PPh}_3)_4$ with Et_3N as base^a.

Entry	L3 (eq.)	$\text{Pd}(0)$ (eq.)	$\text{Cu}(I)$ (eq.)	Et_3N (eq.)	Temp. (°C)	Time (h)	Result ^b
1	3.0	0.1	0.2	4.3	RT	44.0	P/SP 1:1
2	1.5	0.1	0.2	2.1	RT	overnight	P/SP 1:1
3	2.5	0.1	0.2	2.0	40	5.0	P/SP 1:1

^aAll the reactions were carried out in DMF with $\text{Pd}(\text{PPh}_3)_4$, CuI as catalysts and Et_3N as base. The amount of 8-bromoadenosine is 1.0 eq.. ^bP: product, SP: side-product.

The replacement of $\text{Pd}(\text{PPh}_3)_2\text{Cl}_2$ by $\text{Pd}(\text{PPh}_3)_4$ allowed the Sonogashira coupling reactions of **19** and **L3** to take place under milder conditions, but the formation of the above mentioned side-product was still significant (Figure 32A).

The CF_3CO - protecting group has been known to be unstable in basic solutions and the absence of the NH proton signal in the ^1H NMR spectrum of the side-product might indicate the hydrolysis of the amide group in the presence of triethylamine at elevated temperatures. This prompted us to carry out the reaction with *N*-ethyldiisopropylamine (DIPEA) (Table 3, entry 1), a more bulky and weaker base. As can be seen in Figure 32B, after 11 hours at 40 °C, 8-(3-trifluoroacetamidoprop-1-ynyl)adenosine **20** was formed as the major compound. Almost all of the starting material was consumed and only a small amount of the side-product was observed (entry 1, Table 3). After the reaction, DMF was thoroughly removed by co-evaporating the reaction mixture with toluene. The residue was suspended in a small amount of methanol and filtered to remove the yellow precipitate which was supposed to be the palladium catalyst. The

methanol solution was absorbed on silica gel and purified by silica gel column chromatography (MeOH/DCM). The structure and purity of the separated product were confirmed by NMR analysis. The ^1H NMR spectrum of the separated product can nearly be superimposed to that of the starting material, except that it has more signals which can be assigned to the newly introduced linker (see Section 5.7).

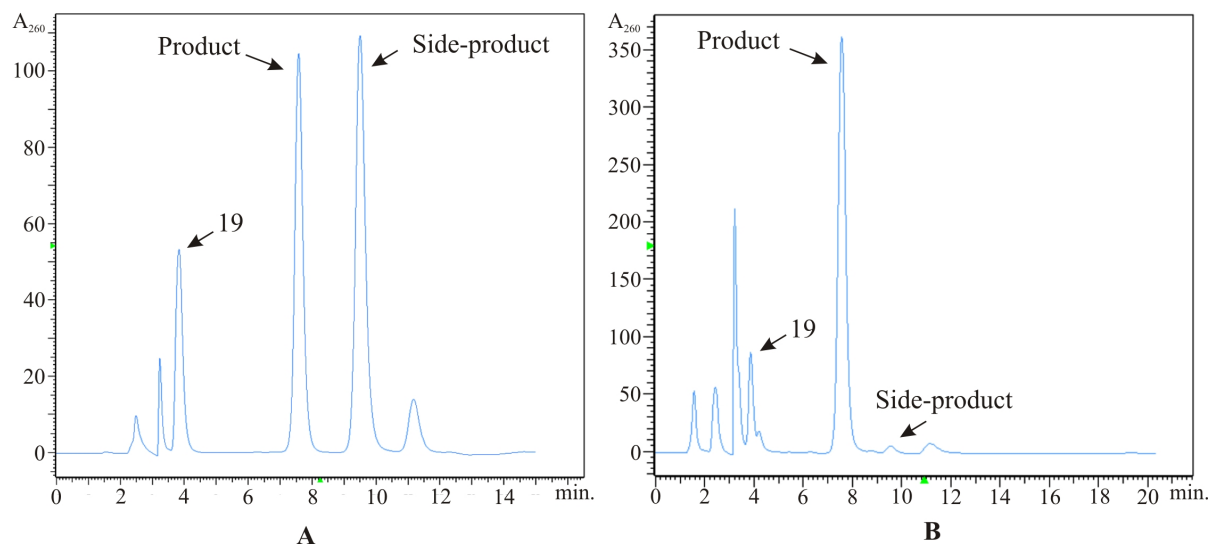


Figure 32 – Reversed-phase HPLC diagram of the Sonogashira coupling of **19** using $\text{Pd}(\text{PPh}_3)_4$ as catalyst, Et_3N (A) or DIPEA (B) as base. The identities of the product and the side-product have been elucidated by NMR analysis.

The amino function of the Sonogashira cross-coupled product **20** was then protected with the phenoxyacetyl protecting group (path A, Figure 31). Various acylation conditions have been tried with different phenoxyacetylating reagents, but no *N*-6-PAC protected product was separated (see Section 3.4). Therefore, the second approach was tested: Firstly, the amino function had been protected with the phenoxyacetyl group to give *N*-6-PAC-8-bromoadenosine **21d** (see Section 3.4) and then the linker was introduced into the C-8 position by the Sonogashira coupling reaction (path B, Figure 31) basing on the reported procedures applied for 8-bromoadenosine and derivatives (Flasche *et al.* 2004; Firth *et al.* 2006). These experiments also did not give rise to the formation of the desired product *N*-6-phenoxyacetyl-8-(3-trifluoroacetamidoprop-1-ynyl)adenosine, but led only to the cleavage of the PAC group (entry 2, Table 3).

The presence of the PAC group in the molecule of compound **21d** should actually support for the introduction of the triple-bond linker by the Sonogashira coupling reaction, since this group causes a negative induction and thus facilitating the oxidative addition of the catalyst $\text{Pd}(0)$ to the $\text{Csp}^2\text{-Br}$ bond (Figure 33a). One possible reason for the unsuccessful combination of the PAC group and **L3** is that this group is relatively bulky and therefore causes steric hindrance, disregarding if it is introduced after or before the linker **L3**. When it is introduced after **L3**, its bulkiness prevents it from accessing the amino function. Similarly, when it is attached to

the amino group before the Sonogashira coupling reaction, its steric hindrance inhibits the formation of the tetravalent complex Pd(II) from the oxidative insertion of the Pd(0) catalyst to the C-8 of adenosine (Figure 33a). If this complex is somehow generated, it would be very unstable, as its triphenylphosphine ligands, which are also bulky, may sterically interact with the PAC group (Figure 33b).

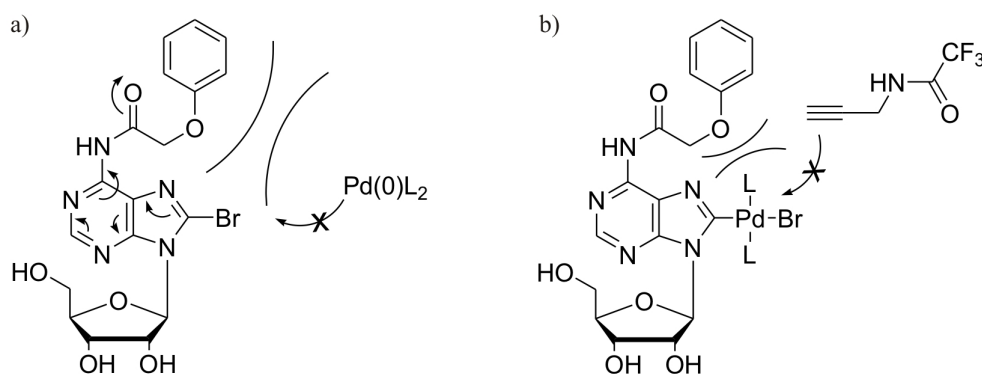


Figure 33 – Unsuccessful Sonogashira cross-coupling reaction of *N*-6-phenoxyacetyl-8-bromoadenosine and **L3** using Pd(PPh₃)₄.

To avoid this problematic steric hindrance, the isobutyryl protecting group, which is less bulky and connected to the amino function by a shorter carbon chain, was chosen. In fact, the protection of the amino function of **20** with isobutyric anhydride was successfully carried out (Section 3.4). Even the diisobutyryl protected nucleoside was easily formed. In addition, the Sonogashira coupling reaction of *N*-6-isobutyryl-8-bromoadenosine **21c** was successfully implemented, although the formation of the product was not as high as expected due to the partial degradation of the isobutyryl protecting group under the Sonogashira reaction condition (entry 3, Table 3).

Table 3 – Sonogashira coupling reactions of **19**, **21c** and **21d** and **L3** catalyzed by Pd(PPh₃)₄ with DIPEA as base^a.

Entry	ArBr ^b	L3 (eq.)	Pd(0) (eq.)	Cu(I) (eq.)	DIPEA (eq.)	Temp. (°C)	Time (h)	Result ^c
1	19	1.2	0.1	0.2	1.2	40	11.0	P: 80% SP: < 5%
2	21d	1.2	0.1	0.2	1.2	40 55	11 overnight	No coupling 21d degraded
3	21c	1.2	0.1	0.2	1.2	40	11	Low yield 21c degraded

^aAll the reactions were carried out in DMF with Pd(PPh₃)₄ and CuI as catalysts, DIPEA as base.

^bThe amounts of 8-bromoadenosine **19**, *N*-6-phenoxyacetyl **21d** and *N*-6-isobutyryl **21c** derivatives (ArBr) were 1.0 eq.. ^cP: product, SP: side-product.

Results of these experiments confirmed the hypothesis that the steric hindrance caused by the PAC group was the main reason for the failure of its introduction simultaneously with the linker **L3** to compound **19**.

3.1.5 Synthesis of 2-(3-trifluoroacetamido-1-prop-1-ynyl)adenosine

The Sonogashira coupling reactions between 2-iodoadenosine **27** and different triple-bond linkers have been investigated before (Matsuda *et al.* 1992; Cristalli *et al.* 1994; Cristalli *et al.* 1995). The cross-coupled products of these reactions showed biological activities, such as A₁ and A₂-receptor agonists.

In helical duplexes of RNA, the proton at the C-8 position of adenosine points into the deep and narrow major groove. On the contrary, the proton at the C-2 position looks into the minor groove which is shallow and wide. In this context, a reporter group attached via a linker arm to the C2 of the purine heterocycle may be more visible for its counterparts, thus more suitable for fluorescence experiments than the one which is located at the C-8 position. Therefore, 2-(3-trifluoroacetamido-1-prop-1-ynyl)adenosine **28** has been synthesized from the commercially available 2-iodoadenosine **27** (Figure 34). In literature procedures, the Sonogashira cross-coupling reactions of **27** and various terminal alkynes have been carried out in DMF at 80 °C with Pd(PPh₃)₂Cl₂ and CuI as catalysts and triethylamine as base (Matsuda *et al.* 1992) or in acetonitril/triethylamine at room temperature with PdCl₂, PPh₃ and CuI (Cristalli *et al.* 1994).

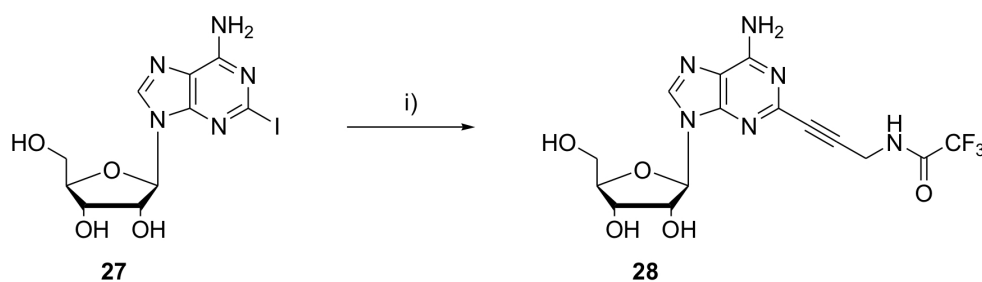


Figure 34 – The Sonogashira cross-coupling reaction of 2-iodoadenosine **27** and **L3**: i) **27**, 1.3 eq. **L3**, 0.1 eq. Pd(PPh₃)₄, 0.2 eq. CuI, 1.2 eq. DIPEA, DMF, 40 °C, 5.0 h, 82%.

In our experiment, the Sonogashira coupling reaction of **27** and the linker **L3** has been conducted according to the condition successfully applied for that of 8-bromoadenosine **19** and **L3** (Table 3, entry 1), which was milder than the reported procedures mentioned above. Thus, to the thoroughly degassed solution of 2-iodoadenosine in DMF were added 0.1 eq. Pd(PPh₃)₄, 1.2 eq. DIPEA, 1.3 eq. **L3** and 0.2 eq. CuI. The mixture was kept under vacuum and then saturated with argon before placed in an oil bath at 40 °C. The progress of the reaction was monitored by TLC (SiO₂; MeOH/DCM) and reversed-phase HPLC (Gradient A1, Table 24).

After 2 hours, the most part of **27** was consumed. Prolonging the reaction time to 5 hours, however, did not lead to the complete conversion of the starting material. DMF was then removed by co-evaporation with toluene under reduced pressure, the residue was resuspended in MeOH and filtered to remove the yellow precipitate and purified by silica gel column chromatography (MeOH/DCM) to afford 2-(3-trifluoroacetamidoprop-1-ynyl)adenosine **28** in 82% yield. The purity and the structure of the newly synthesized compound were confirmed by reversed-phase HPLC (Gradient D, Table 24), NMR and MALDI-MS analyses. In the ^1H NMR spectrum, the signal of the proton of the amide group NHCOCF_3 can be readily recognized at 10.12 ppm as a broad singlet. Accordingly, the two quartets of C=O and CF_3 of the amide group can be clearly seen in the ^{13}C NMR spectrum at 156.22 and 115.79 ppm, respectively.

3.1.6 Synthesis of 8-(3-trifluoroacetamidoprop-1-ynyl)guanosine

For the synthesis of 8-(3-trifluoroacetamidoprop-1-ynyl)guanosine **36** by the Sonogashira coupling reaction, the commercially available 8-bromoguanosine hydrate **35** 98% has been used as the starting material (Figure 35).

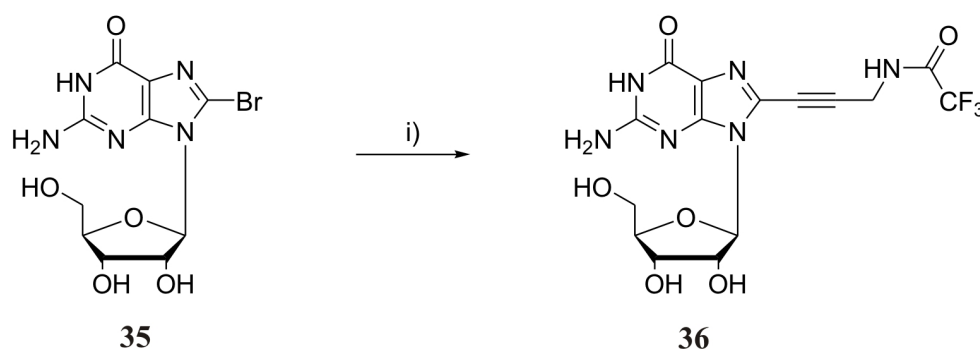


Figure 35 – The Sonogashira cross-coupling reaction of 8-bromoguanosine **35** and **L3**: i) **35**, 2.0 eq. **L3**, 0.1 eq. $\text{Pd}(\text{PPh}_3)_4$, 0.2 eq. CuI , 1.2 eq. DIPEA, 40 °C, 20 h, 80%.

On a general note, the Pd-assisted processes have proved to be more facile with halogenated derivatives of adenosine than with those of guanosine (Western & Shaughnessy 2005). In the case of 8-bromoguanosine and its analogues, various coordination possibilities to [Pd] and presumably also to [Cu] are available such as N-1/N-7 and O-6 coordinations which can hinder the cross-coupling reactions. This could be in part responsible for the fact that only a limited number of protocols for the preparation of 8-alkynylated guanosines (Firth *et al.* 2006) and deoxyguanosines (Saito *et al.* 2008; Crisp & Gore 1997) have been developed. The resulting modified nucleosides have been applied to fluorescence studies or post-synthetic modification. According to these procedures, bromoguanosine and -deoxyguanosine could undergo the Sonogashira coupling reactions with or without the protection of their functional groups. $\text{Pd}(\text{PPh}_2)_2\text{Cl}_2$ or $\text{Pd}(\text{PPh}_3)_4$ and CuI were used as catalyst and co-catalyst, respectively. The organic base was triethylamine.

The ratio of copper(I) to palladium as well as the ratio of catalyst to substrate have a significant effect on the coupling yields and on the purity of the cross-coupled products. A mole ratio of 2:1 CuI to Pd(PPh₃)₄ has been shown to offer the best coupling conditions for the alkynylation of uridine derivatives (Hobbs 1989; Crisp & Flynn 1993). With this ratio, the formation of side-products is minimized and this can also be applied to the cross-coupling of acetylated 8-bromoadenosine to give excellent yields. Surprisingly, the protocol previously considered as standard procedure for 8-brominated guanosine derivatives (0.1 eq. Pd(PPh₂)₂Cl₂, 0.1 eq. CuI, 1.2 eq. terminal alkyne, 3.0 eq. Et₃N in DMF at 110 °C for 18 h) has been proved to be ineffective, giving cross-coupled product in low yield with poor purity due to rapid palladium agglomeration and precipitation (Firth *et al.* 2006). Scaling down the amount of Pd(PPh₃)₂Cl₂ and CuI being used to 0.01 and 0.02 eq., respectively, afforded excellent yields in shorter reaction times. Without copper(I) co-catalyst, the cross-coupling yield is substantially low. Preliminary ³¹P NMR spectroscopic experiments indicated that the excess amount of copper(I) reduced the amount of Pd(0) species bound to the guanosine derivatives, thus releasing the active catalyst back to the catalytic cycle (Firth *et al.* 2006). In other studies, different 8-modified deoxyguanosine derivatives were synthesized in much milder conditions (55 °C in 3.5 h) (Saito *et al.* 2008). The amounts of Pd(PPh₃)₄, CuI and terminal alkynes being used were 0.1-0.5 and 3.0-3.5 eq., respectively, depending on the nature of the amino linker to be cross-coupled. Triethylamine was also used as base.

With regard to these literature procedures, we suggested that the procedure having been successfully applied for the coupling reaction of 8-bromoadenosine (see Section 3.1.4) may be suitable for the Sonogashira coupling reaction of 8-bromoguanosine **35** and the linker **L3**. Basing on this procedure, different Sonogashira reactions of **35** and **L3** have been tested in order to optimize the coupling condition (Table 4). In all cases, the yellow reaction mixture remained homogeneous without the observable black precipitate of the palladium catalyst. Triethylamine was not used as it had been proved to lead to the formation of the side-product in the coupling reaction of 8-bromoadenosine and **L3** (Section 3.1.4, Table 2 and 3). The replacement of DIPEA by the more bulky and weaker base TBA diminished the cross-coupling yield (entry 3). TLC (SiO₂; MeOH/DCM) and reversed-phase HPLC (Gradients A2, Table 24) showed that after 8 hours at 40 °C, only a small amount of 8-bromoguanosine was transformed. Increasing the reaction temperature and prolonging the reaction time led to a polar side-product which was supposed to be guanosine as the result of the reduction of 8-bromoguanosine.

The conditions described in entries 1,2 and 3 (Table 4) have been applied in small scales as tests for the Sonogashira coupling reactions of **35** and **L3**. The amounts of 8-bromoguanosine being used were 0.1-0.2 mmol which were suitable for small reactions in eppendorf tubes. The reaction mixtures were saturated with argon and sealed with parafilm before placed on a shaker at the set temperatures. The condition in entry 4 was applied for preparative scales in which the dissolved oxygen in the reaction mixtures was removed by exchanging several

times between vacuum and a flow of argon. When DIPEA was used (entries 1, 2 and 4), increasing the reaction temperature from 40 to 55 °C did not help to increase the reaction rate. The progress of the reaction was monitored by TLC in high percentages of MeOH (40-50 %) in DCM due to the high hydrophilicity of the unprotected guanosine derivative. The spots of 8-bromoguanosine and the corresponding product were, however, still smeared to some extent. When the reaction finished, the reaction mixture was thoroughly co-evaporated with toluene to remove traces of DMF. The residue was suspended in a small amount of methanol and filtered to remove the yellow precipitate. The resulting solution was absorbed on silica gel and purified by silica gel column chromatography (MeOH/DCM). The cross-coupled product **36** was eluted from silica gel column by high proportions of MeOH in DCM. Using such a polar solvent also had the advantage, as it had washed out all the yellow impurity (supposedly from palladium catalyst), the excess of **L3** and other less polar compounds from the column before the product was eluted.

Table 4 – Sonogashira reaction conditions for the cross-coupling between 8-bromoguanosine hydrate **35** and **L3**^a.

Entry	L3 (eq.)	Pd(0) (eq.)	Cu(I) (eq.)	Base (eq.)	Temp. (°C)	Time (h)	Yield (%)
1	1.8-2.0	0.1	0.2	DIPEA 2.0	40	11	28
2	1.5	0.1	0.2	DIPEA 2.0	55	11	34
3	2.0	0.1	0.2	TBA 2.0	40 55	8 overnight	< 10 Dec. ^b
4	2.0	0.1	0.2	DIPEA	40	20	80

^aAll the reactions were carried out in DMF with Pd(PPh₃)₄ and CuI as catalysts. The amount of 8-bromoguanosine is 1.0 eq.. ^bProlonging the reaction time resulted in the decomposition of **35** to guanosine.

The conditions described in entries 1 and 4 are the same, except that the reaction time in condition 4 was increased to 20 hours. The reaction yield after 11 hours at 40 °C was only 28%, as the amount of the starting 8-bromoguanosine was relatively small and a significant quantity of the product was lost after two times purification by silica gel and reversed-phase chromatography. Under the same condition but for a longer time and with a higher amount of substrates, however, a yield of 80% was obtained.

The purity and the structure of the separated product were confirmed by NMR and MALDI-TOF analyses. The ¹H NMR spectrum of the separated compound indicated the presence of the amide group -NHCOCF₃ of the linker at 10.19 ppm as a broad singlet. In the ¹³C NMR

spectrum, two quartets at 115.74 and 156.27 ppm corresponding to CF_3 and CO of the linker, respectively, were readily recognized.

3.2 Synthesis of modified uridine and adenosine building blocks by the Heck coupling reaction

3.2.1 Retrosynthesis of the modified building blocks by the Heck coupling reaction

The design of suitable reporter groups for attachment to RNA residues should take into account their impact on the overall structure and stability of the molecules, especially on the base-pairing and stacking interactions of the nucleobases located near the labeled sites.

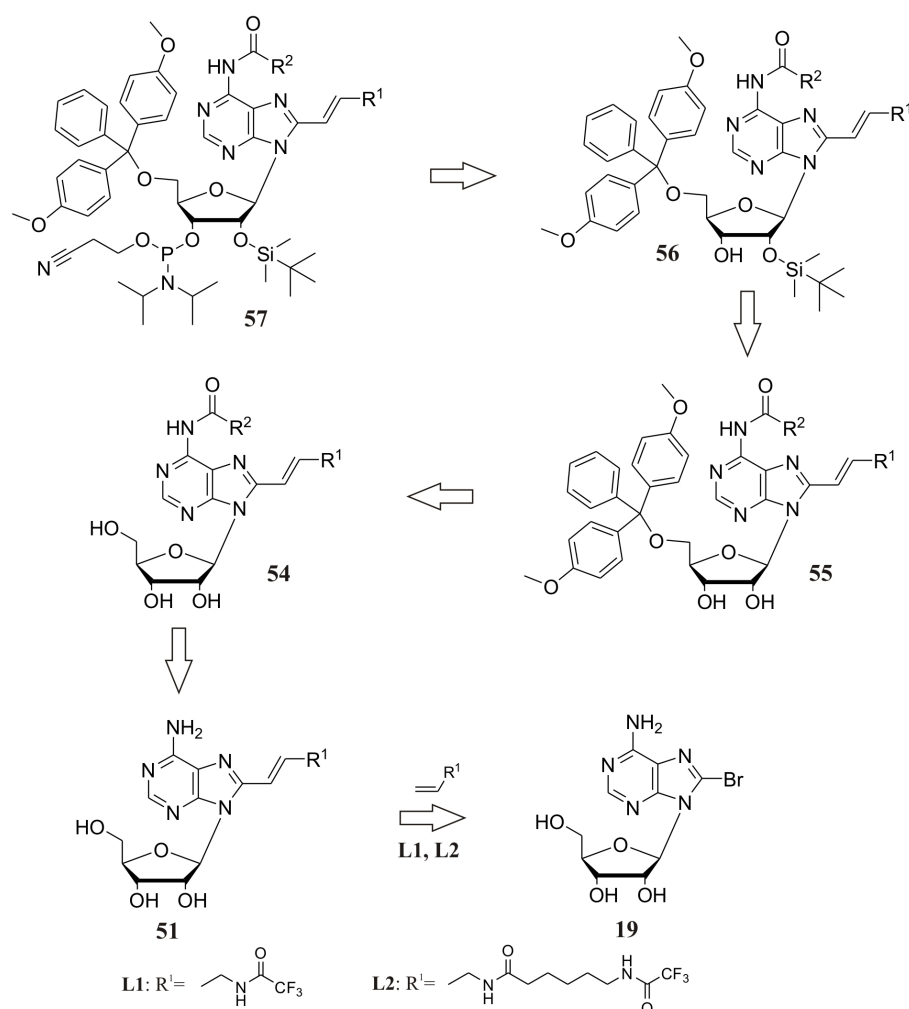


Figure 36 – Retrosynthesis of the amino linker modified adenosine building blocks.

Short and stiff linkers allow the easier control of the motion of the labels, but these labels are more likely to induce structural perturbations than those which are attached via long and flexible linkers. Moreover, labels are more easily coupled via long linkers and may be more

visible to their counterparts. Therefore, besides the rigid triple-bond linker **L3**, the flexible double-bond amino linkers of different lengths **L1** and **L2** have also been attached to the halogenated nucleosides for labeling by the Heck coupling reaction.

As outlined in Figure 36, the modified adenosine phosphoramidite **57** can be synthesized by the acylation, tritylation and silylation of the 8-L1 or -L2 modified adenosine **51** which is synthesized by the Heck coupling reaction of 8-bromoadenosine **19** and the linker **L1** or **L2**. Similar synthetic routes can be applied for the preparation of the 2-modified adenosine building blocks from 2-iodoadenosine **27** and 5-modified uridine building blocks from 5-iodouridine **1**, except that no acylation step for the exo-cyclic amino protection is required for the uridine building blocks.

3.2.2 Synthesis of *N*-allyltrifluoroacetamide **L1**

Allylamine has been used to synthesize the short double-bond linker *N*-allyltrifluoroacetamide **L1**. The amino function of allylamine was protected with the trifluoroacetyl protecting group (TFA) by the acylation reaction with either trifluoroacetic anhydride (Figure 37, path a) (Dey & Sheppard 2001; Cook *et al.* 1988) or the ethyl ester of trifluoroacetic acid (Figure 37, path b) (Cruickshank & Stockwell 1988).

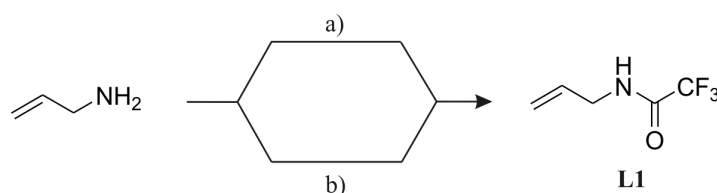


Figure 37 – Synthesis of *N*-allyltrifluoroacetamide **L1**: a) allylamine, 0.5 eq. trifluoroacetic anhydride, ice-cold 45 min., RT overnight, 75%; b) allylamine, 1.3 eq. ethyl trifluoroacetate, MeOH, RT, overnight, 80%.

In the first procedure, trifluoroacetic anhydride was added dropwise and carefully to the ice-cold solution of allylamine, as this acetylating reagent reacted vigorously with the amine in an exothermic reaction. Allylamine was used in an excess amount (2.0 eq.) compared to trifluoroacetic anhydride, since it was required to neutralize the released trifluoroacetic acid. Dey and Sheppard have pointed out that the elimination of the aqueous work-up increased the yield of the highly water-soluble **L1** from 35 to 95%. Thus, after the reaction, the solvent was removed by rotary evaporation. The residue was distilled under vacuum without work-up with aqueous solutions to give the linker *N*-allyltrifluoroacetamide **L1** as a colorless liquid (75%) which solidified when kept at -20 °C.

NMR analysis confirmed the purity and structure of the separated compound. This procedure had, however, some disadvantages: allylamine needed to be used in excess amounts and was sometimes distilled together with **L1**, hence contaminating the product. In this case, the mixture had to be redistilled to give the pure linker product.

Referring to the synthesis of the triple-bond linker **L3** (section 3.1.2), trifluoroacetic anhydride was replaced by ethyl trifluoroacetate which was more readily available. This acylating reagent allowed the reaction to occur under the milder condition. With a slight excess of ethyl trifluoroacetate, allylamine was completely consumed to afford pure **L1** in high yield (80%) after one time distillation. The side-product ethanol and the starting material ethyl ester have low boiling points, thus can be easily removed by rotary evaporation under reduced pressure. The NMR spectrum of the compound synthesized by this method was identical with that of the compound obtained when using trifluoroacetic anhydride.

3.2.3 Synthesis of *N*-allyl-6-(*N*-trifluoroacetylamino)hexanamide **L2**

As outlined in Figure 38, the long double-bond linker **L2** was synthesized by the protection of 6-aminohexanoic acid with ethyl trifluoroacetate to give 6-(*N*-trifluoroacetylamino)hexanoic acid **L2-P1**, followed by the acylation reaction of **L2-P1** with allylamine in the presence of the carboxyl activating reagent 1-ethyl-3-(3-dimethylaminopropyl)carbodiimide hydrochloride (EDAC) (McKeen *et al.* 2003) or 1,1'-carbonyldiimidazole (CDI) (Sinha *et al.* 1995).

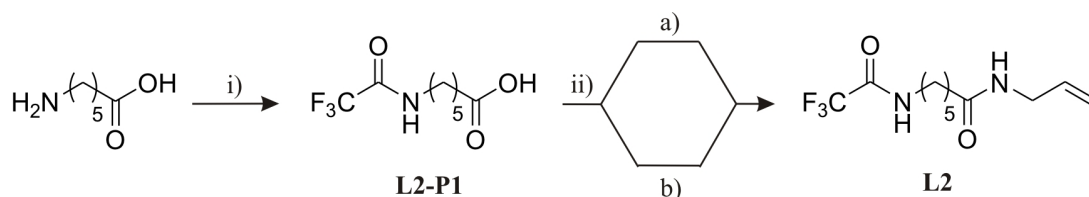


Figure 38 – Synthesis of *N*-allyl-6-(*N*-trifluoroacetylamino)hexanamide **L2**: i) 6-aminohexanoic acid, 1.5 eq. ethyl trifluoroacetate, TEA, MeOH, RT, overnight, 83%; ii) a) **L2-P1**, 1.1 eq. EDAC, 1.1 eq. allylamine, DMF, RT, overnight, 55%. b) **L2-P1**, 1.7 eq. CDI, RT 1 h, 1.7 eq. TEA, MeCN, RT, overnight, 63%.

In the first step, 6-aminohexanoic acid was suspended in methanol and triethylamine followed by the addition of ethyl trifluoroacetate. The mixture became a yellow homogeneous solution after 1 hour and was stirred overnight. The solvents were then removed by rotary evaporation, the residue was treated with HCl and NaCl solutions and recrystallized from diethyl ether to give **L2-P1**.

In the second step, EDAC or CDI was added to the solution of **L2-P1** in dry DMF or MeCN, respectively. Allylamine was then added to the solution of the resulting activated carboxylic acid. The reaction mixtures must be protected from moisture, as the activated carboxylic acids formed *in situ* were readily hydrolyzed by traces of water. After the reaction, the solvent was removed, the residue was treated with dilute solutions of NaHCO_3 and NaCl (when EDAC was used) or HCl and NaCl (when CDI was used) and recrystallized from diethyl ether to give **L2**. The purity and the structure of the separated compounds were verified by NMR analysis. Replacing the hygroscopic carboxyl activating reagent EDAC by CDI helped to improve the yield of the acylation step (from 55 to 63%) and eased the handling. In addition, CDI was

also more easily available. It was important that after the reaction of **L2-P1** with allylamine catalyzed by CDI, the reaction mixture must be carefully treated with diluted HCl solution in order to remove traces of imidazole being formed as a side-product of the reaction. Imidazole could not be completely eliminated only by recrystallization. The contamination of **L2** with imidazole is unacceptable, as the complexation of its heterocyclic nitrogens with palladium led to the entire deactivation of the catalyst in the Heck cross-coupling reaction.

3.2.4 Synthesis of 5-(3-trifluoroacetamidoprop-1-enyl)uridine **8**

The 2'-deoxy analogues of 5-(3-trifluoroacetamidoprop-1-enyl)uridine **8** were first synthesized from 5-chloromercuri-2'-deoxyuridine by the Heck cross-coupling reaction (Cook *et al.* 1988; Bergstrom *et al.* 1981; Langer *et al.* 1981). Sakthivel and Barbas synthesized the C-5 modified deoxyuridine from the commercially available 5-iododeoxyuridine by a similar procedure (Sakthivel & Barbas 1998) which was then modified by Dey and Sheppard (Dey & Sheppard 2001): Using DMF as a co-solvent helped to homogenize the reaction mixture and increasing the reaction temperature to 80 °C improved the cross-coupling yield while decreased significantly the reaction time (from 18 hours at room temperature to 2 hours at 80 °C). Under this Heck coupling condition, the introduction of **L1** into 5'-O-DMT-2'-O-TBDMS-5-iodouridine **3** was unsuccessful, since DMT and TBDMS protecting groups were cleaved off. Thus, the synthesis of **8** was started from the corresponding unprotected nucleoside **1** as shown in Figure 39.

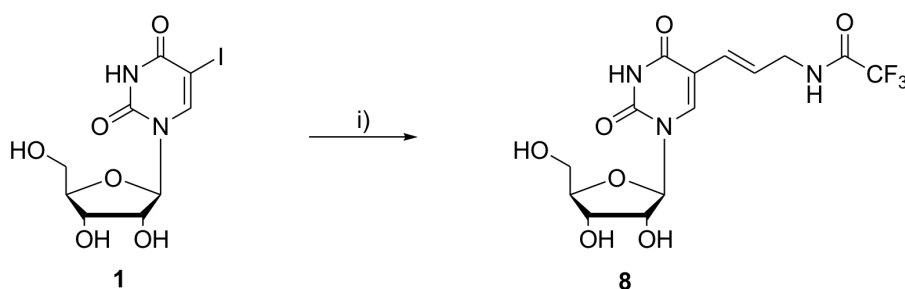


Figure 39 – Synthesis of 5-(3-trifluoroacetamidoallyl)uridine **8** by the Heck coupling reaction: i) **1**, 8.5 eq. **L1**, 0.5 eq. $\text{Na}_2[\text{PdCl}_4]$, 0.1 M NaOAc buffer pH 5.2, DMF, 80 °C, 8.5 h, 89%.

The solution of **1** and **L1** in DMF/acetate buffer was saturated with argon and placed in a preheated oil-bath maintained at 80 °C. A solution of the catalyst $\text{Na}_2[\text{PdCl}_4]$ in DMF was added to the reaction mixture while vigorously stirring. A thick dark-brown solution and the black palladium precipitate were developed during the time of the reaction. After 8.5 h, TLC (MeOH/DCM) indicated that nearly all of **1** was consumed. The reaction mixture was then filtered through Celite 560, treated with NaBH_4 to decompose the excess catalyst and filtered again through Celite 560 to remove the black palladium element. The resulting solution was concentrated by co-evaporation with toluene. The residue was absorbed on silica gel and

purified by silica gel column chromatography (MeOH/DCM).

The treatment with NaBH₄ helped to reduce the excess of palladium catalyst in soluble form to the palladium element which could easily be eliminated by filtration (Cook *et al.* 1988). The solution of this reducing reagent was added slowly and carefully to the reaction mixture until the brown color disappeared. Excess amounts of NaBH₄ can lead to the cleavage of the heterocyclic ring, thus decreasing the yield of the reaction (Blackburn & Gait 1992).

Table 5 – Coupling constants of sp² protons of RCH=CH₂ at different relative positions (taken from Hesse *et al.* 2002).

-R	³ J(Z)	³ J(E)	² J(gem)
-H	11.6	19.1	2.5
-C ₆ H ₅	11.5	18.6	1.1
-OCH ₃	6.7	14.0	-2.2
-F	4.7	12.8	-3.2

In this ligand-free Heck cross-coupling reaction, Na₂[PdCl₄] has been used with high loading in order to compensate the loss of catalytic activity due to the formation of black precipitated palladium at high temperatures in long reaction times. Using excess amounts of linker **L1** also helped to decrease the reaction time because it could reduce the palladium(II) precatalyst to the catalytically active palladium(0) (Figure 16).

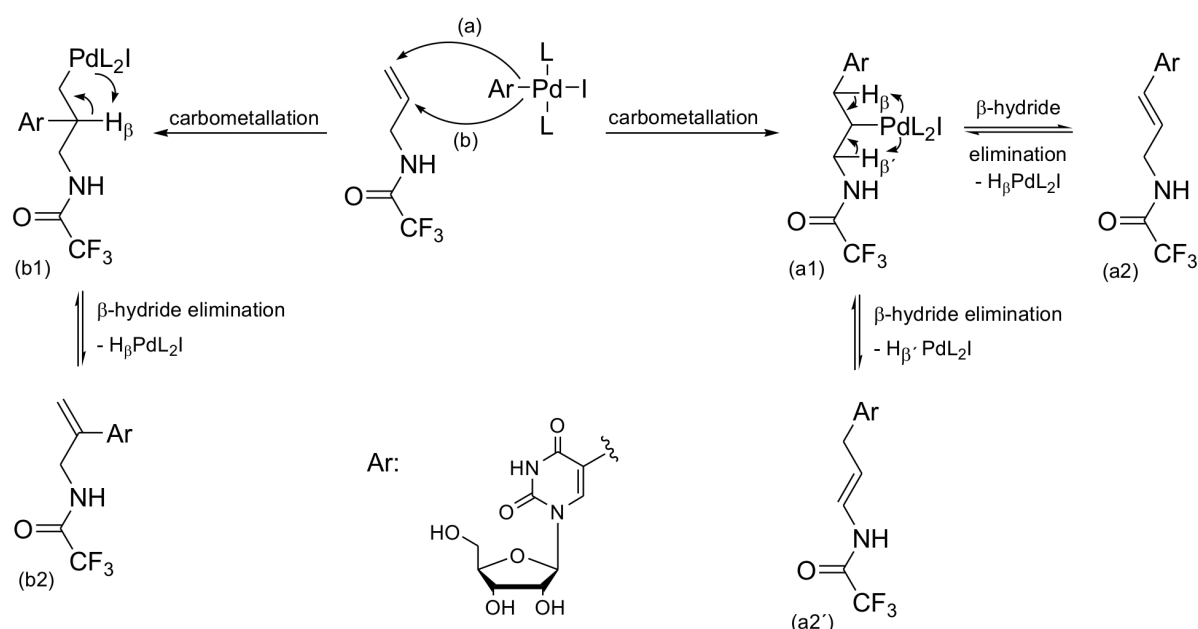


Figure 40 – Different directions in the Heck cross-coupling reaction of **1** and **L1**: a) The heterocycle Ar is added to the terminal carbon of the double-bond; b) The heterocycle Ar is added to the internal carbon of the double-bond.

Because of the asymmetry of the linker arm, the carbometallation could in principle result in the formation of two palladium complexes a1 and b1 (Figure 40) which can undergo β-hydride

elimination to give a mixture of isomers. If the carbometallation happened in direction (b), the corresponding alkene being formed is (b2) which has two terminal protons (*gem*-protons). Two sp^2 *gem*-protons normally have quite small $^2J_{gem}$ coupling constants (Table 5) which are not seen in the spectrum.

In the 1H NMR spectrum of **8**, it is easy to recognize the signals of the two vicinal protons at the double-bond of the linker (Figure 41). The coupling constants are 15.9 Hz, indicating that these protons are *trans* to each other. The splitting motives of the signals also confirmed that the carbometallation happened selectively following direction (a) (Figure 40) in which the nucleophilic attack of the heterocycle (Ar) is preferably on the terminal end of the linker arm.

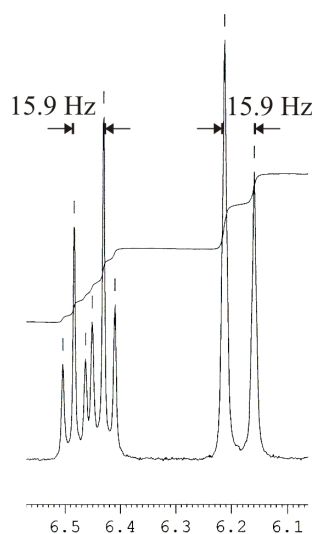


Figure 41 – NMR signals of the protons at the double-bond of the linker in the cross-coupled product **8**.

The attacking direction is compatible with the electron character of the amide group $NHCOCF_3$ which has a negative induction effect. The terminal end of the alkene linker has no substituent and is less sterically hindered, hence facilitating the in-coming of the heterocycle. Both electronic and steric factors are not striking, but strong enough to direct the cross-coupling in a unique manner, as the Heck reactions are very sensitive to the steric difference of the medium around the reaction center.

The β -hydride elimination of (a1) can theoretically lead to the formation of two alkene isomers (a2) and (a2') (Figure 40). The 1H NMR spectrum of the separated compound indicated the presence of only one alkene isomer (a2): The signal of the proton of the $-NHCOCF_3$ amido group appears as a triplet, indicating that it has interactions with two identical protons of the methylene group. (a2) was preferably formed, because it contains the newly generated double-bond which is conjugated with the aromatic system of the heterocycle.

In the β -hydride elimination step, the two leaving-groups $-PdL_2I$ and $-H\beta$ should be co-planar and *syn* to each other. In the configuration required for this elimination, the most bulky groups in the molecule should not eclipse each other, but stagger. Otherwise they will clash with

each other and destabilize the intermediate (Figure 42). Accordingly, the main product is the *trans*-isomer, which is confirmed by NMR data (Figure 41). No *cis*-isomer was detected.

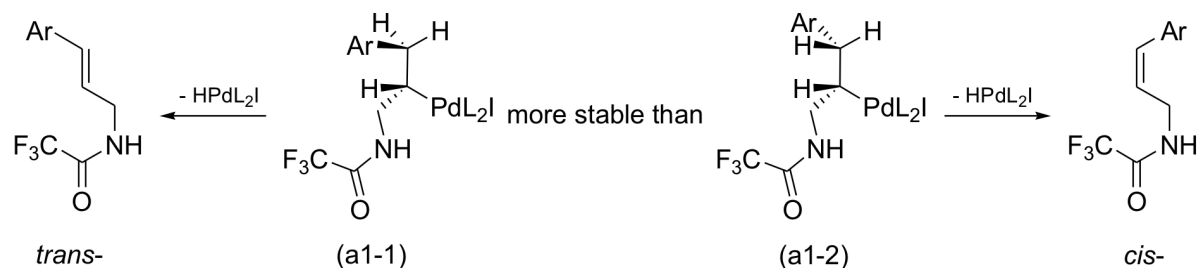


Figure 42 – Configurations of the intermediate formed by carbometallation: (a1-1) Ar- and -CH₂NHCOCF₃ are "gauche" (or "staggered") to each other; (a1-2) Ar- and -CH₂NHCOCF₃ are "eclipsed" by each other.

3.2.5 Synthesis of 5-(3-[6-trifluoroacetylaminohexanamido]prop-1-enyl)uridine

Having been successful with the preparation of the building block **8**, we turned our attention toward the cross-coupling of 5-iodouridine **1** and the long double-bond linker **L2**. Using a similar synthetic route, the building block 5-(3-[6-trifluoroacetylaminohexanamido]prop-1-enyl)uridine **14** was prepared from **1** and the linker **L2** with good yield under the Heck cross-coupling condition (Figure 43).

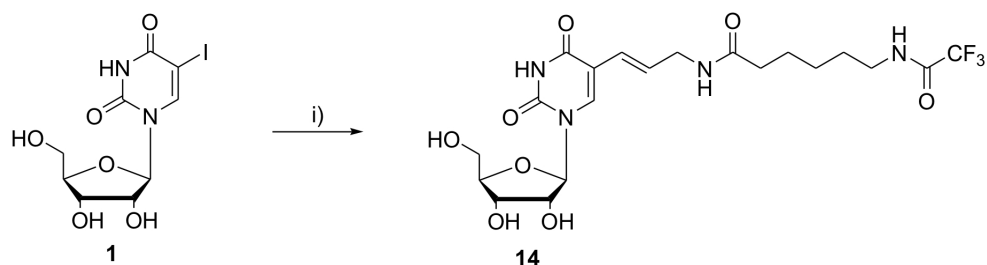


Figure 43 – Synthesis of 5-(3-[6-trifluoroacetylaminohexanamido]prop-1-enyl)uridine **14** by the Heck coupling reaction: **1**, 8.0 eq. **L2**, 0.5 eq. Na₂[PdCl₄], 0.1 M NaOAc buffer pH 5.2, DMF, 81 °C, 9 h, 54%.

Thus, 5-iodouridine **1** and the linker **L2** were dissolved in a mixture of DMF and NaOAc buffer 0.1 M, pH 5.2. To the resulting solution was added the solution of the catalyst Na₂[PdCl₄] in DMF while vigorously stirring. The reaction mixture was purged with argon and placed into a preheated oil-bath at 81 °C. The coupling reaction finished after about 9 hours as indicated by TLC (SiO₂; MeOH/DCM). Solvents were thoroughly removed by co-evaporation with toluene. The residue was taken up in methanol, absorbed on silica gel and purified by silica gel column chromatography (MeOH/DCM).

The purity and the structure of the separated compound were confirmed by NMR and MALDI-TOF analyses (see Section 5.6).

3.2.6 The Heck coupling reaction of 8-bromo-, 8-iodoadenosine and its derivatives with **L1**

In order to introduce the flexible double-bond linker **L1** into the C-8 position of adenosine by the Heck coupling reaction, different 8-bromo and 8-iodoadenosine derivatives have been used in order to optimize the reaction conditions (Figure 44).

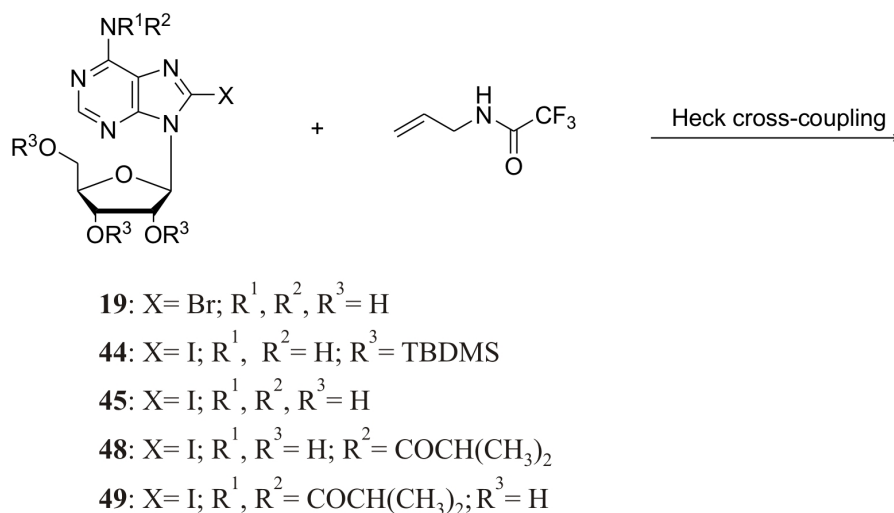


Figure 44 – The Heck cross-coupling reactions of 8-bromo, 8-iodoadenosine and derivatives with the linker **L1**.

3.2.6.1 The Heck coupling reaction of 8-bromoadenosine in non-aqueous solvents

In the first experiments, the commercially available 8-bromoadenosine **19** has been used as the starting material (Figure 44). To the best of our knowledge, the Heck cross-coupling reactions between 8-bromoadenosine and amino linkers have not yet been reported so far. Therefore, the Heck coupling reactions of **19** (summarized in Table 6) have been carried out basing on the reported procedures applied for other non-nucleoside bromo derivatives (Jacobson *et al.* 1993; Herrmann *et al.* 1997; Littke & Fu 1999; Qadir *et al.* 2000).

When the reactions were conducted at high temperatures (over 100 °C), **19** was decomposed to give complicated mixtures of side-products. In some cases, 8-bromoadenine was separated (entries 2 and 5). At lower temperatures that were normally applied for the Heck reactions of iodo derivatives (about 80 °C), no reaction was observed (entries 1, 3 and 4).

The commonly used catalyst systems for the Heck coupling reactions of bromo derivatives Pd(OAc)₂ + triarylphosphine ligands in the presence of inorganic or organic bases (Hermann *et al.* 1995; Whitcombe *et al.* 2001) did not cause any transformation to the direction of the desired compound (entries 2-5). The reaction mixture could not become homogeneous, as the inorganic bases being used were not soluble in DMF and DMA. Increasing the reaction temperature to over 120 °C and prolonging the reaction time led only to the decomposition of

19 (entries 2, 5-7). The addition of phase-transfer reagents according to Jeffery's protocols for low-temperature Heck coupling reactions (Jeffery 1984; Jeffery 1985; Lansky *et al.* 1990) did not help to improve the reactivity of the catalyst (entries 3 and 4). The addition of water (1 ml/1 mmol) did not activate the catalyst system.

Table 6 – Heck cross-coupling reactions of 8-bromoadenosine and **L1** in non-aqueous solvents.

Entry	L1 (eq.)	Catalyst (eq.)	Ligand ^b (eq.)	Base (eq.)	PT-R ^c	Sol. ^d	T./Time (°C) /(h)	Result ^e
1	1.2	Pd(PPh ₃) ₄ 0.1	-	DIPEA 1.2	-	DMF	40-90 /24	NR
2	1.4	Pd(OAc) ₂ 0.02	PAr ₃ 0.08	NaOAc 1.1	-	DMF	70-130 /24	8-BrA
3	1.2	Pd(OAc) ₂ 0.05	-	Et ₃ N 1.0	<i>t</i> Bu ₄ NCl 1.0	PEG- 2000	83/2 100/24	NR
4	2.0	Pd(OAc) ₂ 0.06	-	K ₂ CO ₃ 3.5	<i>t</i> Bu ₄ NCl 1.2	DMF	40-100 /24	NR
5	2.0	Pd(OAc) ₂ 0.1	PAr ₃ 0.2	DIPEA 2.0	-	DMF	85-125 /24	8-BrA
6	8.5	hc ^a 0.2	-	NaOAc 1.1	-	DMA	83-120 /24	Dec.
7	7.5	Pd(dba) ₂ 0.025	PAr ₃ 0.05	NaOAc 1.1	-	DMF	80-125 /24	Dec.

^ahc: Herrmann's catalyst (palladacycle). ^bAr: phenyl or *o*-tolyl. ^cPT-R: phase-transfer reagents.

^dSol.: solvents. ^eNR: no reaction, Dec.: decomposition, 8-BrA: 8-bromoadenosine.

Also, the Herrmann's catalyst (*hc*), palladacycle, which has been reported to be more reactive for bromo substrates than the corresponding (Pd(OAc)₂ + tri(*o*-tolyl)phosphine) system (Herrmann *et al.* 1995) did not effect the cross-coupling reaction, although it could tolerate hard reaction conditions (130 °C for 24 hours) without the formation of the black palladium precipitate (entry 6). The application of poly-ethylenglycol 2000 (PEG-2000), reported as an effective and recyclable medium for the Heck cross-coupling reaction (Chandrasekhar *et al.* 2002), appeared to be unreasonable, as **19** was not soluble in the melted form of PEG-2000. Homogenizing the reaction mixture by the addition of DMF did not have any effect (entry 3).

In the next experiments, aqueous buffers have been used as co-solvents in the Heck coupling reactions of **19** and **L1**.

3.2.6.2 The Heck reaction of 8-bromoadenosine and **L1** in aqueous organic solvents

Water-containing solvent systems have been reported to be more effective than the conventionally used organic reaction solvents for palladium-mediated phosphine-free reactions of halogen derivatives of nitrogen heterocycles (Zhang & Daves 1993; Jeffery 1994; Williams *et al.* 2001; Dey & Sheppard 2001). Therefore, the Heck coupling reaction of **19** and **L1** was repeated in which water was used as co-solvent (Table 7).

Table 7 – The Heck coupling reactions of 8-bromoadenosine and **L1** in aqueous solvents^a.

Entry	L1 (eq.)	Pd(II) (eq.)	Solvent ^b	T./Time (°C)/(h)	Result ^c
1	8.5	1.1	DMF/KOAc buffer	83/5.5	Structure not defined
2	17.0	1.1	DMF/KOAc buffer	75/7 83/1.5	Structure not defined
3	30.0	0.21	DMF/KOAc buffer	83/29	Isomer
4	50.0	0.13	DMF/KOAc buffer	83/24	Red. to adenosine
5	8.5	0.5	DMF/NaOAc buffer	80/11	Isomer
6	8.5	0.5	DMF/NH ₄ OAc buffer	80/11	Isomer
7	8.5	0.5	DMF/LiOAc buffer	80/14	Isomer
8	8.5	0.5	DMF/KOAc buffer	80/14	Isomer

^aIn all cases, Na₂[PdCl₄] was used as catalyst. No ligand was added. ^bNaOAc, LiOAc, KOAc and NH₄OAc buffer: sodium, lithium, potassium and ammonium acetate buffer 0.1 M pH 5.2. ^cIsomer: the formation of the isomer of Heck coupling product with the rearranged double-bond (Figure 46), Red. to adenosine: reduction of 8-bromoadenosine to adenosine.

Thus, the water soluble catalyst Na₂[PdCl₄] has been used without the addition of any phosphine ligands. When the Pd(II) catalyst was used with high loading, the structures of the silica gel purified compounds were not well-defined as they were contaminated by the catalyst and unknown impurities (entries 1 and 2). When the amount of **L1** being used was over 50 eq., the most part of **19** was reduced to adenosine (entry 4). The conditions described in entries 5-8 were similar, but the cations of the buffers were different. The aim of this changing was to investigate if the cations being used in these buffers had any effect on the cross-coupling reaction. These cations may complex with the nitrogen atoms of the heterocycle, thus masking and preventing the nitrogen atoms from intervening in the cross-coupling reaction. In each of these reactions, one main compound and a minor one were formed. The ¹H and ¹³C NMR spectra and MALDI-TOF masses of the main compounds separated from these conditions are identical, indicating that they are one substance. From the NMR analyses, it can be concluded that this main compound was pure, the TFA-protected allylamine linker **L1** was coupled to

the C-8 of the purine ring (two quartets of CO and CF₃ of the TFA group can be recognized in ¹³C NMR). In addition, this compound is a *trans* isomer as indicated by the high coupling constant of the two protons at the double-bond (³*J*(H,H)= 14.4 Hz). However, the signal of the NH proton was significantly shifted downfield (11.32 ppm in comparison with the normal 9.5–10.1 ppm in 5-L1 and -L2 modified uridine analogues, see Section 3.2.4 and 3.2.5) and the signal of the ¹³C of the CH₂ group of the linker appears in a relatively strong field (28.14 ppm in comparison with 41.15 ppm of that of **8**). On the contrary, the ¹H NMR of the minor compound indicated the signal of the NH proton at 9.51 ppm.

One reason for the spectroscopic evidences of the main compound could be the formation of intramolecular hydrogen bonds between the amide group of the linker and the hydroxyl groups or the oxygen of the ribofuranose ring (Figure 45). This was supported by the fact that the ¹H NMR of this compound was not changed while its concentration in the NMR samples changed.

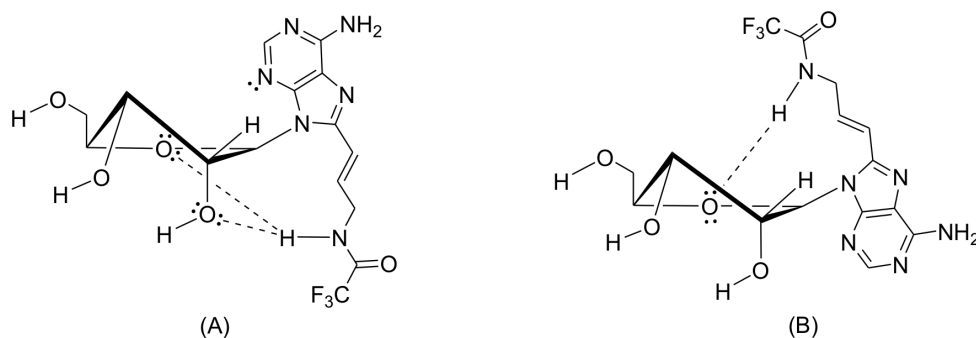


Figure 45 – Possible intramolecular hydrogen bonds of the main compound separated from the Heck reactions of **19** and **L1** in aqueous organic solvents: (A) *syn*-conformation, (B) *anti*-conformation.

Conformation (A) should be favored, since the linker is relatively bulky, thus forcing the nucleobase to the *syn*-conformation. This suggested conformation is supported by the observation: the signal of H2' is shifted significantly to the weak field, indicating that its resonance is affected by the anisotropic effect of N3 which can only perform in the *syn*-conformation. In this conformation, the proton of the amide group forms hydrogen bonds with O2' and O5'. Therefore, its signal is shifted downfield. This hypothesis, however, could not explain convincingly for the fact that in different reaction conditions, the samples have different signal ratios at 11.32 and 9.51 ppm which is not due to the difference in the concentrations of the samples.

In order to clarify the uncertainty, 2D-NMR analysis of the main compound has been carried out (Figure 46). For easy interpretation of the NMR spectra, the linker is numbered as shown in Figure 46. The signal of the proton Hb at the C11-sp² is readily recognized, as it is always a multiplet, regardless of the position of the double-bond. The designated position of the other proton at the double-bond Ha changes according to the rearrangement of the double-bond. In structure (C), it is the proton at the C10, while in structure (D), it is located at the C12.

From the signals in the HMBC spectrum, it can be concluded that the main compound obtained when carrying out the Heck coupling reactions under the conditions summarized in

entries 3 and 5-8 was not the expected Heck cross-coupled product of which the linker double-bond is conjugated to the heterocycle (structure (C), Figure 46), but its isomer of which the double-bond was rearranged (structure (D), Figure 46).

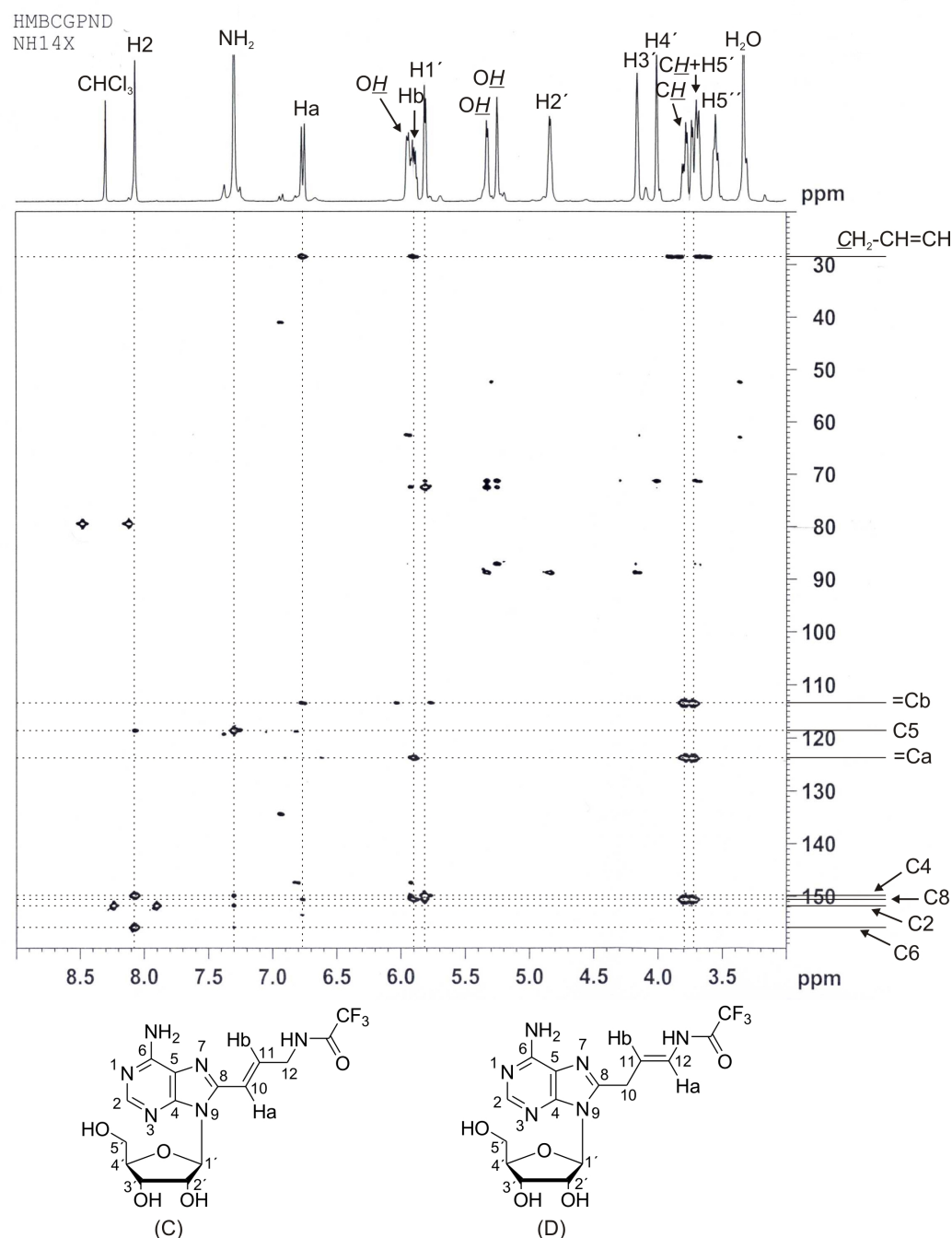


Figure 46 – The HMBC spectrum of the compound separated from the reaction described in entry 5, Table 7. Under the spectrum are the structures of Heck cross-coupled product of **19** with **L1** (C) and its isomer with the rearranged double-bond (D).

This conclusion is supported by the fact that the C8 of the heterocycle which is identified by the strong cross-signal with Hb and H₁' (separated from each other by three bonds) has a weak cross-signal with Ha (separated from each other by four bonds). Moreover, C8 has two strong cross-signals with two protons of the methylene group of the linker. These observations indicate that C8 must be close to the methylene group and far away from Ha. Only structure

(D) in which the two protons of the methylene group and Ha are two-bond and four-bond separated from C8, respectively is in good agreement with those spectroscopic evidences. In structure (C), the cross-signal between C8 and the protons of the methylene group, if exists, should be very weak, as the interaction would be transferred through four bonds.

In Heck coupling reactions, the newly formed double-bond is normally conjugated with the π -system of the halogen substrate. This helps to reduce the energies of the transient states and the resulting product. It was, however, not the case in the Heck cross-coupling reaction of compound **19** and the linker **L1**. This evidence could be explained by the complexation of N7 of the heterocycle with [Pd] during the β -hydride elimination (Figure 47).

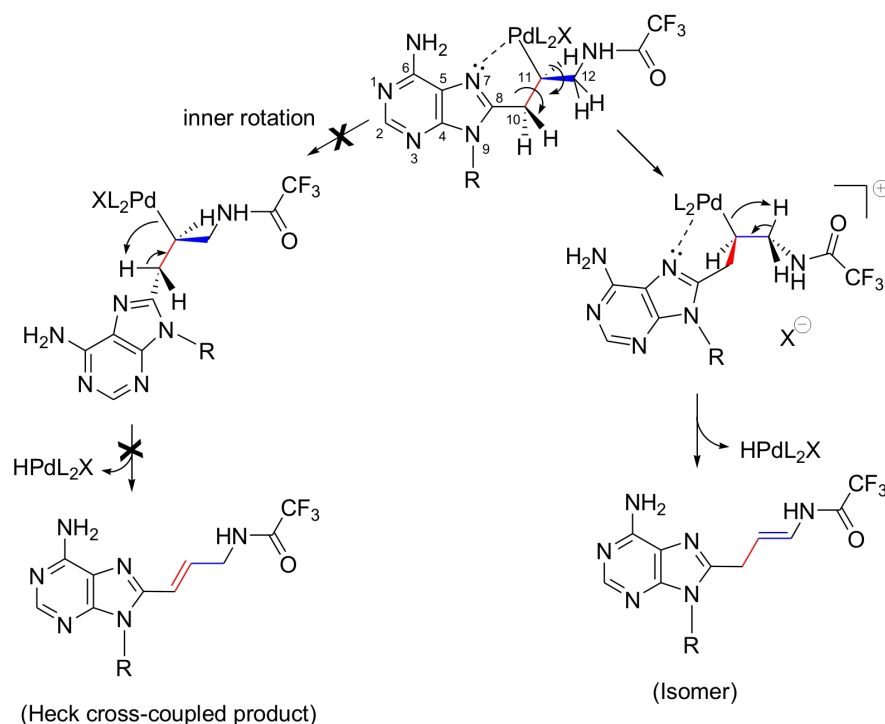


Figure 47 – The restriction of the inner rotation during the Heck cross-coupling reaction of **19** and **L1**. R: D-ribofuranosyl, X: Br[−] or AcO[−].

In the Heck coupling reaction, the insertion step is stereospecifically *syn*, that is, the purine ring and the complex center [Pd] are coplanarily inserted on the same side of the double-bond of the linker (Figure 15). Therefore, the possibility for N7 which has a free electron pair to complex to the [Pd] center is high. This complexation could inhibit the free inner rotation between C8-C10-C11 bonds of the intermediate. Consequently, the formation of the isomer of the Heck cross-coupled product with the rearranged double-bond (Figure 46D) is favored, as it does not interrupt the complexation between N7 and [Pd]. As expected, this isomer also had the *trans* configuration (the coupling constant of the two protons at the newly generated double-bond is 14.4 Hz which is typical for *trans* isomers, see Table 5). Efforts to overcome the complexation of N7 with the catalyst during the β -hydride elimination by changing buffers (entries 3 and 5-8) as well as the amounts of the catalyst and the linker (entries 1-4) were

unsuccessful. Because the position of the double-bond would not affect seriously the rigidity of the linker, the isomer of the Heck coupling reaction between **19** and **L1** can be used to synthesize RNA for FRET experiments.

In another approach to optimize the Heck coupling reaction condition, 8-iodoadenosine and its derivatives have been synthesized and applied as the halogen substrates in the next experiments.

3.2.6.3 Synthesis of 8-iodoadenosine and its derivatives

It has been commonly known that iodinated substrates are more reactive in the Heck coupling reactions than the corresponding brominated analogues. In this context, 8-iodoadenosine may be a more suitable starting material than 8-bromoadenosine **19** for the introduction of double-bond linkers by the Heck coupling reaction. Because 8-iodoadenosine was not commercially available, it was synthesized in our lab basing on the reported procedure (Hayakawa *et al.* 1989).

Firstly, the three hydroxyl groups of adenosine were protected with TBMDMS-Cl in DMF to give 2',3',5'-tri(*tert*-butyldimethylsilyl)adenosine **43** (Figure 48). Imidazole was used as a base to trap the hydrochloric acid formed during the reaction. After being worked up with water, the product was purified by silica gel column chromatography (MeOH/DCM). Secondly, the H-8 proton of the TBDMS-protected adenosine **43** was replaced by an iodine atom upon treatment of the solution of **43** in THF with a solution of lithium diisopropyl amide (LDA) in THF, then with a solution of I₂ in THF. The reaction mixture was neutralized with acetic acid, treated with water and the product 2',3',5'-tri(*tert*-butyldimethylsilyl)-8-iodoadenosine **44** was separated by silica gel column chromatography (hexane/ethyl acetate). The reaction temperature played a decisive role in the success of the substitution reaction. When the reaction temperature was higher than the designated range, side-products were formed due to the reaction of the unprotected amino function of adenosine with LDA. On the contrary, when the reaction temperature was far below -75 °C, there was no reaction.

44 was treated with TBAF·3H₂O to give 8-iodoadenosine **45**. The purification of **45** by silica gel column chromatography or recrystallization failed due to the limited solubility of this compound in organic solvents or water. TBAF could not be completely removed from **45**. A milder fluoride reagent, Et₃N·3HF, was then used. The treatment of **44** with Et₃N·3HF in DMF overnight completely cleaved off the TBDMS protecting groups. After the reaction, DMF was removed by co-evaporation with toluene, the residue was suspended in ethanol and filtered through glass filter. Traces of the fluoride reagent were readily eliminated by thoroughly washing with ethanol and diethyl ether. Both the TBDMS-protected 8-iodoadenosine **44** and 8-iodoadenosine **45** have been used as substrates for the Heck coupling reactions.

In order to synthesize the amino-acylated derivative of **45** (for explanation, see Section 3.2.6.6), the TBDMS-protected 8-iodoadenosine **44** was treated with isobutyric anhydride, since the direct acylation of **45** is impossible due to its low solubility in any organic solvents even at elevated temperatures.

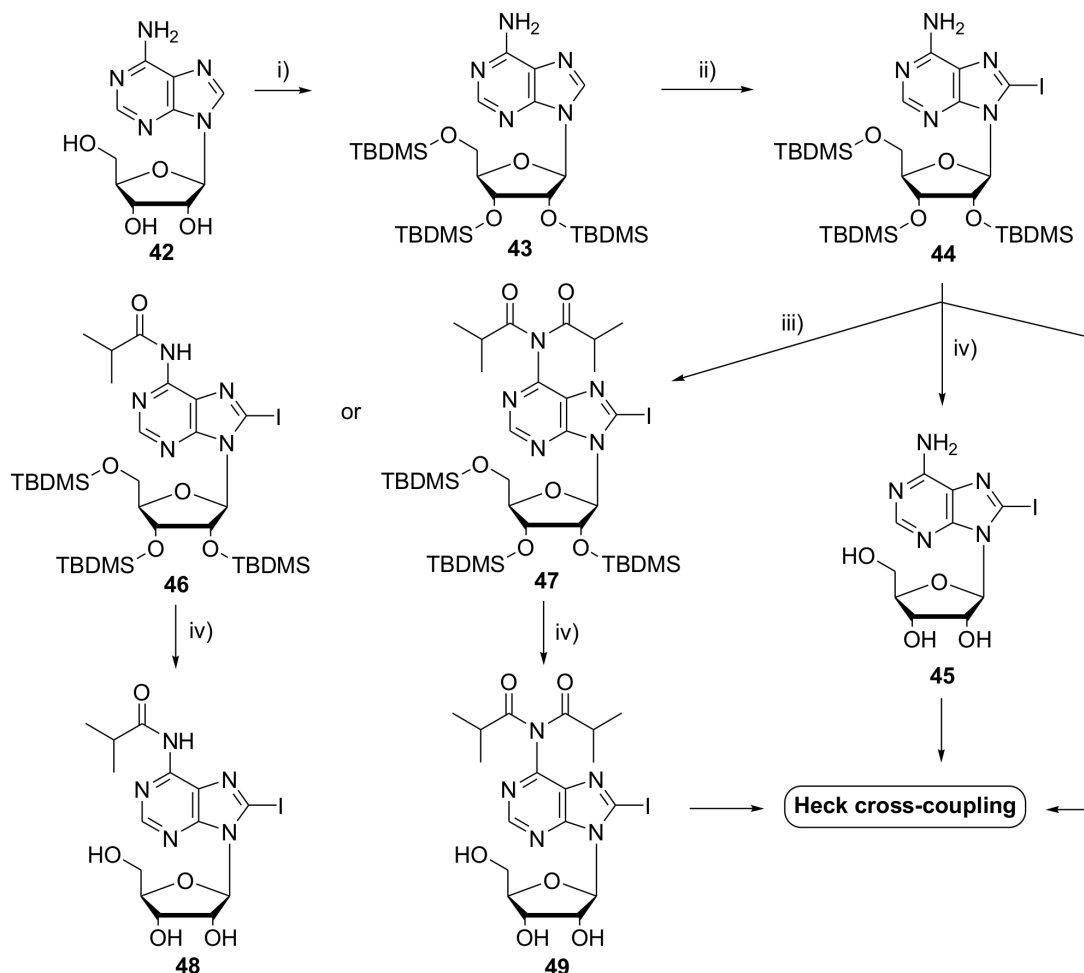


Figure 48 – Synthesis of 8-iodoadenosine and its derivatives for the Heck cross-coupling reaction: i) **42**, 3.5 eq. TBDMS-Cl, 7.8 eq. imidazole, DMF, RT, overnight, 88%; ii) **43**, 1.5 eq. LDA, THF, (-70)-(-75) °C 5.5 h, 1.8 eq. I₂, (-70)-(-75) °C 3 h, 5.0 eq. acetic acid, 10 min., 66%; iii) **44**, 15 eq. isobutyric anhydride, pyridine, RT, 3 days, **46** (69%), **47** (6%); iv) **44**, **46** or **47**, 3.5 eq. Et₃N·3HF, DMF, RT, overnight, **45** (81%), **48** (82%).

The acylation reaction of **44** took place slowly because of the bulkiness of the three TBDMS groups. Even with highly excess amounts of the acylating reagent, **46** could only be obtained with adequate yield only after 3 days. A small amount of **47** was also separated. The deprotection of the TBDMS-protecting groups of **46** and **47** was carried out as described above for **44** to give **48** and **49**, respectively.

8-Iodoadenosine and its derivatives have then been used as the halogen substrates for the introduction of the double-bond linker **L1** into the C-8 position of adenosine by the Heck coupling reaction.

3.2.6.4 The Heck coupling reaction of 2',3',5'-tri(*tert*-butyldimethylsilyl)-8-iodoadenosine and **L1**

Having 8-iodoadenosine and its derivatives in hand, we have first tested the Heck coupling reaction of **44** and **L1** basing on the reported studies (Williams *et al.* 2001; Jefery 1994; Zhang & Daves 1993). The reaction conditions having been investigated are summarized in Table 8.

Table 8 – The Heck cross-coupling reactions of **44** and **L1**.

Entry	L1 (eq.)	Catalyst (eq.)	Ligand (eq.)	Base (eq.)	PT-R ^a (eq.)	Sol. ^b	T./Time (°C)/(h)	Result ^c
1	4.0	Pd(OAc) ₂ 0.2	-	K ₂ CO ₃ 2.5	<i>t</i> Bu ₄ NCl 1.1	DMF	50-80 /24	NR
2	3.0	Pd(dba) ₂ 0.1	PPh ₃ 0.2	<i>n</i> Bu ₃ N 1.5	-	MeCN	60-80 /24	NR
3	60.0	Na ₂ [PdCl ₄] 0.2	-	-	-	DMF/ KOAc	80/2.5	Dec.

^aPT-R: phase-transfer reagent. ^bSol.: solvent. ^cNR: no reaction, Dec.: decomposition of **44**.

In non-aqueous solvents and in the presence or absence of the triphenylphosphine ligand, no reaction has been observed between **44** and **L1** under the Heck coupling reaction conditions (entries 1 and 2).

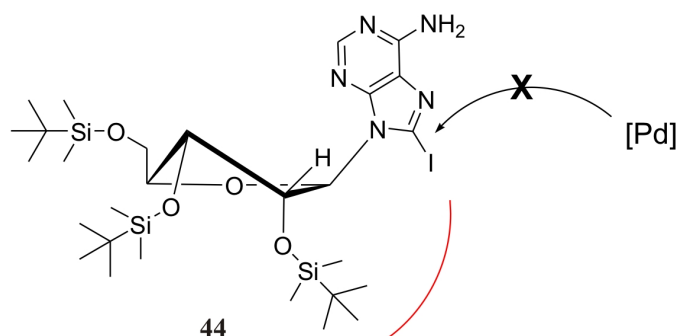


Figure 49 – Suggested steric hindrance of **44** in the Heck coupling reaction with **L1**. The three TBDMS-protecting groups, particularly the one at the 2'-O-position, prevent the catalyst from accessing the C8-I reaction center.

The addition of the phase-transfer reagents according to Jeffery's protocol had no effect. The application of the catalyst Na₂[PdCl₄] in DMF/KOAc buffer 0.1 M, pH 5.2 (Bumagin *et al.* 1989; Dey & Sheppard 2001) led to the cleavage of the 5'-O-TBDMS protecting group and the reduction of **44** to 2',3',5'-tri(*tert*-butyldimethylsilyl)adenosine as could be noticed from ¹H NMR spectrum of the sample (entry 3).

The low reactivity of compound **44** in the Heck coupling reactions with **L1** could be assigned to the three bulky TBDMS protecting groups which inhibit the access of the palladium catalyst to the reaction center, the C8-I bond (Figure 49). Therefore, **44** was deprotected to give 8-iodoadenosine **45** which was applied as the halogenated substrate in the next experiments.

3.2.6.5 The Heck coupling reaction of 8-iodoadenosine and **L1**

By the treatment of **44** with Et₃N.3HF in DMF, 8-iodoadenosine **45** has been prepared in pure form as confirmed by NMR analysis and used as the halogen substrate for the Heck cross coupling reaction with the linker **L1**. The conditions being tried are shown in Table 9.

Table 9 – The Heck coupling reactions of **45** and **L1**.

Entry	L1 (eq.)	Pd(II) ^a (eq.)	PT-R ^b (eq.)	Solvent ^c	T./Time (°C)/(h)	Result ^d
1	8.5	1.1	-	DMF/NaOAc buffer	80/8.5	Red. to A.
2	30.0	0.3	-	DMF/KOAc buffer	81/24	Red. of C=C
3	8.5	1.1	-	DMA/KOAc bufer	80/8	Red. to A.
4	30.0	0.27	<i>t</i> Bu ₄ NCl	DMF/KOAc buffer	81/24	Mix.
5	15.0	0.34	<i>t</i> Bu ₄ NCl	DMF/KOAc buffer	80/24	Red. of C=C

^aIn all cases, Na₂[PdCl₄] was used as catalyst. No ligand was added. ^bPT-R: phase-transfer reagent. ^cNaOAc, KOAc: sodium and potassium acetate buffer 0.1 M pH 5.2; DMF/aqueous buffer 1:1 (v/v). ^dRed. to A.: reduction of **45** to adenosine, Red. of C=C: reduction of the double-bond, Mix.: mixture of Heck cross-coupled product, its isomer with the rearranged double-bond (Section 3.2.6.2, Figure 46) and their reduced form.

8-Iodoadenosine was hardly dissolved in the solvents for Heck reactions (aqueous DMF or DMA) even at 80 °C. Therefore, high amounts of solvents must be added in order to make the reaction mixture homogeneous. As a result of this dilution, the concentrations of the halogen substrate and reagents were significantly lower than in normal Heck coupling reactions. Under these reaction conditions, only undesired by-products have been observed (entries 1-5). Efforts to search for other Heck reaction solvents which can improve the solubility of compound **45** failed.

In many experiments shown in Table 9, KOAc buffer has been used instead of NaOAc buffer, since the former has been reported to allow fast Heck coupling reactions of iodo derivatives at low temperatures (Bumagin *et al.* 1989). In the presence of an excess amount of the palladium catalyst, adenosine was predominantly formed (entries 1 and 3). This is supposedly due to the accelerated oxidative insertion that leads to the formation of high amounts of the intermediate

ArPd(II)L₂Br (Figure 15) which was not transformed fast enough into the cross-coupled product, but protolytically cleaved to adenosine. The protolytical cleavage of the intermediates of the oxidative insertion in Heck coupling reactions has also been observed before (Chu *et al.* 1992; Stokker 1987). Increasing the amount of the linker **L1** and reducing the amount of the palladium(II) catalyst did help to overcome the side-reaction after the oxidative addition step, but again the intermediate of the palladium(II) and linker **L1** was protolytically degraded in part to the reduced form of the Heck cross-coupled compound (Figure 15, path B), as indicated by MALDI-TOF analysis of the samples (entries 2 and 5). After the insertion of the Pd-complex into the double-bond, the reductive β -hydride elimination of PdH is supposed to be delayed due to the complexation of [Pd] with the nitrogen atoms of the heterobase, thus prolonging the exposure of the intermediate of the *syn*-addition to protolytical cleavage. The phase-transfer reagent *t*Bu₄NCl did not have any effect (entries 4 and 5).

In the next experiments, compounds **48** and **49** (Figure 48), the acylated derivatives of compound **45**, have been synthesized and used as the halogen substrates for the Heck coupling reaction.

3.2.6.6 The Heck coupling reaction of *N*-isobutyryl-8-iodoadenosine and *N,N'*-diisobutyryl-8-iodoadenosine with **L1**

The Heck coupling reactions involving nitrogen heterocyclic systems have been reported to be especially challenging, owing to the potential of nitrogen-rich systems to inactivate the catalysts and to lead to side-reactions by N-Pd complexation (Zhang & Daves 1992; Zhang & Daves 1993). In order to suppress the complexation, the amino function of 8-iodoadenosine **45** was protected with isobutyric anhydride to give *N*-isobutyryl-8-iodoadenosine **48** and *N,N'*-diisobutyryl-8-iodoadenosine **49**. In these compounds, the *N*7 atom which can potentially complex with the palladium catalyst due to its vicinity to the reaction center is partly masked by the isobutyryl group. Moreover, this protection may increase the solubility of **45** in the solvents used for the Heck coupling reactions. Thus, different Heck coupling reaction conditions have been tried with these two substrates (Table 10).

In fact, compound isobutyryl *N*-protected 8-iodoadenosine **48** was well dissolved in DMF/acetate buffer. The protecting group, however, was fast and completely cleaved off after 2 hours under the Heck reaction conditions, leading to the precipitation of 8-iodoadenosine. The reaction was allowed to continue during which the precipitated 8-iodoadenosine was gradually dissolved. Different mixtures of the Heck cross-coupled product, its isomer with the rearranged double-bond (Figure 46C and D, respectively) and their reduced form were obtained (entries 1-3) as indicated by MALDI-TOF-MS and NMR analyses. Depending on the amount of the catalyst being used, the ratio of the reduced form to the double-bond isomers in these

mixtures ranged from 1:1 to dominant (entries 1-2). ^1H NMR and MALDI-TOF-MS analyses of the sample in entry 3 indicated the formation of a mixture of Heck cross-coupled product and its isomer: they had the same mass and nearly superimposing ^1H NMR signals, except that the signals supposedly belonging to the *NH* protons of the linker were observed at 9.51 and 11.32 ppm, respectively (Section 3.2.6.2). Increasing the amount of the Pd(II) catalyst to 1.0 eq. led to the reduction of the starting material to adenosine (entry 4).

Table 10 – The Heck coupling reactions of **48** and **49** and **L1**.

Entry	L1 (eq.)	Pd(II) ^a (eq.)	Solvent ^b (1:1)	T./Time (°C)/(h)	Result ^c
1	7.0	0.15	DMF/KOAc buffer	80/72	Red. of C=C
2	7.0	0.25	DMF/KOAc buffer	80/36	Red. of C=C
3	7.0	0.5	DMF/NaOAc buffer	80/32	Mix.
4	7.0	1.0	DMF/KOAc buffer	80/4	Red. to adenosine

^aIn all cases, $\text{Na}_2[\text{PdCl}_4]$ was used as catalyst. No ligand was added. ^bNaOAc, KOAc buffer: sodium and potassium acetate buffer 0.1 M pH 5.2. ^cRed. of C=C: reduction of the double-bond, Mix.: mixture of the Heck cross-coupled product and its isomer with the rearranged double-bond (Section 3.2.6.2, Figure 46), Red. to adenosine: reduction of **48** and **49** to adenosine.

From the experimental evidences in Sections 3.2.6.4-3.2.6.6, it can be concluded that 8-bromo-adenosine is more suitable as the halogen substrate in the Heck reactions with the double-bond linker **L1** than its iodo analogue. Therefore, 8-bromoadenosine was continued to be used for the attachment of the long linker **L2** by the Heck coupling reaction.

3.2.7 The Heck coupling reaction of 8-bromoadenosine and **L2**

The Heck coupling reaction between 8-bromoadenosine **19** and the long double-bond linker **L2** was carried out based on that of **19** and **L1** in aqueous organic solvents (section 3.2.6.2). Thus, **19** and an excess amount of **L2** were dissolved in DMF/NaOAc buffer 1:1 (v/v). To the resulting mixture, a solution of the catalyst $\text{Na}_2[\text{PdCl}_4]$ in DMF was added while vigorously stirring. The reaction mixture was purged with argon and placed into an oil-bath at 80 °C. The formation of the black palladium and adenosine as side-products was observed during the reaction time. After the reaction had finished, the reaction mixture was concentrated by co-evaporation with toluene, the residue was suspended in methanol, filtered to remove the black precipitate and purified by silica gel column chromatography (MeOH/DCM).

^1H and ^{13}C NMR and MALDI-TOF-MS analyses of the separated compound confirmed that it was the isomer of the Heck cross-coupled product with the rearranged double-bond (Figure

50). In this case, the signal of the amide NH proton of the allylamine moiety is a doublet, indicating clearly that it is in the vicinity of only one proton, namely the proton of the methyldiene -CH= group, as the result of the double-bond rearrangement.

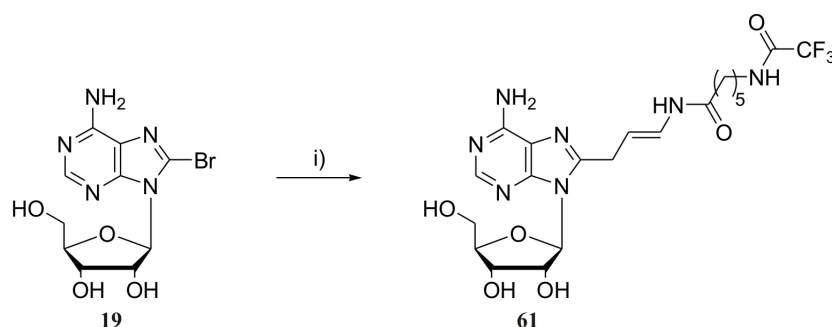


Figure 50 – Synthesis of 8-(3-[6-trifluoroacetamidohexanamido]-prop-2-en-1-yl)adenosine from **19** and **L2**: i) **19**, 8.5 eq. **L2**, 0.5 eq. $\text{Na}_2[\text{PdCl}_4]$, 0.1 M NaOAc buffer pH 5.2, DMF, 80 °C, 10 h, 35%.

3.2.8 The Heck cross-coupling reaction of 2-iodoadenosine and **L1**

After having investigated the Heck coupling reactions of the linkers **L1** and **L2** to the C8 of adenosine, we set out to synthesize adenosine derivatives with linkers attached to the C2. The synthesis of the 2-amino linker modified adenosines by the Heck coupling reaction was conducted with 2-iodoadenosine **27** and the linker **L1** (Figure 51).

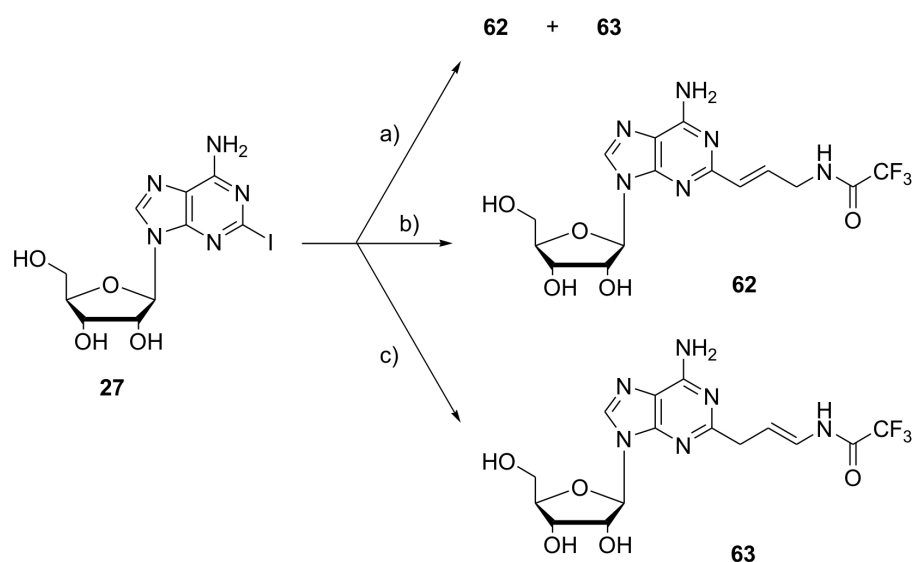


Figure 51 – The Heck cross-coupling reactions of **27** and **L1**: a) **27**, 8.5 eq. **L1**, 0.5 eq. $\text{Na}_2[\text{PdCl}_4]$, 0.1 M NaOAc buffer pH 5.2, DMF, 80 °C, 4.5 h, 1:1 mixture of the Heck cross-coupled product **62** and its isomer **63**. b) **27**, 1.9 eq. **L1**, 0.2 eq. palladacycle, 1.1 eq. NaOAc, 1.1 eq. Bu_3N , DMA, 85 °C 2 h, 100 °C 19 h, **62**, 17%. c) **27**, 2.5 eq. **L1**, 0.17 eq. $\text{Pd}(\text{OAc})_2$, 0.34 eq. AsPh_3 , 1.6 eq. Bu_3N , DMF, 65 °C 14 h, 80 °C 9 h, **63**, 28%.

After the reaction had finished, the reaction mixture was concentrated under reduced pressure. The residue was taken up in methanol and filtered to remove the precipitates. The products

were purified by silica gel column chromatography (MeOH/DCM) and reversed-phase HPLC (Gradient D, Table 24) and analyzed by NMR and MALDI-TOF-MS.

Different reaction conditions have been tested in order to improve the coupling yields and to achieve pure isomers. Depending on the reaction conditions, especially on the nature of the palladium catalysts, different ratios of the Heck cross-coupled product **62** to its isomer with the rearranged double-bond **63** have been observed: a) $\text{Na}_2[\text{PdCl}_4]$ gave rise to the formation of a 1:1 mixture of **62** and **63**; b) palladacycle allowed the production of the expected Heck cross-coupled product **62** as the main compound and c) $\text{Pd}(\text{OAc})_2$ produced exclusively the isomer **63**.

The formation of the mixture of the Heck cross-coupled product and its isomer can again be assigned to the intervention of the nitrogen atoms of the nucleobase, namely N1 and N3, in the β -hydride elimination step (Figure 52).

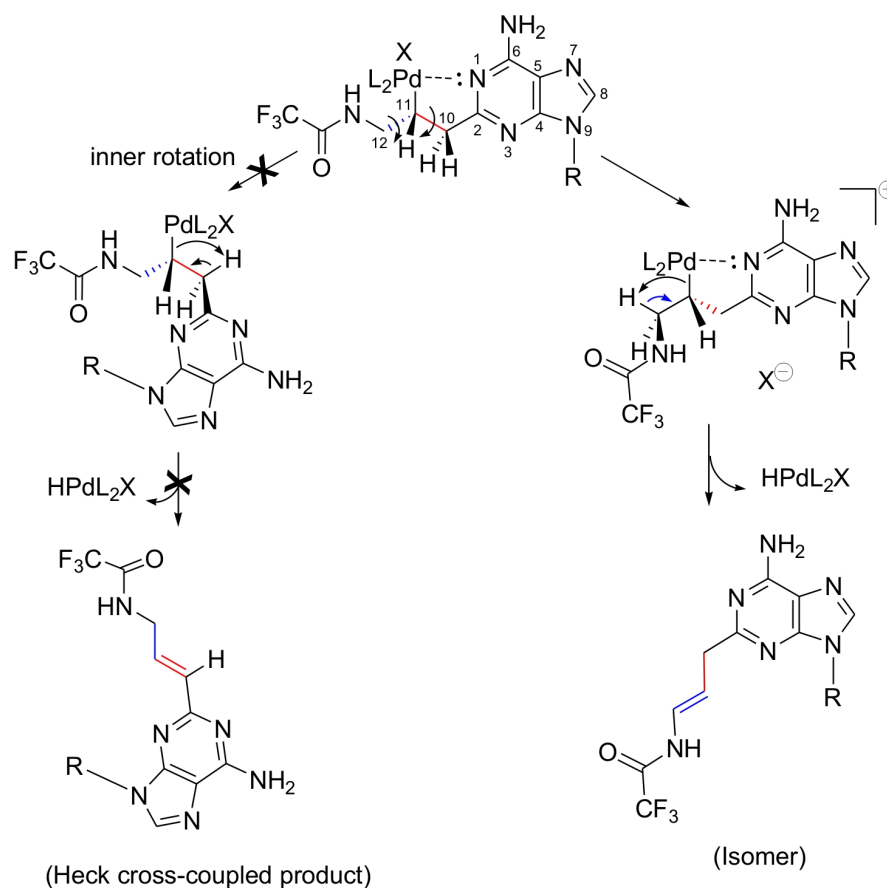


Figure 52 – The restriction of the inner rotation during the Heck cross-coupling reaction of **27** and **L1** due to palladium-nitrogen complexation. R: D-ribofuranosyl, X: Br^- or AcO^- .

The complexation of palladium with the nitrogen atom N3 is less likely, as the access to N3 is partly hindered by the ribofuranose ring. Due to the complexation between [Pd] and N1, the free inner rotation of the two bonds C2-C10-C11 between [Pd] and the heterocycle may be restricted, preventing palladium from reaching to the *syn* position with one of the two β protons on the side of the heterocycle (the two protons at the C10). Therefore, the β -hydride

elimination have to call for the other two β protons on the other side (the two protons at the C12) where the inner rotation is free from restriction. The β -hydride elimination on this side leads to the formation of the isomer of the Heck cross-coupled product with the rearranged double-bond. The *trans*-configuration is favored, since it results from the intermediate having lower energy (see Figure 42, Section 3.2.4). It can be noticed that the isomer distribution depends heavily on the nature of the catalysts. A possible explanation is the sizes of the catalysts that influence the complexation of palladium to N1.

Since compound $\text{Pd}(\text{OAc})_2$ has the smallest size of the three catalysts, it could avoid steric hindrance with the purine ring in the eclipse conformation of the intermediate resulting from the coordination-insertion step. In this conformation, the palladium catalyst and N1 are coplanar. Therefore, the palladium-nitrogen complexation is highly effective. The inner rotation of the C-C bonds between the palladium center and the purine ring may be completely inhibited, leading to the failure of the β -hydride elimination on the ring side, and consequently to the formation of the Heck isomer.

When using Herrmann's catalyst, the palladacycle (Figure 19), as catalyst, no double-bond rearrangement has been observed. The central "Pd" of the palladacycle is surrounded by bulky bidentate ligands, hence being prevented from complexing with the nitrogen atoms of the nucleobase. The palladium-nitrogen complex, if somehow forms, is also not favored due to the steric interactions between the ligands and the ring. Therefore, the free inner rotation may have been recovered, resulting in the formation of the expected Heck cross-coupled product **62**. The disadvantage of palladacycle, in this case, is that it is only active with the iodo-derivative at temperatures above 100 °C.

The catalyst $\text{Na}_2[\text{PdCl}_4]$ has the intermediate size and bulkiness compared to the two above mentioned ones, hence being able to partly complex with the ring nitrogen. In addition, in aqueous organic solutions (condition (a), Figure 51), the complexation is suppressed to some extent as the nitrogen atoms are partly masked by the hydrate shell. The limited palladium-nitrogen complexation allows only partial inner rotation, thus leading to the formation of a mixture of the Heck cross-coupled product and its isomer.

Interestingly, under the same reaction condition, $\text{Na}_2[\text{PdCl}_4]$ led to the complete double-bond isomerization of the C8-coupled product (see Section 3.2.6.2). In this case, more space is provided around the N7-C8 site and there is less steric interaction between the palladium and the ring. Therefore, the palladium-nitrogen complexation becomes more efficient and strictly controls the conformation required for the β -hydride elimination. The higher complexing ability of the nitrogen atom N7 in comparison with N1 may also account for the inhibited rotation at the C-8 position and the dominant formation of the Heck isomer. Unfortunately, the influence of the two catalysts $\text{Pd}(\text{OAc})_2$ and palladacycle on the distribution of the isomers in case of the C8 cross-coupled products can not be evaluated as they do not effect any transformation of the less active 8-bromo analogue.

3.2.9 The Heck coupling reaction of 2-iodoadenosine and L2

Based on the Heck reaction of 5-iodouridine **1** and the linker **L2** (see Section 3.2.5), the cross-coupling between 2-iodoadenosine **27** and **L2** was conducted with an excess amount of **L2** in the presence of the catalyst $\text{Na}_2[\text{PdCl}_4]$ in DMF/NaOAc buffer 1:1 (v/v) at 81 °C for 5 hours (Figure 53). After the reaction, the solvents were removed by co-evaporation with toluene under reduced pressure. The resulting residue was resuspended in methanol, filtered to remove the black precipitate and purified by silica gel column chromatography and reversed-phase HPLC (Gradient D, Table 24).

The sample was analyzed by ^1H NMR and MALDI-TOF-MS. Analysis data showed the formation of a 1:1 mixture of the Heck cross-coupled product **64** and its isomer **65**.

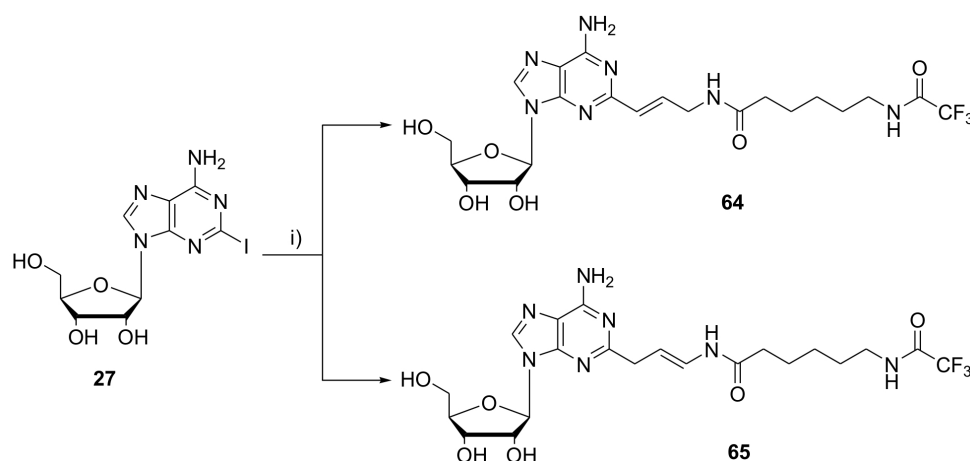


Figure 53 – The Heck cross-coupling reaction of **27** and **L2**: i) **27**, 8.5 eq. **L2**, 0.5 eq. $\text{Na}_2[\text{PdCl}_4]$, 0.1 M NaOAc buffer pH 5.2, DMF, 80 °C, 4.5 h, **64** and **65** (1:1) 18%.

Presumably, results obtained in the Heck coupling reactions of compound **27** and **L2** in the presence of other catalysts such as $\text{Pd}(\text{OAc})_2$ and palladacycle are similar to what has been observed in the coupling reaction of **27** and the short linker **L1**. Nevertheless, more experiments must be done in order to confirm the effects of different catalysts on the ratio of the Heck cross-coupled product **64** to its isomer **65**.

3.3 Amino linker modified nucleosides for further protection and phosphorylation

All the amino linker modified nucleosides which have been synthesized by the Heck and Sonogashira coupling reactions are summarized in Figure 54. Further protection of these building blocks by acylation of the exocyclic amino function, tritylation and silylation of the 5'- and 2'-OH groups, respectively were carried out before they were functionalized by the phos-

by co-evaporation with toluene, the resulting residue was resuspended in MeOH, filtered to remove the precipitate and purified by silica gel column chromatography (MeOH/DCM).

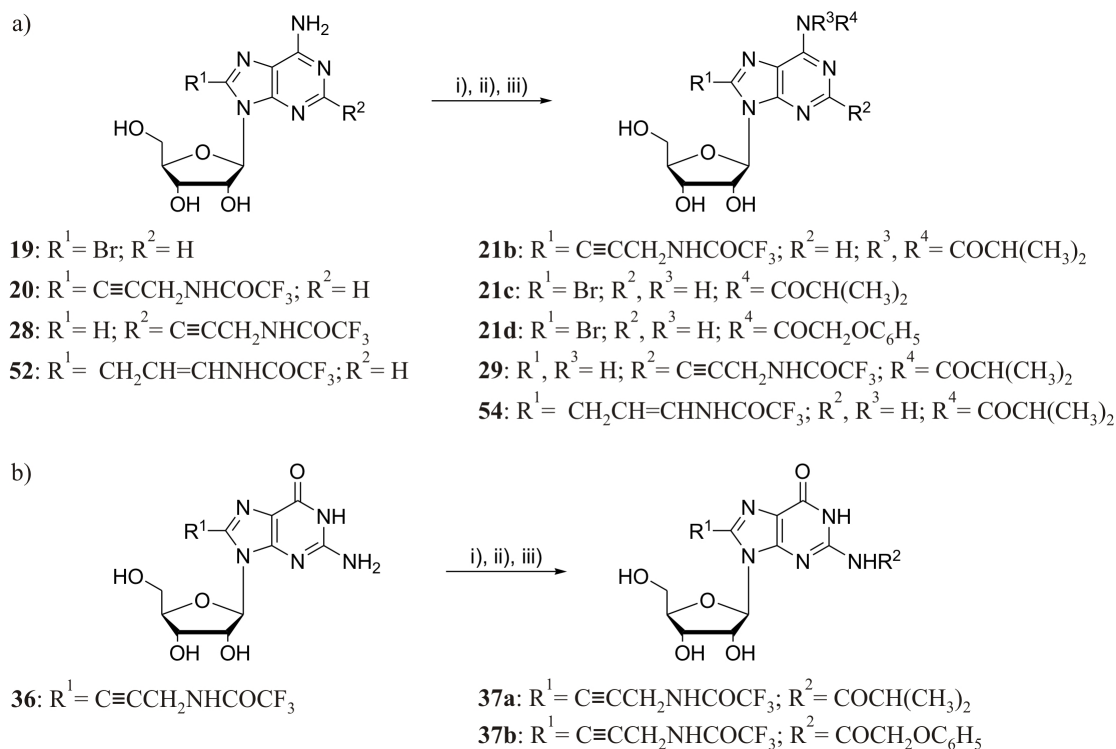


Figure 55 – The protection scheme of the amino functions of a) adenosine and b) guanosine derivatives: i) **19**, **20**, **28**, **36** or **52**, 7.5-15.0 eq. TMS-Cl, pyridine, 0 °C 5 min., RT 2 h; ii) acylating reagent 0 °C 5 min., RT; iii) H₂O 0 °C 10 min., 2.5 M NH₃ 0 °C 30 min.

Different phenoxyacetylating reagents have been tested for the protection of 8-(3-trifluoroacetamidoprop-1-ynyl)adenosine **20** (section 3.1.4). The acylation reaction conditions having been tried are summarized in Table 11. Unfortunately, all attempts were unsuccessful (entries 1-6).

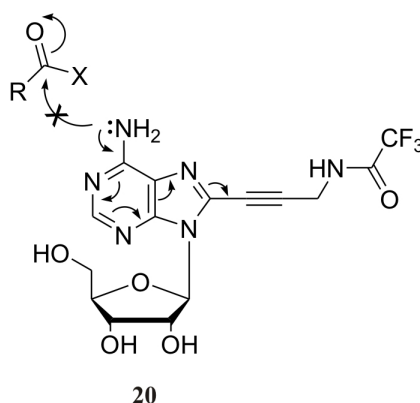


Figure 56 – The unsuccessful protection of 8-(3-trifluoroacetamidoprop-1-ynyl)adenosine **20** with the PAC protecting group supposedly due to the electronic effect of the linker **L3**.

When looking at the structure of **20** (Figure 56), one may suggest that due to the newly attached linker that is conjugated to the purine ring, the electron density on the amino group is shifted

toward the triple bond. This withdrawing-electron effect reduces the nucleophilicity of the amino function, making it impossible to attack the carbonyl carbon of the acetyl moiety.

Table 11 – The protection of the amino function of 8-(3-trifluoroacetamidoprop-1-ynyl)adenosine **20**^a.

Entry	Acylating reagent ^b /(eq.)	T.(°C)/Time(h)	Result ^c
1	(PhOAc) ₂ O/3-8	RT/24	NP
2	PhOAcCl/1.1	-25/5	NP
3	PhOAcCl+HOBT/1.5	RT/24 or 55/4	NP
4	PhOAcCl+triazole/1.5	RT/1; 55/7	NP
5	PhOAcOH+CDI/1.1-1.2	RT/24 or 40/24	NP
6	PhOAcOH+DCC+ <i>p</i> NP/1.0	RT/24	NP
7	(Ibu) ₂ O/1.5-2.0	RT/2	51%

^aThe nucleoside was first protected with TMS-Cl. ^bPhOAc: phenoxyacetyl, HOBT: 1-hydroxybenzotriazole, triazole: 1,2,4-triazole, CDI: carbonyl diimidazole, *p*NP: *p*-nitrophenol. ^cNP: no product was separated.

The synthesis strategy was then changed: the amino group of 8-bromoadenosine **19** was first protected with the phenoxyacetyl group (entries 1-2, Table 12) and then the linker **L3** was introduced into the C-8 by the Sonogashira coupling reaction. The phenoxyacetyl group was successfully introduced into the amino function of **19** to give *N*-6-phenoxyacetyl-8-bromoadenosine **21d** (entry 2, Table 12). Nevertheless, the Sonogashira coupling reaction between **21d** and **L3** again did not proceed (entry 2, Table 3, Section 3.1.4).

Table 12 – The protection of the amino function of 8-bromoadenosine **19**^a.

Entry	Acylating reagent ^b /(eq.)	T.(°C)/Time(h)	Result ^c
1	(PhOAc) ₂ O/5.0	RT/2	NP
2	PhOAcCl+triazole/1.5	55/5	55%
3	(Ibu) ₂ O/2.0	RT/2.5	50%

^a**19** was first protected with TMS-Cl. ^bPhOAc: phenoxyacetyl, triazole: 1,2,4-triazole, (Ibu)₂O: isobutyric anhydride. ^cNP: no product was separated.

On the contrary, the corresponding *N*-6-isobutyryl-8-bromoadenosine (entry 3, Table 12) was able to be cross-coupled with the linker **L3** under the Sonogashira coupling reaction (entry 3, Table 3) and 8-(3-trifluoroacetamidoprop-1-ynyl)adenosine **20** was effectively isobutyrylated (entry 7, Table 11). These evidences indicated that the impossible combination of the linker **L3** and the phenoxyacetyl protecting group is very likely due to steric hindrance. These two

groups can not be introduced together into 8-bromoadenosine, as the first attached one inhibits the in-coming of the other, regardless which one is introduced first (for more detailed discussion, see Section 3.1.4, Figure 33). The isobutyryl group has a shorter carbon chain and is less bulky, hence causing less steric hindrance.

The final concentration of ammonia in solution during the alkaline treatment was important. When the final concentration of ammonia in the reaction mixtures was lower than 1.5 M and the treatment was shorter than 20 minutes, *N,N'*-6-diisobutyryl-8-(3-trifluoroacetamidoprop-1-ynyl)adenosine **21b** was obtained. Prolonging the treatment time to over 4 hours helped to completely cleave off the second isobutyryl, but led unfortunately to the deprotection of the linker as well. A final concentration of 2.5 M of ammonia and an alkaline treatment for 30 minutes at 0 °C gave the desired protected product *N*-6-isobutyryl-8-(3-trifluoroacetamidoprop-1-ynyl)adenosine **21a** (entry 7, Table 11).

Basing on this reaction condition, the amino functions of all of other amino-linker modified building blocks were successfully protected with isobutyric anhydride (Table 13).

Table 13 – The protection of the amino functions of the amino linker modified nucleosides **20**, **28**, **36** and **52** nucleosides with isobutyric anhydride (Ibu)₂O^a.

Entry	Nucleoside ^b (1.0 eq.)	(Ibu) ₂ O(eq.)	Time(h)	Yield(%)
1	8-L3-A 20	1.7	2.0	51
2	2-L3-A 28	2.3	2.0	81
3	8-L1'-A 52	3.8	2.0	38
4	8-L3-G 36	2.2	2.0	73

^aAll of the nucleosides were first transiently protected by the reaction with 7.5-15.0 eq. TMS-Cl in 1-2 h. ^bL3: linker **L3**, L1': the linker **L1** with the rearranged double-bond, A: adenosine, G: guanosine.

The three OH groups of the nucleosides were first transiently protected with excess amounts of TMS-Cl in pyridine basing on reported procedures (Ti *et al.* 1982). The TMS-protected nucleosides were then treated with slight excess of isobutyric anhydride. After the reactions had finished, the reaction mixtures were treated with the ammonium solution to cleave off the TMS-protecting groups and the second isobutyryl group on the amino functions (if any).

This protection procedure has also been successfully applied to other building blocks: 2-(3-trifluoroacetamidoprop-1-ynyl)adenosine **28**, 8-(3-trifluoroacetamidoprop-1-ynyl)guanosine **36**, 8-(3-trifluoroacetamidoprop-2-en-1-yl)adenosine **52**. Noticeably, 8-(3-trifluoroacetamidoprop-1-ynyl)guanosine could be protected with the phenoxyacetyl group, since the amino function on the C-2 and the C-8 position are on different sides of the heterocycle and are not effected by steric hindrance (see Figure 33, Section 3.1.4). The phenoxyacetylation yield was, however, modest (28%).

Interestingly, the *N,N'*-6-diisobutyryl-8-(3-trifluoroacetamidoprop-1-ynyl)guanosine runs significantly more slowly than the corresponding *N*-monoisobutyryl, as indicated by TLC (SiO_2 ; MeOH/DCM). This can be explained by the fact that the 2-amide group of the monoisobutyryl protected nucleoside can form intramolecular hydrogen-bonds with one of the hydroxyl groups of the sugar (Figure 57), hence reducing the hydrophilicity of the nucleoside. On the contrary, the imide group of the *N,N'*-diisobutyryl protected nucleoside can not generate intramolecular hydrogen-bonds and does not affect the polarity of the molecule (Hakimelahi *et al.* 1982).

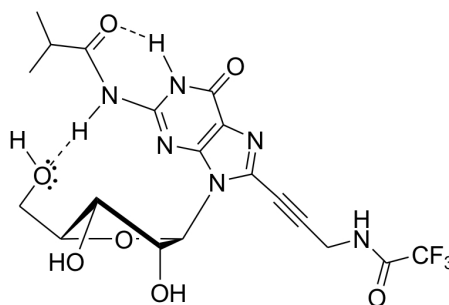


Figure 57 – Intramolecular hydrogen bonding of *N*-6-isobutyryl-8-(3-trifluoroacetamidoprop-1-ynyl)guanosine.

MALDI-TOF-MS analysis of an 8-mer RNA containing the isobutyryl-protected **28** showed that the isobutyryl protecting group was completely cleaved off under the standard deblocking procedure used for RNA synthesized from PAC-protected phosphoramidites (Table 18).

3.5 The protection of the 5'-OH group by dimethoxytritylation

The 5'-OH group is the only primary hydroxyl group of the three hydroxyl functions of a ribonucleoside. It is not only the least influenced by the electron-withdrawing effects of other substituents of the sugar moiety but also the least sterically hindered. Therefore, it shows the highest activity of the nucleoside's OH groups in nucleophilic substitution reactions.

In the 2'-*O*-TBDMS-3'-*O*-phosphoramidite chemistry, the 5'-OH group of the phosphoramidite building blocks is standardly protected by the DMT group (Figure 58). During the chemical synthesis of an oligonucleotide, this 5'-*O*-protecting group is periodically cleaved off after every cycle of the chain assembly under mild acidic conditions. The freed 5'-OH group of the growing chain can then be coupled with the in-coming phosphoramidite.

The 5'-*O*-protection of the modified nucleosides by the dimethoxytritylation reactions with DMT-Cl has been carried out basing on literature procedures (Hakimelahi *et al.* 1982; Shah *et al.* 1994). As the tritylating reagent and the tritylated nucleoside are easily hydrolyzed by protonic acids in the presence of water, the starting material must thoroughly be dried by co-evaporation with anhydrous pyridine and dry DCM and kept overnight under vacuum. In

addition, the tritylation reaction mixture must be protected from moisture by an argon stream introduced through a drying tube during the reaction time.

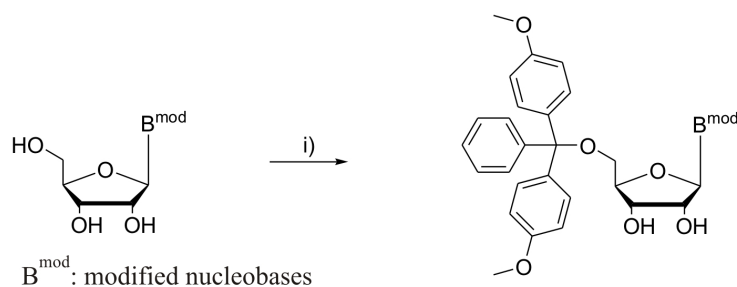


Figure 58 – The protection of the 5'-OH groups of the modified nucleoside building blocks by dimethoxytritylation: modified uridine, adenosine or guanosine nucleoside, 1.3-1.5 eq. DMT-Cl, pyridine, ice-cold or RT, 50-87%.

For the tritylation of the uridine derivatives (entries 1-3, Table 14), 1.2 eq. DMT-Cl was added all at once in solid form to the ice-cold solution of the nucleoside in pyridine. The ice-bath was then removed, the reaction mixture was stirred at room temperature and the progress of the tritylation was monitored by TLC (SiO_2 ; MeOH/DCM). After 2-3 hours, another 0.1-0.2 eq. DMT-Cl was added to the mixture, as TLC indicated the presence of the starting material. The most part of the starting nucleoside was consumed after 8-9 hours. Keeping the reaction overnight did not lead to the complete conversion of the starting material. Also, the addition of DMAP (Chaudhary & Hernandez 1979) did not accelerate the velocity or improve the transformation. Anhydrous MeOH was added to quench the unreacted DMT-Cl and the reaction mixture was treated with solutions of NaHCO_3 and NaCl. The work-up with the solution of NaHCO_3 is necessary, as it helps to neutralize the hydrochloric acid formed during the reaction and prevents the detritylation.

Table 14 – The protection of 5'-OH group by dimethoxytritylation^a.

Entry	Nucleoside ^b (1.0 eq.)	DMT-Cl(eq.)	T(°C)/Time(h)	Yield(%)
1	5-I-U 1	1.2	RT/overnight	59
2	5-L1-U 8	1.2	RT/overnight	66
3	5-L2-U 14	1.2	RT/6	50
4	N6-Ibu-8-L3-A 21a	1.5	0/2; RT/4	80
5	N6-Ibu-2-L3-A 29	1.5	0/2; RT/6	71
6	N6-Ibu-8-L1'-A 54	1.5	0/2; RT/10.5	22
7	N2-Ibu-8-L3-G 37a	1.5	0/2; RT/0.5	87

^aAll of the reactions were carried out in anhydrous pyridine. ^bL1, L2 and L3: linker **L1**, **L2** and **L3**, L1': linker **L1** with the rearranged double-bond, U: uridine, A: adenosine, G: guanosine.

The residue was then purified by silica gel column chromatography (MeOH/DCM) to afford the 5'-*O*-DMT-protected nucleoside with the yields of 50-55%. The moderate yields for the tritylation reactions can be assigned to the formation of the 3',5'-*O*-ditritylated nucleoside side-products. The formation of these side-products may result from the fast addition of the tritylating reagent (Hakimelahi *et al.* 1982).

Several modifications of the tritylation procedure for the uridine nucleosides have been tested. Thus, 1.3-1.5 eq. solid DMT-Cl were added portionwise as solid into the ice-cold solution of the nucleoside in pyridine (Ahmadian *et al.* 2000). This change did reduce the formation of side-products to some extent and improved the yields up to 66%.

For the tritylation of guanosine and adenosine derivatives (entries 4-7, Table 14), DMT-Cl was dissolved in a small amount of anhydrous pyridine and added dropwise over 2 hours into the ice-cold solution of the nucleoside in anhydrous pyridine. TLC (SiO₂; MeOH/DCM) indicated the completion of the reactions after about 6 hours for adenosine derivatives and after only 2.5 hours for the tritylation of the guanosine derivative without any detectable by-product. The tritylated nucleosides were separated with yields up to 87%. Unfortunately, the application of this procedure for the pyrimidine nucleosides was unsuccessful. The tritylation of the uridine derivatives could only be completed by keeping the reaction mixtures at ambient temperature for 6-8 hours after all of the tritylating reagent was added.

The structures and the purity of the separated compounds have been controlled by NMR and MALDI-TOF-MS analyses (Chapter 5, Section 5.4 - 5.10).

3.6 The protection of the 2'-OH group by *tert*-butyldimethylsilylation

After the 5'-*O*-tritylation, the modified nucleosides have been selectively silylated at the 2'-position (Figure 59) basing on the standard TBDMS chemistry (Ogilvie *et al.* 1974). In contrary to the simple silylating protecting groups like TMS, the bulky TBDMS group produces ether linkages with hydroxyl groups which are much more stable to acids and bases. The 2'-*O*-protection is permanent, that is, the 2'-OH groups stay protected through all the stages of the chemical synthesis of the oligonucleotides. After the synthesis, the TBDMS protecting groups will be cleaved off in the last deprotection step with fluorides to give the fully functional RNA (see Section 3.8.1).

The success of the silylation reaction can be affected by a number of critical factors. The reagents of the silylation reaction are sensitive to water and precautions should be taken to exclude moisture. Thus, the nucleoside must be co-evaporated with anhydrous pyridine and dry DCM and kept under vacuum overnight. The air inlet to the rotary evaporator was connected to an argon source via a drying tube to prevent moist air from getting into the apparatus. The dried nucleoside was dissolved in anhydrous THF followed by the addition of pyridine and

AgNO₃. The mixture was stirred until AgNO₃ was dissolved (the solution became a white emulsion) and TBDMS-Cl was added all at once.

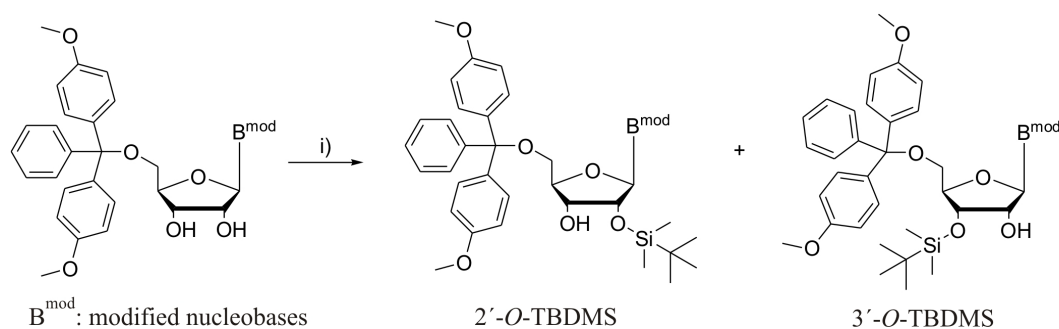


Figure 59 – The protection of the 2'-OH groups of the modified nucleoside building blocks by *tert*-butyldimethylsilylation: i) 5'-O-DMT protected nucleoside, 1.3-1.7 eq. TBDMS-Cl, 1.2-1.5 eq. AgNO₃, 3.7-4.0 eq. pyridine, THF, RT, 6-66%.

The slow addition of the silylating reagent at lower temperature gave no significant improvement in the regioselectivity of the silylation reaction. The reaction flask was protected from moisture and should be opened only long enough for the addition and removal of materials. The progress of the reaction was monitored by TLC (SiO₂; ethyl acetate/hexane). The most part of the starting nucleoside was consumed after different time periods depending on which nucleoside was silylated. Adding more silylating reagent or prolonging the reaction time did not necessarily help to improve the transformation, but increased the amount of side-products (3'-isomer and disilylated nucleosides). When the silylation reaction finished, the reaction mixture was diluted with ethyl acetate or DCM, filtered to remove the AgCl precipitate. The treatment of the resulting solution with a dilute solution of NaHCO₃ prevents detritylation.

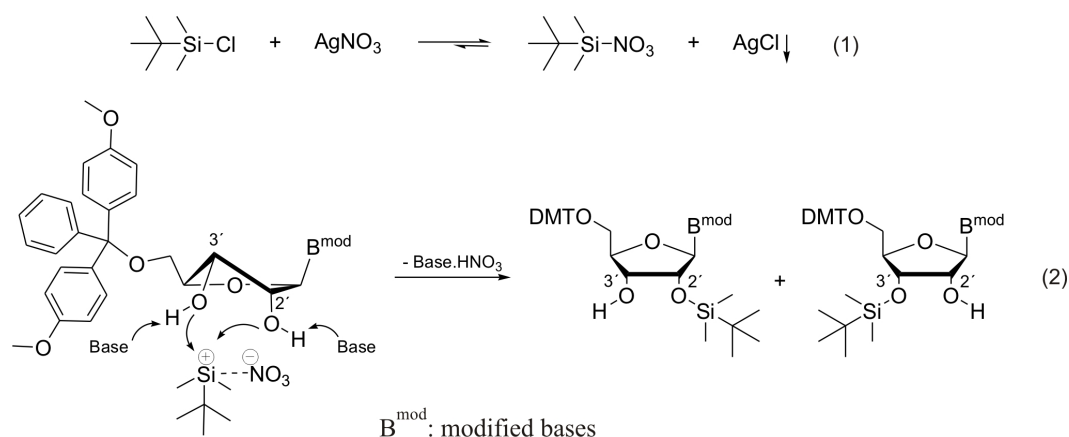


Figure 60 – Effects of AgNO₃ on the silylation reaction: (1) AgNO₃ reacts with TBDMS-Cl to produce the suggested more reactive silylating reagent TBDMS-NO₃; (2) 2'-O-Silylation is favored due to kinetic control.

The addition of AgNO₃ helps to improve the regioselectivity of the silylation reaction. AgNO₃ reacts with TBDMS-Cl to give the more reactive silylating reagent TBDMS-NO₃ (Barton & Tully 1978), as NO₃⁻ is a better leaving group (reaction (1), Figure 60). This reaction is supported by the formation of the AgCl precipitate. The nucleophilic attack of the 2'-OH group on

TBDMS-NO₃ is very likely S_N1 and faster than that of the 3'-OH group, since the OH group at the 2'-position is less sterically hindered (reaction (2), Figure 60). However, beside the 2'-O-TBDMS desired product, the 3'-O-TBDMS isomer as well as the 2',3'-O-di(TBDMS) side-product have always been observed to some extent. On silica gel TLC run in ethyl acetate/hexane, the 2',3'-O-di(TBDMS) protected nucleoside runs the fastest, followed by the 2'-O-TBDMS isomer and the 3'-O-TBDMS is the most slowly. In addition, the 2'-isomer can be readily recognized as it normally appears as the main compound.

The 2'-O-TBDMS isomer was separated from the by-products by silica gel column chromatography (hexane/ethyl acetate). The most important consideration of all is the absolute isomeric purity of the 2'-protected nucleosides which is required for the synthesis of high quality RNA. After chromatographic purification, these products should be carefully examined by heavily loading them on a TLC plate and checking for the presence of traces of the contaminating 3'-isomer by UV-shadowing, exposing to trifluoacetic acid vapor or by NMR analysis. The DMT-protected nucleosides turn orange when exposed to the vapor of the acid. This color reaction is a simple test but more sensitive than UV-shadowing. If any trace of the 3'-isomer was found, the contaminated products must be repurified. In fact, it is better to sacrifice several last product fractions that may overlap those containing the 3'-isomer. MALDI-TOF and NMR analyses have been done to confirm the structure and the purity of the separated 2'-O-TBDMS protected nucleosides. ¹H NMR spectra of the samples indicated the presence of only one free hydroxyl group, namely, the 3'-OH group (Chapter 5, Section 5.4 - 5.10).

Table 15 – The protection of the 2'-OH groups of the nucleoside building blocks with TBDMS-Cl^a.

Entry	Nucleoside ^b (1.0 eq.)	TBDMS-Cl (eq.)	AgNO ₃ (eq.)	Time (h)	2'- ^c (%)	3'- ^c (%)	2',3'- ^c (%)
1	5'-DMT-5-I-U 2	1.3	1.2	2.5	71	-	-
2	5'-DMT-5-L1-U 9	1.3	1.2	6.5	48	<20	-
3	5'-DMT-5-L2-U 15	1.3	1.2	10.0	47	<10	<25
4	5'-DMT-N6-Ibu-8-L3-A 22	1.3	1.2	5.5	40	37	5
5	5'-DMT-N6-Ibu-2-L3-A 30	1.3	1.2	4.5	63	12	-
6	5'-DMT-N6-Ibu-8-L1'-A 55	1.7	1.2	6.5	7	6	-
7	5'-DMT-N2-Ibu-8-L3-G 38	1.7	1.5	8.5	26	21	8

^aIn all cases, the silylation was done in THF with 3.7-4.0 eq. pyridine. ^bL1, L2 and L3: linker **L1**, **L2**, **L3**, L1': the isomer of linker **L1**, U: uridine, A: adenosine, G: guanosine. ^c2'-, 3'- and 2',3'- are the 2'-, 3'-O-TBDMS and 2',3'-O-di(TBDMS) protected nucleosides, respectively.

The 2'-O-TBDMS ribonucleosides should be treated with care, since the TBDMS group is known to isomerize between the 2'- and 3'-OH groups of the ribofuranose ring in protic sol-

vents such as methanol or aqueous pyridine (Ogilvie *et al.* 1979). These environments should be avoided. THF was used as the solvent for all the silylation reactions, as it has been proved that in THF alone, isomerization could not be detected even after 24 hours (Scaringe *et al.* 1990). A small amount of pyridine is normally added as an acid-scavenger. It has also been reported that pyridine when used as solvent could support for the selective silylation of the 2'-OH group, but the reaction took place in a significantly longer time (Ogilvie *et al.* 1978; Hakimelahi *et al.* 1982).

From Table 15, it can be noticed that the silylation reaction of 5'-*O*-(4,4'-dimethoxytrityl)-5-iodouridine (5'-DMT-5-I-U) **2** has high conversion and selectivity, while those of 5'-*O*-(4,4'-dimethoxytrityl)-*N*-6-isobutyryl-2-(3-trifluoroacetamidoprop-1-ynyl)adenosine (5'-DMT-N6-Ibu-2-L3-A) **30**, 5'-*O*-(4,4'-dimethoxytrityl)-5-(3-trifluoroacetamidoprop-1-ynyl)uridine (5'-DMT-5-L1-U) **9**, 5'-*O*-(4,4'-dimethoxytrityl)-5-(3-[6-trifluoroacetylaminohexanamido]prop-1-enyl)uridine (5'-DMT-5-L2-U) **15** and 5'-*O*-(4,4'-dimethoxytrityl)-*N*-6-isobutyryl-8-(3-trifluoroacetamidoprop-1-ynyl)adenosine (5'-DMT-N6-Ibu-8-L3-A) **22** are from good to medium. The presence of the linkers at the C-5 position of uridine and at the C-8 position of adenosine does reduce the selectivity of the 2'-OH group over the 3'-OH group, as they cause more steric hindrance about the 2'-position. The selectivity and conversion is particularly low in case of 5'-*O*-(4,4'-dimethoxytrityl)-*N*-2-isobutyryl-8-(3-trifluoroacetamidoprop-1-ynyl)guanosine (5'-DMT-N2-Ibu-8-L3-G) **38**. The worst silylation yield was obtained from 5'-*O*-(4,4'-dimethoxytrityl)-*N*-6-isobutyryl-8-(3-trifluoroacetamidoprop-2-en-1-yl)adenosine (5'-DMT-N6-Ibu-8-L1-A) **55**. All attempts to improve the 2'-*O*-silylation yield of this nucleoside failed.

3.7 Synthesis of amino linker modified phosphoramidite building blocks

The functionalization of the 3'-OH groups of the modified nucleosides by phosphitylation is the key step in the preparation of the phosphoramidite building blocks for the chemical synthesis of RNA (Figure 61). In all cases, phosphitylation reactions have been conducted by 2-cyanoethyl-*N,N'*-diisopropylamino-chlorophosphoramidite with slight modifications of the reported procedure (McBride & Caruthers 1983). The phosphitylation reaction is extremely moisture sensitive. Therefore, all reagents and the solvent must be anhydrous. The reaction bottle must be carefully oven dried and cooled down in a desiccator before use. Importantly, the starting material must be of high purity, as the phosphoramidite product can only tolerate fast chromatographic purification by silica gel column.

Thus, the 5'-*O*-DMT-2'-*O*-TBDMS (-*N*6) protected nucleoside was dried by co-evaporation with anhydrous pyridine and dry DCM and kept overnight under vacuum. The kept cold phosphitylating reagent was allowed to be warmed up to ambient temperature before opened. The serum-capped reagent and reaction bottles were connected to argon-filled balloons via

drying tubes. This provided a convenient system to withdraw or inject materials under inert atmosphere with pressure equalization. Dry freshly distilled DIPEA (Hünig's base) was added to the bottle containing the dried nucleoside, followed by dry DCM. When the nucleoside was completely dissolved, the phosphitylating reagent was added dropwise to the resulting solution. The progress of the reaction was monitored by silica gel TLC (ethyl acetate/hexane containing 1-2% triethylamine; triethylamine reduces the resolution of the TLC, but in the absence of the base, the phosphoramidite product tends to degrade when extendedly exposed to silica gel).

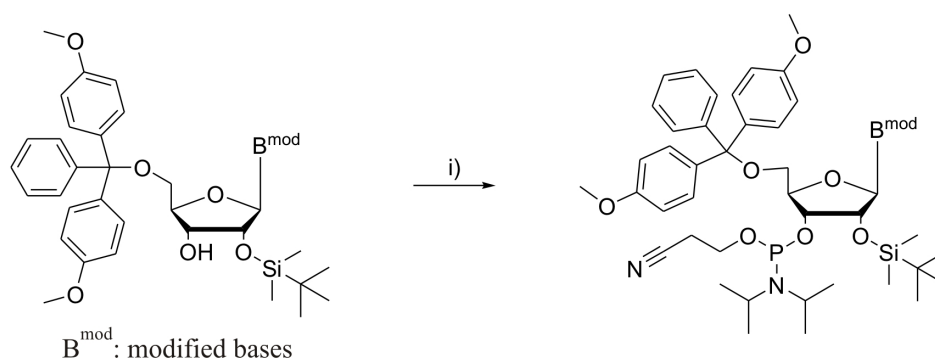


Figure 61 – The functionalization of the 3'-OH groups of the modified nucleosides by phosphitylation - The synthesis of modified phosphoramidite building blocks: i) 5'-O-DMT-2'-O-TBDMS (-N6) protected nucleoside, 1.5 eq. 2-cyanoethyl-*N,N'*-diisopropylamino-chlorophosphoramidite, 4.0 eq. DIPEA, DCM, RT, 2.5-5.5 h, yield 60-87%.

Theoretically, the phosphoramidite with all hydroxyl groups being protected is the least polar compound in the reaction mixture and should therefore run the fastest. In fact, the phosphitylated uridine derivatives with **L1** or **L3** linker at the C-5 position ran approximately as fast as the starting nucleosides. The phosphoramidite products, however, could be readily recognized, since they always appeared as an eight-shaped spot or even two clearly separated spots, because the solvent system could partially resolve the two diastereomers of the chiral phosphorus atom. Moreover, the phosphoramidite could be detected by the yellow color when sprayed with ninhydrin reagent, while the starting material did not have this color reaction.

The phosphitylation reactions of the modified ribonucleosides were considerably more slowly than those of the deoxyribose analogues due to the bulky 2'-O-TBDMS group as well as the modifications. Prolonging the reaction time to increase the conversion, however, is not suggested, because the phosphoramidite products are gradually degraded in solution. Also, adding more phosphitylating reagent should be carefully considered, as it may complicate the purification. In addition, HCl from the hydrolysis of the excess phosphitylating reagent during the aqueous work-up can lead to the degradation of the product. Therefore, after 5-6 hours, when almost all of the starting material was consumed, the excess of the phosphitylating reagent was quenched by anhydrous methanol. This helps to avoid the hydrolysis of the phosphitylating reagent during aqueous work-up. The reaction mixture was diluted with ethyl acetate which had been neutralized with NaHCO₃ and contained 1% triethylamine. The solution was washed

with a dilute solution of NaHCO_3 and the phosphoramidite product was purified by fast silica gel column chromatography.

Chromatographic purification of the phosphoramidite is necessary as it helps to : i) remove DIPEA. This base has a high boiling-point and is difficult to be removed by rotary evaporation. Its traces can disturb the activation of the phosphoramidites by tetrazoles. ii) remove the excess amount of the nucleoside educt, reagents and other impurities. Therefore, the amount of the phosphoramidite product can be quantitatively determined. The contamination of the phosphoramidite with the nucleoside educt should be avoided, as it can also be coupled with the activated phosphoramidite, hence reducing the coupling efficiency. The commonly used solvent system ethyl acetate/hexane/triethylamine 45:45:10 (Atkinson & Smith 1990) has proved to be too polar. Optimal purification can only be obtained by adjusting the ratio of these solvents for each building block (Table 16).

Table 16 – The synthesis of the phosphoramidite building blocks from the modified nucleosides^a.

Entry	Nucleoside ^b	Time(h)	EtOAc(%) ^c	Yield(%)
1	5'-DMT-2'-TBDMS-5-L3-U 4	5.0	35	80
2	5'-DMT-2'-TBDMS-5-L1-U 10	3.0	40-60	87
3	5'-DMT-2'-TBDMS-5-L2-U 16	4.0	10-70	82
4	5'-DMT-2'-TBDMS-N6-Ibu-2-L3-A 31	3.5	10-60	87
5	5'-DMT-2'-TBDMS-N6-Ibu-8-L1'-A 56	3.5	10-60	70

^aIn all reactions, the amounts of the phosphitylating reagent and DIPEA are 1.5 and 4.0 eq., respectively. All of the reactions were carried out at room temperature. ^bL1, L2 and L3: linker **L1**, **L2** and **L3**, L1' is the linker **L1** with the rearranged double-bond, U: uridine, A: adenosine.

^cThe gradients of ethyl acetate in hexane for SiO_2 -chromatography. In all cases, 1-5% Et_3N was added to neutralize SiO_2 .

It should also be noticed that the work-up and chromatographic purification must be done as fast as possible so as not to leave the phosphoramidite product in solution any longer than necessary, since it will start to decompose. Before being used for oligonucleotide synthesis, the phosphoramidite product must be thoroughly dried by co-evaporation with dry DCM to remove traces of triethylamine and other solvents and kept in an evacuated decicator over P_2O_5 overnight. Rotary evaporation of solvents should be done at temperatures not higher than 35 °C to avoid the degradation of the phosphoramidite.

The structures and purity of the phosphoramidite building blocks have been checked by ^1H and ^{31}P NMR analysis (Chapter 5, Section 5.4 - 5.10). NMR spectra always show the presence of a mixture of two phosphoramidite diastereomers. In some cases, small amounts of the 2-cyanoethyl *H*-phosphonate has been recognized by TLC and ^{31}P NMR. The formation of

this side-product may result from the decomposition of the phosphoramidite catalyzed by the excess phosphitylating reagent hydrolyzed during the aqueous work-up of the reaction mixture.

3.8 RNA: chemical synthesis, purification, labeling, analysis and hybridization

In order to test the possibility of the modified phosphoramidite building blocks to be incorporated into the RNA chains by chemical synthesis, the thermally stable stems (Donor D1, Acceptor A1 and A2) as well as the modified full-length sequence of the fourU-thermometer (4U-Ther.) (Waldminghaus *et al.* 2007) have been prepared. The fourU-thermometer (Figure 62) is a new type of RNA thermometer that regulates translation of the *Salmonella enterica agsA* gene by four consecutive uracil residues that pair with the Shine-Dalgarno (SD) sequence.

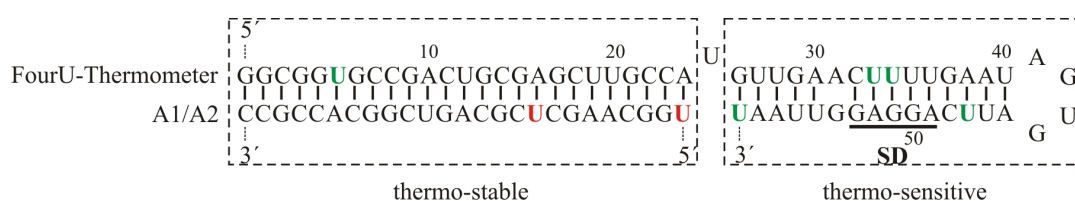


Figure 62 – Secondary structure of the modified fourU-thermometer of the *Salmonella enterica agsA* gene: (left) modified thermo-stable stem for FRET experiments; (right) thermo-sensitive hairpin. The four consecutive uracil residues pair with the SD sequence.

In vivo and *in vitro* experiments have demonstrated dynamic temperature-dependent conformational changes in the 5'-untranslated region (5'-UTR) of *agsA* that control ribosome access to the SD sequence. The start codon region of the RNA thermometer has been modified to be the thermo-stable stem (Figure 62, left) required for FRET experiments. The green and red Us are different amino linker modified uridine residues at which the RNAs will be labeled with donor and acceptor dyes, respectively.

In addition, strands c and d of the four-way RNA junction of the hairpin ribozyme (Walter *et al.* 1998), the hairpin aptazyme HPAR2 (Rublack 2009) and short test sequences (2-L3-A and 8-L1-A) for MALDI-MS analysis have also been synthesized (Table 17).

The hairpin ribozyme is a small nucleolytic RNA motif found in the negative strand of the satellite RNA of the *tobacco ringspot* virus (Buzayan *et al.* 1986). The hairpin ribozyme consists of two loop-carrying duplexes that are adjacent arms of a four-way junction in its natural context in the viral RNA. Conformational analyses by FRET experiments have revealed that the junction undergoes an ion-induced transition to the antiparallel conformation upon the addition of divalent metal ions, while in the absence of added metal ions, the junction adopts

the stacked 90° cross structure (Walter *et al.* 1998). In order to reinvestigate the conformational changes of the junction in the presence of different cations by smFRET, its strands c (RNA-26) and d (RNA-25) have been synthesized with the incorporation of the 5-L2 modified uridine building block 5-(3-[6-trifluoroacetylaminohexanamido]prop-1-enyl)uridine **14** (Figure 63, left).

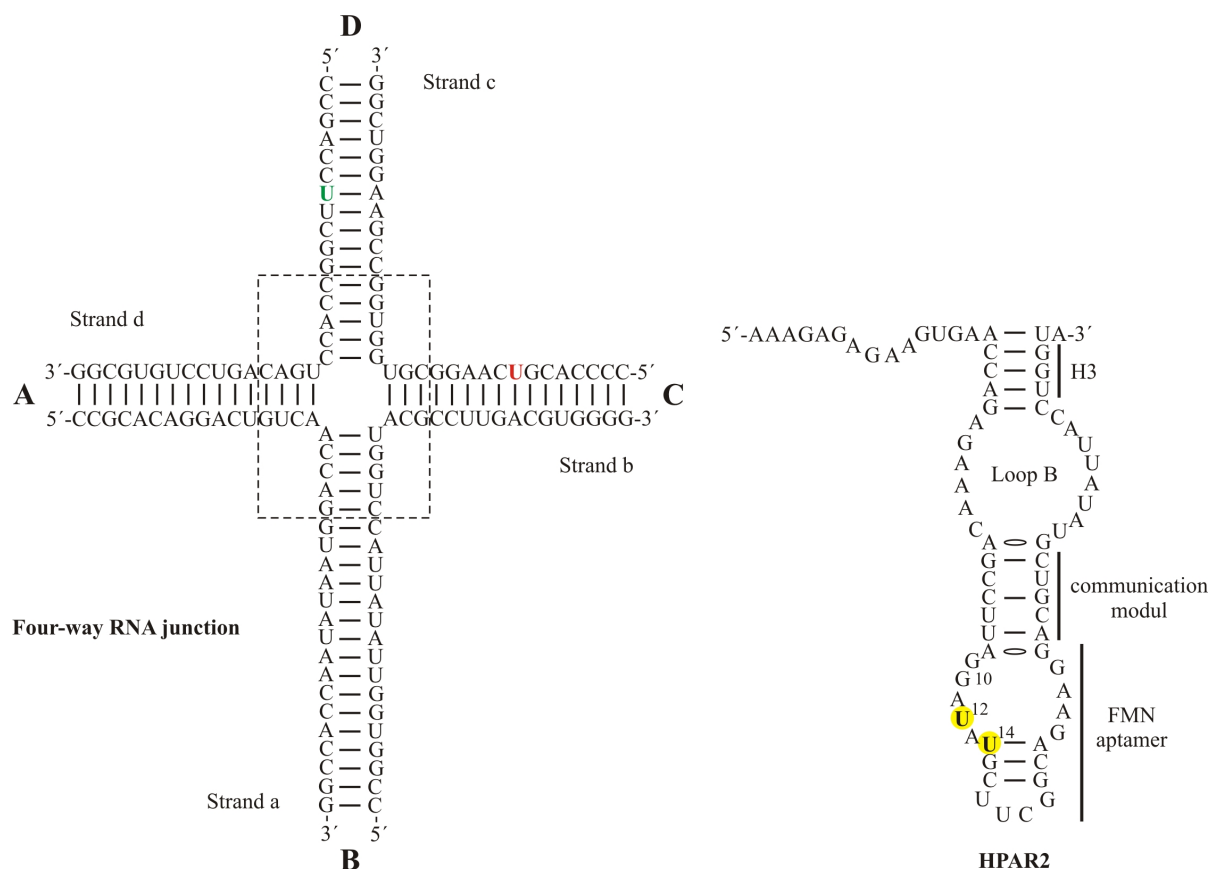


Figure 63 – Secondary structures of the modified four-way RNA junction and the hairpin aptazyme HPAR2 : (left) The four-way RNA junction. The junction (in the box with dash-line) remained intact, while the stems and loops were modified for FRET experiments. The green and red Us are the L2-modified uridine **14** where the donor and acceptor dyes are located, respectively. (right) The hairpin aptazyme HPAR2. The hairpin aptazyme HPAR2 was modified at the U12 or U14 positions (marked yellow) with the L1-modified uridine **8** to which the FMN derivative was connected.

The hairpin aptazyme HPAR2 has been designed in the working group of Prof. Müller based on the hairpin ribozyme found in the *tobacco ringspot* virus (Buzayan *et al.* 1986). HPAR2 is able to cleave an oligonucleotide in the presence of FMN in oxidative state. The cleavage activity decreases dramatically when the effector FMN is reduced (Strobach *et al.* 2006). In order to connect the aptazyme HPAR2 with a FMN derivative and thus to create a reversibly switchable molecular device (Rublack 2009), the 5-L1 modified uridine derivative 5-(3-trifluoroacetamidoprop-1-enyl)uridine **8** was incorporated into the aptazyme RNA (HPAR2a and HPAR2b) (Figure 63, right).

Table 17 – Sequences of amino linker modified RNAs

Name	Length	Sequence (5' → 3')	Mod.	Dye
A1L1	25-mer	UGG CAA GCU CGC AGU CGG CAC CGC C	U-L1	Cy5
A1L2	25-mer	UGG CAA GCU CGC AGU CGG CAC CGC C	U-L2	Cy5, ATTO 647N
A1L3	25-mer	UGG CAA GCU CGC AGU CGG CAC CGC C	U-L3	Cy5
A2L1	25-mer	UGG CAA GCU CGC AGU CGG CAC CGC C	U-L1	Cy5
A2L2	25-mer	UGG CAA GCU CGC AGU CGG CAC CGC C	U-L2	Cy5, ATTO 647N
A2L3	25-mer	UGG CAA GCU CGC AGU CGG CAC CGC C	U-L3	Cy5
D1L1	25-mer	GGC GGU GCC GAC UGC GAG CUU GCC A	U-L1	Alexa 488
D1L2	25-mer	GGC GGU GCC GAC UGC GAG CUU GCC A	U-L2	Alexa 488
D1L3	25-mer	GGC GGU GCC GAC UGC GAG CUU GCC A	U-L3	Alexa 488
L2-TEST	8-mer	GGA AUU CC	U-L2	-
2-L3-A	8-mer	GGA AAU CC	2-L3-A	ATTO 647N
8-L1-A	8-mer	UU A GUA CU	8-L1'-A	-
RNA-25	32-mer	CCC CAC GUC AAG GCG UGG UGG CCG AAG GUC GG	U-L2	Cy5
RNA-26	32-mer	CCG ACC UUC GGC CAC CUG ACA GUC CUG UGG GG	U-L2	Alexa 488
HPAR2a	43-mer	AAA GAG AGA AGU GAA CCA GAG AAA CAG CCU UGA GAU AUG CUG G	U-L1	-
HPAR2b	43-mer	AAA GAG AGA AGU GAA CCA GAG AAA CAG CCU UGA GAU AUG CUG G	U-L1	-
4U-Ther.	60-mer	GGC GGU GCC GAC UGC GAG CUU GCC AUG UUG AAC UUU UGA AUA GUG AUU CAG GAG GUU AAU	U-L2	Alexa 488
4U-Ther.	60-mer	GGC GGU GCC GAC UGC GAG CUU GCC AUG UUG AAC UUU UGA AUA GUG AUU CAG GAG GUU AAU	U-L2	Alexa 488
4U-Ther.	60-mer	GGC GGU GCC GAC UGC GAG CUU GCC AUG UUG AAC UUU UGA AUA GUG AUU CAG GAG GUU AAU	U-L2	Alexa 488
4U-Ther.	60-mer	GGC GGU GCC GAC UGC GAG CUU GCC AUG UUG AAC UUU UGA AUA GUG AUU CAG GAG GUU AAU	U-L2	Alexa 488

3.8.1 Chemical synthesis and purification of modified RNAs

The chemical synthesis of the RNAs being used in this work was carried out following the standard phosphoramidite procedure in our working group (see Section 5.2.4). All the reagents and solvents for the oligonucleotide synthesis should have the highest quality. Solutions of all of the phosphoramidites should be prepared just before used, as they start immediately to degrade in solution at room temperature.

In the first step, the 5'-O-DMT group of the support-bound nucleoside is cleaved off by a dilute solution of dichloroacetic acid in DCE to give a free 5'-OH group. After the column has been washed with DCE and MeCN, a solution of a phosphoramidite in MeCN activated by BMT (solution in MeCN) is flowed through the column and performs the coupling reaction with the free 5'-OH group. The excess amounts of the uncoupled phosphoramidite and BMT are washed with MeCN. In the capping step, unreacted 5'-OH groups are acetylated by a solution of acetic anhydride in MeCN in the presence of 2,4,6-trimethylpyridine (collidine). Collidine catalyzes the acetylation reaction. The coupling reaction will not continue from these truncated fragments in the next coupling rounds. The unstable phosphite triester intermediate is oxidized to its corresponding phosphate triester by a solution of I₂ in MeCN/H₂O in the presence of collidine. This compound makes the medium basic that is required for the oxidation reaction. After being detritylated, the growing oligomer again has a free 5'-OH group and can participate in the next coupling round. The UV-absorption intensity of the solution of the released DMT cations can be used to quantitatively evaluate the efficiency of each coupling. The coupling cycle is repeated until the oligonucleotide of the desired sequence is assembled. During the whole synthesis, all protecting groups other than the DMT group stay intact.

The modified phosphoramidite building blocks have been incorporated into the growing RNA chain during the chemical synthesis. Before being coupled, the modified phosphoramidites must be thoroughly dried by co-evaporation with dry DCM. If necessary, the standard coupling condition must be adjusted for each modified building block. Thus, two modified procedures have been tested (Table 25): The coupling time of the modified phosphoramidite was prolonged in order to increase the coupling yield. Alternatively, the coupling time was kept as standard and the coupling reaction was repeated twice. After the first coupling, the column was washed with MeCN and a new batch of the modified phosphoramidite and BMT was circulated through the column and served for the second coupling reaction. In all cases, the coupling efficiencies of the modified phosphoramidites under the standard or modified conditions were comparable with those of the natural ones.

After the chemical synthesis of the RNA, it is important that the protecting groups are completely removed and that no nucleoside base modification or phosphodiester linkage isomerization occurs. Using the ensemble of the standard protecting groups, only two steps are required

to completely deprotect the synthetic oligonucleotide. Firstly, the alkaline treatment of the support-bound oligonucleotide removes the *N*-acyl and the β -cyanoethyl phosphate protecting groups and cleaves off the oligonucleotide from the CPG support. Secondly, the treatment of the oligonucleotide with fluoride reagents removes the TBDMS protecting groups.

In the first deprotection step, the synthetic RNA was treated with a 1:1 (v/v) mixture of concentrated NH_3 and ethanolic methylamine (AMA) at 65 °C for 1 hour. Ethanol was used as the solvent for methylamine. In addition, ethanol helped to increase the solubility of the silyl protected oligonucleotide in the reaction mixture. It has also been reported that the addition of ethanol could strongly suppress the hydrolysis of the silyl protecting groups in alkaline solutions (Stawinski *et al.* 1988). In the absence of ethanol, a significant number of TBDMS groups was removed by NH_4OH , leading to the cleavage of the phosphodiester linkage of the RNA. In the second deprotection step, the 2'-*O*-TBDMS protecting groups were removed upon treatment of the RNA with a 1:3 (v/v) mixture of DMF and $\text{Et}_3\text{N} \cdot 3\text{HF}$ at 55 °C for 1.5 hours. The dilute solution of $\text{Et}_3\text{N} \cdot 3\text{HF}$ in DMF has been proved to cleave off the silyl protecting groups more effectively under milder conditions than TBAF (Westman & Stromberg 1994). The extra desalting step required to remove the excess of the TBAF reagent (Scaringe *et al.* 1990) could then be avoided.

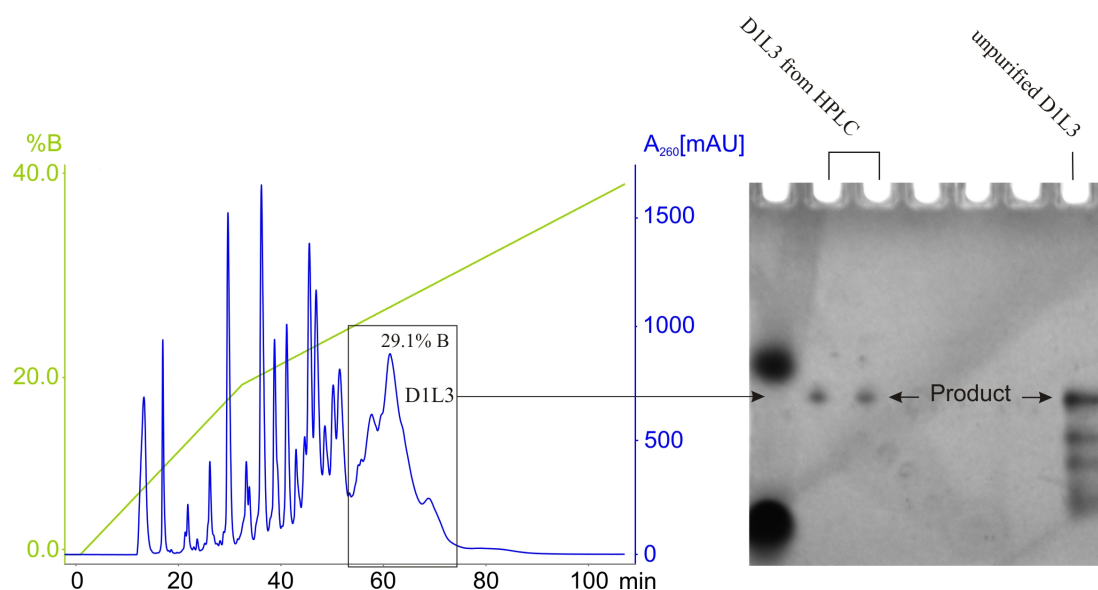


Figure 64 – Purification of the modified oligonucleotide D1L3 by anion exchange HPLC (left, Gradient F, see Table 24) and 15% denaturing PAA-gel of the fractions collected at 29.1% B (right).

The completely deprotected oligonucleotide was precipitated from cold butanol overnight. The resulting crude RNA was purified by anion-exchange HPLC or denaturing PAGE. Figure 64 (left) shows exemplarily the purification of the 25-mer modified RNA D1L3 (see Table 17) by anion-exchange HPLC. As can be seen from the HPLC diagram, the product fraction at 29.1%B appears to be a broadened peak, resulting supposedly from different secondary structures of the oligonucleotide. These secondary structures were so stable, that they could not be disrupted under the denaturing condition (6 M urea, 70 °C). The broadened peak was collected,

urea buffer was eliminated by reversed-phase chromatography and the sample was analyzed by an analytical denaturing PAA-gel (Figure 64, right). In fact, the broad peak contained only one RNA sequence which corresponded to the oligonucleotide product. In this context, all the synthetic oligonucleotides have later been purified to complete homogeneity by denaturing PAGE. The concentrations of PAA-gels were varied depending on the length of the oligonucleotides. The synthetic RNA product was the longest one and therefore ran the most slowly on the gel. The bands corresponding to the oligonucleotide product were detected by UV-shadowing at 254 nm and excised from the gel. The RNA product was eluted from the gel pieces with eluting buffer and precipitated from the eluent by the addition of a 1:1 (v/v) mixture of absolute ethanol and acetone.

The identity of the purified RNAs was confirmed by MALDI-TOF-MS (see Section 3.8.3). From the UV-absorption at 260 nm, the amounts of the oligonucleotides obtained can be determined by the Lambert-Beer law (see Section 5.2.4).

3.8.2 Labeling of amino linker modified RNAs

For FRET experiments, the synthetic RNAs have been labeled with different fluorescent dyes via the amide bonds formed in the reactions of the primary amines of the linkers and the active *N*-hydroxysuccinimidyl- (NHS) or tetrafluorophenyl- (TFP) esters of the dyes (Figure 65).

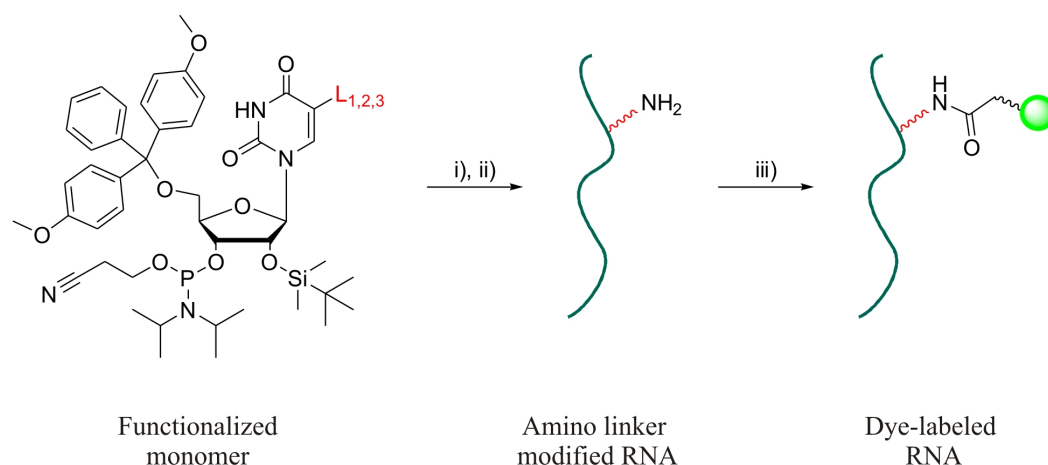


Figure 65 – Synthesis and labeling reaction of the amino-modified oligonucleotides: i) Chemical synthesis of the oligonucleotides from modified phosphoramidite building blocks using solid phase method; ii) Deprotection of the synthetic oligonucleotides; iii) Labeling reaction of the amino-modified oligonucleotides with fluorescent dyes.

The donor RNAs have been labeled with Alexa 488 dyes, while the acceptor sequences have been labeled with either Cy5 or ATTO 647N dyes (Figure 66). The structure of the ATTO 647N NHS-ester is not available due to patent protection.

The fluorophores have been attached to the synthetic RNAs via linkers at the C-5 position of

uridine, the C-2 or C-8 positions of adenosine and the C-8 position of guanosine. At these positions, effects of the modifications upon base-pairing ability of the nucleobases and the stability of the RNA duplexes are minimal. The active esters react selectively with the amino functions of the linkers, as they are more nucleophilic than the aromatic amines of the nucleobases and the hydroxyl groups of the sugars. The labeling solutions must be buffered in slightly basic ranges to maintain the amino function in non-protonated form, i.e. in active form.

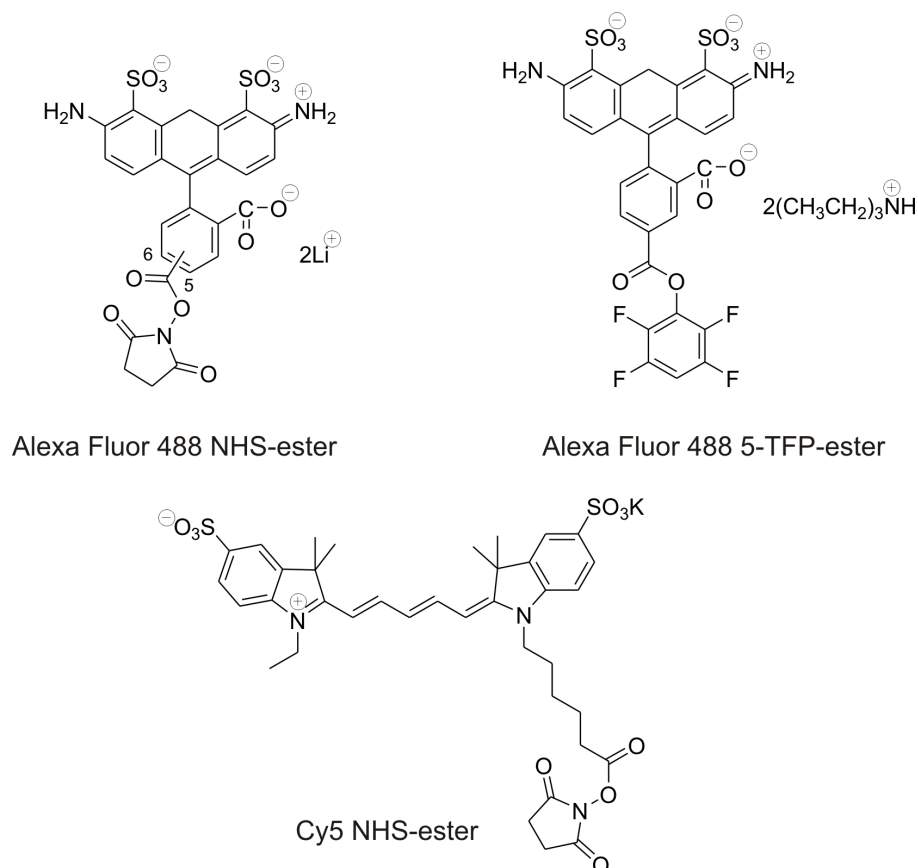


Figure 66 – Structures of Alexa Fluor 488 5(6)-NHS-, TFP-esters and Cy5 NHS-ester.

To ensure that the oligonucleotide is free of interfering compounds, especially amines such as Tris, it is strongly recommended to extract the sample with chloroform and/or precipitating the oligonucleotide prior to the labeling reaction. The solution of the dye should be freshly prepared for each reaction, because the reactive portion of the dye is hydrolyzed quickly back to the corresponding acid. The rate of the hydrolysis is increased with the increase in pH. Borax buffer was chosen in most cases, as it could maintain a stable pH for a longer time. Other buffers such as bicarbonate and hydrophosphate buffers can also be used, but buffers containing primary amines such as Tris should be avoided. DMF is used as a co-solvent which helps to increase the solubility of the dye in aqueous solutions.

Thus, for a labeling reaction, the amino-modified RNA was dissolved in Borax buffer. To the resulting solution, a freshly prepared solution of the fluorescent dye (10-30 eq.) in DMF was added. The reaction mixture was mixed, protected from light and placed on a shaker

at room temperature. The reaction solution was gently vortexed every half hour for the first two hours to ensure that it remained well mixed. After the labeling reaction, the excess dye was removed by gel filtration (Sephadex G-25). The labeled oligonucleotide was separated from the unlabeled by denaturing PAGE or reversed-phase HPLC. The labeled and unlabeled oligonucleotides were located by UV-shadowing at 254 and 365 nm. All the dye-labeled RNAs showed visible fluorescence when exposed to UV-light at 365 nm, but with different intensities depending on the absorption maxima of the dyes. The dye-labeled oligonucleotide runs more slowly than the unlabeled, as its molecular weight is higher.

It should be noticed that the commercially available Alexa Fluor 488 and ATTO 647N NHS-esters were not isomerically pure. In fact, oligonucleotides labeled with different isomers may run differently in reversed-phase HPLC and denaturing PAA-gel. The bands containing the labeled and unlabeled oligonucleotides were separately excised and eluted with eluting buffers. The oligonucleotides were precipitated from the eluents by the addition of a 1:1 (v/v) mixture of absolute ethanol and acetone. The samples were analyzed by analytical reversed-phase HPLC and MALDI-TOF-MS (see Section 3.8.3). Yields of the labeling reactions vary from dye to dye and from linker to linker (16-36% with Alexa Fluor 488 and 25-54% with Cy5 and ATTO 647N). They also depend on the coupling times, temperatures and especially on the pHs of the labeling reactions and the ratios between dyes and oligonucleotides. The fluorescently labeled oligonucleotides can be used directly to prepare hybrids for FRET experiments. The unlabeled oligonucleotide can be used for later labeling reactions.

The concentration of the dye-labeled oligonucleotide can be determined by measuring the absorbance of the nucleic acid at 260 nm or the absorbance of the dye at its absorption maximum. The calculation is based on the Beer-Lambert law (see Section 5.2.4).

Labeling reactions of amino-modified RNAs with Alexa Fluor 488 5(6)-NHS- and 5-TFP-esters

Alexa Fluor 488 active ester (λ_{max} = 495 nm) belongs to the best green-fluorescent reactive dyes available. It can offer great fluorescence and photostability in the conjugates with biomolecules. Its spectra are relatively insensitive to pH over a broad range. Moreover, it is well water soluble due to the multiple negatively charged sulfonate groups, hence suitable for labeling reactions in aqueous buffers. Alexa Fluor 488-labeled oligonucleotides are suitable for FRET experiments as they have high FRET efficiency, high quantum yields and long fluorescent life times. The *N*-hydroxysuccinimidyl (NHS) ester of Alexa Fluor 488 carboxylic acid is available as a mixture of 5- and 6-isomers, while its analogue, the tetrafluorophenyl (TFP) ester can be commercially obtained as an isomerically pure 5-isomer (Figure 66).

In the labeling reactions with amino-modified RNAs, Alexa Fluor 488 active dye had relatively low coupling yields, especially with the ones bearing short linkers (the thermo-stable

stems D1L1 and D1L3). The coupling yields of the labeled oligonucleotides being separated ranged from only 6 to 16%. In order to improve the coupling efficiencies, modifications of the labeling conditions have been made basing on literature procedures (Cox & Singer 2004).

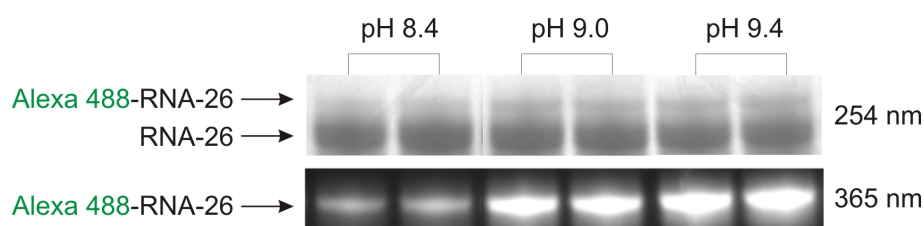


Figure 67 – Coupling reactions of the RNA-26 with Alexa Fluor 488 TFP-ester at different pHs: amino-modified RNA, 30 eq. Alexa Fluor 488 active ester, Borax buffer 0.1 M, pH 8.4, 9.0 and 9.4, RT, overnight. The labeling reactions were analyzed by 15% denaturing PAA-gel.

Heat denaturing and snap-cooling the oligonucleotide on ice before the coupling reaction to disrupt secondary structures did not help to increase the coupling efficiencies. Increasing the reaction temperatures (45 °C) or prolonging the coupling times (48 hours) had only little effect. Changing buffer concentrations (0.1-0.3 M) has also been tried, but no difference has been observed. The low labeling yields of the Alexa Fluor 488 reagents may in part due to the steric hindrance associated with its large ring structure as well as the static repulse between the negatively charged phosphate backbone of the RNA and the sulfonate groups. Coupling yields of the oligonucleotides modified with the long linker **L2** (the thermo-stable stem D1L2, the full length fourU-thermometers and strand d (RNA-26)) increased to some extent (yields of labeled RNAs up to 36%). The coupling efficiency of the TFP-ester was higher than that of the NHS-ester, as it is more resistant to hydrolysis. The best coupling efficiencies of Alexa Fluor 488 dyes have been obtained in Borax or carbonate/bicarbonate buffer at high pHs (Figure 67).

Labeling reactions of amino-modified RNAs with Cy5 and ATTO 647N NHS-esters

Cy5 (λ_{max} = 646 nm) and ATTO 647N (λ_{max} = 644 nm) NHS-esters are the red-fluorescent active dyes. These fluorophores have been proved to have strong absorption, high fluorescence quantum yields and good solubility in aqueous buffers. Of the two, ATTO 647N dye shows higher photostability. Cy5 NHS-ester possesses one negative charge, but has a long linker arm, while ATTO 647N is a cationic dye. Therefore, active NHS-esters of these two dyes may be more easily accessible for the amino linkers, as steric interactions and static repulses are minimized or eliminated. In fact, the coupling yields of the Cy5 and ATTO 647N NHS-esters with amino modified RNAs (25-54%) are much higher than those of the Alexa Fluor 488 dyes. Figure 68 (upper) shows an exemplary denaturing gel for the purification of ATTO 647N-labeled A1L2. As can be seen from the gel, the most part of the amino modified A1L2 was labeled with ATTO 647N. The bands containing the labeled product could be nicely excised from the small bands beneath which were supposed to be a certain secondary structure. The

labeled product was eluted from the gel, precipitated from ethanol/acetone and analyzed by reversed-phase HPLC (Figure 68, Gradient E, Table 24) and MALDI-TOF-MS (Table 19).

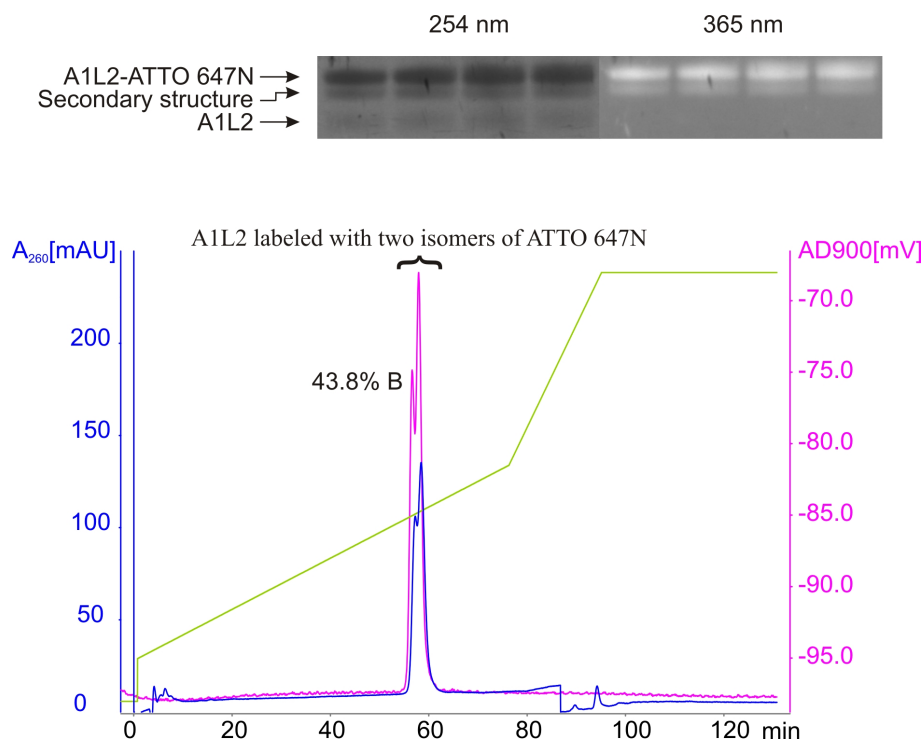


Figure 68 – Purification and analysis of ATTO 647N-labeled A1L2 by denaturing gel and reversed-phase HPLC. Upper: 15% Denaturing PAA-gel of ATTO 647N-labeled A1L2; lower: Analytical reversed-phase HPLC (Gradient E, Table 24). A1L2 sequences which are labeled with different isomers of the dye run differently.

The product was free of the unlabeled oligonucleotide and the uncoupled dye. It can also be noticed from the HPLC diagram that the A1L2 sequences which are labeled with different isomers of the ATTO 647N NHS-ester are partially separated by the reversed-phase column.

3.8.3 Analysis of modified and dye-labeled RNAs by MALDI-TOF-MS

Synthetic and dye-labeled oligonucleotides which had been purified by denaturing PAA-gel or reversed-phase HPLC were analyzed by MALDI-TOF-MS. Prior to mass determination, the ethanol/acetone precipitated oligonucleotides must be desalted by gel filtration (see Section 5.2.3) through which the most part of salts and buffers are removed. The desalted sample and the matrix solution (saturated solution of 3-hydroxypicolinic acid (3-HPA) in MeCN/H₂O) were then treated with cation-exchange beads (DOWEX 50 WX8, H⁺ or NH₄⁺-form). Desalination by gel filtration and treatment with cation-exchange beads prevent the formation of the salt adducts of the oligonucleotide by the association of any cations in the solution with the negatively charged phosphate backbone. The desalted mixture of the oligonucleotide and matrix solutions was loaded on a MALDI-plate and dried in open air during which the sample was crystallized. The sample was measured using the linear negative-ion mode. The RNA samples

must be analyzed right after desalination with a freshly prepared matrix solution in order to get optimal MALDI-MS spectra. Molecular weights of unlabeled and labeled oligonucleotides having been measured by MALDI-TOF-MS are shown in Table 18 and 19.

Table 18 – Masses of the synthetic RNAs determined by MALDI-TOF-MS (linear negative-ion mode, found $M = [M-H]^-$).

Sequence	Cal. M	Found M	ΔM	Error (%)
L2-TEST	2677.73	2675.99	0.77	0.027
2-L3-A	2585.63	2583.99	0.64	0.024
8-L1-A	2526.53	2525.96	0.43	0.017
A1L1	8041.95	8040.41	0.53	0.010
A1L2	8155.03	8153.15	0.88	0.011
		8237.61	82.57	-
A1L3	8039.93	8039.23	0.30	0.003
A2L1	8041.93	8044.29	3.36	0.040
A2L2	8155.03	8156.71	2.68	0.030
		8237.00	82.97	-
A2L3	8039.93	8041.17	2.24	0.030
D1L1	8098.93	8098.62	0.69	0.010
D1L2	8212.03	8211.46	0.43	0.005
		8293.32	82.29	-
D1L3	8096.93	8099.73	3.80	0.040

From the MALDI-TOF-MS spectrum of each sequence A1, A2 and D1 with the long linker **L2**, it can be noticed that beside the peak of the correct mass M , there is always a signal corresponding to the mass of $[M+82]$ (Table 18).

Table 19 – Masses of dye-labeled oligonucleotides determined by MALDI-TOF-MS (linear negative-ion mode, found $M = [M-H]^-$).

Labeled sequence	Cal. M	Found M	ΔM	Error (%)
2-L3-A-ATTO 647N	3213.63	3212.44	0.19	0.006
A1L2-ATTO 647N	8783.03	8782.28	0.25	0.003
A2L2-ATTO 647N	8783.03	8776.95	5.08	0.057
A2L2-Cy5	8793.25	8791.53	0.72	0.008

In order to check the quality of 5-(3-[6-trifluoroacetylaminohexanamido]prop-1-enyl)uridine **14**, the short test sequence L2-TEST (Table 17) incorporating this building block was syn-

thesized and analyzed by MALDI-MS. Figure 69 indicates a good agreement between the calculated and the found mass of the test sequence. No side product was observed. From these evidences, it can be concluded that the modified building block **14** and its incorporation into the RNAs during the chemical synthesis are reliable. In order to figure out the identity of the unknown $[M+82]$ signal mentioned above, further enzymatic analyses of the oligonucleotide D1L2 has been carried out (see Section 3.8.4).

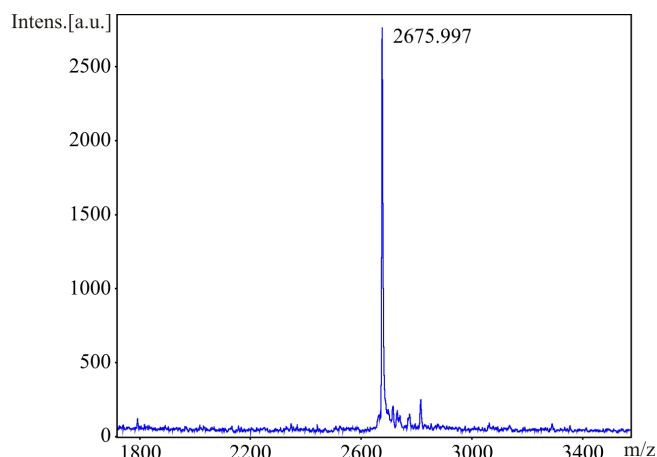


Figure 69 – MALDI-TOF mass spectrum of the test sequence L2-TEST: calculated mass 2677.73; found 2675.997 $[M-H]^-$.

Figure 70 shows exemplary MALDI-TOF mass spectra of the short test sequence 2-L3-A (left) and its corresponding conjugate with ATTO 647N NHS-ester (right).

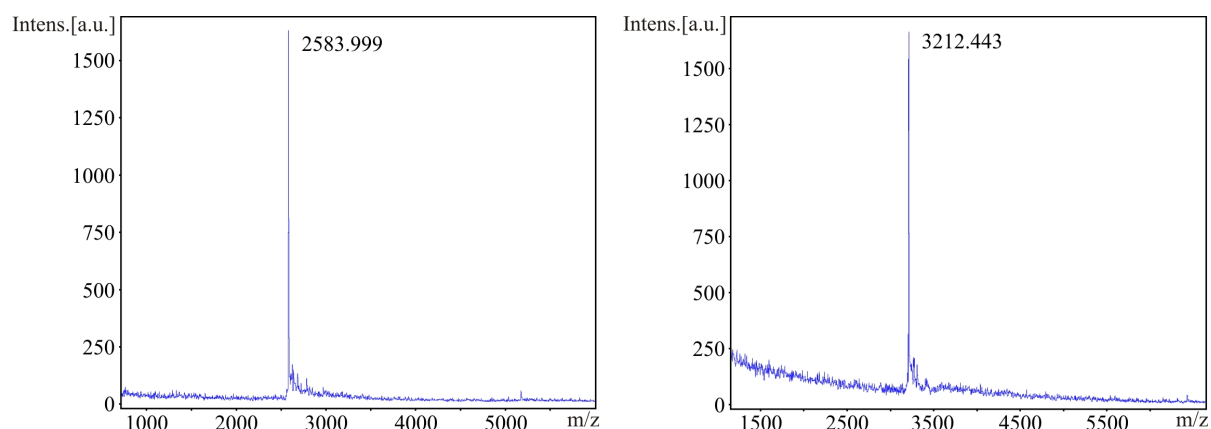


Figure 70 – MALDI-TOF mass spectra of the test RNA 2-L3-A and its corresponding ATTO 647N-labeled sequence: (left): 2-L3-A, calculated mass 2583.99, found: 2583.999 $[M-H]^-$; (right): 2-L3-A-ATTO 647N, calculated mass 3212.44, found 3212.443 $[M-H]^-$.

3.8.4 Treatment of the oligonucleotide D1L2 with calf intestinal alkaline phosphatase (CIAP) and snake venom phosphodiesterase (SVP)

When analyzing the 25-mer L2-modified oligonucleotide D1L2 by MALDI-MS (see Table 18), besides the desired RNA with the mass of $[M]$, a by-product with the mass of $[M+82]$

was observed in different ratios to the main product. They are named D1L2-lower and D1L2-upper, respectively, according to their relative positions on the gel (Figure 71, lane 1). This ΔM deviation did not correspond to any protecting group which was not cleaved. The only group which has the closest mass to the deviation is the phosphate group ($-O-PO_3$, $M = 78.96$). In order to investigate if the RNA had an extra phosphate group somewhere in the sequence, the D1L2-upper oligonucleotide with the molecular weight of $[M+82]$ was treated with calf intestinal alkaline phosphatase (CIAP) in CIAP or NE buffer. The enzyme was then removed by phenol-chloroform extraction. The oligonucleotide sample was precipitated from ethanol and analyzed by a 15% denaturing PAA-gel (Figure 71, lane 2).

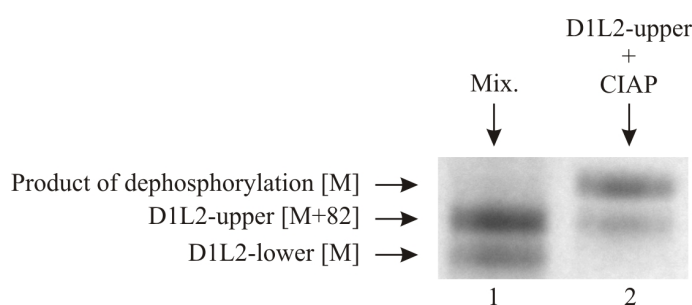


Figure 71 – Analysis of D1L2 by the treatment with CIAP: (left) crude synthetic D1L2 RNA; (right) treatment of D1L2-upper (molecular weight= $[M+82]$) with CIAP: 500 pmol D1L2-upper, 50 μ l CIAP buffer (10 x), 25 units CIAP, total volume 500 μ l, 36 °C, 2 h. 15% Denaturing PAA-gel.

As can be seen from the gel, the CIAP enzyme did have effect on the oligonucleotide D1L2-upper, indicating that there may be an extra phosphate group in the sequence of the synthetic D1L2. Surprisingly, the phosphorylated sequence which possesses one more negative charge from the phosphate group runs more slowly than the right product. It is even more surprising that the product of dephosphorylation, which according to MS analysis is identical to D1L2-lower, runs differently. Such unusual effects have also been observed before (Pieper *et al.* 2007).

Another experiment was carried out in which the D1L2-lower and D1L2-upper RNAs were treated with CIAP and snake venom phosphodiesterase (SVP) to compare their nucleoside compositions. Thus, each of the two oligonucleotides was incubated with CIAP and SVP in Tris-HCl buffer in the presence of $MgCl_2$. After the reactions, the mixtures were analyzed by reversed-phase HPLC (Figure 72). From the HPLC diagrams, four peaks corresponding to the four nucleosides A, U, G and C can be readily seen. These peaks can be integrated and the resulting areas under the UV-curve at 260 nm can be considered to be proportional to the UV-absorptions of the nucleosides at 260 nm. With this assumption, the ratio of the four nucleotides in an RNA sequence can be evaluated from their integrated areas by the Beer-Lambert law:

$$A : U : G : C = (A_A/\varepsilon_A) : (A_U/\varepsilon_U) : (A_G/\varepsilon_G) : (A_C/\varepsilon_C)$$

Where A_A , A_U , A_G and A_C are the integrated areas of the peaks of the nucleosides A, U, C

and G, respectively (Figure 72, A and B, right). $\varepsilon_A = 15.4 \times 10^3$, $\varepsilon_U = 10.1 \times 10^3$, $\varepsilon_G = 11.5 \times 10^3$, $\varepsilon_C = 7.4 \times 10^3$ ($\text{M}^{-1}\text{cm}^{-1}$) are the corresponding extinction coefficients of the nucleosides A, U, G and C at 260 nm.

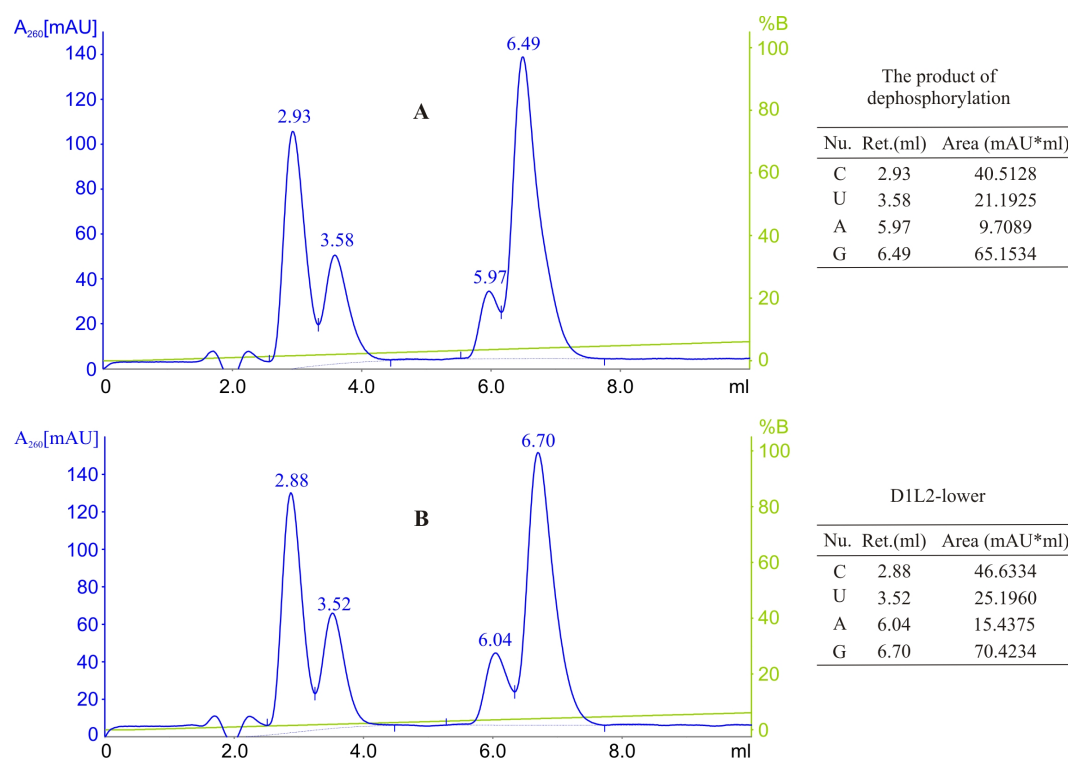


Figure 72 – Analysis nucleoside components of the product of dephosphorylation and D1L2-lower by treatment with CIAP and phosphodiesterase: 1200 pmol oligonucleotide, 1 μl Tris-HCl 0.4 M, pH 8.9, 1 μl MgCl_2 0.4 mM, 22 units CIAP, 0.04 units phosphodiesterase, total volume 10 μl , 37 $^\circ\text{C}$, 3 hours. Reversed-phase HPLC: (A) The digestion of the product of dephosphorylation by phosphodiesterase and CIAP, (B): the digestion of D1L2-lower by phosphodiesterase and CIAP (Gradient G, Table 24).

Using the equation above, the ratios of the four nucleosides in the sequences of the product of dephosphorylation and D1L2-lower can be calculated as followed:

Sequence	A : U : G : C
Product of dephosphorylation	1.21 : 4.00 : 10.78 : 10.40
D1L2-lower	1.60 : 4.00 : 9.83 : 10.10
Calculated	3 : 4 : 10 : 8

The experimentally found ratios between U, G and C of the two sequences are comparable and roughly match the calculated ratio, while the found numbers of A are rather deviated from calculation. The deviation may result from the non-baseline separation of the peaks, leading to intergration errors. The intergration errors have the most influence on the ratio of A, as A has the highest extinction coefficient and the number of A in D1L2 is the smallest. Concerning the fact that the masses of the two sequences are identical and in good agreement with the calculated value, it can be concluded that they have the identical composition. In this context,

their different behaviors on the PAA-gel can only be explained with the assumption that they possess different stable secondary structures which can not be disrupted under the denaturing conditions being used in PAGE.

3.8.5 Hybridization of single-stranded RNAs

In order to demonstrate that the amino linkers as well as the fluorescent labels do not intervene in the hybridization of the single-stranded oligonucleotides, the hybrid of Alexa Fluor 488-labeled D1L3 and Cy5-labeled A1L3 has been prepared. Thus, the two dye-labeled oligonucleotides were dissolved in Tris buffer containing MgCl_2 . The mixture was thoroughly mixed, heat denatured at 78 °C and slowly cooled down to room temperature. The hybrid was analyzed by 15% native PAA-gel (Figure 73). The oligonucleotides and their hybrid were located by illumination with UV-light at 254 and 365 nm. As can be seen from the gel, the two dye-labeled single-stranded oligonucleotides were quantitatively hybridized. The hybrid runs more slowly than the single-stranded oligonucleotides, since its size and weight are higher.

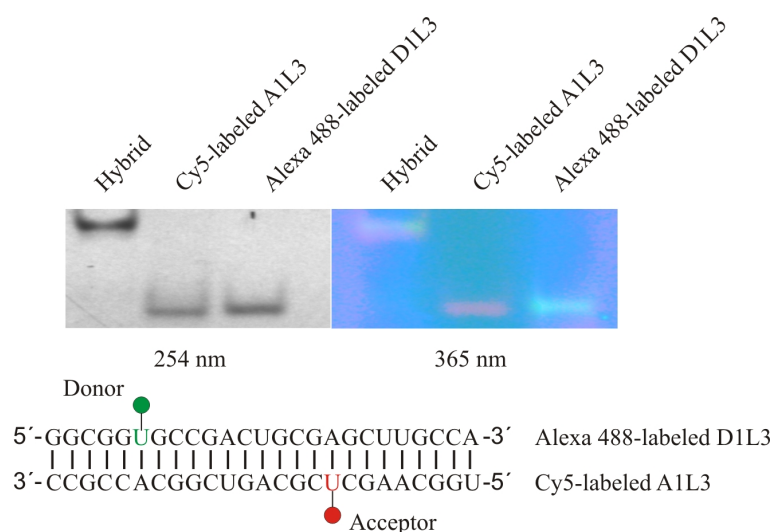


Figure 73 – Preparation of the hybrid of Alexa 488-labeled D1L3 and Cy5-labeled A1L3: 3 μM Alexa 488-labeled D1L3, 3 μM Cy5-labeled A1L3, 10 mM MgCl_2 , 50 mM Tris buffer, pH 7.4, total volume 100 μl , 78 °C 3 min., slowly cooling to RT. The hybrid was analyzed by 15% native PAA-gel: (left) illuminated at 254 nm, (right) illuminated at 365 nm.

In another test, Alexa 488-labeled D1L3 and Cy5-labeled A1L3 were dissolved in KH_2PO_4 - K_2HPO_4 buffer containing MgCl_2 and KCl. The mixture was mixed, incubated at 78 °C for 3 minutes, then slowly cooled down to room temperature. The mixture was analyzed by native PAA-gel (gel pictures not shown). Under this condition, the hybridization was also quantitative. Therefore, it can be concluded that the linkers and fluorescent labels have no negative effect on the hybridization of the modified single-stranded RNAs.

For FRET experiments, different hybrids of the Alexa 488-labeled (donor) and Cy5-labeled RNAs (acceptor) have been prepared. The hybridization between a donor and an acceptor

single-stranded RNA was conducted in $\text{K}_2\text{HPO}_4/\text{KH}_2\text{PO}_4$ buffer, pH 6.5 in the presence of MgCl_2 and KCl. The concentrations of the RNA molecules ranged between 2 and 10 μM . For FRET molecules, different ratios of the acceptor to the donor ranging from 1.5 to 3.0 have been tested. The reaction mixture was heated up to 90 °C in a water-bath and then slowly cooled down to room temperature overnight. The hybrids have been used in single molecule detection (SMD) and time correlated single photon counting (TCSPC) bulk experiments.

3.8.6 Influences of linker length and rigidity on the quantitative FRET experiments of dye-labeled RNAs

The progress in the single-molecule FRET technique (smFRET) in the last years (Karunatilaka & Rueda 2009) has solved many problems of the ensemble FRET approach such as species and time averaging, incomplete or unspecific labeling and position dependent donor or acceptor quenching artifacts. However, quantitative FRET measurements still have to deal with two problems: the uncertainty in dye position due to long flexible linkers and the influence of the relative orientation of the transition dipole moments of the two dyes. The uncertainty in dye position causes significant errors in quantitative distance measurements by FRET and prevents experiments with short donor-acceptor distances because of dye-dye interactions.

To overcome the first problem, fluorescently labeled RNAs with short dye linkers, namely **L1** and **L3**, have been tested in cooperation with the working group of Prof. Claus Seidel at the University of Düsseldorf. Firstly, the influences of the linker nature and length on the fluorescence properties of the Alexa Fluor 488 and Cy5 dyes for RNA have been studied. Secondly, quantitative FRET distance measurements using internally labeled dsRNA as test systems have been done.

Rigid and short linkers may, however, restrict dye reorientation what makes the estimation of the orientational factor difficult. Moreover, they may induce structural perturbation. Therefore, for experiments which must avoid any possible sterical constraints such as benchmark studies, RNAs with dye labels attached via the long flexible linker **L2** have been used. The errors caused by the application of the short and stiff linkers have also been calculated. For comparison, the corresponding experiments for DNA have been carried out in parallel.

Initial FRET studies on these dsRNA test systems have demonstrated that the new short dye linkers **L1** and **L3** for RNA labeling are adequate for quantitative measurements (Sindbert *et al.*, close to submission). The short linkers are particularly suitable for unknown environments of the fluorescent dyes, as the dye position can be well defined and hence modeling is less important. Moreover, for the short linkers, the errors related to the orientational factor are only slightly higher than for long linkers. Currently, further FRET experiments are in progress.

4 Summary

The discovery of a number of catalytic RNAs since the beginning of the 80s has led to an increasing need for structural investigation of RNA as well as the relationship between structure and function. Among the physical techniques used nowadays in molecular biology, single-molecule FRET (smFRET) experiments can provide structural and dynamic information of RNAs and help better understanding their folding and interacting with substrates during actions. FRET measurements of RNA demand that fluorescent labels are site-specifically attached to the oligonucleotide samples. To this end, a simple, but effective approach is to functionalize the dyes with amine-reactive functions such as isothiocyanate or activated ester, while the RNAs are modified with amino-linkers. Except from a limited number of amino linkers for 3'- and 5'-labeling and only a few of C-5 amino-modified thymidine derivatives, amino-modified ribonucleoside building blocks are in fact rarely available. FRET experiments on the one hand require linkers variable in length and rigidity to obtain optimal signals. The replacement of ribonucleoside building blocks in the chemical synthesis of RNA by their corresponding deoxy analogues on the other hand may cause deviations from the real pictures of the RNA, as deoxy- and ribonucleotides have different sugar conformations. Concerning these problems, we aimed to synthesize ribonucleoside phosphoramidite building blocks modified with amino linkers of different designs for the chemical synthesis of RNA and subsequently for post-synthetic labeling. The amino linkers were not only introduced into the C-5 position of the pyrimidine heterocycle, but also into the C-2 and C-8 positions of the purine ring, hence providing more choices for internal labeling. Theoretically, modifications at these positions will not disturb the hybridization of the modified single-stranded RNAs, because they do not intervene in the hydrogen-bond formation between the nucleobases.

From the synthetic works in solution and on solid-phase, the following results have been obtained:

- Three amino linkers with different lengths and rigidities were prepared. The primary amino functions of these linkers were protected with the trifluoroacetyl (TFA) protecting group. The short and rigid triple-bond linker *N*-propargyltrifluoroacetamide **L3** was attached to the C-5 position of uridine, C-2 and C-8 positions of adenosine and C-8 position of guanosine by the Sonogahira coupling reaction. These nucleosides were also modified at the same positions with more flexible double-bond linkers (*N*-allyltrifluoroacetamide **L1** and *N*-allyl-6-(*N*-trifluoroacetyl-amino)hexanamide **L2**) of different lengths basing on the Heck chemistry. Three amino-modified nucleoside derivatives were synthesized from 5-iodouridine, six from 8-bromo- and 2-

iodoadenosine and one from 8-bromoguanosine. For the Heck coupling reaction of adenosine at the C-8 position, 8-iodoadenosine and its derivatives were also synthesized.

- In the Heck coupling reactions of 8-bromo, 8-iodo and 2-iodoadenosine with the linkers **L1** and **L2**, the rearrangement of the double-bond was observed. By fine-tuning the reaction conditions, especially the catalysts, isomerically pure products could be synthesized with medium yields.
- From the above mentioned amino-modified nucleosides, five phosphoramidite building blocks were synthesized. Using the standard protecting groups, the exo-cyclic amino functions of adenosine and guanosine derivatives were protected with the isobutyryl groups, while the 5'- and 2'-OH functions were capped with the 4,4'-dimethoxytrityl (DMT) and *tert*-butyldimethylsilyl (TBDMS) groups, respectively. The 3'-OH group was functionalized with the phosphoramidite group. All of the modified phosphoramidites were successfully incorporated into RNA chains during the chemical synthesis of oligonucleotides by the 2'-*O*-TBDMS-3'-*O*-phosphoramidite chemistry. The coupling efficiencies of these building blocks were comparable with those of the natural ones under the same coupling conditions.
- The synthetic compounds were analyzed by one-dimensional (^1H , ^{13}C , DEPT 135 and ^{31}P), two-dimensional (HMBS and HSQC) NMR and MALDI-TOF-MS. Data obtained from these analytical methods confirm that they have the desired structures and adequate purity.
- Using these modified phosphoramidites, short test oligonucleotides (8-mer), the thermostable stem of the fourU-thermometer (25-mer), its complements (25-mer) and the full length fourU-thermometer (60-mer) were synthesized. Furthermore, sequences of the four-way RNA junction (32-mer) and the hairpin aptazyme HPAR2 (43-mer) were also prepared with these modified nucleosides specifically incorporated at desired positions.
- The synthetic amino-modified oligonucleotides were labeled with Cy5, ATTO 647N and Alexa Fluor 488 NHS-esters and Alexa Fluor 488 TFP-ester. The unlabeled and labeled oligonucleotides were purified to homogeneity by denaturing PAA-gel or HPLC. The labeled oligonucleotides were purified to free of the uncoupled dyes and unlabeled sequences. The identity of the product sequences was confirmed by HPLC and MALDI-TOF-MS. In all cases, the found masses of the synthetic oligonucleotides and their dye-labeled sequences are in good agreement with the calculated values. Several oligonucleotides modified with the linker **L2** were accompanied by unknown side-products having 82 Da higher in mass compared to the right sequences. By the enzymatic analyses with CIAP and SVP, it has been proved that these RNA sequences contain an extra phosphate group.

- Dye-labeled oligonucleotides were quantitatively hybridized, indicating that the linkers and fluorescent labels at the chosen positions did not disturb the hydrogen bonding needed to form hybrids. These hybrids have been used in the working group of Prof. Claus Seidel at the University of Düsseldorf in quantitative FRET experiments.

The experimental evidences mentioned above indicate that the modified phosphoramidites with amino-linkers of different structures are suitable for the solid-phase synthesis of oligonucleotides under the conventional conditions. Moreover, these building blocks can afford various possibilities for the post-synthetic labeling of oligonucleotides, not only at the 3'- and 5'-ends, but also at internal positions with linkers of various designs. Modified RNAs can now be synthesized with genuine modified ribonucleoside building blocks, making their nucleotide components as well as their secondary structures more close to the studied sequences. With these improvements, the FRET experiments using the fluorescent labels can always be optimized to get more authentic structural and dynamic information. In terms of nucleoside chemistry, it was the first time double-bond amino linkers were successfully introduced into different positions of the purine ring of the riboadenosine derivatives by the Heck coupling reaction. With regard to these achievements, the synthetic part can be continued with linkers of other structures which may be easier for introduction into the nucleosides. In addition, linkers functionalized with groups other than primary amines are of interest, because they can provide the possibility of orthogonal labeling. Moreover, one can also think of preparing modified cytidine derivatives to complete the set of modified ribonucleosides for RNA synthesis.

In conclusion, the present work has established the conjugation chemistry for RNA. With the newly synthesized building blocks, not only fluorescent dyes, but also spin labels or any other desired reporter groups can be introduced at desired positions in the RNA sequence with minimal structural disturbance.

5 Experimental

5.1 Materials

5.1.1 General remarks

Chemicals were obtained from commercial suppliers (Merck, Aldrich, Sigma, Acros, Fluka and VWR) and used without further purification unless otherwise noted. P.a Pyridine was kept over granulate KOH for 24 hours, refluxed for 2 hours, distilled and stored over molecular sieve 4. DIPEA and triethylamine was freshly distilled over CaH_2 just before used. DMT-Cl and 2-cyanoethyl-*N,N'*-diisopropylamino-chlorophosphoramidite were synthesized in the working group by standard procedures. Palladacycle was synthesized from $\text{Pd}(\text{OAc})_2$ and $\text{P}(o\text{-tolyl})_3$ as described in literature (Herrmann *et al.* 1995). All the technical organic solvents for extraction and silica gel column chromatography were distilled by rotary evaporation before used.

5.1.2 Buffers

Table 21 – Buffers

Borax buffer	0.1 M sodium tetraborate, adjusted with conc. HCl to pH 8.0, 8.5, 8.7, 9.0 and 9.4
Carbonate buffer	0.1 M or 0.2 M NaHCO_3 , adjusted with conc. HCl to pH 8.5
Carbonate/bicarbonate buffer	0.2 M NaHCO_3 - Na_2CO_3 , pH 9.2, 9.5, 9.8
CIAP buffer	BioLabs
Denaturing gel solution	20% Acrylamide/bisacrylamide 19:1 (Roth), 1 x TBE, 7 M urea
Eluting buffer	0.5 M LiOAc
Hybridizing buffer 1	10 mM MgCl_2 , 100 mM KCl, 20 mM KH_2PO_4 - K_2HPO_4 pH 6.5
Hybridizing buffer 2	10 mM MgCl_2 , 50 mM Tris-HCl, pH 8.0
Loading denaturing buffer	98 vol% Formamide, 2 vol% 0.5 M EDTA
Loading native buffer	50 vol% Glycerine, 50 vol% 1 x TBE
Na-, K-, Li-, NH_4OAc buffer	0.1 M Na-, K-, Li-, and NH_4OAc , adjusted by conc. HCl to pH 5.2

Native gel solution	20% Acrylamide/bisacrylamide 19:1 (Roth), 1 x TBE
Solution for Phenol-chloroform-extraction	1) saturated Phenol in 1 x TE, 2) CHCl ₃ /isoamylic alcohol 24:1, 3) CHCl ₃
TEAAc buffer	0.05 M Triethylammoniumacetate, pH 7.0
TBE (1 x)	0.1 M Tris, 1 mM EDTA, 85 mM boric acid, pH 8.3
TBK buffer	Triethylammonium bicarbonate buffer, pH 8.5 (Fluka)
Tris-HCl buffer	1 M Tris, adjusted by conc.HCl to pH 8.0, 8.9

5.1.3 Enzymes

Table 22 – Enzymes

Alkaline phosphatase, calf intestinal (CIP)	10000 u/ml, BioLabs
Phosphodiesterase I from <i>Crotalus adamanteus</i> venom, Type VI	≥ 0.01 u/mg, Sigma

5.1.4 Apparatus

Table 23 – Apparatus

Centrifuge	Centrifuge 5804 R and 5804, Eppendorf
DNA synthesizer	Gene Assembler Special, Pharmacia
Gel electrophoresis	Electrophoresis Power Supply, EPS 3500
HPLC	1) LaChrom, Merck Pump: L-7100, Merck UV-detector: L-7420, Merck 2) Äkta Purifier, Amersham Biosciences Pump: P-900, Amersham Biosciences UV-detector: UV-900, Amersham Biosciences Fluorescence-detector: SHIMAZU RF-535
Lyophilisator	Speed Vac SC 110, Savant UNIVAPO 100H
Mass spectrometer	microflex MALDI-TOF MS, Bruker Daltonics
NMR spectrometer	300 MHz Bruker, 600 MHz Bruker
pH-meter	Knick
Rotary evaporator	Heidolph
ThermoShaker	Biometra

UV-VIS camera system	VILBER LOURMAT
UV-VIS spectrometer	NanoDrop ND-1000 Spectrometer
UV-Lamp	SVL

5.2 Methods for purification and analysis of the samples

5.2.1 Chromatographic methods

Thin layer chromatography (TLC)

Silica gel 60 F₂₅₄ on aluminium plate from Merck. Detection was carried out under UV light at 254 nm and 365 nm. The following mixtures were used as spraying reagents: 1) Ninhydrin reagent: 400 mg ninhydrin, 50 ml methanol and 0.76 ml acetic acid, 2) 0.5% KMnO₄ in water, 3) Trifluoroacetic acid (TFA).

Column chromatography

Column chromatography was performed with silica gel 60 0.063-0.2 mm/70-230 mesh ASTM from MACHEREY-NAGEL. The length and diameter of the silica gel bed are customarily made depended on the amounts of substances as well as the difficulty of the separation.

HPLC

Buffers for reversed-phase HPLC purification were filtered through 0.45 μ l membrane and degassed in ultra-sonic bath before used. Buffers used in RNA purification and labeling were prepared from autoclaved micro-pore water and filtered through 0.20 μ l membrane. The analysis of the chemical reaction mixtures were carried out in LaChrom HPLC system, while the purification of the reaction products and oligonucleotides were achieved with Äkta Purifier system. The samples were filtered through 0.45 μ m membrane before injected into the HPLC system. The components of the samples were detected by UV-detector at 260 nm or by fluorescence-detector at the corresponding excitation-emission wavelengths of the dyes. In most cases, reversed-phase HPLC column C-18 were used. The mobile phase is mixed in suitable scale from buffer A containing low percentage of MeCN (or MeOH) and buffer B containing high percentage MeCN (or MeOH). When oligonucleotides were purified, buffers containing TEAAc (0.1 M, pH 7.0) were required. TEAAc can mask the negatively charged phosphate backbone, increasing the hydrophobicity of the oligonucleotides, therefore improve

the separation. The flow rate was set to optimize the separation and to keep the system under allowed pressure. Before each run, the column was equilibrated with buffer A. After the separation of the sample, the column was washed with buffer B (3-5 column volumes). The column is normally store in 70-80% MeCN. Additional washing is required, if the pressure is unnormally high or samples are contaminated with unknown substances. The gradients being used in this work are listed in the table below:

Table 24 – Gradients

Gradient A

Column	250/4.6 Eurospher 80 5 μ m C18
Flow rate	0.8 ml/min
Buffer A	100% H ₂ O
Buffer B	100% MeCN
Gradient	isocratic 20% B (Gradient A1) isocratic 13% B (Gradient A2)

Gradient B

Column	VP 125/21 Nucleosil 120-10 C18 (Macherey-Nagel)
Flow rate	0.6 ml/min
Buffer A	5% MeCN
Buffer B	30% MeCN
Gradient	0% B for 15 min, 15-90% B in 385 min, 100% B for 140 min

Gradient C

Column	VP 125/21 Nucleosil 120-10 C18 (Macherey-Nagel)
Flow rate	0.5 ml/min
Buffer A	5% MeCN
Buffer B	30% MeCN
Gradient	0% B for 15 min, 15-70% B in 840 min, 100% B for 168 min

Gradient D

Column	VP 125/21 Nucleosil 120-10 C18 (Macherey-Nagel)
Flow rate	0.6 ml/min
Buffer A	5% MeCN
Buffer B	30% MeCN
Gradient	0% B for 15 min, 12-75% B in 700 min, 100% B for 140 min

Gradient E

Column	EC 250/4 Nucleodur 100-5 C18 ec (Macherey-Nagel)
Flow rate	0.5 ml/min
Buffer A	0.1 M TEAAc (pH 7), 5% MeCN
Buffer B	0.1 M TEAAc (pH 7), 70% MeCN

Gradient	0% B for 5 min, 10-55% B in 76 min, 55-100% B in 19 min
Gradient F	
Column	Dionex BioLC, DNAPac PA-100
Flow rate	3.0 ml/min
Buffer A	10 mM Tris-HCl, 6 M urea, 10 mM NaClO ₄
Buffer B	10 mM Tris-HCl, 6 M urea, 500 mM NaClO ₄
Gradient	0% B for 32 min, 0-70% B in 158 min, 100% B for 95 min
Gradient G	
Column	EC 250/4 Nucleodur 100-5 C18 ec (Macherey-Nagel)
Buffer A	0.1 M TEAAc (pH 5.5), 5% MeOH
Buffer B	MeOH
Gradient	0-30% B in 95 min, 30-100% B in 19 min, 100%B for 19 min

5.2.2 NMR

The samples were analyzed on Bruker Avance 300 and 600 MHz NMR spectrometer. For elucidation of the structure of the synthesized compounds, the one-dimensional ¹H NMR, proton-decoupled ¹³C NMR and DEPT 135 spectra were measured in most cases. In the case of compound 8-(3-trifluoroacetamidoprop-2-en-1-yl)adenosine, two-dimensional HSQC and HMBC spectroscopic data were required. All NMR measurements were performed in DMSO-d₆ and the chemical shift of the solvent at 25 °C ($\delta(\text{ppm}) = 2.5$) was chosen as the internal reference. Chemical shifts of the samples are given in ppm, coupling constants are given in Hz. For ³¹P NMR spectra of the phosphoramidites, H₃PO₄ ($\delta(\text{ppm}) = 0$) was added as the internal reference. Abbreviations of the multiplicities are given as following: s= singlet, d= doublet, t= triplet, q= quartet, sept= septet, m= multiplet, br= broad. More complex coupling patterns are presented by combinations of the respective symbols, for example: dd indicates a doublet from doublets.

5.2.3 MALDI-TOF

Chemical substances: 1-2 mg of the sample was dissolved in 100 μl methanol or water. 1.5 μl of the solution of the sample and 1.5-3.0 μl of the saturated matrix solution (30-40 mg 3-hydroxypicolinic acid (3-HPA) in 500 μl MeCN/H₂O 1:1, vortexed for 30 seconds) were mixed. 1-2 μl of the mixture was loaded on a MALDI-plate. After dried, the sample was analyzed by Bruker microflex Daltonics mass spectrometer in reflective positive (or negative) mode with 40-50 shoots/measurement. The laser intensity was adjusted, so that the intensity of the desired signals was about 1000.

RNA samples: Is it suggested to desalt the RNA samples, even when they have been precipitated from ethanol or purified by reverse-phase HPLC. For the desalination of the RNA, Sephadex G25 fine (GE Healthcare, suitable for RNAs larger than 10-mer) was used. The desalted samples were then dissolved in autoclaved micro-pore water to give a concentration of about 100-500 pmol/ μ l. 1 μ l RNA solution and 1-2 μ l matrix solution were treated with cation-exchange beads (Dowex 50 WX8, NH_4^+ -form, 100-200 mesh, Serva Feinbiochemica; 4-7 μ l suspension of the beads in autoclaved micro-pore water was pipetted in a 250 μ l eppendorf and dried by withdrawing water with a 2.5 μ l tip. To the beads were added the mixture of the oligonucleotide and matrix solutions). The mixture was allowed to stand for about 10 minutes, then loaded on the MALDI-plate and dried in open air. The samples were measured using linear negative (or positive) mode with 40-50 shoots/measurement. The sample is heterogeneously crystallized, meaning, that at different positions there are different signal abundances and intensities. Good signals can normally be found around the edge of the crystals. Besides the main peak $[\text{M}-1]^-$ (negative mode), the signals corresponding to $[\text{M}-2]^{2-}/2$ were in some cases also observed.

5.2.4 Chemical synthesis and purification of RNAs

Chemical synthesis of RNA

The synthesis of the RNAs was performed by a DNA-synthesizer (Gene Assembler Special, Pharmacia) using phosphoramidite building blocks and CPG-support which are commercially available from ChemGenes Corporation and link technologies. The modified phosphoramidites were incorporated into the growing sequences at the designed positions.

Table 25 – Phosphoramidite building blocks and CPG-supports

Phosphoramidites	
A	5'-DMT-2'- <i>t</i> BDMSilyl-ribo Adenosine (<i>n</i> -PAC) CED (ChemGenes) Pac-A-CE phosphoramidite (link)
U	5'-DMT-2'- <i>t</i> BDMSilyl-ribo Uridine CED phosphoramidite U-CE phosphoramidite (link)
G	5'-DMT-2'- <i>t</i> BDMSilyl-ribo Guanosine (<i>n</i> -PAC) CED phosphoramidite (ChemGenes) <i>i</i> Pr-Pac-G-CE phosphoramidite (link)
C	5'-DMT-2'- <i>t</i> BDMSilyl-ribo Cytidine (<i>n</i> -PAC) CED phosphoramidite (ChemGenes)

	Ac-C-CE phosphoramidite (link)
Supports	
A-support	Adenosine (<i>n</i> -PAC) 3'- <i>t</i> BDMSilyl 2'- <i>lcaa</i> A, CPG 500, 45 μ mol/g (ChemGenes)
U-support	Uridine 3'- <i>t</i> BDMSilyl 2'- <i>lcaa</i> , CPG , 35.9 μ mol/g (ChemGenes) U RNA Synbase, CPG 1000/110, 44 μ mol/g (link)
G-support	Guanosine (<i>n</i> -PAC) 3'- <i>t</i> BDMSilyl 2'- <i>lcaa</i> G, CPG 500, 37 μ mol/g (ChemGenes) <i>i</i> Pr-Pac-rG Synbase, CPG 1000/110, 23 μ mol/g (link)
C-support	Cytidine (<i>n</i> -PAC) 3'- <i>t</i> BDMSilyl 2'- <i>lcaa</i> , CPG 500, 37 μ mol/g (ChemGenes) Ac-rC Synbase, CPG 1000/110S, 36 μ mol/g (link)
Universal support	Custom Primer Support Universal 40, 38 μ mol/g (GE Healthcare)

The syntheses were carried out in 1 μ mol scale following the standard phosphoramidite procedure. The unmodified phosphoramidites were used in 0.1 M solution in dry MeCN containing less than 0.001% water. With this concentration, the on-going phosphoramidite will have ten equivalents excess compared to the 5'-OH of the growing chain. The modified building blocks were applied in 0.1-0.15 M solution in MeCN. A 0.3 M solution of 5-benzylmercaptotetrazole (BMT; H₂O content < 75 ppm; emp Biotech GmbH) in dry MeCN was used as the activator. All syntheses were carried out using the "trityl-off" mode. The system was kept under argon during the whole procedure. The solutions of phosphoramidites, BMT and MeCN were kept over molecular sieve 0.3 nm (Merck). The reagents and steps in the cycles of the chemical synthesis of RNA according to the phosphoramidite methodology are summarized in Table 26.

Table 26 – Reagents and steps in the chemical synthesis of RNA

Step	Reagent	Time
5'-Detritylation	3% Dichloroacetic acid in 1,2-dichloroethane	36 s
Activation/Coupling	0.3 M BMT in MeCN	6 min
	Phosphoramidite: 0.1 M (unmodified) or 0.1-0.15 M (modified) in MeCN	or 2 x 6 min
Capping	Cap A: <i>N</i> -Methylimidazole/MeCN 1:5 (v/v) Cap B: Acetic anhydride/2,4,6-trimethylpyridine/MeCN 2:3:5 (v/v/v)	48 s
Oxidation	0.01 M I ₂ in 2,4,6-trimethylpyridine/MeCN/H ₂ O 1:10.8:5 (v/v/v)	18 s

The concentration as well as the coupling time of modified phosphoramidites were adjusted from the standard procedure in order to optimize the coupling efficiency.

Deprotection of the chemically synthesized oligonucleotides

The column containing the CPG-support with the synthesized oligonucleotide was placed in a vial and centrifuged to remove MeCN. The dry CPG-support was transferred into two other 1.5 ml vials. To each of these two vials, 750 μ l NH₃ 30% and 750 μ l ethanolic methylamine were added. These vials were then sealed and incubated at 65 °C for 1 hour during which the mixture was from time to time vortexed. The mixture was then cooled down to room temperature, the supernatant was transferred into two new 2.0 ml vials. The support was washed with ethanol/water 1:1 (v/v) (3 x 150 μ l). The solutions and the washing fractions were collected, frozen in liquid nitrogen and lyophilized in a Speed Vac to dryness. The residue in each vial was dissolved in 800 μ l of a 1:3 (v/v) mixture of DMF/Et₃N.3HF and incubated at 55 °C for 1.5 hours. After the reaction, the solutions in the vials were cooled down and transferred into a 50-ml falcon tube. To the falcon tube were added 200 μ l H₂O (to stop the reaction) and 20 ml butanol. The mixture was well mixed and kept at -20 °C overnight. The solution was centrifuged for 30 minutes at 6000 rpm, the supernatant was decanted, the RNA pellet was washed several times with cold 80% ethanol and dried at room temperature in open air (or under vacuum for a few minutes). The following purification step was performed with HPLC or denaturing PAGE.

PAGE

Native PAGE: Native gels were used to analyze the hybridization reaction of two single-stranded oligonucleotides. All the native gels were made from 15% native gel solution and in analytical scale with the size of 80 x 100 x 1.5 mm. Thus, 15 ml 20% stock native gel solution (see Table 21) were diluted with 5 ml 1 x TBE buffer to get 20 ml 15% native gel solution. The gel solution was polymerized by the addition of 20 μ l TEMED and 250 μ l 10% solution of APS in water (w/v). The electrophoresis was carried out in 1 x TBE buffer. The gel was prerun at 80 V for 30 minutes. The hybridizing mixture was dried, dissolved again in H₂O/native loading buffer 1:1 (v/v) and loaded on the gel (no more than 15 μ l in each well). The gel was run at 100-120 V. After the electrophoresis had finished, the gel was exposed to UV- and/or fluorescence lamp at 254 and/or 365 nm, respectively.

Denaturing PAGE: Denaturing gels were applied to purify all of the unlabeled and labeled oligonucleotides being synthesized and used in this work. Depending on the purpose (analyti-

cal or preparative) as well as the length of the oligonucleotides, the preparation of the gel and the electrophoresis procedure are summarized in Table 27.

Table 27 – Denaturing analytical and preparative PAGE

	Analytical gel	Preparative gel
Size	80 x 100 x 1.5 mm	200 x 200 x 1.5 mm
Gel solution volume	V= 20 ml (15%)	V= 100 ml (8, 12 or 15%)
Polymerizing reagents	20 μ l TEMED 250 μ l 10% APS solution in water (w/v)	30 μ l TEMED 1 ml 10% APS solution in water (w/v)
Loaded sample volume	< 15 μ l	< 40 μ l
Prerun at	80 V, 30 min	200 V, 30-60 min
Run at	80-100 V	400 V

To prepare a denaturing gel in preparative scale, 20% stock gel solution (see Table 21) was diluted with 7 M urea to get the desired concentration in a total volume of 100 ml (8, 25 and 32-mer oligonucleotides: 15%, 60-mer oligonucleotides: 10-12% gel) which was used to make a gel of 200 x 200 x 1.5 ml. The polymerization of the gel was conducted by the addition of 30 μ l TEMED and 1 ml 10% solution (w/v) of APS in water. After polymerized, the gel was prerun at 200 V for 30-60 minutes in 1 x TBE buffer. The RNA samples were dissolved in H₂O/loading buffer 1:1 (v/v), denatured at 90 °C for 3-5 minutes and loaded on the gel when hot (less than 40 μ l for every well). A mixture of bromophenol blue and xlenecyanol was used as reference. After the electrophoresis, the bands corresponding to the desired oligonucleotides were detected by UV- and/or fluorescence shadowing at 254 and/or 365 nm, respectively. The product bands were cut out and eluted with suitable buffer.

To perform an analytical gel, the same procedure was applied, but with a smaller gel size (see Table 27). If necessary, the analytical gels were stained for 10 minutes with ethidium bromide (5 μ g/ml in 1 x TBE), washed with water and exposed to a transilluminator.

Elution of oligonucleotides from gel

The bands corresponding to the desired oligonucleotide products were excised from the gel and cut into small pieces. The gel pieces were placed in a falcon tube and covered with 0.5 M LiOAc buffer ("crush-and-soak" method). The falcon was then shaken at 10 °C overnight. On the next day, the eluting buffer was changed by a new solution of LiOAc and the oligonucleotides were eluted at 10 °C for another 4 hours. The procedure was repeated one more

time so most of the oligonucleotide samples were eluted out from the gel pieces. The oligonucleotide products were separated from the solution by precipitation from ethanol/acetone.

Precipitation of RNA from solution

Precipitation from butanol: This method was used to precipitate the crude oligonucleotides after the unblocking of the protecting groups and of the synthesized oligonucleotides from the support. To the deprotection reaction, 20 ml butanol was added, the mixture was thoroughly mixed and kept at -20 °C overnight. After centrifuged at 6000 rpm for 30 minutes, the supernatant was decanted, the pellet was dried in open air or *in vacuo* for a few minutes, dissolved in water and purified by denaturing PAGE or HPLC.

Precipitation from ethanol/acetone: This method was used to separate oligonucleotides from eluents in LiOAc buffer. The eluents were collected and concentrated in a Speed Vac until the concentration of LiOAc was about 1.0-1.5 M. Five volumes of ethanol/acetone 1:1 (v/v) were added. The mixture was then well mixed and kept at -20°C overnight. After centrifuged at 6000 rpm for 45 minutes, the supernatant was decanted, the pellet was washed with cold 70% ethanol, dried in open air (or under vacuum for a few minutes), dissolved in a defined amount of water and the concentration was calculated from the absorption at 260 nm and/or at the absorption wavelength of the fluorescence dyes if the oligonucleotides were labeled with these dyes.

Precipitation from ethanol: This method can be used to precipitate RNA sample from the reaction with CIAP enzyme. To the reaction solution, 0.1 volume 3 M NaCl and 2.5 M volume of absolute ethanol were added. The mixture was vortexed, stored -20 °C overnight. The solution was centrifuged at 14000 rpm for 45 minutes, the supernatant was decanted, the pellet was washed with cold 70% ethanol and dried in vacuum for a few minutes.

Desalination

Gel filtration: This method was used to remove buffers and the excess amounts of dyes in the labeling reaction from oligonucleotides larger than 10-mer. Thus, 1.1 g Sephadex G25 (GE Healthcare) was suspended in 10 ml autoclaved micro-pore water and allowed to swell for at least 3 hours. The swollen material was used to pack a column of 4.0 x 1.5 cm which was equilibrated with 20 ml water. The oligonucleotide sample was dissolved in 300-500 μ l water and loaded on the column. After the sample had sunken into the column bed, water was added slowly to elute the oligonucleotide. 0.5-ml Fractions were collected and checked for the presence of the oligonucleotide by UV-VIS spectrometer at 260 nm and/or at the absorption wavelength of the chromophores, if the oligonucleotide was labeled with dyes.

Reversed-phase chromatography: The desalination of an oligonucleotide sample was performed with a reversed-phase column (Sep-Pak Vac 12cc (2g), C18) as following: i) Wash the prepacked column with 10 ml MeCN, then equilibrate it with 10 ml 0.1 M TBK buffer pH 8.5; ii) 0.5-1.0 ml RNA sample in water was loaded on the column; iii) Wash the column again with 2 ml 0.1 TBK buffer and 20 ml water; iv) Elute the sample with MeCN/H₂O 6:4 (v/v) and collect 1-ml fractions (about 10 fractions). Fractions containing the oligonucleotide sample were detected by UV-VIS spectrometer at 260 nm.

Phenol-chloroform extraction

This extraction was used to eliminate CIP and phosphodiesterase I from the reaction mixtures. The reaction mixture was vigorously mixed with the same volume of phenol (the under layer in the saturated solution of phenol in 1 x TBE buffer). The mixture was vortexed for 30 seconds and the phenol phase was removed. The extraction with phenol was repeated one more time. Afterwards, the sample was extracted with chloroform/isoamyl alcohol 24:1 (v/v) (2 times) and chloroform (2 times) using the same procedure. The oligonucleotides can be obtained by ethanol/acetone precipitation.

Concentration determination of RNA

The concentration of the RNA samples can be determined by measuring the UV- and/or fluorescence absorption at 260 nm or at the absorption wavelength of the chromophores, when the RNAs are labeled with dyes, by a UV-VIS spectrometer. The relationship between the absorption of the sample and its concentration is presented by the Lambert-Beer law:

$$A = \varepsilon lc$$

Where: A: Absorption
 ε (cm⁻¹M⁻¹): Extinction coefficient
 l (cm): Thickness of the cell
 c (mol/l): Concentration

The extinction coefficient of the RNA at 260 nm can be calculated with IDT SciTools - Oligo-Analyzer 3.1 (online at: <http://eu.idtdna.com/analyzer/Applications/OligoAnalyzer/>). Informations of the dyes being used in this work can be obtained from the corresponding suppliers.

Table 29 – Optical data of the fluorescent labels

Dye	λ_{abs} (nm)	ε_{abs} (cm ⁻¹ M ⁻¹)	λ_{fl} (nm)	Supplier
ATTO 647N	644	1.5 x 10 ⁵	669	ATTO-Tec

Alexa Fluor 488	495	7.1×10^4	519	invitrogen
Cy5	646	2.5×10^5	665	GE Healthcare

When the absorption A , the thickness of the cell l and the extinction coefficient ε of the sample are known, its concentration can be calculated by the following equation:

$$c = A/(\varepsilon l)$$

The calculations based on the UV absorption at 260 nm and the fluorescence at the λ_{abs} of the dyes gave compatible results.

5.3 Synthesis of linkers

5.3.1 *N*-Allyltrifluoroacetamide **L1**

Method A: Trifluoroacetic anhydride (4.56 g; 3 ml; 21.7 mmol) was added dropwise to an ice-cold solution of allylamine (2.48 g; 3.3 ml; 43.4 mmol) under argon atmosphere over a period of 45 minutes with stirring. The mixture was then warmed up gradually to room temperature and stirred at room temperature overnight. The *N*-allyltrifluoroacetamide **L1** was then isolated as a colorless liquid from the dark-red viscous oil by a short-path distillation under reduced pressure (0.25 mbar; 40-45 °C) which was solidified when kept at -20°C.

Yield: 2.82 g (18.4 mmol; 85%).

^1H NMR (300 MHz, DMSO- d_6): δ (ppm)= 3.81 (2 H, t, J 5.5; CH_2), 5.10 (2 H, m, $=\text{CH}_2$), 5.75-5.88 (1 H, m, $=\text{CH}$), 9.63 (1 H, br s, NH).

^{13}C NMR (300 MHz, DMSO- d_6): δ (ppm)= 41.33, (110.26, 114.08, 117.90 and 121.72, q, J 288, CF_3), 116.17, 133.28, (155.47, 155.95, 156.43 and 156.91, q, J 36, $(\text{C}=\text{O})\text{CF}_3$).

Method B: Ethyl trifluoroacetate (20.3 ml; 170.3 mmol; 1.3 eq.) was added dropwise to an ice-cold solution of allylamine (9.84 ml; 131 mmol; 1.0 eq.) in anhydrous methanol (20 ml). The resulting solution was stirred at room temperature overnight. Methanol and the excess of the starting materials were then removed by rotary evaporation under vacuum, the residue was then distilled under reduced pressure (0.51 mbar, 50 °C) to afford **L1** as a colorless liquid which has the same analytical properties as the product obtained in method A.

Yield: 1.6 g (104.8 mmol; 80%).

5.3.2 *N*-Allyl-6-(*N*-trifluoroacetyl amino)hexanamide **L2**

6-(N-Trifluoroacetyl amino)hexanoic acid

6-Aminohexanoic acid (10 g; 75 mmol) was suspended in anhydrous methanol (50 ml) and triethylamine (53 ml). To the resulting suspension, ethyl trifluoroacetate (13.5 ml; 115 mmol; 1.5 eq.) was added dropwise while stirring. The reaction mixture became clear after one hour having a pale yellow color. The mixture was stirred under argon overnight at room temperature. The solvent was removed by rotary evaporation under reduced pressure to give a viscous yellow oil. The oil was then dissolved in ethyl acetate (200 ml), washed with 1 M HCl (100 ml x 3), saturated NaCl (100 ml x 3) and then dried over Na₂SO₄. The dried solution was filtered through filter paper to remove drying reagent and evaporated under reduced pressure to give a viscous pale yellow oil which was recrystallized from hot diethyl ether to afford 6-(*N*-trifluoroacetyl amino)hexanoic acid as white crystals.

Yield: 14.3 g (63 mmol; 84%).

¹H NMR (300 MHz, DMSO-*d*₆): δ(ppm)= 1.20-1.30 (2 H, m, CH₂), 1.42-1.54 (4 H, m, CH₂-CH₂), 2.19 (2 H, t, *J* 7.2, CH₂(C=O)), 3.13-3.19 (2 H, m, CH₂NH), 9.38 (1 H, br s, NH), 11.99 (1 H, br s, COOH).

N-Allyl-6-(*N*-trifluoroacetyl amino)hexanamide **L2**

Method A: 6-(*N*-Trifluoroacetyl amino)hexanoic acid (10.7 g; 47.3 mmol) and EDAC (10 g; 52 mmol; 1.1 eq.) were dissolved in anhydrous DMF (20 ml). Allylamine (3.9 ml; 53.9 mmol; 1.1 eq.) was added dropwise to the resulting solution while stirring. The reaction was stirred under argon at room temperature overnight. DMF was then removed *in vacuo* to give a viscous yellow oil. This oil was dissolved in DCM (500 ml), washed with water (100 ml x 2), saturated NaHCO₃ solution (100 ml x 2), brine (100 ml x 2) and dried over Na₂SO₄. Na₂SO₄ was then filtered off and the solvent was removed. The residue was crystallized from hot diethyl ether to furnish *N*-allyl-6-(*N*-trifluoroacetyl amino)hexanamide **L2** as a white solid.

Yield: 6.89 g (25.87 mmol; 55%).

¹H NMR (300 MHz, DMSO-*d*₆): δ(ppm)= 1.23 (2 H, m, CH₂), 1.48 (4 H, m, CH₂-CH₂), 2.09 (2 H, t, *J* 7.3, CH₂(C=O)), 3.15 (2 H, m, CH₂-NH), 3.66 (2 H, m, CH₂-NH), 5.06 (2 H, m, =CH₂), 5.78 (1 H, m, =CH), 7.92 (1 H, t, *J* 5.18, NH), 9.38 (1 H, br s, NH).

¹³C NMR (300 MHz, DMSO-*d*₆): δ(ppm)= 24.89, 25.84, 28.03, 35.14, 40.73, (110.27, 114.08, 117.90 and 121.72, q, *J* 288, CF₃), 114.81, 135.55, (155.42, 155.90, 156.37 and 156.85, q, *J* 36, (C=O)CF₃), 171.78.

Method B: 6-(*N*-Trifluoroacetylamino)hexanoic acid (1.31 g; 5.77 mmol) was dissolved in dry MeCN (6 ml). 1,1'-Carbonyldiimidazole (1.62 g; 10 mmol; 1.7 eq.) was added portionwise to the resulting solution to avoid the overreleasing of CO₂. The reaction mixture was stirred for 1 hour at room temperature under argon. Allylamine (0.75 ml; 10 mmol; 1.7 eq.) was added dropwise to the solution of the activated acid. The reaction mixture was stirred at room temperature overnight. The solvent was then removed, the residue was dissolved in DCM (50 ml), washed with 1 M HCl (20 ml x 3), brine (20 ml), water (20 ml) and dried over Na₂SO₄. The solvent was then evaporated under reduced pressure. The resulting solid was then recrystallized from hot diethyl ether to give a white solid which has the identical analytical properties as the product obtained in method A.

Yield: 0.97 g (3.65 mmol; 63%).

5.3.3 *N*-Propargyltrifluoroacetamide **L3**

To a magnetically-stirred, ice-cold solution of propargylamine (110 mg; 128 μ l, 2 mmol) in methanol (4 ml) was added ethyl trifluoroacetate (370 mg; 310 μ l; 2.6 mmol). The resulting solution was stirred at room temperature for 24 hours. The reaction mixture was then concentrated *in vacuo*, the residue was dissolved in CHCl₃ (10 ml) and washed with saturated NaHCO₃ solution (2 x 5 ml) and water (5 ml), dried over Na₂SO₄ and finally rotary evaporated to give a dark-red oil. This oil was then distilled under reduced pressure to give *N*-trifluoroacetylpropargylamine **L3** as a colorless liquid, which was solidified when kept at -20 °C.

Yield: 196 mg (1.3 mmol; 65%).

¹H NMR (300 MHz, DMSO-d₆): δ (ppm)= 3.23 (1 H, t, *J* 2.7, CH), 3.99 (2 H, d, *J* 2.4, CH₂), 9.97 (1 H, br s, NH).

5.4 5'-*O*-(4,4'-Dimethoxytrityl)-2'-*O*-*tert*-butyldimethylsilyl-3'-(2-cyanoethyl-*N,N'*-diisopropylamino phosphoramidite)-5-(3-trifluoroacetamidoprop-1-ynyl)uridine

5'-*O*-(4,4'-Dimethoxytrityl)-5-iodouridine **2**

5-Iodouridine **1** (740 mg; 2 mmol) was co-evaporated with anhydrous pyridine (5 ml x 3) and dissolved in anhydrous pyridine. DMT-Cl was added in three portions every 30 minutes (270

mg x 3; 2.4 mmol; 1.2 eq.). The reaction mixture was protected from moisture by connecting with a balloon of argon via a drying tube and stirred at room temperature. After 3 hours, TLC (SiO₂; DCM/MeOH 95:5 (v/v)) showed that there was still starting material left. Therefore, DMT-Cl (34 mg; 0.1 mmol; 0.05 eq.) was added and the reaction mixture was stirred overnight. Methanol (1 ml) was added to quench the unreacted DMT-Cl and after 10 minutes, the reaction mixture was concentrated to dryness *in vacuo*. The residue was dissolved in DCM (100 ml), washed with 5% solution of NaHCO₃ (20 ml x 2). The aqueous phase was extracted with DCM (2 x 20 ml). The organic extracts were then collected, dried over Na₂SO₄ and concentrated by rotary evaporation to a yellow gum which was purified by silica gel column chromatography (DMC/MeOH 99.5:0.5 to 95:5 (v/v)) to give **2** as yellow solid.

Yield: 793 mg (1.18 mmol; 59%).

R_f(SiO₂; DCM/MeOH 95:5 (v/v)): 0.34.

¹H NMR (300 MHz, DMSO-d₆): δ(ppm)= 3.18 (2 H, m, *H*-5' and *H*-5''), 4.00 (2 H, m, *H*-4' and *H*-3'), 4.18 (1 H, q, *J* 5.4, *H*-2'), 5.15 (1 H, d, *J* 5.7, OH), 5.47 (1 H, d, *J* 5.4, OH), 5.74 (1 H, d, *J* 5.1, *H*-1'), 6.89 (4 H, d, *J* 8.7, aromatic), 7.31 (9 H, m, aromatic), 8.00 (1 H, s, *H*-6), 11.76 (1 H, s, N-*H*).

5'-*O*-(4,4'-Dimethoxytrityl)-2'-*O*-*tert*-butyldimethylsilyl-5-iodouridine **3**

5'-*O*-(4,4'-Dimethoxytrityl)-5-iodouridine **2** (670 mg; 1 mmol) was co-evaporated with anhydrous pyridine (2 ml x 2), dry DCM (5 ml x 2), kept under vacuum overnight and then dissolved again in anhydrous THF (8 ml). To the solution were added anhydrous pyridine (0.4 ml; 5 mmol; 5.0 eq.) and AgNO₃ (200 mg; 1.2 mmol; 1.2 eq.). The reaction mixture was stirred for 15 minutes to give a white emulsion and TBDMS-Cl (200 mg; 1.3 mmol; 1.3 eq.) was added. The reaction was protected from moisture and stirred at room temperature until TLC (SiO₂; hexane/ethyl acetate 1:1 (v/v)) showed no starting material left (2.5 hours). The reaction mixture was diluted with ethyl acetate (50 ml), filtered through filter paper to remove the precipitation and washed with saturated solution of NaHCO₃ (20 ml x 2). The organic layer was dried over Na₂SO₄, concentrated under reduced pressure to give a white gum which was then purified by silica gel column chromatography (hexane/ethyl acetate 80:20 (v/v)) to furnish **3** as a white foam.

Yield: 558.2 mg (0.71 mmol; 71%).

R_f(SiO₂; hexane/ethyl acetate 1:1 (v/v)): 0.76.

¹H NMR (300 MHz, DMSO-d₆): δ(ppm)= 0.04 (6 H, 2 x s, Si(CH₃)₂), 0.84 (9 H, s, C(CH₃)₃), 3.22 (2 H, s, *H*-5' and *H*-5''), 3.74 (6 H, s, 2 x OCH₃), 4.01 (2 H, m, *H*-3' and *H*-4'), 4.31 (1

H, t, J 5.4 and 5.1, H -2'), 5.13 (1 H, d, J 5.7, OH -3'), 5.80 (1 H, d, J 5.4, H -1'), 6.90 (4 H, d, J 8.7, *aromatic*), 7.53 (9 H, m, *aromatic*), 8.05 (1 H, s, H -6), 11.81 (1 H, br s, N - H).

^{13}C NMR (300 MHz, DMSO-d_6): $\delta(\text{ppm})$ = -5.22, -4.83, 17.90, 25.58, 55.06, 59.74, 69.87, 70.23, 75.42, 83.55, 85.99, 87.87, 113.32, 126.78, 127.54, 127.99, 129.73, 135.23, 143.74, 144.73, 150.25, 158.13, 160.37, 164.91.

5'-*O*-(4,4'-Dimethoxytrityl)-2'-*O*-*tert*-butyldimethylsilyl-5-(3-trifluoroacetamidoprop-1-yn-yl)uridine 4

5'-*O*-(4,4'-Dimethoxytrityl)-2'-*O*-*tert*-butyldimethylsilyl-5-iodouridine **3** (300 mg; 0.38 mmol) was dissolved in anhydrous DMF (3 ml) in a round-bottom flask. Any dissolved oxygen in the solution was removed by exchanging between vacuum and a stream of argon (3 times) before the reagents were added. To the argon saturated solution, the following reagents were added in the indicated order: i) 228 μl (1.63 mmol; 4.3 eq.) freshly distilled triethylamine, ii) 182 mg (1.2 mmol; 3.0 eq.) *N*-propargyltrifluoroacetamide **L3**, iii) 44 mg (0.038 mmol; 0.1 eq.) $\text{Pd}(\text{PPh}_3)_4$, and iv) 14.4 mg (0.076 mmol; 0.2 eq.) CuI . The reaction mixture was stirred for 8 hours in the dark when TLC (SiO_2 ; hexane/ethyl acetate 55:45(v/v)) showed only traces of the starting material. The reaction mixture was then concentrated by rotary evaporation to remove DMF. The residue was dissolved in ethyl acetate, washed with 5% solution of EDTA (20 ml x 4) and dried over Na_2SO_4 . The dried solution was filtered through filter paper to remove the drying reagent, concentrated under vacuum to give a dark yellow solid which was then purified by silica gel column chromatography (hexane/ethyl acetate 75:25 to 70: 30 (v/v)) to furnish **4** as a pale yellow foam.

Yield: 212.2 mg (0.26 mmol; 69%)

$R_f(\text{SiO}_2$; hexane/ethyl acetate 55:45(v/v)): 0.65.

^1H NMR (300 MHz, DMSO-d_6): $\delta(\text{ppm})$ = 0.03 and 0.05 (6 H, 2 x s, $\text{Si}(\text{CH}_3)_2$), 0.88 (9 H, s, $\text{C}(\text{CH}_3)_3$), 3.08 (1 H, m, H -5'), 3.38 (1 H, m, H -5''), 3.74 (6 H, s, 2 x OCH_3), 3.93 (2 H, d, J 5.4, CH_2), 4.05 (2 H, m, H -4' and H -3'), 4.34 (1 H, t, J 4.5 and 4.8, H -2'), 5.17 (1 H, d, J 6.0, OH), 5.74 (1 H, d, J 5.7, H -1'), 6.89 (4 H, dd, J 9.0 and 3.3, *aromatic*), 7.33 (9 H, m, *aromatic*), 7.97 (1 H, s, H -6'), 9.97 (1 H, t, J 5.1 and 5.7, N - H), 11.74 (1 H, s, N - H).

^{13}C NMR (300 MHz, DMSO-d_6): $\delta(\text{ppm})$ = -5.14, -4.78, 17.92, 25.63, 29.31, 55.00, 59.75, 63.03, 69.62, 74.87, 75.56, 83.28, 85.92, 87.41, 88.86, 98.08, 113.22, 113.30, (110.01, 113.83, 117.65 and 121.47, q, J 289, CF_3), 126.65, 127.42, 127.93, 129.67, 129.73, 134.96, 135.54, 143.34, 144.84, 149.46, (155.21, 155.69, 156.17 and 156.65, q, J 37, $(\text{C}=\text{O})\text{CF}_3$), 158.10, 161.41.

5'-O-(4,4'-Dimethoxytrityl)-2'-O-tert-butyldimethylsilyl-3'-(2-cyanoethyl-*N,N'*-diisopropyl-amino phosphoramidite)-5-(3-trifluoroacetamidoprop-1-ynyl)uridine **5**

5'-O-(4,4'-Dimethoxytrityl)-2'-O-tert-butyldimethylsilyl-5-(3-trifluoroacetamidoprop-1-ynyl)-uridine **4** (296 mg; 0.36 mmol) was co-evaporated two times with 5 ml dry DCM containing 10% pyridine. The nucleoside and a dry magnetic bar was then kept under vacuum over P₂O₅ overnight in a decicator. On the next day, the decicator was slowly filled with argon, so that the bottle containing the nucleoside was also filled with the inert gas. Dry freshly distilled DIPEA (320 μ l; 1.44 mmol; 4.0 eq.) was added, followed by dry DCM (2 ml). When the nucleoside was already dissolved, 2-cyanoethyl-*N,N'*-diisopropylamino-chlorophosphoramidite (120 μ l; 0.54 mmol; 1.5 eq.) was added dropwise to the solution. After 2 hours, the progress of the reaction was checked by TLC (SiO₂; hexane/ethyl acetate/triethylamine 45:45:10). The presence of the phosphoramidite was proved by the color reaction with ninhydrin reagent: the phosphoramidite product produced a pale yellow color, while the educt did not. The phosphoramidite product, however, run as fast as the starting material on the TLC, so another 0.3 eq. phosphitylating reagent was added to completely consume the excess of the starting material, if any. After 3 hours, anhydrous methanol (0.2 ml) was added to quench the excess amount of the phosphitylating reagent. The reaction mixture was diluted with ethyl acetate containing 10% triethylamine (150 ml), washed with saturated solution of NaHCO₃ (10 ml), saturated solution of NaCl (10 ml), dried over Na₂SO₄ and concentrated under vacuum to remove the solvents. The residue was purified by silica gel short column chromatography (hexane/ethyl acetate/triethylamine 60:35:5) to give **5** as a pale yellow foam. Before being used for RNA synthesis, the phosphoramidite was co-evaporated with dry DCM (3 times), kept under vacuum to remove trace of solvents, then overnight over P₂O₅ in an evacuated decicator.

Yield: 290.7 mg (0.29 mmol; 80%).

R_f(SiO₂; hexane/ethyl acetate/triethylamine 45:45:10 (v/v/v)): 0.69. The phosphoramidite product appeared to be a broaden spot as the two isomers of the chiral phosphorus were partially resolved by the solvent system.

¹H NMR (300 MHz, DMSO-d₆): δ (ppm)= 0.01, 0.03, 0.05 and 0.09 (6 H, 4 x s, Si(CH₃)₂), 0.83 and 0.86 (9 H, 2 x s, C(CH₃)₃), 1.35 (12 H, m, CH(CH₃)₂), 2.77 (t, *J* 5.8) and 2.88 (t, *J* 5.8) (2 H, CH₂-CN), 3.45 (2 H, m, CH(CH₃)₂), 3.74 (6 H, s, 2 x OCH₃), 3.97 (2 H, t, *J* 5.7, OCH₂), 4.19 (2 H, m, *H*-4' and *H*-3'), 4.52 (1 H, m, *H*-2'), 5.78 (d, *J* 5.7) and 5.84 (d, *J* 6.3) (1 H, *H*-1'), 6.89 (4 H, m, aromatic), 7.35 (9 H, m, aromatic), 7.99 and 8.01 (1 H, 2 x s, *H*-6), 9.98 (1 H, m, N-H), 11.75 (1 H, br s, N-H).

³¹P NMR (300 MHz, DMSO-d₆): δ (ppm)= 148.24, 149.27.

5.5 5'-O-(4,4'-Dimethoxytrityl)-2'-O-*tert*-butyldimethylsilyl-3'-(2-cyanoethyl-*N,N'*-diisopropylamino phosphoramidite)-5-(3-trifluoroacetamidoprop-1-enyl)uridine

5-(3-Trifluoroacetamidoprop-1-enyl)uridine **8**

5-Iodouridine **1** (740 mg; 2 mmol) was dissolved in DMF (7 ml). To the resulting solution, NaOAc buffer (7.1 ml; 0.1M; pH 5.2) and *N*-allyltrifluoroacetamide (2601 mg; 17 mmol; 8.5 eq.) were added. The space in the reaction bottom was filled with argon and a solution of Na₂[PdCl₄] (294.2 mg; 1.0 mmol; 0.5 eq.) in DMF (7 ml) was added while stirring vigorously. The reaction bottom was then placed in an oil bath at 80 °C for 8 hours. TLC (SiO₂; DCM/MeOH 8.5:1.5 (v/v)) showed that there was only trace of the starting material. The reaction mixture was filtered through celite (560 mess) to remove the black precipitated palladium element. The filtrate was treated with a solution of NaBH₄ in DMF until the brownish color disappeared. The solution was filtered again through celite and concentrated to a viscous yellowish oil which was then purified by silica gel column chromatography (DCM/MeOH 98:2 to 93.5:6.5 (v/v)) to give **8** as a white solid.

Yield: 458.3 mg (1.16 mmol; 58%).

R_f(SiO₂; DCM/MeOH 8.5:1.5 (v/v)): 0.17.

¹H NMR (300 MHz, DMSO-d₆): δ(ppm)= 3.62 (2 H, m, *H*-5' and *H*-5''), 3.85 (3 H, m, *H*-4' and CH₂), 3.99 (1 H, br s, *H*-3'), 4.07 (1 H, m, *H*-2'), 5.09 (1 H, br s, OH), 5.22 (1 H, br s, OH), 5.41 (1 H, br d, OH), 5.77 (1 H, d, *J* 4.8, *H*-1'), 6.18 (1 H, d, *J* 15.9, =CH), 6.46 (1 H, tt, *J* 15.9 and 6.1, =CH), 8.12 (1 H, s, *H*-6), 9.69 (1 H, t, *J* 5.4, *N*-H).

¹³C NMR (300 MHz, DMSO-d₆): δ(ppm)= 41.59, 60.51, 69.51, 73.73, 84.75, 88.13, 109.86, (110.24, 114.06, 117.88 and 121.70, q, *J* 288, CF₃), 123.92, 124.23, 138.20, 149.90, (155.34, 155.82, 156.30 and 156.77, q, *J* 36, (C=O)CF₃), 162.25.

5'-O-(4,4'-Dimethoxytrityl)-5-(3-*N*-trifluoroacetamidoprop-1-enyl)uridine **9**

The reaction was carried out as described for **2**: 5-(3-*N*-Trifluoroacetamidoprop-1-enyl)uridine **8** (677 mg; 1.7 mmol), DMT-Cl (700 mg; 2.1 mmol; 1.2 eq.), anhydrous pyridine, room temperature, overnight. **9** was then purified by silica gel column chromatography (DCM/MeOH 99:1 to 95:5 (v/v)) to give **9** as a white foam.

Yield: 778.7 mg (1.11 mmol; 66%).

R_f (SiO₂; DCM/MeOH 95:5 (v/v)): 0.62.

¹H NMR (300 MHz, DMSO-d₆): δ (ppm)= 3.14 (1 H, m, *H*-5'), 3.26 (1 H, m, *H*-5''), 3.64 (2 H, m, CH₂), 3.96 (1 H, m, *H*-4'), 4.08 (1 H, q, *J* 5.4, *H*-3'), 4.18 (1 H, q, *J* 5.1, *H*-2'), 5.16 (1 H, d, *J* 5.7, OH), 5.48 (1 H, d, *J* 5.4, OH), 5.74 (2 H, m, =CH and *H*-1'), 6.36 (1 H, tt, *J* 15.9 and 6.3, =CH), 6.88 ((4 H, d, *J* 8.7, aromatic), 7.32 (9 H, m, aromatic), 7.66 (1 H, s, *H*-6), 9.59 (1 H, t, *J* 5.4, NH), 11.53 (1 H, s, NH).

5'-O-(4,4'-Dimethoxytrityl)-2'-O-tert-butyltrimethylsilyl-5-(3-N-trifluoroacetamidoprop-1-enyl)uridine 10

The procedure was similar to that described for **3**: 5'-O-(4,4'-Dimethoxytrityl)-5-(3-N-trifluoroacetamidoprop-1-enyl)uridine **9** (751 mg; 1.1 mmol), anhydrous pyridine (0.35 ml; 4.4 mmol; 4.0 eq.), AgNO₃ (216 mg; 1.27 mmol; 1.15 eq.), TBDMS-Cl (216 mg; 1.43 mmol; 1.3 eq.), anhydrous THF (10 ml), room temperature, 6.5 hours. **10** was separated from the reaction mixture by silica gel column chromatography (hexane/ethyl acetate 90:10 to 75:25) to a white foam.

Yield: 428.4 mg (0.53 mmol; 48%).

R_f (hexane/ethyl acetate 1:1 (v/v)): 0.66.

¹H NMR (300 MHz, DMSO-d₆): δ (ppm)= 0.05 and 0.07 (6 H, 2 x s, Si(CH₃)₂), 0.85 (9 H, s, C(CH₃)₃), 3.18 (1 H, m, *H*-5'), 3.34 (1 H, m, *H*-5''), 3.57 (2 H, m, CH₂), 4.02 (2 H, m, *H*-4' and *H*-3'), 4.31 (1 H, t, *J* 4.7, *H*-2'), 5.12 (1 H, d, *J* 4.8, OH), 5.65 (1 H, d, *J* 15.9, =CH), 5.81 (1 H, d, *J* 4.8, *H*-1'), 6.32 (1 H, tt, *J* 15.8 and 6.4, =CH), 6.89 (4 H, d, *J* 8.7, aromatic), 7.31 (9 H, m, aromatic), 7.68 (1 H, s, *H*-6), 9.58 (1 H, t, *J* 5.4, NH), 11.54 (1 H, br s, NH).

¹³C NMR (300 MHz, DMSO-d₆): δ (ppm)= -5.12, -4.75, 17.94, 25.63, 41.82, 55.02, 63.39, 69.79, 75.24, 79.91, 83.14, 85.90, 88.51, 110.22, (110.22, 114.01, 117.83 and 121.65, q, *J* 288, CF₃), 113.30, 124.08, 124.88, 126.86, 127.61, 127.98, 129.72, 129.77, 135.02, 135.41, 137.67, 144.70, 149.51, (155.25, 155.73, 156.21 and 156.69, q, *J* 36, (C=O)CF₃), 158.18, 161.92.

5'-O-(4,4'-Dimethoxytrityl)-2'-O-tert-butyltrimethylsilyl-3'-(2-cyanoethyl-*N,N'*-diisopropylamino phosphoramidite)-5-(3-trifluoroacetamidoprop-1-enyl)uridine 11

The reaction was carried out as described for **5**: 5'-O-(4,4'-Dimethoxytrityl)-2'-O-tert-butyltrimethylsilyl-5-(3-trifluoroacetamidoprop-1-enyl)uridine **10** (243 mg; 0.3 mmol), anhydrous

DIPEA (0.27 ml; 1.2 mmol; 4.0 eq.), 2-cyanoethyl-*N,N'*-diisopropylamino-chlorophosphoramidite (0.1 ml; 0.45 mmol; 1.5 eq.), dry DCM (2 ml), room temperature, 3 hours. The phosphoramidite product **11** was purified by short silica gel column chromatography (hexane/ethyl acetate 60:40 to 40:60 (v/v), 1% triethylamine) to a white foam.

Yield: 263 mg (0.26 mmol; 87%).

R_f (SiO₂; hexane/ethyl acetate 55:45 (v/v), 1% triethylamine): 0.47; 0.53.

¹H NMR (300 MHz, DMSO-*d*₆): δ (ppm)= (0.01, 0.03, 0.05 and 0.08, 6 H, 4 x s, Si(CH₃)), (0.83 and 0.85, 9 H, 2 x s, C(CH₃)₃), 1.10 (12 H, m, N-CH(CH₃)₂), 2.77 (2 H, t, *J* 6.0, CH₂), 3.59 (4 H, *H*-5', *H*-5'' and N-CH(CH₃)₂), 3.73 (6 H, s, OCH₃), 3.78 (2 H, m, OCH₂), 4.19 (2 H, m, *H*-4' and *H*-3'), 4.51 (1 H, m, *H*-2'), (5.64 and 5.66, 1 H, 2 x d, *J* 15.8, =CH), (5.84 and 5.88, 1 H, 2 x d, 5.96 and 6.38, *H*-1'), 6.30 (1 H, m, =CH), 6.89 (4 H, m, aromatic), 7.33 (9 H, m, aromatic), (7.68 and 7.69, 1 H, 2 x s, *H*-6), 9.56 (1 H, br s, NH), 11.59 (1 H, br s, NH).

³¹P NMR (300 MHz, DMSO-*d*₆): δ (ppm)= 148.2; 149.23.

5.6 5'-*O*-(4,4'-Dimethoxytrityl)-2'-*O*-*tert*-butyldimethylsilyl-3'-(2-cyanoethyl-*N,N'*-diisopropylamino phosphoramidite)-5-(3-[6-trifluoroacetylaminohexanamido]prop-1-enyl)uridine

5-(3-[6-Trifluoroacetylaminohexanamido]prop-1-enyl)uridine **14**

The synthesis was the same as that described for **8**: 5-Iodoadenosine **1** (740 mg; 2 mmol), *N*-allyl-6-(*N*-trifluoroacetamino)hexanamide L2 (4250 mg; 16 mmol; 8.0 eq.), Na₂[PdCl₄] (294 mg; 1.0 mmol; 0.5 eq.), DMF (7 ml), NaOAc buffer (0.1M; pH 5.2; 7.1 ml), 81 °C, 8 hours. **14** was purified by silica gel column chromatography (DCM/MeOH 95:5 (v/v)) to a white solid.

Yield: 544 mg (1.07 mmol; 53%).

R_f (SiO₂; DCM/MeOH 8.5:1.5 (v/v)): 0.49.

¹H NMR (300 MHz, DMSO-*d*₆): δ (ppm)= 1.25 (2 H, m, CH₂), 1.48 (4 H, m, CH₂-CH₂), 2.09 (2 H, t, *J* 7.4, CH₂), 3.16 (2 H, m, CH₂), 3.57 (2 H, m, *H*-5' and *H*-5''), 3.74 (2 H, t, *J* 5.4, CH₂), 3.84 (1 H, m, *H*-4'), 3.99 (1 H, q, *J* 4.7, *H*-3'), 4.06 (1 H, m, *H*-2'), 5.07 (1 H, d, *J* 5.1, OH), 5.2 (1 H, t, *J* 4.8, OH), 5.39 (1 H, d, *J* 5.45, OH), 5.78 (1 H, d, *J* 4.9, *H*-1'), 6.12 (1 H, d, *J* 16.0, =CH), 6.40 (1 H, tt, *J* 15.9 and 5.8, =CH), 7.96 (1 H, t, *J* 5.6, NH), 8.08 (1 H, s, *H*-6), 9.39 (1 H, br s, NH), 11.42 (1 H, br s, NH).

^{13}C NMR (300 MHz, DMSO- d_6): $\delta(\text{ppm})$ = 25.11, 25.79, 28.04, 35.06, 40.80, 43.20, 60.55, 69.57, 73.68, 84.75, 88.04, 110.32, (113.09, 114.99, 116.90 and 118.82, q, J 289, CF_3), 122.09, 126.90, 137.34, 149.79, (155.74, 155.98, 156.22 and 156.45, q, J 36, $(\text{C}=\text{O})\text{CF}_3$), 162.06, 171.69.

5'-O-(4,4'-Dimethoxytrityl)-5-(3-[6-trifluoroacetylaminohexanamido]prop-1-enyl)uridine **15**

The reaction was carried out as described for **2**: 5-(3-[6-Trifluoroacetylaminohexanamido]prop-1-enyl)uridine **14** (697 mg; 1.37 mmol), DMT-Cl (558 mg; 1.65 mmol), anhydrous pyridine (5 ml), room temperature, 6 hours. **15** was purified by silica gel column chromatography (DCM/MeOH 99.5:0.5 to 93:7 (v/v) containing 0.25% triethylamine) to a pale yellow foam.

Yield: 550.6 mg (0.68 mmol; 49%).

$R_f(\text{SiO}_2; \text{DCM/MeOH } 95:5 \text{ (v/v)})$: 0.52.

^1H NMR (300 MHz, DMSO- d_6): $\delta(\text{ppm})$ = 1.22 (2 H, m, CH_2), 1.47 (2 H, m, $\text{CH}_2\text{-CH}_2$), 2.04 (2 H, t, J 7.4, CH_2), 3.14 (2 H, m, CH_2), 3.26 (1 H, m, $H\text{-}5'$), 3.47 (3 H, m, $H\text{-}5''$ and CH_2), 3.73 (6 H, s, OCH_3), 3.97 (1 H, m, $H\text{-}4'$), 4.08 (1 H, q, J 5.4, $H\text{-}3'$), 4.21 (1 H, q, J 5.3, $H\text{-}2'$), 5.16 (1 H, d, J 5.7, OH), 5.48 (1 H, d, J 5.3, OH), 5.70 (1 H, d, J 15.8, $=\text{CH}$), 5.79 (1 H, d, J 4.9, $H\text{-}1'$), 6.29 (1 H, tt, J 15.8 and 6.1, $=\text{CH}$), 6.89 (4 H, d, J 8.9, *aromatic*), 7.31 (9 H, m, *aromatic*), 7.62 (1 H, s, $H\text{-}6$), 7.82 (1 H, t, J 5.4, NH), 9.39 (1 H, t, J 5.1, NH), 11.50 (1 H, s, NH).

^{13}C NMR (300 MHz, DMSO- d_6): $\delta(\text{ppm})$ = 24.83, 25.90, 28.05, 35.12, 41.06, 55.02, 63.64, 69.99, 73.02, 82.87, 85.79, 88.68, (110.26, 114.08, 117.90 and 121.72, q, J 289, CF_3), 110.45, 110.59, 113.27, 122.30, 126.80, 127.66, 127.95, 129.69, 129.75, 135.20, 135.52, 137.42, 144.68, 149.69, (155.41, 155.89, 156.37 and 156.85, q, J 36, $(\text{C}=\text{O})\text{CF}_3$), 158.14, 162.04, 171.63.

5'-O-(4,4'-Dimethoxytrityl)-3'-(tert-butyldimethylsilyl)-5-(3-[6-trifluoroacetylaminohexanamido]prop-1-enyl)uridine **16**

The synthesis was similar to that described for **3**: 5'-O-(4,4'-Dimethoxytrityl)-5-(3-[6-trifluoroacetylaminohexanamido]prop-1-enyl)uridine **15** (607 mg; 0.75 mmol), anhydrous pyridine (240 μl ; 3.0 mmol; 4.0 eq.), AgNO_3 (153 mg; 0.9 mmol; 1.2 eq.), TBDMS-Cl (147 mg; 0.97 mmol; 1.3 eq.), anhydrous THF (4 ml), room temperature, 10 hours. **16** was then purified by silica gel column chromatography (hexane/ethyl acetate 95:5 to 50:50) to a white foam.

Yield: 298.1 mg (0.32 mmol; 43%).

R_f (SiO₂; hexane/ethyl acetate 2.5:7.5 (v/v)) 0.55.

¹H NMR (300 MHz, DMSO-d₆): δ (ppm)= 1.23 (2 H, m, CH₂), 1.46 (2 H, m, CH₂-CH₂), 2.10 (2 H, t, J 7.4, CH₂), 3.14 (2 H, m, CH₂), 3.30 (1 H, m, H-5'), 3.46 (3 H, m, H-5'' and CH₂), 3.73 (6 H, s, OCH₃), 4.02 (2 H, m, H-4' and H-3'), 4.31 (1 H, t, J 4.8, H-2'), 5.21 (1 H, d, J 5.9, OH), 5.63 (1 H, d, J 15.8, =CH), 5.83 (1 H, d, J 5.1, H-1'), 6.25 (1 H, tt, J 15.8 and 6.1, =CH), 7.64 (1 H, s, H-6), 7.79 (1 H, t, J 5.4, NH), 9.48 (1 H, t, J 5.4, NH), 11.54 (1 H, s, NH).

¹³C NMR (300 MHz, DMSO-d₆): δ (ppm)= -5.15, -4.78, 17.92, 24.82, 25.61, 25.88, 28.05, 35.09, 55.03, 63.42, 69.88, 75.20, 83.28, 85.91, 88.16, (110.75, 114.07, 117.89 and 121.71, q, J 289, CF₃), 113.29, 122.71, 126.86, 127.75, 127.98, 129.70, 129.74, 135.01, 135.36, 136.73, 144.68, 149.59, (155.39, 155.78, 156.35 and 156.83, q, J 36, (C=O)CF₃), 158.71, 161.95, 171.61.

5'-O-(4,4'-Dimethoxytrityl)-2'-O-tert-butyl dimethylsilyl-3'-(2-cyanoethyl-*N,N'*-diisopropylamino phosphoramidite)-5-(3-[6-trifluoroacetylaminohexanamido]prop-1-enyl)uridine **17**

The procedure was similar to that used for **5**: 5'-O-(4,4'-Dimethoxytrityl)-2'-O-tert-butyl dimethylsilyl-5-(3-[6-trifluoroacetylaminohexanamino]prop-1-enyl)uridine **16** (278 mg; 0.3 mmol), anhydrous DIPEA (270 μ l; 1.2 mmol; 4.0 eq.), 2-cyanoethyl-*N,N'*-diisopropylaminochlorophosphoramidite (100 μ l, 0.45 mmol, 1.6 eq.), dry DCM (2 ml), room temperature, 4 hours. The phosphoramidite product **17** was purified by short column chromatography (hexane/ethyl acetate 90:10 to 40:60 (v/v), containing 1% triethylamine) to a white foam.

Yield: 277.6 mg (0.25 mmol; 82%).

R_f (SiO₂; hexane/ethyl acetate 20:80 (v/v) containing 1% triethylamine): 0.74, 0.84 (two isomers).

¹H NMR (300 MHz, DMSO-d₆): δ (ppm)= 0.00, 0.02, 0.05 and 0.08 (6 H, 4 x s, Si-CH₃), 0.83 and 0.85 (9 H, 2 x s, C(CH₃)₃), 1.11 (12 H, d, J 6.9, CH(CH₃)₂), 1.17 (2 H, m, CH₂), 1.45 (2 H, m, CH₂), 2.00 (2 H, m, CH₂), 2.75 and 2.86 (2 H, 2 x t, J 5.8, CH₂CN), 3.15 (2 H, m, CH₂), 3.27 (2 H, m, H-5' and H-5'), 3.52 (2 H, m, CH), 3.73 (8 H, m, OCH₃ and CH₂), 3.80 (2 H, m, OCH₂), 4.15 (1 H, m, H-4'), 4.23 (1 H, m, H-3'), 4.52 (1 H, m, H-2'), 5.63 and 5.65 (1 H, 2 x d, J 15.8, =CH), 5.86 and 5.90 (1 H, 2 x d, J 6.4, H-1'), 6.22 (1 H, m, =CH), 6.89 (4 H, m, aromatic), 7.33 (9 H, m, aromatic), 7.65 (1 H, 2 x s, H-6), 7.78 (1 H, m, NH), 9.39 (1 H, m, NH), 11.6 (1 H, br s, NH).

³¹P NMR (300 MHz, DMSO-d₆): δ (ppm)= 149.39, 148.22.

5.7 5'-O-(4,4'-Dimethoxytrityl)-N-6-isobutyryl-8-(3-trifluoroacetamidoprop-1-ynyl)adenosine

8-(3-Trifluoroacetamidoprop-1-ynyl)adenosine **20**

8-Bromoadenosine (173 mg; 0.5 mmol) was dissolved in dry DMF **19** (4 ml). Any dissolved oxygen in the solution was removed by the exchange between vacuum and the introduction of argon (3 times). Pd(Ph₃P)₄ (58 mg; 0.05 mmol; 0.1 eq.) was added. The solution was again kept under vacuum and then saturated with argon. DIPEA (100 μ l; 0.6 mmol; 1.2 eq., freshly distilled over CaH₂) was added via syringe, followed by the addition of *N*-propynyltrifluoroacetamide **L3** (90.6 mg; 0.6 mmol; 1.2 eq.) and CuI (19 mg; 0.1 mmol; 0.2 eq.). The mixture was stirred at 40 °C for 11 hours. The solvent was then removed to give a brown viscous oil which was dissolved in DCM/MeOH 1:1 (v/v) and filtered through filter to remove the precipitation. The residue was purified by silica gel column chromatography to provide **20** as a yellow foam.

Yield: 151.0 mg (0.36 mmol; 73%).

R_f(SiO₂; DCM/MeOH 93:7): 0.31.

¹H NMR (300 MHz, DMSO-d₆): δ (ppm)= 3.54 (1 H, m, *H*-5'), 3.68 (1 H, m, *H*-5''), 3.98 (1 H, m, *H*-4'), 4.20 (1 H, m, *H*-3'), 4.35 (2 H, s, CH₂), 4.98 (1 H, q, *J* 6.0, *H*-2'), 5.2 (1 H, m, *J* 4.2, OH), 5.42 (1 H, d, *J* 6.3, OH), 5.51 (1 H, dd, *J* 8.2 and 3.7, OH-5'), 5.92 (1 H, d, *J* 6.9, *H*-1'), 7.63 (2 H, br s, NH₂), 8.16 (1 H, s, *H*-2), 10.25 (1 H, br s, NHCOCF₃).

¹³C NMR (300 MHz, DMSO-d₆): δ (ppm)= 29.39, 62.18, 70.91, 71.59, 71.82, 86.69, 89.35, 91.09, (110.01, 113.83, 117.65 and 121.47, q, *J* 288.2, CF₃), 119.31, 132.92, 148.36, 153.44, (155.61, 156.12, 156.59 and 157.07, q, *J* 36.7, (C=O)CF₃), 156.12.

N-6-Isobutyryl-8-(3-trifluoroacetamidoprop-1-ynyl)adenosine **21a**

8-(3-Trifluoroacetamidoprop-1-ynyl)adenosine **20** (416 mg; 1.0 mmol) was co-evaporated with anhydrous pyridine (3 x 4 ml), dissolved in anhydrous pyridine (4 ml). The resulting solution was protected from moisture (drying tube), purged with argon and placed on ice. To the ice cold solution, TMS-Cl (1.0 ml; 7.5 mmol; 7.5 eq.) was added dropwise via syringe. The ice bath was then removed and the mixture was stirred for 2 hours. The solution was then cooled on ice and isobutyric anhydride (0.25 ml; 1.5 ml; 1.5 eq.) was added dropwise via syringe and the ice bath was removed. After stirred for another 2 hours at room temperature, the reaction was placed again on ice, ice cold water (20 ml) was slowly added, followed after 15 minutes

by concentrated ammonia solution (1.5 ml) to get the final concentration 2.5M of ammonia. The mixture was kept on ice for 30 minutes, then the solvents were immediately evaporated. The residue was co-evaporated with toluene (3 x 5 ml) to remove traces of water, resuspended in MeOH and filtered through filter paper to remove the precipitation. The filtrate was then concentrated, dissolved in a small amount of MeOH, absorbed on silica gel and purified by column chromatography (DCM/MeOH 96:4 to 95:5(v/v)) to give **21a** as a yellow solid.

Yield: 247.9 mg (0.51 mmol; 51%).

R_f (SiO₂; DCM/MeOH 95:5 (v/v)): 0.22.

¹H NMR (300 MHz, DMSO-d₆): δ (ppm)= 1.13 (6 H, d, J 6.9, CH(CH₃)₂), 2.95 (1 H, sept, J 6.9, CH(CH₃)₂), 3.53 (1 H, m, H -5'), 3.70 (1 H, m, H -5''), 3.96 (1 H, m, H -4'), 4.27 (1 H, m, H -3'), 4.47 (2 H, d, J 3.3, CH₂), 5.04 (2 H, m, H -2' and OH), 5.24 (1 H, d, J 4.8, OH), 5.47 (1 H, d, J 6.0, OH), 6.00 (1 H, d, J 6.3, H -1'), 8.69 (1 H, s, H -2), 10.27 (1 H, br s, NH), 10.81 (1 H, s, NH).

¹³C NMR (300 MHz, DMSO-d₆): δ (ppm)= 19.17, 29.42, 34.45, 61.87, 70.51, 71.29, 71.49, 86.27, 89.34, 92.86, (110.00, 113.81, 117.62 and 121.43, q, J 287.4, CF₃), 123.66, 135.82, 150.15, 150.92, 152.62 (155.66, 156.15, 156.64 and 157.13, q, J 37.4, (C=O)CF₃), 175.26.

When the final concentration of ammonia in the solution is only 1.0 M and the solvent was removed immediately after 10 minutes kept on ice, the main product was *N,N'*-6-diisobutyl-8-(3-trifluoroacetamido-1-ynyl)adenosine **21b**.

¹H NMR (300 MHz, DMSO-d₆): δ (ppm)= 1.12 (12 H, d, J 6.6, 2 x CH(CH₃)₂), 2.88 (2 H, sept, J 6.6, 2 x CH(CH₃)₂), 3.56 (1 H, m, H -5'), 3.71 (1 H, m, H -5''), 3.97 (1 H, m, H -4'), 4.30 (1 H, m, H -3'), 4.49 (1 H, d, J 5.4, CH₂), 4.90 (1 H, m, OH), 5.12 (1 H, q, J 5.7, H -2'), 5.29 (1 H, d, J 4.8, OH), 5.54 (1 H, d, J 6.0, OH), 6.04 (1 H, d, J 6.3, H -1'), 9.00 (1 H, s, H -2), 10.26 (1 H, t, J 5.4, NH).

***N*-6-Isobutyladenosine 21c**

The reaction was carried as described for the synthesis of **21a**: 8-Bromoadenosine **19** (346 mg; 1.0 mmol), TMS-Cl (1.0 ml; 7.5 mmol; 7.5 eq.) 2 hours at room temperature, isobutyric anhydride (340 μ l; 2.0 mmol; 2.0 eq.) 2 hours at room temperature. Silica gel column chromatography: DCM/MeOH 98:2 to 96:4 (v/v).

Yield: 207.5 mg (0.5 mmol; 50%).

R_f (DCM/MeOH 95:5 (v/v)): 0.20.

^1H NMR (300 MHz, DMSO- d_6): $\delta(\text{ppm}) = 1.13$ (6 H, d, J 6.9, $\text{CH}(\text{CH}_3)_2$), 2.93 (1 H, sept, J 6.9, $\text{CH}(\text{CH}_3)_2$), 3.53 (1 H, m, $H-5'$), 3.69 (1 H, m, $H-5''$), 3.97 (1 H, m, $H-4'$), 4.27 (1 H, m, $H-3'$), 5.00 (1 H, dd, J 4.8 and 7.2, OH), 5.20 (1 H, q, J 5.9, $H-2'$), 5.28 (1 H, d, J 4.8, OH), 5.51 (1 H, J 6.0, OH), 5.91 (1 H, d, J 6.3, $H-1'$), 8.65 (1 H, s, $H-2$), 10.78 (1 H, s, NH).

***N*-6-Phenoxyacetyl-8-bromoadenosine 21d**

8-Bromoadenosine **19** (346 mg; 1.0 mmol) was co-evaporated with anhydrous pyridine (3 x 5 ml) and dissolved in anhydrous pyridine (5 ml). The solution was protected from moisture (drying tube) and cooled in an ice bath. To the ice cold solution was added TMS-Cl (1.0 ml; 7.5 mmol; 7.5 eq.) dropwise via syringe. The ice bath was then removed and the reaction was stirred for 2 hours. In another flask, 1,2,4-triazole (104 mg; 1.5 mmol; 1.5 eq.) was dissolved in anhydrous pyridine (2.5 ml) and anhydrous MeCN (2.5 ml). To this solution, phenoxyacetyl chloride (0.2 ml; 1.5 mmol; 1.5 eq.) was added dropwise via syringe. After 10 minutes, the phenoxyacetylating solution was added via syringe to the solution of the TMS-protected nucleoside over 1 hour, during the time the temperature was elevated to 55 °C. The reaction was stirred at 55 °C for another 6 hours. The reaction mixture was then cooled on ice and ice cold water (1 ml) was slowly added. After 10 minutes, the solvents were removed. The residue was purified by silica gel column chromatography (DCM/MeOH 98:2 to 96:4 (v/v)) to give **21d** as a yellow solid.

Yield: 263.5 mg (0.55 mmol; 55%).

R_f (DCM/MeOH 96:4 (v/v)): 0.4.

^1H NMR (300 MHz, DMSO- d_6): $\delta(\text{ppm}) = 3.49$ (1 H, m, $H-5'$), 3.69 (1 H, m, $H-5''$), 3.97 (1 H, m, $H-4'$), 4.27 (1 H, m, $H-3'$), 4.97 (3 H, m, CH_2 and OH), 5.15 (1 H, q, J 5.8, $H-2'$), 5.29 (1 H, d, J 5.1, OH), 5.54 (1 H, J 6.0, OH), 5.94 (1 H, d, J 6.1, OH), 7.13 (5 H, m, C_6H_5), 8.71 (1 H, s, $H-2$), 11.10 (1 H, s, NH).

***5'*-*O*-(4,4'-Dimethoxytrityl)-*N*-6-isobutyryl-8-(3-trifluoroacetamidoprop-1-ynyl)adenosine 22**

N-6-Isobutyryl-8-(3-trifluoroacetamidoprop-1-ynyl)adenosine (524 mg; 1.1 mmol) was co-evaporated with anhydrous pyridine (3 x 3 ml) and dissolved in anhydrous pyridine (5.0 ml). DMT-Cl (549 mg; 1.62 mmol; 1.5 eq.) was dissolved in anhydrous pyridine (3.0 ml) and added dropwise to the ice cold solution of the nucleoside over 2 hours. After 6 hours at ice cold temperature, TLC (DCM/MeOH 95:5(v/v)) showed that the starting material was completely consumed. Methanol (1.0 ml) was added to quench the unreacted DMT-Cl and after

10 minutes, the solution was concentrated to dryness *in vacuo*. The residue was dissolved in DCM (100 ml), washed with a 5% solution of NaHCO₃ (2 x 20 ml) and water (2 x 20 ml). The organic layer was then dried over Na₂SO₄ and concentrated to give a yellow gum which was purified by silica gel column chromatography (DCM/MeOH 98:2 to 97:3 (v/v)) to give **22** as a pale yellow foam.

Yield: 693.7 mg (0.88 mmol; 80%).

R_f(SiO₂; DCM/MeOH 95:5 (v/v)): 0.5.

¹H NMR (300 MHz, DMSO-d₆): δ(ppm)= 1.12 (6 H, d, *J* 6.9, CH(CH₃)₂), 2.95 (1 H, sept, *J* 6.9, CH(CH₃)₂), 3.21 (2 H, m, *H*-5' and *H*-5'), 3.69 and 3.71 (6 H, 2 x s, 2 x OCH₃), 4.09 (1 H, m, *H*-4'), 4.43 (1 H, d, *J* 5.4, CH₂), 4.52 (1 H, m, *H*-3'), 5.14 (1 H, q, *J* 5.1, *H*-2'), 5.25 (1 H, d, *J* 5.7, OH), 5.52 (1 H, d, *J* 5.4, OH), 6.02 (1 H, d, *J* 4.5, *H*-1'), 6.77 (4 H, 2 x d, *J* 9.0, aromatic), 7.22 (9 H, m, aromatic), 8.49 (1 H, s, *H*-2), 10.27 (1 H, t, *J* 5.4, NH), 10.78 (1 H, s, NH).

¹³C NMR (300 MHz, DMSO-d₆): δ(ppm)= 19.17, 29.39, 34.43, 54.94, 63.44, 70.24, 71.16, 71.47, 83.53, 85.24, 89.86, 92.80, (110.00, 113.81, 117.62 and 121.43, q, *J* 287.4, CF₃), 112.95, 113.00, 123.50, 126.50, 127.61, 129.56, 129.67, 135.56, 135.61, 136.12, 144.89, 150.00, 150.75, 152.51, (155.64, 156.13, 156.62 and 157.11, q, *J* 37.4, (C=O)CF₃), 157.97, 175.22.

5'-O-(4,4'-Dimethoxytrityl)-2'-(*tert*-butyldimethylsilyl)-N-6-isobutyryl-8-(3-trifluoroacetamidoprop-1-ynyl)adenosine **23**

23 was synthesized as described for **3**: 5'-O-(4,4'-Dimethoxytrityl)-N-6-isobutyryl-8-(3-trifluoroacetamidoprop-1-ynyl)adenosine **22** (233.5 mg; 0.3 mmol), anhydrous pyridine (90 μl; 1.17 mmol; 3.9 eq.), AgNO₃ (60 mg; 0.36 mmol; 1.2 eq.), TBDMS-Cl (60 mg; 3.9 mmol; 1.3 eq.), anhydrous THF (3.0 ml), room temperature, 5.5 hours. **23** was then purified by silica gel column chromatography (hexane/ethyl acetate 85:15 to 60:40 (v/v)) to a white foam.

Yield: 108.3 mg (0.12 mmol; 40%).

R_f(SiO₂; hexane/ethyl acetate 40:60 (v/v)): 0.43.

¹H NMR (300 MHz, DMSO-d₆): δ(ppm)= -0.22 and -0.08 (6 H, 2 x s, Si(CH₃)₂), 0.72 (9 H, s, SiC(CH₃)₃), 1.12 (6 H, d, *J* 6.6, CH(CH₃)₂), 2.94 (1 H, sept, *J* 6.9, CH(CH₃)₂), 3.25 (2 H, m, *H*-5' and *H*-5'), 3.70 and 3.71 (6 H, 2 x s, 2 x OCH₃), 4.12 (1 H, m, *H*-4'), 4.38 (2 H, d, *J* 4.2, CH₂), 4.46 (1 H, m, *H*-3'), 5.16 (2 H, m, *H*-2' and OH), 6.03 (1 H, d, *J* 5.1, *H*-1'), 6.79 (4

H, m, *aromatic*), 7.25 (9 H, m, *aromatic*), 8.49 (1 H, s, *H*-2), 10.24 (1 H, t, *J* 5.4, *NH*), 10.80 (1 H, s, *NH*).

¹³C NMR (300 MHz, DMSO-*d*₆): δ (ppm)= -5.48, -4.89, 17.73, 19.14, 19.17, 29.30, 34.44, 54.95, 63.16, 70.04, 71.18, 73.02, 83.79, 85.28, 89.66, 92.99, (109.96, 113.78, 117.60 and 121.42, q, *J* 288.01, CF₃), 113.00, 123.46, 126.53, 127.42, 127.63, 129.63, 129.69, 135.64, 135.76, 144.91, 150.07, 150.74, 152.57, (155.60, 156.09, 156.58 and 157.07, q, *J* 37.15, (C=O)CF₃), 157.95, 157.98, 175.20.

5.8 5'-*O*-(4,4'-Dimethoxytrityl)-2'-(*tert*-butyldimethylsilyl)-3'-(2-cyanoethyl-*N,N'*-diisopropylaminophosphoramidite)-*N*-6-isobutyryl-2-(3-trifluoroacetamidoprop-1-ynyl)adenosine

2-(3-Trifluoroacetamidoprop-1-ynyl)adenosine **28**

The reaction was carried out as described for **20**: 2-Iodoadenosine **27** (1134 mg; 2.88 mmol), *N*-propynyltrifluoroacetamide **L3** (565.3 mg; 3.69 mmol; 1.3 eq.), Pd(Ph₃P)₄ (334.08 mg; 0.288 mmol; 0.1 eq.), CuI (109 mg; 0.572 mmol; 0.2 eq.), DIPEA (576 μ l; 3.39 mmol; 1.2 eq.), dry DMF (23 ml), 40 °C, 5 hours. **28** was separated from the reaction mixture by silica gel column chromatography (DCM/MeOH 93:7 to 89:11 (v/v)) to a white solid.

Yield: 952.9 mg (2.38 mmol; 82%).

R_f(SiO₂; DCM/MeOH 85:15 (v/v)): 0.32.

HPLC: Gradient A1 (see Table 24).

¹H NMR (300 MHz, DMSO-*d*₆): δ (ppm)= 3.56 (1 H, m, *H*-5'), 3.66 (1 H, m, *H*-5''), 3.95 (1 H, m, *H*-4'), 4.13 (1 H, m, *H*-3'), 4.26 (2 H, s, CH₂), 4.50 (1 H, m, *H*-2'), 5.16 (2 H, m, 2 x OH), 5.46 (1 H, d, *J* 6.3, OH), 5.86 (1 H, d, *J* 6.0, *H*-1'), 7.49 (2 H, s, NH₂), 8.43 (1 H, s, *H*-8), 10.12 (1 H, br s, *NH*).

¹³C NMR (300 MHz, DMSO-*d*₆): δ (ppm)= 29.01, 61.34, 70.33, 73.82, 79.31, 82.47, 85.60, 87.39, (110.06, 113.88, 117.70 and 121.51, q, *J* 288.2, CF₃), 118.82, 140.38, 144.80, 149.22, (155.49, 155.98, 156.46 and 156.95, q, *J* 36.70, (C=O)CF₃), 155.85.

MALDI-TOF: C₁₅H₁₅F₃N₆O₅, calculated 416.11, found 416.96 [M+H]⁺.

***N*-6-Isobutyryl-2-(3-trifluoroacetamidoprop-1-ynyl)adenosine 29**

The procedure was the same as that described for **21a**: 2-(3-Trifluoroacetamidoprop-1-ynyl)-adenosine **28** (778 mg; 1.87 mmol), anhydrous pyridine (11.23 ml), TMS-Cl (3.66 ml; 23.92 mmol; 12.75 eq.) 1 hour, isobutyric anhydride (0.72 ml; 4.31 mmol; 2.3 eq.) 2 hours. **29** purified by column chromatography (DCM/MeOH 98:2 to 95:5 (v/v)) to a yellow solid.

Yield: 739.1 mg (1.52 mmol; 81%).

R_f (SiO₂; DCM/MeOH 90:10 (v/v)): 0.30.

¹H NMR (300 MHz, DMSO-d₆): δ (ppm)= 1.12 (6 H, d, J 6.9, CH(CH₃)₂), 2.89 (1 H, sept, J 6.9, CH(CH₃)₂), 3.57 (1 H, m, H -5'), 3.68 (1 H, m, H -5''), 3.97 (1 H, m, H -4'), 4.13 (1 H, m, H -3'), 4.33 (2 H, d, J 4.8, CH₂), 4.52 (1 H, m, H -2'), 5.09 (1 H, m, OH), 5.22 (1 H, d, J 4.8, OH), 5.55 (1 H, d, J 5.7, OH), 5.98 (1 H, d, J 5.4, H -1'), 8.76 (1 H, s, H -8), 10.18 (1 H, br s, NH), 10.79 (1 H, s, NH).

¹³C NMR (300 MHz, DMSO-d₆): δ (ppm)= 19.18, 29.07, 34.43, 61.04, 70.09, 73.97, 81.39, 81.78, 85.56, 87.37, (110.06, 113.88, 117.70 und 121.52, q, J 288.1, CF₃), 123.73, 143.37, 143.86, 149.84, 152.04, (155.55, 156.04, 156.52 and 157.02, q, J 36.8, (C=O)CF₃), 175.19.

MALDI-TOF: C₁₉H₂₁F₃N₆O₆, calculated 486.15, found 486.77 [M+H]⁺.

***5'*-O-(4,4'-Dimethoxytrityl)-*N*-6-isobutyryl-2-(3-trifluoroacetamidoprop-1-ynyl)adenosine 30**

The synthesis was carried out as described for **22**: *N*-6-Isobutyryl-2-(3-trifluoroacetamidoprop-1-ynyl)adenosine **29** (739.2 mg; 1.52 mmol), DMT-Cl (770.8 mg; 2.27 mmol; 1.5 eq.), anhydrous pyridine (7.5 ml), ice-cold, 8 hours. **30** was purified by silica gel column chromatography (DCM/MeOH 99.5:0.5 to 96.5:3.5) to a pale yellow foam.

Yield: 845.7 mg (1.07 mmol; 71%).

R_f (SiO₂; DCM/MeOH 92:8 (v/v)): 0.57.

¹H NMR (300 MHz, DMSO-d₆): δ (ppm)= 1.12 (6 H, d, J 6.9, CH(CH₃)₂), 2.90 (1 H, sept, J 6.9, CH(CH₃)₂), 3.23 (2 H, m, H -5' and H -5''), 3.71 and 3.72 (6 H, 2 x s, 2 x OCH₃), 4.10 (1 H, m, H -4'), 4.26 (1 H, m, H -3'), 4.32 (2 H, d, J 5.7, CH₂), 4.63 (1 H, m, H -2'), 5.24 (1 H, d, J 6.0, OH), 5.65 (1 H, d, J 5.7, OH), 6.02 (1 H, d, J 4.2, H -1'), 6.83 (4 H, m, aromatic), 7.25 (9 H, m, aromatic), 8.60 (1 H, s, H -8), 10.14 (1 H, t, J 5.4, NH), 10.79 (1 H, s, NH).

^{13}C NMR (300 MHz, DMSO- d_6): $\delta(\text{ppm}) = 19.15, 29.06, 34.43, 54.98, 63.66, 70.22, 73.66, 81.22, 81.86, 83.21, 85.52, 87.82, (110.07, 113.88, 117.70 \text{ and } 121.52, q, J 288.1, \text{CF}_3), 123.62, 126.66, 127.66, 127.79, 129.67, 135.43, 135.50, 143.15, 143.97, 144.76, 149.88, 151.93, (155.54, 156.03, 156.51 \text{ and } 157.00, q, J 36.70, (\text{C}=\text{O})\text{CF}_3), 158.04, 175.16$.

MALDI-TOF: $\text{C}_{40}\text{H}_{39}\text{F}_3\text{N}_6\text{O}_8$, calculated 788.28, found 788.95 $[\text{M}+\text{H}]^+$.

5'-O-(4,4'-Dimethoxytrityl)-2'-(tert-butyl dimethylsilyl)-N-6-isobutyryl-2-(3-trifluoroacetamidoprop-1-ynyl)adenosine 31

The reaction was similar to that of **23**: 5'-O-(4,4'-dimethoxytrityl)-N-6-isobutyryl-2-(3-trifluoroacetamidoprop-1-ynyl)adenosine **30** (845.7 mg; 1.07 mmol), dry pyridine (321 μl ; 4.24 mmol; 4.0 eq.), AgNO_3 (218 mg; 1.28 mmol; 1.2 eq.), TBDMS-Cl (218 mg; 1.42 mmol; 1.3 eq.), anhydrous THF (10.7 ml), room temperature, 4.5 hours. **31** was purified by silica gel column chromatography (hexane/ethyl acetate 65:35 to 40:60 (v/v)) to a white foam.

Yield: 607.3 mg (0.67 mmol; 63%).

$R_f(\text{SiO}_2; \text{hexane/ethyl acetate } 2:3 \text{ (v/v)})$: 0.60.

^1H NMR (300 MHz, DMSO- d_6): $\delta(\text{ppm}) = -0.07 \text{ and } 0.01 (6 \text{ H}, 2 \times \text{s}, \text{Si}(\text{CH}_3)_2), 0.79 (9 \text{ H}, \text{s}, \text{Si}(\text{CH}_3)_3), 1.12 (6 \text{ H}, \text{d}, J 6.9, \text{CH}(\text{CH}_3)_2), 2.90 (1 \text{ H}, \text{sept}, J 6.9, \text{CH}(\text{CH}_3)_2), 3.30 (2 \text{ H}, \text{m}, H-5' \text{ and } H-5''), 3.73 (6 \text{ H}, \text{s}, 2 \times \text{OCH}_3), 4.17 (2 \text{ H}, \text{m}, H-4' \text{ and } H-3'), 4.28 (2 \text{ H}, \text{d}, J 5.4, \text{CH}_2), 4.70 (1 \text{ H}, \text{t}, J 4.5, H-2'), 5.20 (1 \text{ H}, \text{d}, J 6.0, \text{OH}), 6.05 (1 \text{ H}, \text{d}, J 4.2, H-1'), 6.85 (4 \text{ H}, 2 \times \text{d}, J 9.0, \text{aromatic}), 7.29 (9 \text{ H}, \text{m}, \text{aromatic}), 8.57 (1 \text{ H}, \text{s}, H-8), 10.16 (1 \text{ H}, \text{t}, J 5.4, \text{NH}), 10.83 (1 \text{ H}, \text{s}, \text{NH})$.

^{13}C NMR (300 MHz, DMSO- d_6): $\delta(\text{ppm}) = -5.30, -4.82, 17.84, 19.16, 25.54, 28.98, 34.43, 54.99, 63.48, 69.99, 75.56, 81.21, 81.70, 83.41, 85.59, 88.08, (110.07, 113.88, 117.70 \text{ and } 121.52, q, J 288.0, \text{CF}_3), 113.16, 123.53, 126.71, 127.66, 127.82, 129.72, 135.33, 135.43, 142.62, 144.04, 144.76, 149.87, 151.76, (155.49, 155.97, 156.46 \text{ and } 156.95, q, J 36.70, (\text{C}=\text{O})\text{CF}_3), 158.08, 175.14$.

MALDI-TOF: $\text{C}_{46}\text{H}_{53}\text{F}_3\text{N}_6\text{O}_8\text{Si}$, calculated 902.36, found 903.10 $[\text{M}+\text{H}]^+$.

5'-O-(4,4'-Dimethoxytrityl)-2'-(tert-butyl dimethylsilyl)-3'-(2-cyanoethyl-N,N'-diisopropylaminophosphoramidite)-N-6-isobutyryl-2-(3-trifluoroacetamidoprop-1-ynyl)adenosine 32

The reaction was carried out as described for **5**: 5'-O-(4,4'-Dimethoxytrityl)-2'-(tert-butyl dimethylsilyl)-N-6-isobutyryl-2-(3-trifluoroacetamidoprop-1-ynyl)adenosine **31** (108.28 mg;

0.12 mmol), DIPEA (108 μ l; 0.48 mmol; 4.0 eq.), 2-cyanoethyl-*N,N'*-diisopropylamino-chlorophosphoramidite (39.6 μ l; 0.18 mmol; 1.5 eq.), DCM (3 ml). The phosphoramidite product **32** was purified by short column chromatography (hexane/ethyl acetate 90:10 to 40:60 (v/v) containing 1% triethylamine) to a pale yellow foam.

Yield: 114.8 mg (0.10 mmol; 87%).

R_f (SiO₂; hexane/ethyl acetate 1:1 containing 1% triethylamine): 0.70.

¹H NMR (300 MHz, DMSO-d₆): δ (ppm)= (-0.21, -0.18, -0.05, -0.02, 12 H, 4 x s, 4 x Si-CH₃), (0.741 and 0.744, 9 H, 2 x s, C(CH₃)₃), 1.01 (6 H, d, *J* 6.9, (C=O)CH(CH₃)₂), 1.12 (12 H, d, *J* 6.9, N-CH(CH₃)₂), 2.77 (2 H, t, *J* 6.0, CH₂-CN), 2.89 (1 H, m, (C=O)CH(CH₃)₂), 3.31 (2 H, m, *H*-5' and *H*-5''), 3.57 (2 H, m, N-CH(CH₃)₂), 3.72 (6 H, s, 2 x OCH₃), 3.70 (2 H, m, O-CH₂CH₂-CN), 4.29 (2 H, m, *H*-4', *H*-3' and CH₂), 4.96 (1 H, m, *H*-2'), 6.01 (1 H, m, *H*-1'), 6.85 (4 H, m, aromatic), 7.30 (9 H, m, aromatic), 8.60 (1 H, s, *H*-8), 10.14 (1 H, t, *J* 5.4, NH), 10.83 (1 H, s, NH).

³¹P NMR (300 MHz, DMSO-d₆): δ (ppm)= 148.41, 149.22.

5.9 5'-*O*-(4,4'-Dimethoxytrityl)-2'-(*tert*-butyldimethylsilyl)-*N*-2-isobutyryl-1-8-(3-trifluoroacetamidoprop-1-ynyl)guanosine

8-Trifluoroacetamidoprop-1-ynyl)guanosine **36**

The reaction was carried out as described for **20**: 8-Bromoguanosine hydrate 98% **35** (1448.4 mg; 4.0 mmol), *N*-propynyltrifluoroacetamide **L3** (1208 mg; 8.0 mmol, 2.0 eq.), Pd(Ph₃P)₄ (464 mg; 0.4 mmol; 0.1 eq.), CuI (152 mg; 0.8 mmol; 0.2 eq.), DIPEA (816 μ l; 4.8 mmol; 1.2 eq.), DMF (32 ml), 40 °C, 20 hours. **36** was purified by silica gel column chromatography (DCM/MeOH 90:10 to 84:16 (v/v)) to a pale yellow solid.

Yield: 2765.4 mg (6.4 mmol, 80%).

R_f (SiO₂; DCM/MeOH 60:40 (v/v)): 0.80.

HPLC: Gradient A2 (see Table 24).

¹H NMR (300 MHz, DMSO-d₆): δ (ppm)= 3.50 (1 H, m, *H*-5'), 3.64 (1 H, m, *H*-5''), 3.84 (1 H, m, *H*-4'), 4.12 (1 H, m, *H*-3'), 4.36 (2 H, d, *J* 5.4, CH₂), 4.88 (2 H, m, *H*-2' and OH), 5.04 (1 H, d, *J* 4.8, OH), 5.40 (1 H, d, *J* 6.0, OH), 5.76 (1 H, d, *J* 6.3, *H*-1'), 6.57 (2 H, br s, NH₂), 10.20 (1 H, t, *J* 5.4, NH), 10.90 (1 H, br s, NH).

^{13}C NMR (300 MHz, DMSO- d_6): $\delta(\text{ppm}) = 29.40, 62.06, 70.47, 70.85, 72.75, 85.77, 88.38, 89.12, (110.03, 113.84, 117.65 \text{ and } 121.47, q, J 288.02, \text{CF}_3), 117.24, 129.04, 150.90, 154.12, (155.54, 156.03, 156.51 \text{ and } 157.00, q, J 36.76, (\text{C}=\text{O})\text{CF}_3), 156.24$.

MALDI-TOF: $\text{C}_{15}\text{H}_{15}\text{F}_3\text{N}_6\text{O}_6$, calculated 432.10, found 432.82 $[\text{M}+\text{H}]^+$.

***N*-2-Isobutyryl-8-(3-trifluoroacetamidoprop-1-ynyl)guanosine 37a**

The procedure was similar to that of **21a**: 8-(3-Trifluoroacetamidoprop-1-ynyl)guanosine **36** (216.5 mg; 0.5 mmol), anhydrous pyridine (2 ml), TMS-Cl (0.55 ml; 4.1 mmol; 8.2 eq.) 2 hours, isobutyric anhydride (0.13 ml; 1.1 mmol; 2.2 eq.) 2 hours. **37a** was purified by silica gel column chromatography (DCM/MeOH 95:5 to 91:9 (v/v)) to a yellow solid.

Yield: 183.3 mg (0.37 mmol; 73%).

$R_f(\text{SiO}_2; \text{DCM/MeOH } 80:20 \text{ (v/v)})$: 0.63.

^1H NMR (300 MHz, DMSO- d_6): $\delta(\text{ppm}) = 1.13$ (6 H, d, J 6.9, $\text{CH}(\text{CH}_3)_2$), 2.79 (1 H, sept, J 6.9, $\text{CH}(\text{CH}_3)_2$), 3.53 (1 H, m, $H-5'$), 3.68 (1 H, m, $H-5''$), 3.84 (1 H, m, $H-4'$), 4.17 (1 H, br s, $H-3'$), 4.40 (2 H, s, CH_2), 4.81 (1 H, br s, $H-2'$), 4.91 (1 H, br s, OH), 5.09 (1 H, br s, OH), 5.50 (1 H, br s, OH), 5.86 (1 H, d, J 6.0, $H-1'$), 10.21 (1 H, br s, NH), 11.62 (1 H, br s, NH), 12.16 (1 H, br s, NH).

MALDI-TOF: $\text{C}_{19}\text{H}_{21}\text{F}_3\text{N}_6\text{O}_7$, calculated 502.14, found 502.84 $[\text{M}+\text{H}]^+$.

***N*-2-Phenoxyacetyl-8-(3-trifluoroacetamidoprop-1-ynyl)guanosine 37b**

The reaction was carried out as for the synthesis of **37a**: 8-(3-Trifluoroacetamidoprop-1-ynyl)guanosine **36** (216.5 mg; 0.5 mmol), TMS-Cl (0.5 ml; 3.75 mmol; 7.5 eq.), phenoxyacetic anhydride (286.3 mg; 1.0 mmol; 2.0 eq.). **37b** was purified by silica gel column chromatography (DCM/MeOH 92:8 to 86:14 (v/v)) and obtained as a white solid.

Yield: 78.4 mg (0.14 mmol; 28%).

$R_f(\text{SiO}_2; \text{DCM/MeOH } 85:15 \text{ (v/v)})$: 0.52.

^1H NMR (300 MHz, DMSO- d_6): $\delta(\text{ppm}) = 3.53$ (1 H, m, $H-5'$), 3.66 (1 H, m, $H-5''$), 3.86 (1 H, m, $H-4'$), 4.20 (1 H, m, $H-3'$), 4.40 (2 H, s, CH_2), 4.91 (4 H, m, $H-2'$, OCH_2 and OH), 5.11 (1 H, br s, OH), 5.51 (1 H, br s, OH), 5.86 (1 H, d, J 6.0, $H-1'$), 6.96 (3 H, m, aromatic), 7.31 (2 H, t, J 8.0, aromatic), 10.22 (1 H, br s, NH), 11.82 (2 H, br s, 2 x NH).

^{13}C NMR (300 MHz, DMSO-d_6): $\delta(\text{ppm})$ = 29.44, 61.93, 66.44, 70.27, 71.00, 72.15, 85.75, 88.66, 90.53, (110.05, 113.87, 117.68 and 121.50, q, J 288.1, CF_3), 114.47, 114.59, 121.37, 129.54, 129.59, 148.54, 154.03, (155.64, 156.13, 156.61 and 157.11, q, J 36.7, $(\text{C}=\text{O})\text{CF}_3$), 157.58, 157.63, 171.17.

MALDI-TOF: $\text{C}_{23}\text{H}_{21}\text{F}_3\text{N}_6\text{O}_8$, calculated 566.14, found 567.02 $[\text{M}+\text{H}]^+$.

5'-O-(4,4'-Dimethoxytrityl)-N-6-isobutyryl-8-(3-trifluoroacetamidoprop-1-ynyl)guanosine 38

The synthesis was carried in the same way as described for **22**: *N*-2-Isobutyryl-8-(3-trifluoroacetamidoprop-1-ynyl)guanosine **37a** (1174.4 mg; 2.4 mmol), DMT-Cl (1219.8 mg; 3.6 mmol; 1.5 eq.), anhydrous pyridine (10 ml), ice-cold, 2.5 hours. **38** was purified by column chromatography (DCM/MeOH 97:3 to 95:5 (v/v) containing 1% triethylamine) to a pale yellow foam.

Yield: 1671.6 mg (2.08 mmol; 87%).

R_f (DCM/MeOH 90:10 (v/v)): 0.44.

^1H NMR (300 MHz, DMSO-d_6): $\delta(\text{ppm})$ = 1.11 (6 H, 2 x d, J 6.9 and 6.6, $\text{CH}(\text{CH}_3)_2$), 2.72 (1 H, sept, J 6.9, $\text{CH}(\text{CH}_3)_2$), 3.11 and 3.45 (2 H, m, H -5' and H -5''), 3.69 and 3.71 (6 H, 2 x s, 2 x OCH_3), 4.04 (1 H, m, H -4'), 4.31 (3 H, br s, H -3' and CH_2), 4.91 (1 H, m, H -2'), 5.04 (1 H, br s, OH), 5.61 (1 H, br s, OH), 5.94 (1 H, d, J 4.5, H -1'), 6.73 (4 H, 2 x d, J 8.7 and 9.0, aromatic), 7.23 (9 H, m, aromatic), 10.85 (3 H, br s, 3 x NH).

^{13}C NMR (300 MHz, DMSO-d_6): $\delta(\text{ppm})$ = 18.71, 18.94, 29.33, 34.80, 54.86, 54.91, 64.72, 70.49, 71.36, 72.06, 84.21, 85.21, 89.91, 90.49, (110.02, 113.82, 117.65 and 121.47, q, J 288.5, CF_3), 112.73, 112.82, 120.83, 126.45, 127.47, 127.78, 129.64, 129.80, 131.52, 135.58, 144.87, 148.24, 154.33, (155.55, 156.05, 156.53 and 157.03, q, J 37.0, $(\text{C}=\text{O})\text{CF}_3$), 157.88, 157.95, 180.09.

MALDI-TOF: $\text{C}_{40}\text{H}_{39}\text{F}_3\text{N}_6\text{O}_9$, calculated 804.27, found 805.24 $[\text{M}+\text{H}]^+$.

5'-O-(4,4'-Dimethoxytrityl)-2'-(tert-butyldimethylsilyl)-N-2-isobutyryl-8-(3-trifluoroacetamidoprop-1-ynyl)guanosine 39

The reaction was carried out similarly to that of **23**: 5'-O-(4,4'-Dimethoxytrityl)-N-2-isobutyryl-8-(3-trifluoroacetamidoprop-1-ynyl)guanosine **38** (1623 mg; 2.02 mmol), anhydrous pyridine (606 μl ; 7.47 mmol; 3.7 eq.), AgNO_3 (505 mg; 3.0 mmol; 1.5 eq.), TBDMS-Cl (528 mg;

3.43 mmol; 1.7 eq.), anhydrous THF (20 ml), room temperature, 8.5 hours. **39** was purified by silica gel column chromatography (hexane/ethyl acetate 85:15 to 40:60 (v/v)) to a pale yellow foam.

Yield: 482.3 mg (0.53 mmol; 26%).

R_f (SiO₂; hexane/ethyl acetate 1:1 (v/v) containing 4% MeOH): 0.41.

¹H NMR (300 MHz, DMSO-d₆): δ (ppm)= -0.14 and -0.02 (6 H, 2 x s, Si(CH₃)₂), 0.76 (9 H, s, SiC(CH₃)₃), 1.09 (6 H, 2 x d, J 6.6 and 6.9, CH(CH₃)₂), 2.70 (1 H, sept, J 6.6 and 6.9, CH(CH₃)₂), 3.19 (1 H, m, H -5'), 3.51 (1 H, m, H -5''), 3.67 and 3.69 (6 H, 2 x s, 2 x OCH₃), 4.09 (1 H, m, H -4'), 4.20 (1 H, br m, H -3'), 4.38 (2 H, br d, J 5.1, CH₂), 4.79 (1 H, m, H -2'), 5.95 (1 H, d, J 4.8, H -1'), 6.75 (4 H, 2 x d, J 8.7, aromatic), 7.27 (9 H, m, aromatic), 10.16 (1 H, t, J 5.1 and 5.4, NH), 11.38 (1 H, br s, NH), 12.14 (1 H, br s, NH).

¹³C NMR (300 MHz, DMSO-d₆): δ (ppm)= -5.40, -4.91, 17.81, 18.63, 18.88, 25.47, 29.24, 34.77, 54.89, 54.93, 64.49, 70.16, 71.95, 73.74, 84.26, 85.30, 90.66, (109.97, 113.79, 117.61 and 121.43, q, J 288.40, CF₃), 112.82, 112.87, 126.51, 127.55, 127.76, 129.70, 129.78, 135.50, 135.58, 144.86, 148.52, 154.10, (155.54, 156.03, 156.52 and 157.01, q, J 37.0, (C=O)CF₃), 157.93, 157.98, 180.07.

MALDI-TOF: C₄₆H₅₃F₃N₆O₉Si, calculated 918.36, found 919.19 [M+H]⁺.

5.10 5'-O-(4,4'-Dimethoxytrityl)-2'-(tert-butyldimethylsilyl)-3'-(2-cyanoethyl-*N,N'*-diisopropylaminophosphoramidite)-*N*-6-isobutyryl-8-(3-trifluoroacetamidoprop-2-en-1-yl)adenosine

8-(3-Trifluoroacetamidoprop-2-en-1-yl)adenosine **52**

The procedure was similar to that of **8**: 8-Bromoadenosine (2064 mg; 6.0 mmol), *N*-allyltrifluoroacetamide (7803 mg; 4.25 mmol; 8.5 eq.), Na₂[PdCl₄] (882 mg; 3.0 mmol; 0.5 eq.), DMF (18 ml), NaOAc buffer (21.6 ml; 0.1 M; pH 5.2), 80 °C, 22 hours. **52** was purified by silica gel column chromatography (DCM/MeOH 95:5 to 93:7 (v/v)) to a yellow solid. For a NMR sample, 15 mg of the product chromatographed by silica gel column was then purified again by reversed-phase HPLC.

Yield: 822.7 mg (1.97 mmol; 33%).

R_f (DCM/MeOH 90:10 (v/v)): 0.28.

HPLC: Gradient B (see Table 24).

^1H NMR (300 MHz, DMSO- d_6): $\delta(\text{ppm})$ = 3.51 (1 H, m, H -5'), 3.73 (3 H, m, H -5'' and CH_2 -linker), 4.01 (1 H, m, H -4'), 4.16 (1 H, br s, H -3'), 4.84 (1 H, m, H -2'), 5.25 (1 H, d, J 4.2, OH), 5.33 (1 H, d, J 7.2, OH), 5.81 (1 H, d, J 7.2, H -1'), 5.91 (2 H, m, OH and =CH-linker), 6.77 (1 H, d, J 14.1, =CH-linker), 7.30 (2 H, s, NH_2), 8.07 (1 H, s, H -2), 11.32 (1 H, s, NH).

^{13}C NMR (300 MHz, DMSO- d_6): 28.14 (CH_2 -linker), 62.18 (C -5'), 70.92 (C -3'), 72.19 (C -2'), 86.81 (C -4'), 88.42 (C -1'), (109.99, 113.80, 117.61 and 121.41, q, J 287.2, CF_3), 113.09 (=C-linker), 118.27 (C -5), 123.44 (=C-linker), 149.56 (C -4), 150.27 (C -8), 151.46 (C -2), (152.88, 153.38, 153.87 and 154.36, q, J 37.2, ($\text{C}=\text{O}$) CF_3), 155.61 (C -6).

MALDI-TOF: $\text{C}_{15}\text{H}_{17}\text{F}_3\text{N}_6\text{O}_5$, calculated 418.12, found 419.03 $[\text{M}+\text{H}]^+$.

***N*-6-Isobutyryl-8-(3-trifluoroacetamidoprop-2-en-1-yl)adenosine 54**

The preparation of **54** was carried out as for the synthesis of **21a**: 8-(3-Trifluoroacetamidoprop-2-en-1-yl)adenosine **52** (756.58 mg; 1.81 mmol), TMS-Cl (4.11 ml; 31 mmol; 17.2 eq.), isobutyric anhydride (1.16 ml; 6.93 mmol; 3.83 eq.). **54** was purified by silica gel column chromatography (DCM/MeOH 95:5 to 94:6) and obtained as a yellow solid.

Yield: 488.1 mg (0.69 mmol; 37.9%).

$R_f(\text{SiO}_2; \text{DCM/MeOH } 90:10 \text{ (v/v)})$: 0.56.

^1H NMR (300 MHz, DMSO- d_6): $\delta(\text{ppm})$ = 1.12 (6 H, d, J 6.9, $\text{CH}(\text{CH}_3)_2$), 2.97 (1 H, sept, J 6.9, $\text{CH}(\text{CH}_3)_2$), 3.57 (1 H, m, H -5'), 3.70 (1 H, m, H -5'), 3.87 (2 H, d, J 6.9, CH_2), 3.98 (1 H, m, H -4'), 4.22 (1 H, m, H -3'), 4.94 (1 H, m, H -2'), 5.25 (2 H, m, 2 x OH), 5.37 (1 H, d, J 6.6, OH), 5.91 (2 H, m, H -1' and =CH), 6.82 (1 H, dd, J 14.1 and 7.8, =CH), 8.59 (1 H, s, H -2), 10.57 (1 H, s, NH), 11.35 (1 H, d, J 8.1, NH).

^{13}C NMR (300 MHz, DMSO- d_6): $\delta(\text{ppm})$ = 19.26 ($\text{CH}(\text{CH}_3)_2$), 28.34 (CH_2 -linker), 34.31 ($\text{CH}(\text{CH}_3)_2$), 61.81 (C -5'), 70.50 (C -3'), 71.73 (C -2'), 86.33 (C -4'), 88.36 (C -1'), (110.24, 114.05, 117.86 and 121.67, q, J 287.2, CF_3), 112.86 (=C-linker), 123.45 (C -5), 123.78 (=C-linker), 149.03 (C -4), 150.77 (C -8), 152.59 (C -2), (153.17, 153.67, 154.16 and 154.65, q, J 37.4, ($\text{C}=\text{O}$) CF_3), 154.10 (C -6), 175.32 ($\text{C}=\text{O}$).

MALDI-TOF: $\text{C}_{19}\text{H}_{23}\text{F}_3\text{N}_6\text{O}_6$, calculated 488.16, found 488.86 $[\text{M}+\text{H}]^+$.

***5'*-O-(4,4'-Dimethoxytrityl)-*N*-6-isobutyryl-8-(3-trifluoroacetamidoprop-2-en-1-yl)adenosine 55**

The preparation of **55** was the same as for **22**: *N*-6-Isobutyryl-8-(3-trifluoroacetamido-2-en-1-yl)adenosine (187.9 mg; 0.385 mmol), DMT-Cl (195.6 mg; 0.58 mmol; 1.5 eq.), room temper-

ature, 10.5 hours. **55** was purified by silica gel column chromatography (DCM/MeOH 98:2 to 96.5:3.5 (v/v)) and was obtained as a yellow foam.

Yield: 66.0 mg (0.08 mmol; 22%).

R_f (DCM/MeOH 93:7 (v/v)): 0.38.

^1H NMR (300 MHz, DMSO- d_6): 1.11 (6 H, d, J 6.6, $\text{CH}(\text{CH}_3)_2$), 2.95 (1 H, m, $\text{CH}(\text{CH}_3)_2$), 3.16 (1 H, m, $H-5'$), 3.26 (1 H, m, $H-5'$), 3.91 (2 H, d, J 6.3, CH_2), 4.07 (1 H, m, $H-4'$), 4.55 (2 H, m, $H-3'$ and $H-2'$), 5.26 (1 H, m, OH), 5.45 (1 H, d, J 6.0, OH), 5.95 (2 H, m, $H-1'$ and $=\text{CH}$), 6.75 (5 H, m, $=\text{CH}$ and aromatic), 7.20 (9 H, m, aromatic), 8.45 (1 H, s, $H-2$), 10.54 (1 H, s, NH), 11.37 (1 H, d, J 9.3, NH).

MALDI-TOF: $\text{C}_{40}\text{H}_{41}\text{F}_3\text{N}_6\text{O}_8$, calculated 790.29, found 791.13 $[\text{M}+\text{H}]^+$.

5'-O-(4,4'-Dimethoxytrityl)-2'-(tert-butyldimethylsilyl)-N-6-isobutyryl-8-(3-trifluoroacetamidoprop-2-en-1-yl)adenosine **56**

The preparation of **56** was carried out as described for **23**: 5'-O-(4,4'-Dimethoxytrityl)-N-6-isobutyryl-8-(3-trifluoroacetamidoprop-2-en-1-yl)adenosine **22** (155.35 mg; 0.2 mmol), anhydrous pyridine (60 μl ; 0.74 mmol; 3.7 eq.), AgNO_3 (40.8 mg; 0.24 mmol; 1.2 eq.), TBDMS-Cl (52.8 mg; 0.34 mmol; 1.7 eq.), THF (3.5 ml), room temperature, 6.5 hours. The product **56** was separated by silica gel column chromatography (hexane/ethyl acetate 85:15 to 40:60 (v/v)).

Yield: 12.4 mg (0.014 mmol; 6.9%).

R_f (SiO_2 ; hexane/ethyl acetate 1:1 (v/v) containing 4% MeOH): 0.44.

MALDI-TOF: $\text{C}_{46}\text{H}_{55}\text{F}_3\text{N}_6\text{O}_8\text{Si}$, calculated 904.38, found 905.40 $[\text{M}+\text{H}]^+$.

5'-O-(4,4'-Dimethoxytrityl)-2'-(tert-butyldimethylsilyl)-3'-(2-cyanoethyl-N,N'-diisopropylaminophosphoramidite)-N-6-isobutyryl-8-(3-trifluoroacetamidoprop-2-en-1-yl)adenosine **57**

The preparation of **57** was based on the same procedure used for the synthesis of **32**: 5'-O-(4,4'-Dimethoxytrityl)-2'-(tert-butyldimethylsilyl)-N-6-isobutyryl-8-(3-trifluoroacetamidoprop-2-en-1-yl)adenosine **56** (69 mg; 0.076 mmol), DIPEA (68.4 μl ; 0.30 mmol; 4.0 eq.), 2-cyanoethyl-N,N'-diisopropylamino-chlorophosphoramidite (25.1 μl ; 0.114 mmol; 1.5 eq.), DCM (2 ml), room temperature 3.5 hours. The phosphoramidite product was purified by

short silica gel column chromatography (hexane/ethyl acetate 90:10 to 40:60 (v/v) containing 1% triethylamine).

Yield: 54.6 mg (0.05 mmol; 70%).

R_f (SiO₂; hexane/ethyl acetate 1:1(v/v) containing 1% triethylamine): 0.65.

5.11 8-(3-[6-Trifluoroacetylaminohexanamido]prop-2-en-1-yl)adenosine

The same condition for the synthesis of **52** was applied to prepare **61**.

Yield: 26%.

¹H NMR (300 MHz, DMSO-d₆): δ (ppm)= 1.23 (2 H, m, CH₂), 1.49 (4 H, m, 2 x CH₂), 2.14 (2 H, t, J 7.2, CH₂), 3.15 (2 H, m, CH₂), 3.61 (3 H, m, H -5', H -5'' and CH₂), 4.00 (1 H, m, H -4'), 4.16 (1 H, m, H -3'), 4.83 (1 H, m, H -2'), 5.25 (1 H, d, J 4.2, OH), 5.80 (1 H, d, J 7.2, H -1'), 5.99 (1 H, dd, J 9.6 and 3.0, OH), 6.77 (1 H, dd, J 14.4 and 10.2, =CH), 7.22 (1 H, m, =CH), 7.29 (2 H, br s, NH₂), 8.06 (1 H, s, H -2), 9.38 (1 H, br s, NH), 9.81 (1 H, d, J 9.9, NH).

¹³C NMR (300 MHz, DMSO-d₆): δ (ppm)= 24.51, 25.81, 28.00, 28.28, 35.04, 38.89, 105.27, (110.23, 114.05, 117.86 and 121.68, q, J 288.10, CF₃), 118.32, 125.28, 149.49, 151.06, 151.35, (155.41, 155.88, 156.36 and 156.83, q, J 35.8, (C=O)CF₃), 155.62.

MALDI-TOF: C₂₁H₂₈F₃N₇O₆, calculated 531.21, found 532.31 [M+H]⁺.

5.12 2-(3-Trifluoroacetamidoprop-1-enyl)adenosine and 2-(3-trifluoroacetamidoprop-2-en-1-yl)adenosine

Condition A: 2-Iodoadenosine (39.3 mg; 0.1 mmol), *N*-allyltrifluoroacetamide **L1** (130.0 mg; 0.85 mmol, 8.5 eq.) and Na₂[PdCl₄] (14.7 mg; 0.05 mmol; 0.5 eq.) were dissolved in DMF (500 μ l). To this solution was added NaOAc buffer (360 μ l; 0.1 M; pH 5.2). The solution was then saturated with argon and placed on a shaker at 80 °C for 4.5 hours, when TLC (DCM/MeOH 90:10 (v/v)) indicated that all the starting material was consumed. The solvents were then removed by co-evaporation with toluene (3 x 1 ml), dissolved again in methanol (2 ml), absorbed on silica gel and purified by column chromatography (DCM/MeOH 90:10 to 87:13 (v/v)) and then reversed-phase HPLC (Gradient C) to give a mixture of 2-(3-trifluoroacetamidoprop-1-enyl)adenosine **62** and 2-(3-trifluoroacetamidoprop-2-en-1-yl)adenosine **63** in a ratio of nearly 1:1 as a white solid.

MALDI-TOF: $C_{15}H_{17}F_3N_6O_5$, calculated 418.12, found 418.77 $[M+H]^+$.

Condition B: 2-Iodoadenosine (39.3 mg; 0.1 mmol), $Pd(OAc)_2$ (3.87 mg; 0.017 mmol; 0.17 eq.) and $AsPh_3$ (10.1 mg; 0.033 mmol; 0.33 eq.) were placed in a 2-ml vial. DMF (1.3 ml) was added to dissolve the reagents. To the resulting solution were added *N*-allyltrifluoroacetamide **L1** (38.3 mg; 0.25 mmol; 2.5 eq.) and tributylamine (38 μ l; 0.16 mmol; 1.6 eq.). The reaction solution was stirred at 65 °C for 14 hours after which there was no reaction. The temperature was then increased to 80 °C and the reaction was stirred for another 9 hours. The reaction mixture was then concentrated, co-evaporated with toluene to remove DMF, dissolved again in a small amount of methanol and absorbed on silica gel and purified by silica gel column chromatography (DCM/MeOH 95:5 to 85:15 (v/v)), then by reversed-phase HPLC (Gradient D) to give **63** as white solid.

Yield: 10.0 mg (0.024 mmol; 24%).

1H NMR (300 MHz, DMSO- d_6): δ (ppm)= 3.42 (2 H, d, J 7.2, CH_2), 3.58 (1 H, m, $H-5'$), 3.65 (1 H, m, $H-5''$), 3.98 (1 H, m, $H-4'$), 4.14 (1 H, m, $H-3'$), 4.62 (1 H, m, $H-2'$), 5.18 (1 H, d, J 4.2, OH), 5.40 (1 H, d, J 6.3, OH), 5.59 (1 H, m, OH), 5.86 (1 H, d, J 6.6, $H-1'$), 5.93 (1 H, m, =CH), 6.68 (1 H, d, J 14.1, =CH), 7.32 (2 H, s, NH_2), 8.27 (1 H, s, $H-8$), 11.19 (1 H, s, NH). About 15% of the isomer **62** was also formed as can be seen in the spectrum.

^{13}C NMR (300 MHz, DMSO- d_6): δ (ppm)= 39.20, 61.90, 70.97, 73.32, 86.21, 87.71, (110.02, 113.83, 117.64 and 121.45, q, J 287.8, CF_3), 115.97, 117.82, 122.15, 139.74, 149.70, (152.74, 153.23, 153.72 and 154.17, q, J 37.3, (C=O) CF_3), 156.03, 156.10, 162.45.

MALDI-TOF: $C_{15}H_{17}F_3N_6O_5$, calculated 418.12, found 419.04 $[M+H]^+$.

Condition C: 2-Iodoadenosine (39.3 mg; 0.1 mmol), pallacycle (18.79 mg; 0.02 mmol; 0.2 eq.) and NaOAc (9.0 mg; 0.11 mmol; 1.1 eq.) were placed in a 2 ml vial. DMA (400 μ l) was added to dissolve the reagents. To the resulting solution were added *N*-allyltrifluoroacetamide **L1** (29.42 mg; 0.19 mmol; 1.9 eq.). The reaction solution was stirred at 80 °C for 2.5 hours and no reaction occurred. Because NaOAc was not dissolved in DMA, tributylamine was added. The reaction mixture was then let to stir for another 2 hours at 85 °C when there was still no reaction. The temperature was then increased to 100 °C and the reaction was stirred for 19 hours. The reaction mixture was then concentrated, co-evaporated with toluene to remove DMA, dissolved again in a small amount of methanol and absorbed on silica gel and purified by silica gel column chromatography, then by reverse-phase HPLC (Gradient D) to give the Heck coupling product **62** as the major compound.

Yield: 8.4 mg (0.02 mmol; 20%).

^1H NMR (300 MHz, DMSO- d_6): $\delta(\text{ppm})$ = 3.55 (1 H, m, $H-5'$), 3.66 (1 H, m, $H-5''$), 3.96 (1 H, m, $H-4'$), 4.03 (2 H, t, J 5.4, CH_2), 4.14 (1 H, m, $H-3'$), 4.61 (1 H, m, $H-2'$), 5.20 (1 H, d, J 4.2, OH), 5.40 (2 H, m, 2 x OH), 5.87 (1 H, d, J 6.3, $H-1'$), 6.35 (1 H, d, J 15.6, =CH), 6.84 (1 H, tt, J 15.6 and 5.4, =CH), 7.29 (2 H, s, NH_2), 8.31 (1 H, s, $H-8$), 9.83 (1 H, t, J 5.4, NH).

MALDI-TOF: $\text{C}_{15}\text{H}_{17}\text{F}_3\text{N}_6\text{O}_5$, calculated 418.12, found 419.02 $[\text{M}+\text{H}]^+$.

When applying condition A for the Heck coupling reaction of 2-iodoadenosine with **L2**, again a 1:1 mixture of Heck coupling product 2-(3-[6-trifluoroacetylaminohexanamido]prop-1-enyl)adenosine **64** and its isomer 2-(3-[6-trifluoroacetylaminohexanamido]prop-2-en-1-yl)adenosine **65** was also obtained (^1H NMR data not shown).

MALDI-TOF: $\text{C}_{21}\text{H}_{28}\text{F}_3\text{N}_7\text{O}_6$, calculated 531.21, found 532.28 $[\text{M}+\text{H}]^+$.

5.13 8-Iodoadenosine

2',3',5'-Tris-*O*-(*tert*-butyldimethylsilyl)adenosine **43**

Adenosine **42** (1602 mg; 6 mmol) was dissolved in dry DMF. To the resulting solution were added imidazole (3168 mg; 46.5 mmol; 7.8 eq.) and TBDMS-Cl (3168 mg; 21.0 mmol; 3.5 eq.). The reaction mixture was protected from moisture and stirred under argon overnight at room temperature. TLC (DCM/MeOH 95:5 (v/v)) showed that there was no starting material left. DMF was then removed under vacuum. The rest of the reaction was extracted several times with ethyl acetate (300 ml). The extracts were collected, washed with water (3 x 40 ml), dried over Na_2SO_4 and concentrated to a colorless oil which was purified by silica gel column chromatography (DCM/MeOH 99.5:0.5 to 97:3 (v/v)) to get the desired product as white foam.

Yield: 3217.4 mg (5.28 mmol; 88%).

$R_f(\text{SiO}_2; \text{DCM/MeOH } 95:5 \text{ (v/v)})$: 0.30.

^1H NMR (300 MHz, DMSO- d_6): $\delta(\text{ppm})$ = -0.35, -0.11, 0.07, 0.10 and 0.12 (18 H, 5 x s, 3 x $\text{Si}(\text{CH}_3)_2$), 0.77, 0.89 and 0.91 (27 H, 3 x s, 3 x $\text{Si}(\text{CH}_3)_3$), 3.72 (1 H, m, $H-4'$), 3.99 (2 H, m, $H-5'$ and $H-5''$), 4.32 (1 H, m, $H-3'$), 4.90 (1 H, m, $H-2'$), 5.92 (1 H, d, J 6.3, $H-1'$), 7.28 (2 H, s, NH_2), 8.12 (1 H, s, $H-8$), 8.31 (1 H, s, $H-2$).

2',3',5'-Tris-*O*-(*tert*-butyldimethylsilyl)-8-iodoadenosine 44

2',3',5'-Tris-*O*-(*tert*-butyldimethylsilyl)adenosine **43** (2440 mg; 4 mmol) was co-evaporated with dry DCM (3 x 10 ml) and kept over P₂O₅ in an evacuated decicator overnight. On the next day, argon was slowly introduced into the decicator to fill up the bottle containing the nucleoside. Anhydrous THF (40 ml) was added to dissolve the solid and the resulting solution was placed in an isopropanol/liquid nitrogen bath at (-70)-(-75 °C). To this solution, lithium diisopropyl amide (LDA) (11.1 ml 1.8 M solution of LDA in THF/heptane/ethyl benzene; 5 eq.; diluted in 36 ml dry THF) was added slowly, so that the internal temperature did not exceed -70 °C. The solution was stirred for 5.5 hours at (-70)-(-75 °C), then I₂ (1929 mg; 7.2 mmol; 1.8 eq.) in anhydrous THF (30 ml) was added slowly in order to keep the reaction temperature under -70 °C. The reaction mixture was stirred for another 3 hours while the reaction temperature was maintained between -70 and -75 °C. Acetic acid (1.2 ml; 5.0 eq.) was added and after 10 minutes, the reaction was diluted with ethyl acetate (400 ml) and washed with water until the water phase was colorless. The ethyl acetate phase was dried over Na₂SO₄, concentrated under vacuum to give a yellow solid which was purified by silica gel column chromatography (hexane/ethyl acetate 85:15 to 78:22 (v/v)) to afford **44** as a white solid.

Yield: 1938.1 mg (2.64 mmol; 66%).

R_f(SiO₂; hexane/ethyl acetate 60:40 (v/v)): 0.60.

¹H NMR (300 MHz, DMSO-d₆): δ(ppm)= -0.40, -0.11, -0.05, -0.01, 0.13 and 0.14 (18 H, 6 x s, 3 x Si(CH₃)₂), 0.75, 0.81 and 0.94 (27 H, 3 x s, 3 x SiC(CH₃)₃), 3.66 (1 H, m, *H*-5'), 4.08 (1 H, m, *H*-5''), 3.95 (1 H, m, *H*-4'), 4.53 (1 H, m, *H*-3'), 5.58 (1 H, m, *H*-2'), 5.80 (1 H, d, *J* 6.0, *H*-1'), 7.41 (2 H, br s, NH₂), 8.02 (1 H, s, *H*-2).

MALDI-TOF: C₂₈H₅₄IN₅O₄Si₃, calculated 735.92, found 737.27 [M+H]⁺.

8-Iodoadenosine 45

2',3',5'-Tris-*O*-(*tert*-butyldimethylsilyl)adenosine (735.9 mg; 1.0 mmol) was dissolved in 10.0 ml dry DMF. To this solution, Et₃N.3HF (600 μl; 3.5 mmol; 3.5 eq.) was added and the reaction mixture was let to stir under argon overnight. TLC showed that there was no starting material left. The reaction mixture was then concentrated, co-evaporated with toluene (3 x 2 ml) to remove trace of DMF. The rest was then resuspended in ethanol, filtered through glass filter. The yellow solid in fine powder form was washed several times with ethanol, diethyl ether and dried under vacuum to give **45** as yellow solid.

Yield: 318.3 mg (0.81 mmol; 81%).

^1H NMR (300 MHz, DMSO- d_6): δ (ppm)= 3.52 (1 H, m, $H-5'$), 3.68 (1 H, m, $H-5''$), 3.98 (1 H, m, $H-4'$), 4.19 (1 H, m, $H-3'$), 5.10 (1 H, m, $H-2'$), 5.21 (1 H, d, J 4.5, OH), 5.40 (1 H, d, J 6.3, OH), 5.64 (1 H, dd, J 9.0 and 9.0, OH), 5.77 (1 H, d, J 6.9, $H-1'$), 7.52 (2 H, br s, NH_2), 8.04 (1 H, s, $H-2'$).

^{13}C NMR (300 MHz, DMSO- d_6): 62.21, 70.99, 71.13, 86.71, 92.28, 103.72, 122.38, 149.56, 151.88, 155.01.

2',3',5'-Tris-*O*-(*tert*-butyldimethylsilyl)-6-*N*-isobutyryl-8-iodoadenosine 46

2',3',5'-Tris-*O*-(*tert*-butyldimethylsilyl)-8-iodoadenosine **44** (1103.88 mg; 1.5 mmol) was co-evaporated with anhydrous pyridine (3 x 5 ml), dissolved in anhydrous pyridine (7.5 ml). The solution was protected from moisture, purged with argon and placed on ice. To this ice-cold solution, isobutyric anhydride (3.86 ml; 22.5 mmol; 15 eq.) was added dropwise. The reaction was run in 3 days when TLC (hexane/ethyl acetate 80:20 (v/v)) indicated that there was only a small amount of the starting material. The reaction was stopped by the addition of 1 ml ice cold water, solvents were then removed under vacuum, the residue was redissolved in ethyl acetate, washed with a saturated solution of NaHCO_3 (2 x 40 ml) and water (50 ml) and purified by silica gel column chromatography (hexane/ethyl acetate 90:10 to 87:13 (v/v)) to give **46** as a white foam.

Yield: 833.5 mg (1.04 mmol; 69%).

R_f (SiO_2 ; hexane/ethyl acetate 80:20 (v/v)): 0.50.

MALDI-TOF: $\text{C}_{32}\text{H}_{60}\text{IN}_5\text{O}_5\text{Si}_3$, calculated 805.01, found 806.16 $[\text{M}+\text{H}]^+$.

6-*N,N'*-Diisobutyryl-2',3',5'-tris-*O*-(*tert*-butyldimethylsilyl)adenosine was also obtained in 6% yield; MALDI-TOF: $\text{C}_{36}\text{H}_{66}\text{IN}_5\text{O}_6\text{Si}_3$, calculated 876.1, found 898.76 $[\text{M}+\text{Na}]^+$.

6-*N*-Isobutyryl-8-iodoadenosine 48

Compound **48** was synthesized from 2',3',5'-tris-*O*-(*tert*-butyldimethylsilyl)-*N*-6-isobutyryl-8-iodoadenosine **46** as described above in the preparation of 8-iodoadenosine **45**. After the reaction finished, DMF was removed under vacuum, the residue was resuspended in DCM, filtered through glass filter, washed several times with DCM and diethyl ether to give **48** as a white solid.

Yield: 82%.

^1H NMR (300 MHz, DMSO-d_6) = 1.12 (6 H, d, J 6.9, $\text{CH}(\text{CH}_3)_2$), 2.95 (1 H, sept, J 6.9, $\text{CH}(\text{CH}_3)_2$), 3.54 (1 H, m, $H-5'$), 3.70 (1 H, m, $H-5''$), 3.97 (1 H, m, $H-4'$), 4.27 (1 H, m, $H-3'$), 5.07 (1 H, m, OH), 5.23 (2 H, m, $H-2'$ and OH), 5.46 (1 H, d, J 6.3, OH), 5.85 (1 H, d, J 6.6, $H-1'$), 8.57 (1 H, s, $H-2$), 10.74 (1 H, s, NH).

MALDI-TOF: $\text{C}_{14}\text{H}_{18}\text{IN}_5\text{O}_5$, calculated 463.04, found 463.98 $[\text{M}+\text{H}]^+$.

5.14 Post-synthetic labeling of the modified oligonucleotides

Labeling protocol for amino linker modified oligonucleotides with Alexa Fluor 488 NHS- and TFP-esters

Amino linker modified oligonucleotides (5-10 nmol) were dissolved in Borax buffer (25 μl ; 0.1 M; pH 9.4) and added to a solution of Alexa Fluor 488 NHS- or TFP-ester (100 μg) in DMF (5 μl) (the solution of the dye in DMF was freshly prepared just before the coupling reaction). The mixture was well mixed, protected from light and placed on a shaker at room temperature overnight. The most part of the excess amount of the dye was removed via gel filtration (Sephadex G25 fine, GE Healthcare). The labeled RNA was then purified by denaturing PAGE in the dark. The labeled RNA ran more slowly than the free RNA and showed fluorescence when exposed to UV light at 365 nm. The bands corresponding to the labeled RNA were excised; the labeled RNA was eluted from the gel with LiOAc buffer, precipitated from ethanol/acetone and analyzed by MALDI-TOF-MS.

Yield: 15-37%.

Labeling protocol for amino modified oligonucleotides with Cy5 NHS-ester

The labeling reaction of amino linker modified oligonucleotides with Cy5 mono NHS-ester was carried out as described for Alexa Fluor 488 NHS or TFP-ester: Amino linker modified RNA (5-10 nmol) in Borax buffer (15-25 μl ; 0.1 M; pH 8.7), Cy5 mono NHS-ester (100 μg) in DMF (5 μl), room temperature, overnight. The labeled RNAs were separated by gel filtration and denaturing PAGE.

Labeling protocol for amino modified RNAs with ATTO 647N NHS-ester

Amino linker modified oligonucleotides were labeled with ATTO 647N NHS-ester using the same procedure for the labeling reaction of Alexa Fluor 488 NHS or TFP-ester: Amino linker

modified RNAs (5 nmol) in Borax buffer (15 μ l; 0.1 M; pH 8.7), ATTO 647N ester (100 μ g) in DMF (5 μ l), room temperature, overnight. The ATTO 647N-labeled oligonucleotides were purified by denaturing PAGE or reversed-phase HPLC (Gradient E, Table 24).

5.15 Preparation of hybrids

Condition A: For the hybridization of unlabeled single-stranded oligonucleotides, D1L3 (300 pmol) and A1L3 (300 pmol) were dissolved in 50 mM Tris buffer, pH 7.4 in the presence of 10 mM MgCl_2 in a total volume of 100 μ l. The solution was then well mixed, incubated at 78 °C for 3 minutes, centrifuged to collect the vapor on the cap of the eppendorf, wrapped in aluminium film and slowly cooled down to room temperature. The hybrid was analyzed by 15% native PAA gel.

Condition B: Alexa Fluor 488-labeled D1L3 (25 pmol) and Cy5-labeled A1L3 (25 pmol) were dissolved in 20 mM KH_2PO_4 - K_2HPO_4 buffer, pH 6.5 in the presence of 10 mM MgCl_2 and 100 mM KCl in a total volume of 50 μ l. The components were then vortexed, centrifuged and incubated at 78 °C for 3 minutes. The mixture was slowly cooled down to room temperature in aluminium film. The hybridization was checked by 15% native PAA gel.

5.16 Analyses of D1L2 with enzymes

Testing for the presence of the phosphate group by the treatment with alkaline phosphatase (CIAP)

In order to check if D1L2-upper has a phosphate monoester group, the RNA sample was treated with the enzyme alkaline phosphatase from calf intestine (CIAP, Fermentas or BioLabs): 500 pmol D1L2-upper in 10 μ l water were added to a solution of 50 μ l CIAP buffer (10 x, Fermentas) (or NE buffer, 10 x, BioLabs) and 25 units of CIAP in a total volume of 500 μ l in water. The solution was well mixed and incubated at 36 °C for 2 hours. The enzyme was removed by phenol-chloroform extraction. The oligonucleotides were separated by ethanol precipitation and analyzed by 15% denaturing PAA-gel.

Digestion of D1L2-upper and -lower oligonucleotides with phosphodiesterase and alkaline phosphatase

1200 pmol of the oligonucleotide were taken up in 2.8 μ l water. To this solution were added 1 μ l Tris-HCl buffer, pH 8.9, 1 μ l MgCl_2 0.4 mM, 2.2 μ l solution of CIAP (10 u/ μ l) and 3 μ l

solution of snake venom phosphodiesterase (0.04 u/3 μ l). The solution was thoroughly mixed and incubated at 37 °C for 3 hours. The reaction was stopped by heat denaturing the enzymes at 80 °C for 1 minute. The reaction mixture was filled up to a volume of 100 μ l with water and analyzed by reversed-phase HPLC (Gradient G, Table 24).

List of Tables

1	Sonogashira reaction of 8-bromoadenosine and L3 catalyzed by Pd(PPh ₃) ₂ Cl ₂	34
2	Sonogashira reactions of 8-bromoadenosine and L3 catalyzed by Pd(PPh ₃) ₄ with Et ₃ N as base.	35
3	Sonogashira coupling reactions of 19 , 21c and 21d and L3 catalyzed by Pd(PPh ₃) ₄ with DIPEA as base.	37
4	Sonogashira reaction conditions for the cross-coupling between 8-bromoguanosine hydrate and L3	41
5	Coupling constants of sp ² protons of RCH=CH ₂ at different relative positions.	46
6	Heck cross-coupling reactions of 8-bromoadenosine and L1 in non-aqueous solvents.	50
7	The Heck cross-coupling reactions of 8-bromoadenosine and L1 in aqueous solvents.	51
8	The Heck cross-coupling reactions of 44 and L1	57
9	The Heck coupling reactions of 45 and L1	58
10	The Heck coupling reactions of 48 and 49 and L1	60
11	The protection of the amino function of 8-(3-trifluoroacetamidoprop-1-ynyl)-adenosine 20	67
12	The protection of the amino function of 8-bromoadenosine 19	67
13	The protection of the amino functions of the amino linker modified nucleosides 20 , 28 , 36 and 52 with isobutyric anhydride (iBu) ₂ O.	68
14	The protection of the 5'-OH group by dimethoxytritylation.	70
15	The protection of the 2'-OH groups of the nucleoside building blocks with TBDMS-Cl.	73
16	The synthesis of the phosphoramidite building blocks from modified nucleosides.	76
17	Sequences of amino linker modified RNAs	79
18	Masses of the synthetic RNAs determined by MALDI-TOF-MS.	87
19	Masses of the dye-labeled oligonucleotides determined by MALDI-TOF-MS.	87
21	Buffers	96
22	Enzymes	97
23	Apparatus	97
24	Gradients	99

25	Phosphoramidite building blocks and CPG-supports	101
26	Reagents and steps in the chemical synthesis of RNA	102
27	Denaturing analytical and preparative PAGE	104
29	Optical data of the fluorescent labels	106

List of Figures

1	Selected examples of modifications that can be incorporated at the phosphodiester backbone, sugar and base moieties of RNA using the chemical synthesis of oligonucleotides.	2
2	Preferred conformations of pentose sugars.	3
3	The structures of the building blocks to be prepared for RNA synthesis based on the 2'-O-TBDMS-3'-O-phosphoramidite chemistry.	4
4	Phosphoramidite approach.	5
5	Structure of building blocks for automated RNA synthesis based on 2'-O-TBDMS-3'-O-phosphoramidite chemistry.	5
6	<i>Lcaa</i> -CPG used as solid support used for RNA synthesis.	6
7	Synthesis cycle of the 2'-O-TBDMS-3'-O-phosphoramidite method.	6
8	Activation mechanism of 1 <i>H</i> -tetrazole and derivatives.	7
9	Phosphoramidite building blocks based on "ACE" and "TOM" chemistry. . .	10
10	New phosphoramidite building blocks for RNA synthesis using 2'-O-thiomorpholine-4-carbothioate (2'-O-TC) protection.	10
11	The Sonogashira coupling reaction.	11
12	The mechanism of the Sonogashira coupling reaction.	12
13	Regioselective Pd(0)-catalyzed alkynylation.	13
14	The Heck coupling reaction.	15
15	The general mechanism of Heck coupling reaction.	15
16	The <i>in situ</i> formation of Pd(0) by the reduction of Pd(II) in the presence of amines, phosphine, organometallics or alkenes.	16
17	The coordination-insertion process.	17
18	Regio- and stereoselectivity in Heck coupling reaction.	18
19	The preparation of Palladacycle.	19
20	Amino linkers for post-synthetic 3'- and 5'-end labeling.	21
21	Post-synthetic 3'-labeling chemistry based on the selective periodate-mediated oxidation.	22
22	Phosphoramidite building blocks for internal labeling.	22
23	Reactions of primary amines with amino-reactive reporter groups.	23
24	The principles of FRET spectroscopy.	25

25	Structures of matrices commonly used for MALDI-MS analysis of oligonucleotides.	27
26	Retrosynthesis of the modified uridine building block by the Sonogashira coupling reaction.	28
27	Retrosynthesis of adenosine building blocks by the Sonogashira coupling reaction.	29
28	Synthesis of <i>N</i> -propargyltrifluoroacetamide L3	30
29	Synthesis of 5'- <i>O</i> -(4,4'-dimethoxytrityl)-2'- <i>O</i> - <i>tert</i> -butyldimethylsilyl-5-(3-trifluoroacetamidoprop-1-ynyl)uridine 4	31
30	Cyclization of 5-alkynyl uracine derivatives.	32
31	Two strategies to introduce the amino linker L3 into the C-8 position of adenosine by the Sonogashira coupling reaction.	33
32	Reversed-phase HPLC diagram of the Sonogashira coupling reactions of 19 using Pd(PPh ₃) ₄ as catalyst, Et ₃ N (A) or DIPEA (B) as base.	36
33	Unsuccessful Sonogashira cross-coupling reaction of <i>N</i> -6-phenoxyacetyl-8-bromoadenosine and L3 using Pd(PPh ₃) ₄	37
34	The Sonogashira cross-coupling reaction of 2-iodoadenosine 27 and L3	38
35	The Sonogashira cross-coupling reaction of 8-bromoguanosine 35 and L3	39
36	Retrosynthesis of the amino linker modified adenosine building blocks.	42
37	Synthesis of <i>N</i> -allyltrifluoroacetamide L1	43
38	Synthesis of <i>N</i> -allyl-6-(<i>N</i> -trifluoroacetyl-amino)hexanamide L2	44
39	Synthesis of 5-(3-trifluoroacetamidoallyl)uridine 8 by the Heck coupling reaction.	45
40	Different directions in the Heck cross-coupling reaction of 1 and L1	46
41	NMR signals of the protons at the double-bond of the linker in the cross-coupled product 8	47
42	Configurations of the intermediate formed by carbometallation.	48
43	Synthesis of 5-(3-[6-trifluoroacetamidohexanamido]prop-1-enyl)uridine 14 by the Heck coupling reaction	48
44	The Heck coupling reactions of 8-bromo, 8-iodoadenosine and derivatives with the linker L1	49
45	Possible intramolecular hydrogen bonds of the main compound separated from the Heck reactions of 19 and L1 in aqueous organic solvents.	52
46	The HMBC spectrum of the main compound separated from the reaction described in entry 5, Table 7.	53
47	The restriction of the inner rotation during the Heck cross-coupling reaction of 19 and L1	54

48	Synthesis of 8-iodoadenosine and its derivatives for the Heck cross-coupling.	56
49	Suggested steric hindrance of 44 in the Heck coupling reaction with L1	57
50	Synthesis of 8-(3-[6-trifluoroacetamidohexanamido]-prop-2-en-1-yl)adenosine from 19 and L2	61
51	The Heck cross-coupling reactions of 27 and L1	61
52	The restriction of the inner rotation during the Heck cross-coupling reaction of 27 and L1	62
53	The Heck cross-coupling reaction of 27 and L2	64
54	Amino linker modified building blocks for further protection and phosphitylation.	65
55	The protection scheme of the amino functions of adenosine and guanosine derivatives.	66
56	The unsuccessful protection of 8-(3-trifluoroacetamidoprop-1-ynyl)adenosine 20 with the PAC group supposedly due to the electronic effect of the linker L3 .	66
57	Intramolecular hydrogen bonding of <i>N</i> -6-isobutyryl-8-(3-trifluoroacetamidoprop-1-ynyl)guanosine.	69
58	The protection of the 5'-OH groups of the modified nucleoside building blocks by dimethoxytritylation.	70
59	The protection of the 2'-OH groups of the modified nucleoside building blocks by <i>tert</i> -butyldimethylsilylation.	72
60	Effects of AgNO ₃ on the silylation reaction.	72
61	The functionalization of the 3'-OH groups of the modified nucleosides by phosphitylation - The synthesis of modified phosphoramidite building blocks.	75
62	Secondary structure of the modified fourU-thermometer of the <i>Salmonella enterica agsA</i> gene.	77
63	Secondary structures of the modified four-way RNA junction and the hairpin aptazyme HPAR2.	78
64	Purification of the modified oligonucleotide D1L3 by anion exchange HPLC and denaturing PAGE.	81
65	Synthesis and labeling reaction of the amino-modified oligonucleotides. . . .	82
66	Structure of Alexa Fluor 488 5(6)-NHS-, TFP-esters and Cy5 NHS-ester. . . .	83
67	Coupling reactions of the RNA-26 with Alexa Fluor 488 TFP-ester at different pHs.	85
68	Purification and analysis of ATTO 647N-labeled A1L2 by denaturing gel and reversed-phase HPLC.	86
69	MALDI-TOF mass spectrum of the test sequence L2-TEST.	88
70	MALDI-TOF mass spectra of the test RNA 2-L3-A and its corresponding ATTO 647N-labeled sequence.	88
71	Analysis of D1L2 by the treatment with CIAP.	89

72	Analysis nucleoside components of the product of dephosphorylation and D1L2-lower by treatment with CIAP and phosphodiesterase.	90
73	Preparation of the hybrid of Alexa 488-labeled D1L3 and Cy5-labeled A1L3.	91

Literatures

- Acevedo, O. L.; Andrews, R. S.; Dunkel, M.; Dan Cook, P. *J. Heterocycl. Chem.* **1994**, *31*, 989.
- Agarwal, K. L.; Yamazaki, A.; Cashion, P. J.; Khorana, H. G. *Angew. Chem., Int. Ed.* **1972**, *11*, 451.
- Ahmadian, M.; Klewer, D. A.; Berstrom, D. E. *Curr. Prot. Nucl. Acid Chem.* **2000**, 1.1.5.
- Albert, K.; Gisdakis, P.; Rosch, N. *Organometallics* **1998**, *17*, 1608.
- Alemán, E. A.; Lamichhane, R.; Rueda, D. *Curr. Opin. Chem. Biol.* **2008**, *12*, 647.
- Altenhoff, G.; Würtz, S. Glorius, F. *Tetrahedron Lett.* **2006**, *47*, 2925.
- Amatore, C.; Carré, E.; Jutand, A.; M'Barki, M. *Organometallics*, **1995**, *14*, 1818.
- Amatore, C.; Jutand, A. *Acc. Chem. Res.* **2000**, *33*, 314.
- Amatore, C.; Bensalem, S.; Ghalem, S.; Jutand, A.; Medjour, Y. *Eur. J. Org. Chem.* **2004**, 366.
- Andersen, W.; Hayes, D. H.; Michelson, A. M.; Todd, A. R. *J. Chem. Soc.* **1954**, 1882.
- Atkinson, T.; Smith, M. In *Oligonucleotide Synthesis: a practical approach*, Ed. Gait, M. J., Oxford University Press **1990**, pp 35.
- Balraju, V.; Reddy, D. S.; Periasamy, M.; Iqbal, J. *J. Org. Chem.* **2005**, *70*, 9626.
- Barton, T. J.; Tully, C. R. *J. Org. Chem.* **1978**, *43*, 3649.
- Beaucage, S. L.; Caruthers, M. H. *Tetrahedron Lett.* **1981**, *22*, 1859.
- Beletskaya, I. P.; Cheprakov, A. V. *Chem. Rev.* **2000**, *100*, 3009.
- Beletskaya, I. P.; Cheprakov, A. V. *J. Organomet. Chem.* **2004**, *689*, 4055.
- Bergbreiter, D. E.; Osburn, P. L.; Wilson, A.; Sink, E. M. *J. Am. Chem. Soc.* **2000**, *122*, 9058.
- Bergmann, F.; Pfeleiderer, W. *Helv. Chim. Acta* **1994**, *77*, 481.
- Bergstrom, D. E.; Ogawa, M. K. *J. Am. Chem. Soc.* **1978**, *100*, 8106.
- Bergstrom, D. E.; Ruth, J. L.; Warwick, P. *J. Org. Chem.* **1981**, *46*, 1432.

- Berry, D. A.; Jung, K.-Y.; Wise, D. S.; Sercel, A. D.; Pearson, W. H.; Mackie, H.; Randolph, J. B.; Somers, R. L. *Tetrahedron Lett.* **2004**, 45, 2457.
- Bertus, P.; Fécourt, F.; Bauder, C.; Pale, P. *New J. Chem.* **2004**, 28, 12.
- Blackburn, G. M.; Gait, M. J. In *Nucleic Acid in Chemistry and Biology*, Oxford University Press **1992**, pp 262.
- Böhm, V. P. W.; Herrmann, W. A. *Eur. J. Org. Chem.* **2000**, 3679.
- Brückner, R.; In *Reaktionsmechanismen*, Spektrum, 3. Auflage **2004**, pp 715.
- Buback, M.; Perkovic, T.; Redlich, S.; de Meijere, A. *Eur. J. Org. Chem.* **2003**, 2375.
- Bumagin, N. A.; More, P. G.; Baletskaya, I. P. *J. Organomet. Chem.* **1989**, 371, 397.
- Buzayan, J. M.; Gerlach, W. L.; Bruening, G. *Nature* **1986**, 323, 349.
- Cabri, W.; Candiani, I.; Bedeschi, A.; Santi, R. *Tetrahedron Lett.* **1991**, 32, 1753.
- Cabri, W.; Candiani, I.; Bedeschi, A.; Penco, S.; Santi, R. *J. Org. Chem.* **1992**, 57, 1481.
- Cabri, W.; Candiani, I. *Acc. Chem. Res.* **1995**, 28, 2.
- Cacchi, S.; Fabrizi, G.; Gasparri, F.; Villani, C. *Synlett* **1999**, 345.
- Casado, A. L.; Espinet, P. *Organometallics* **1998**, 17, 954.
- Cassar, L. *J. Organomet. Chem.* **1975**, 93, 253.
- Čerňa, I.; Pohl, R.; Hocek, M. *Chem. Commun.* **2007**, 4729.
- Chaix, C.; Duplaa, A. M.; Molko, D.; Téoule, R. *Nucl. Acids Res.* **1989**, 17, 7381.
- Chandrasekhar, S.; Narsihmulu, Ch.; Sultana, S. S.; Reddy, N. R. *Org. Lett.* **2002**, 4, 4399.
- Chaudhary, S. K.; Hernandez, O. *Tetrahedron Lett.* **1979**, 20, 95.
- Chichilla, R.; Nájera, C. *Chem. Rev.* **2007**, 107, 874.
- Chou, C.-W.; Limbach, P. A. *Curr. Prot. Nucl. Acid Chem.* **2000**, 10.1.1
- Chowrira, B. M.; Berzal-Herranz, A.; Keller, C. F.; Burke, J. M. *J. Biol. Chem.* **1993**, 268, 19458.
- Chu, K. S.; Negrete, N. R.; Konopelski, J. P.; Lakner, F. J.; Woo, N.-T.; Olmstead, M. M. *J. Am. Chem. Soc.* **1992**, 114, 1800.

- Clayden, J.; Greeves, N.; Warren, S.; Wothers, P. In *Organic Chemistry*, Oxford University Press, **2006**.
- Cohen, S. B.; Cech, T. R. *J. Am. Chem. Soc.* **1997**, *119*, 6259.
- Comins, D. L.; Nolan, J. M.; Bori, I. D. *Tetrahedron Lett.* **2005**, *46*, 6697.
- Cook, A. F.; Vuocolo, E.; Brakel, C. L. *Nucl. Acids Res.* **1988**, *16*, 4077.
- Cox, W. G.; Singer, V. L. *BioTechniques* **2004**, *36*, 114.
- Crisp, G.; Flynn, B. L. *J. Org. Chem.* **1993**, *58*, 6614.
- Crisp, G. T.; Gore, J. *Tetrahedron*, **1997**, *53*, 1523.
- Cristalli, G.; Eleuteri, A.; Vittori, S.; Volpini, R.; Lohse, M. J.; Klotz, K.-N.; *J. Med. Chem.* **1992**, *35*, 2363.
- Cristalli, G.; Volpini, R.; Vittori, S.; Camaioni, E.; Monopoli, A.; Conti, A.; Dionisotti, S.; Zocchi, C.; Ongini, E. *J. Med. Chem.* **1994**, *37*, 1720.
- Cristalli, G.; Camaioni, E.; Vittori, S.; Volpini, R.; Borea, P. A.; Conti, A.; Dionisotti, S.; Ongini, E.; Monopoli All, A. *J. Med. Chem.* **1995**, *38*, 1462.
- Cruickshank, K. A.; Stockwell, D. L. *Tetrahedron Lett.* **1988**, *29*, 5221.
- Davis, G. D., Jr.; Hallberg, A. *Chem. Rev.* **1989**, *89*, 1433.
- De Meijere, A.; Meyer, F. E. *Angew. Chem., Int. Ed.* **1994**, *33*, 2379.
- Demik, N. N.; Kabachnik, M. M.; Novikova, Z. S.; Baletskaya, I. P. *Russ. J. Org. Chem.* **1995**, *31*, 57.
- Deng, B.-L.; Hartman, T. L.; Buckheit, R. W., Jr.; Pannecouque, C.; De Clerck, E.; Fanwick, P. E.; Cushman, M. *J. Med. Chem.* **2005**, *48*, 6140.
- DeRose, V. J. *Curr. Opin. Struct. Biol.* **2003**, *13*, 317.
- DeVasher, R. B.; Moore, L. R.; Shaughnessy, K. H. *J. Org. Chem.* **2004**, *69*, 7919.
- De Vries, J. G. *Can. J. Chem.* **2001**, *79*, 1086.
- Dey, S.; Sheppard, T. L. *Org. Lett.* **2001**, *3*, 3983.
- Diek, H. A.; Heck, F. R. *J. Organomet. Chem.* **1975**, *93*, 259.
- Dounay, B.; Overman, L. E. *Chem. Rev.* **2003**, *103*, 2945.

- Duggan, L. J.; Hill, T. M.; Wu, S.; Garrison, K.; Zhang X. L.; Gottlieb, P. A. *J. Biol. Chem.* **1995**, *270*, 28049.
- Eckhardt, M.; Fu, G. C. *J. Am. Chem. Soc.* **2003**, *125*, 13642.
- Eckstein, F. *Annu. Rev. Biochem.* **1985**, *54*, 367.
- Edwards, T. E., Sigurdsson, S. T. In *Handbook of RNA Biochemistry* **2005** Wiley-VCH Verlag, GmbH & Co., pp 112.
- Erlanson, D. A.; Chen, L.; Verdine, G. L. *J. Am. Chem. Soc.* **1993**, *115*, 12583.
- Ferré-D'Amaré, A. R.; Doudna, J. A. *Nucl. Acids Res.* **1996**, *24*, 977.
- Firth, A. G.; Fairlamb, I. J. S.; Darley, K.; Baumann, C. G. *Tetrahedron Lett.* **2006**, *47*, 3529.
- Flasche, W.; Cismas, C.; Herrmann, A.; Liebscher, J. *Synthesis* **2004**, *14*, 2335.
- Förster, T. *Ann. Phys.* **1948**, *2*, 55.
- Förster, U.; Lommel, K.; Sauter, D.; Grünewald, C.; Engels, J. W.; Wachweitzl, J. *Chem-BioChem.* **2010**, *11*, 664.
- Giller, G.; Tasara, T.; Angerer, B.; Mühlegger, K.; Amacker, M.; Winter, H. *Nucl. Acids. Res.* **2003**, *31*, 2630.
- Glaser, C. *Ber. Dtsch. Chem. Ges.* **1869**, *2*, 422.
- Goodchild, J. *Bioconjugate Chem.* **1990**, *1*, 165.
- Gough, G. R.; Brunden, M. J.; Gilham, P.T. *Tetrahedron Lett.* **1981**, *22*, 4177.
- Gramlich, P. M. E.; Wirges, C. T.; Manetto, A.; Carell, T. *Angew. Chem., Int. Ed.* **2008**, *47*, 8350.
- Gramlich, P. M. E.; Warncke, S.; Gierlich, J.; Carell, T. *Angew. Chem., Int. Ed.* **2008**, *47*, 3442.
- Griffin, B. E.; Jarman, M.; Reese, C. B. *Tetrahedron* **1968**, *24*, 639.
- Grigg, R.; Loganathan, V.; Santhakumar, V.; Sridharan, V.; Teasdale, A. *Tetrahedron Lett.* **1991**, *32*, 687.
- Grushin, V. V.; Alper, H. *Chem. Rev.* **1994**, *94*, 1047.
- Guerrier-Takada, C.; Gardiner, K.; Marsh, T.; Pace, N.; Altman, S. *Cell* **1983**, *35*, 849.

- Guo, Z.; Karunatilaka, K. S.; Rueda, D. *Nat. Struct. Mol. Biol.* **2009**, *16*, 1154.
- Hakimelahi, G.; Proba, Z. A.; Ogilvie, K. K. *Can. J. Chem.* **1982**, *60*, 1106.
- Haraguchi, K.; Itoh, Y.; Tanaka, H.; Miyasaka, T. *Tetrahedron Lett.* **1991**, *32*, 3391.
- Haralambidis, J.; Chai, M.; Treager, G. W. *Nucl. Acids Res.* **1987**, *15*, 4857.
- Hayakawa, H.; Takana, H.; Sasaki, K.; Haraguchi, K.; Saitoh, T.; Takai, F.; Miyasaka, T. *J. Het. Chem.* **1989**, *26*, 189.
- Heck, R. F. *J. Org. Chem.* **1969**, *91*, 6707.
- Heck, R. F.; Nolley, J. P. *J. Org. Chem.* **1972**, *14*, 2320.
- Helm, M.; Brule, H.; Giege, R.; Florentz, C. *RNA*, **1999**, *5*, 618.
- Hengesbach, M.; Kobitski, A.; Voigts-Hoffmann, F.; Frauer, C.; Nienhaus, G. U.; Helm, M. *Curr. Prot. Nucl. Acid Chem.* 2008, 11.12
- Herrmann, W. A.; Brossmer, C.; Öfele, K.; Reisinger, C.-P.; Priermeier, T.; Beller, M.; Fischer, H. *Angew. Chem., Int. Ed.* **1995**, *34*, 1844.
- Hesse, M. ; Meier, H.; Zeeh, B. In *Spektroskopische Methoden in der organischen Chemie*, Georg Thieme Verlag **2002**, pp 110.
- Hii, K. K.; Claridge, T. D. W.; Brown, J. M. *Angew. Chem., Int. Ed.* **1997**, *36*, 984.
- Hobbs, Jr. F. W. *J. Org. Chem.* **1989**, *54*, 3420.
- Hocek, M.; Fojta, M. *Org. Biomol. Chem.* **2008**, *6*, 2233.
- Hundertmark, T.; Littke, A. F.; Buchwald, S. L.; Fu, G. C. *Org. Lett* **2000**, *2*, 1729.
- Ikonen, S.; Macíčková-Cahová, H.; Pohl, R.; Šanda, M.; Hocek, M. *Org. Biomol. Chem.* **2010**, *8*, 1194.
- Iwai, S.; Ohtsuka, E. *Nucl. Acids. Res.* **1988**, *16*, 9443.
- Jacobson, K. A.; Shi, D.; Gallo-Rodriguez, C.; Manning, Jr. M.; Müller, C.; Daly, J. W.; Neumeyer, J. L.; Kiriass, L.; Pfeleiderer, W. *J. Med. Chem.* **1993**, *36*, 2639.
- Jäger, S.; Rasched, G.; Kornreich-Reshem, H.; Engeser, M.; Thum, O.; Famulok, M. *J. Am. Chem. Soc.* **2005**, *127*, 15071.
- Jeffery, T. *J. Chem. Soc., Chem. Commun.* **1984**, 1287.

- Jeffery, T. *Tetrahedron Lett.* **1985**, 26, 2667.
- Jeffery, T. *Synthesis*, **1987**, 1, 70.
- Jeffery, T. *Tetrahedron Lett.* **1994**, 35, 3051.
- Jeffery, T. *Tetrahedron* **1996**, 52, 10113.
- Karunatilaka, K. S.; Rueda, D. *Chem. Phys. Lett.* **2009**, 476, 1.
- Kawai, R.; Kimoto, M.; Ikeda, S.; Mitsui, T.; Endo, M.; Yokoyama, S.; Hirao, I. *J. Am. Chem. Soc.* **2005**, 127, 17286.
- Khan, S. I.; Grinstaff, M. W. *J. Am. Chem. Soc.* **1999**, 121, 4704.
- Khorana, H. G.; Tener, G. M.; Moffatt, J. G.; Pol, E. H. *Chem. Ind.* **1956**, 1523.
- Khorana, H. G.; Razzell, W. E.; Gilham, P. T.; Tener, G. M.; Pol, E. H. *J. Am. Chem. Soc.* **1957**, 79, 1002.
- Kolpashchikov, D. M.; Ivanova, T. M.; Boghachev, V. S.; Nasheuer, H. P.; Weisshart, K.; Favre, A.; Pestryakov, P. E.; Lavrik, O. I. *Bioconjugate Chem.* **2000**, 11, 445.
- Kreutz, C.; Kählig, H.; Konrat, R.; Micura, R. *J. Am. Chem. Soc.* **2005**, 127, 11558.
- Krstić, I.; Frolow, O.; Sezer, D.; Endeward, B.; Weigand, J. E.; Suess, B.; Engels, J.W.; Prisner, T. F. *J. Am. Chem. Soc.* **2010**, 132, 1454.
- Kruger, K.; Grabowski, P. J.; Zaug, A. J.; Sands, J.; Gottschling, D. E.; Cech, T. R. *Cell* **1982**, 31, 147.
- Kumar, T. S.; Madsen A. S.; Sau, S. P.; Wengel, J.; Hrdlichka, P. J. *J. Org. Chem.* **2009**, 74, 1070.
- Kuusela, S.; Lönnberg, H. *J. Chem. Soc., Perkin Trans.* **1994**, 2, 2109.
- Kuwahara, M.; Nagashima, J.; Hasegawa, M.; Tamura, T.; Kitarata, R.; Hanawa, K.; Hososhima, S.; Kasamtshu, T.; Ozaki, H.; Sawai, H. *Nucl. Acids. Res.* **2006**, 34, 5383.
- Lagisetty, P.; Zhang, L.; Lakshman, M. K. *Adv. Synth. Catal.* **2008**, 350, 602.
- Lang, P.; Magnin, G.; Mathis, G.; Burger, A.; Biellmann, J.-F. *J. Org. Chem.* **2000**, 65, 7825.
- Langer, P. R.; Waldrop, A. A.; Ward, D. C. *PNAS* **1981**, 78, 6633.
- Lansky, A.; Reiser, O.; de Meijere, A. *Synlett* **1990**, 405.

- Larock, R. C.; Gong, W. H.; Baker, B. E. *Tetrahedron Lett.* **1989**, 30, 2603.
- Larsen, R. D. *Curr. Opin. Drug Discovery Dev.* **1999**, 2, 651.
- Latham, M. P.; Zimmermann, G. R.; Pardi, A. *J. Am. Chem. Soc.* **2009**, 131, 5052.
- Lehmann, C.; Xu, Y. Z.; Christodoulou, C.; Tan, Z. K.; Gaiz, M. J. *Nucl. Acids. Res.* **1989**, 17, 2379.
- Létinois-Halbes, U.; Pale, P.; Berger, S. J. *J. Org. Chem.* **2005**, 70, 9185.
- Letsinger, R. L.; Ogilvie K. K. *J. Am. Chem. Soc.* **1967**, 89, 4801.
- Letsinger, R. L.; Lunsford, W. B. *J. Am. Chem. Soc.* **1976**, 98, 3655.
- Li, P.; Medon, P. P.; Skingle, D. C.; Lanser, J. A.; Symons, R. H. *Nucl. Acids Res.* **1987**, 15, 5275.
- Lieber, E.; Enkoji, T. *J. Org. Chem.* **1961**, 26, 4472.
- Littke, A. F.; Fu, G. C. *J. Org. Chem.* **1999**, 64, 10.
- Liu, Q.; Burton, J. D. *Tetrahedron Lett.* **1997**, 38, 4371.
- Lu, K.; Miyazaki, Y.; Summers, M. F. *J. Biomol. NMR* **2009**, 46, 113.
- Martadinata, H.; Phan, A. T. *J. Am. Chem. Soc.* **2009**, 131, 2570.
- Matsuda, A.; Shinozaki, M.; Yamaguchi, T.; Homma, H.; Nomoto, R.; Miyasaka, T.; Watanabe, Y.; Abiru, T. *J. Med. Chem.* **1992**, 35, 241.
- McBride, L. J.; Caruthers, M. H. *Tetrahedron Lett.* **1983**, 24, 245.
- McKeen, C. M.; Brown, L. J.; Nicol, J. T. G.; Mellor, J. M.; Brown, T. *Org. Biomol. Chem.* **2003**, 1, 2267.
- Michelson, A. M.; Todd, A. R. *J. Chem. Soc.* **1955**, 2632.
- Milligan, J. F.; Groeber, D. R.; Witherrell G. W.; Uhlenbeck, O. C. *Nucl. Acids Res.* **1987**, 21, 8783.
- Mizoroki, T.; Mori, K.; Ozaki, A. *Bull. Chem. Soc. Jpn.* **1971**, 44, 581.
- Mooers, B. H. *Methods* **2009**, 47, 168.
- Murray J. B.; Adams C. J.; Arnold J. R. P.; Stockley, P. G. *Biochem. J.* **1995**, 311, 487.
- Nagy, A.; Novák, Z.; Kotschy, A. *J. Organomet. Chem.* **2005**, 690, 4453.

- Negishi, E.; de Meijere, A. In *Handbook of Organopalladium Chemistry for Organic Synthesis*, Wiley: New York **2002**.
- Nicolaou, K. C.; Bulger, P. G.; Sarlah, D. *Angew. Chem., Int. Ed.* **2005**, *44*, 4442.
- Ogilvie, K. K.; Sandana, K. L.; Thompson, E. A.; Quilliam, M. A.; Westmore, J. B. *Tetrahedron Lett.* **1974**, *15*, 2861.
- Ogilvie, K. K.; Beaucage, S. L.; Schiffman, A. L.; Theriault, N. Y.; Sadana, K. L. *Can. J. Chem.* **1978**, *56*, 2768.
- Ogilvie, K. K.; Schiffman, A. L.; Penney, C. L. *Can. J. Chem.* **1979**, *57*, 2230.
- Pallan P. S., Egli, M. *Nat. Protoc.* **2007**, *2*, 640.
- Paoletta, G.; Sproat B. S.; Lamond A. I. *EMBO J.* **1992**, *11*, 1913.
- Pastre, J. C.; Correia, C. R. D. *Org. Lett.* **2006**, *8*, 1657.
- Pieken, W. A.; Olsen, D. B.; Benseler, F.; Aurup, H.; Eckstein, F. *Science* **1991**, *253*, 314.
- Pieper, S. ; Vauléon, S.; Müller, S. *Biol. Chem.* **2007**, *388*, 743.
- Piton, N.; Mu, Y.; Stock, G.; Prisner, T. F.; Schiemann, O.; Engels, J. W. *Nucl. Acids Res.* **2007**, *35*, 3128.
- Pitsch, S.; Weiss, P. A.; Jenny, L.; Stutz, A.; Wu, X. *Helv. Chim. Acta.* **2001**, *84*, 3773.
- Pleiss J. A.; Derrick, M. L.; Uhlenbeck, O. C. *RNA* **1998**, *4*, 1313.
- Prober, J. M.; Trainor, G. L.; Dam, R. J.; Hobbs, F. W.; Robertson, C. W.; Zagursky, R. J.; Cocuzza, A. J.; Jensen, M. A.; Baumeister, K. *Science* **1987**, *238*, 336.
- Proudnikov, D.; Mirzabekov, A. *Nucl. Acids. Res.* **1996**, *24*, 4535.
- Puffer, B; Moroder, H.; Aigner, M.; Micura, R. *Nucl. Acids. Res.* **2008**, *36*, 970.
- Puffer, B. Kreutz, C.; Rieder, U.; Elbert, M. O.; Konrat, R.; Micura, R. *Nucl. Acids. Res.* **2009**, *37*, 7728.
- Pyle, A. M.; Cech, T. R. *Nature* **1991**, *350*, 628.
- Quadir, M.; Möchel, T.; (Mini) Hii, K. K. *Tetrahedron* **2000**, *56*, 7975.
- Quin, P. Z.; Pyle, A. M. *Methods* **1999**, *18*, 60-70.
- Robins, M. J.; Barr, P. J. *Tetrahedron Lett.* **1981**, *22*, 421.

- Robins, M. J.; Vinayak, R. S.; Wood, S. G. *Tetrahedron Lett.* **1990**, *31*, 3731.
- Roskey, M. T.; Juhasz, P.; Smirnov, I. P.; Takach, E. J.; Martin, S. A.; Haff, L. A. *PNAS USA* **1996**, *93*, 4724.
- Rublack, N. *Diploma Thesis*, **2009**, Ernst-Moritz-Arndt Universität Greifswald.
- Ruparel, H.; Bi, L.; Li, Z.; Bai, X.; Kim, D. H.; Turro, N. J.; Ju, J. *PNAS* **2005**, *102*, 5932.
- Saito, Y.; Hanawa, K.; Motegi, K.; Omoto, K.; Okamoto, A.; Saito, I. *Tetrahedron Lett.* **2005**, *46*, 7605.
- Saito, Y.; Matsumoto, K.; Bag, S. S.; Ogasawara, S.; Kujimoto, K.; Hanawa, K.; Saito, I. *Tetrahedron* **2008**, *64*, 3578.
- Salon, J.; Sheng, J.; Jiang, J.; Cheng, G.; Caton-William, J.; Huang, Z. *J. Am. Chem. Soc.* **2007**, *129*, 4862.
- Salon, J.; Jiang, J.; Sheng, J.; Gerlits, O. O.; Huang, Z. *Nucl. Acids. Res.* **2008**, *36*, 7009.
- Scaringe, S. A.; Francklyn, C.; Usman, N. *Nucl. Acids Res.* **1990**, *18*, 5433.
- Scaringe, S. A.; *Methods* **2001**, *23*, 206.
- Schiemann, O.; Piton, N.; Plackmayer, J.; Bode, B. E.; Prisner, T. F.; Engels, J. W. *Nat. Protoc.* **2007**, *2*, 904.
- Schiemann, O. Prisner, T. F. *Q. Rev. Biophysics* **2007**, *40*, 1.
- Schmidt, A. F.; Smirnov, V. V. *Kinet. Catal.* **2001**, *42*, 800.
- Schreiber, S. L.; Kiessling, L. L. *J. Am. Chem. Soc.* **1988**, *110*, 631.
- Schulhof, J. C.; Molko, D.; Teoule, R. *Nucl. Acids Res.* **1987**, *15*, 397.
- Serganov, A.; Keiper, S.; Malinina, L.; Tereshko, V.; Skripkin, E.; Hörbartner, C.; Polonskaia, A.; Phan, A.T.; Wombacher, R.; Micura, R.; Dauter, Z.; Jäschke, A.; Patel, D. J. *Nat. Struct. Mol. Biol.* **2005**, *12*, 218.
- Serganov, A.; Huang, L.; Patel, D. J. *Nature* **2009**, *458*, 233.
- Sessler, J. L.; Wang, R. *J. Org. Chem.* **1998**, *63*, 4079.
- Shah, K.; Wu, H.; Rana, T. M. *Bioconjugate Chem.* **1994**, *5*, 508.
- Shakthivel, K.; Barbas, C. F. *Angew. Chem., Int. Ed.* **1998**, *37*, 2872.

- Sindbert, S.; Kalinin, S.; Woźniak, A.; Felekyan, S.; Kühnemuth, R.; Kienzler, A.; Clima, L.; Bannwarth, W.; Nguyen, H.; Appel, B.; Müller, S.; Seidel, C. A. M., *close to submission*.
- Sinha, N. D.; Biernat, J.; Köster, H. *Tetrahedron Lett.* **1983**, 24, 5843.
- Sinha, N. D.; Davis, P.; Schultze, L. M.; Upadhyaya, K. *Tetrahedron Lett.* **1995**, 36, 9277.
- Smalley, M. K.; Silverman, S. K. *Nucl. Acids. Res.* **2006**, 34, 152.
- Smith, M.; Rammler, D. H.; Goldberg, I. H.; Khorana, H. G. *J. Am. Chem. Soc.* **1962**, 84, 430.
- Sonogashira, K.; Tohda, Y.; Hagihara, N. *Tetrahedron Lett.* **1975**, 16, 4467.
- Sonogashira, K. *J. Organomet. Chem.* **2002**, 653, 46.
- Sowa, G. Z.; Quin, P. Z. *Prog. Nucleic Acid Res. Mol. Biol.* **2008**, 82, 147.
- Spencer, A. *J. Organomet. Chem.* **1982**, 240, 209.
- Spencer, A. *J. Organomet. Chem.* **1983**, 258, 101.
- Spencer, A. *J. Organomet. Chem.* **1984**, 270, 115.
- Štambaský, J.; Hocek, M.; Kočouřský, P. *Chem. Rev.* **2009**, 109, 6729.
- Stawinski, J.; Stromberg, R.; Thelin, M.; Westman, E. *Nucl. Acids Res.* **1988**, 16, 9285.
- Stemmler, E. A.; Buchanan, M. V.; Hurst, G. B.; Hettich, R. L. *Anal. Chem.* **1995**, 67, 2924.
- Steiner, M.; Karunatilaka, K. S.; Sigel, R. K.; Rueda, D. *Proc. Natl. Acad. Sci. USA* **2008**, 105, 13853.
- Stokker, G. E. *Tetrahedron Lett.* **1987**, 28, 3179.
- Stone M. D.; Mihalusova, M.; O'Connor, C. M.; Prathapam, R.; Collins, K.; Zhuang, X. *Nature* **2007**, 446, 458.
- Strohbach, D.; Novak, N.; Müller, S. *Angew. Chemie.* **2006**, 118, 2181.
- Tanaka, H.; Baba, M.; Hayakawa, H.; Sakamaki, T.; Miyasaka, T.; Ubasawa, M.; Takashima, H.; Sekiya, K.; Nitta, I.; Shigeta, S.; Walker, R. T.; Balzarini, J.; De Clercq, E. *J. Med. Chem.* **1991**, 34, 349.
- Ti, G. S.; Gaffney, B. L.; Jones, R. A. *J. Am. Chem. Soc.* **1982**, 104, 1316.
- Toberman, T.; Dvořák, D. *Eur. J. Org. Chem.* **2008**, 2923.

- Vauléon, S. *Dissertation* **2006**, Ernst-Moritz-Arndt Universität Greifswald.
- Volpini, R.; Costanzi, S.; Lambertucci, C.; Vittori, S.; Klotz, K.-N.; Lorenzen, A.; Cristalli, G. *Bioorg. Med. Chem. Lett.* **2001**, *11*, 1931.
- Vrábel, M.; Horáková, P.; Pivoňková, H.; Kalachova, L.; Černoká, H.; Cahová, H.; Pohl, R.; Šebest, P.; Fojta, M. *Chem. Eur. J.* **2009**, *15*, 1144.
- Wachowius, F.; Höbartner, C. *ChemBioChem.* **2010**, *11*, 469.
- Waldminghaus, T.; Heidrich, N.; Brantl, S.; Narberhaus, F. *Mol. Microbiol.* **2007**, *65*, 413.
- Walter, F.; Murchie, A. I. H.; Lilley, D. M. J. *Biochem.* **1998**, *37*, 17629.
- Waring, R. B. *Nucl. Acids Res.* **1989**, *17*, 10281.
- Watts, J. K.; Johnston, B. D.; Jayakanthan, K.; Wahba, A. S.; Pinto, B. M.; Damha, M. J. *J. Am. Chem. Soc.* **2008**, *130*, 8578.
- Welz, R.; Müller, S. *Tetrahedron Lett.* **2002**, *43*, 795.
- Wenter, P.; Reymond, L.; Auweter, S. D.; Allain, F. H.; Pitsch, S. *Nucl. Acids. Res.* **2006**, *34*, e79.
- Wenter, P.; Bodenhausen, G.; Dittmer, J.; Pitsch, S. *J. Am. Chem. Soc.* **2006**, *128*, 7579.
- Western, E. C.; Shaughnessy, K. H. *J. Org. Chem.* **2005**, *70*, 6378.
- Whale, R. F.; Coe, P. L.; Walker, R. T. *Nucleosides & Nucleotides* **1991**, *10*, 1615.
- Wellington, K. W.; Benner, S. A. *Nucleosides, Nucleotides & Nucleic Acids* **2006**, *25*, 1309.
- Westmann, E.; Stromberg, R. *Nucl. Acids Res.* **1994**, *22*, 2430.
- Whitcombe, N. J.; (Mimi) Hii, K. K.; Gibson, S. E. *Tetrahedron*, **2001**, *57*, 7449.
- Williams, D. B. G.; Lombard, H.; Holzapfel, C. W. *Syn. Commun.* **2001**, *31*, 2077.
- Wnuk, S. F.; Lewandowska, E.; Sacasa, P. R.; Crain, L. N.; Zhang, J.; Borchardt, R. T.; de Clercq, E. J. *Med. Chem.* **2004**, *47*, 5251.
- Wolfe, S. A.; Ferentz, A. E.; Grantcharova, V.; Churchill M. E. A.; Verdine G. L. *Chem. Biol.* **1995**, *2*, 213.
- Wu, K. J.; Steding, A.; Becker, C. H. *Rapid Commun. Mass Spectrom.* **1993**, *7*, 142.
- Wu, T.; Ogilvie, K. K.; Pon, R. T. *Nucl. Acids. Res.* **1989**, *17*, 3501.

Zhang, H.-C.; Daves, G. D., Jr. *J. Org. Chem.* **1992**, *57*, 4690.

Zhang, H.-C.; Daves, G. D., Jr. *Organometallics* **1993**, *12*, 1499.

Zhang, Q.; Stelzer, A. C.; Fischer, C. K.; Al-Hashimi, H. M. *Nature* **2007**, *450*, 1263.

Zhao, L.; Xia, T. *Methods* **2009**, *49*, 128.

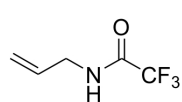
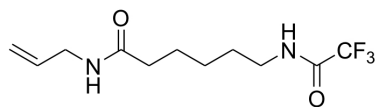
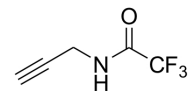
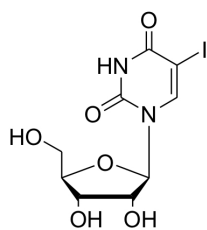
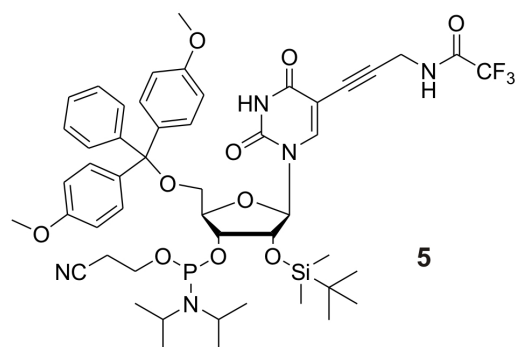
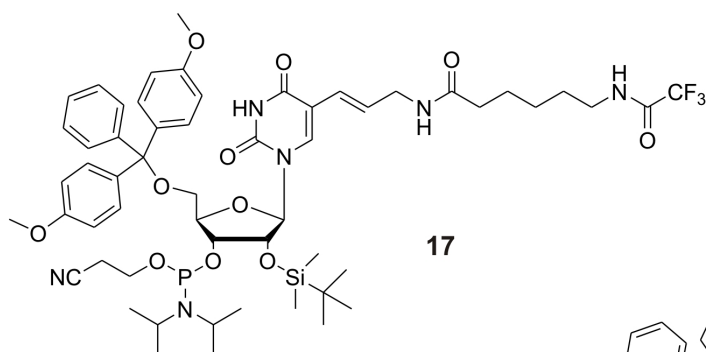
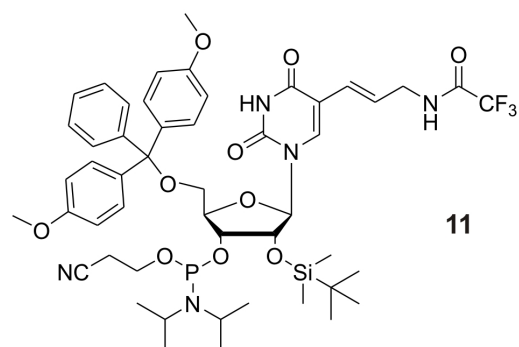
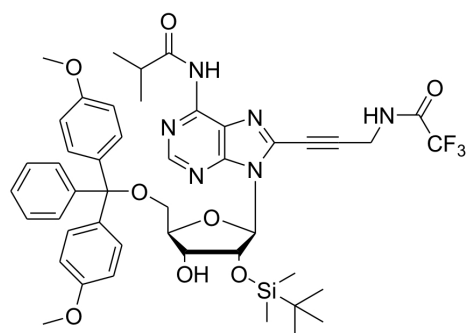
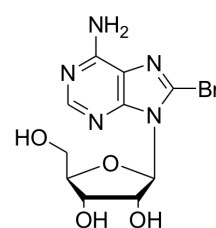
Zhang, X.; Cekan, P.; Sigurdsson, S. Th, Qin, P. Z. *Methods Enzymol.* **2009**, *469*, 303.

Zoppellaro, G.; Baumgarten, M. *Eur. J. Org. Chem.* **2005**, 2888.

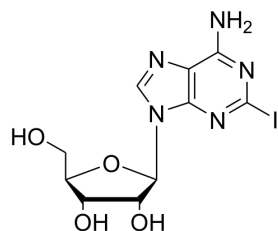
Appendix

Structures of the starting materials and the synthesized building blocks.

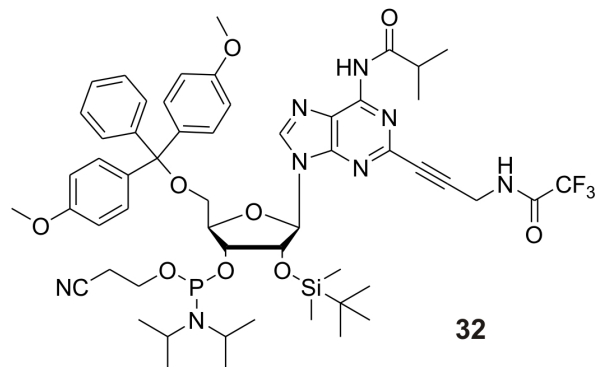
Structures of the starting materials and the synthesized building blocks

**L1****L2****L3****1****5****17****11****23****19**

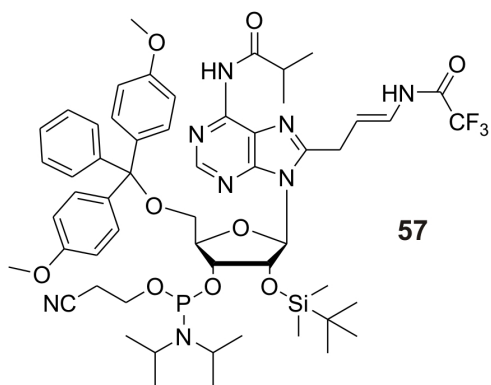
Structures of the starting materials and the synthesized building blocks



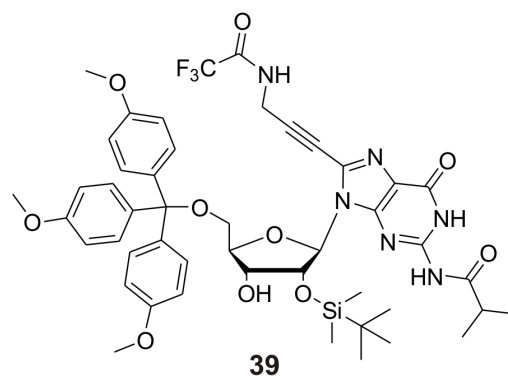
27



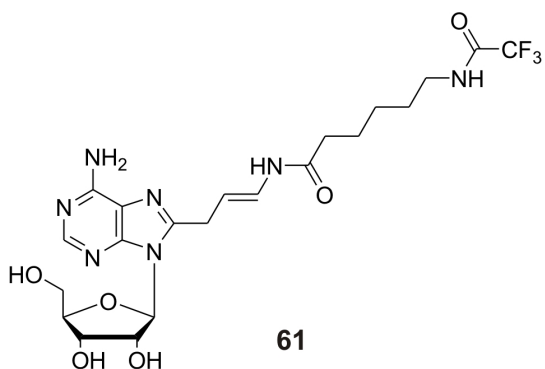
32



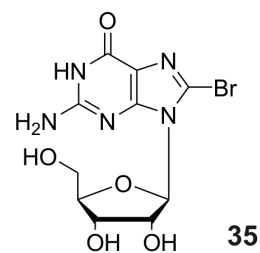
57



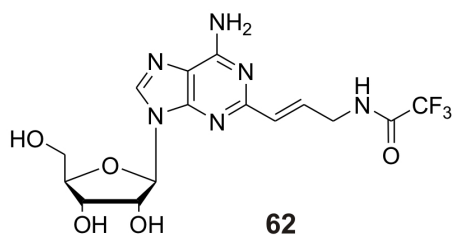
39



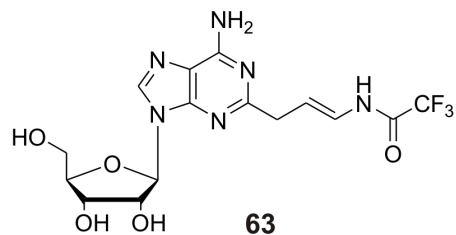
61



35



62



63

Acknowledgments

This Ph.D Thesis has been completed in the working group of Prof. Dr. Sabine Müller in the Institute for Biochemistry, University of Greifswald, Germany with the support of many people and organizations.

First of all, I would like to express my deep gratitude to my supervisor, Prof. Dr. Sabine Müller, for giving me a chance to work in her researching group and providing me with an interesting project and opportunities to learn biochemistry and to gain practical experiences in organic synthesis and RNA chemistry. In the last three years, Prof. Dr. Müller has been kindly guiding and encouraging me, so that I can go through difficulties and finish my Ph.D work in time. With her support, I also have had chances to go to different national and international conferences.

I would like to thank Prof. Dr. Willi Bannwarth at the Albert-Ludwigs University of Freiburg for the review of my Ph.D Thesis.

I wish to thank Prof. Dr. Claus Seidel and Simon Sindbert at the Heinrich-Heine University of Düsseldorf for their cooperation in the FRET experiments.

I wish to thank Prof. Dr. Klaus Weisz, Dr. Zhou Xiao, Fanny Riechert-Krause and all the members of the working group for their helpful 2D-NMR measurements and structural discussions about my synthetic compounds.

Many thanks to the NMR Laboratory at the University of Greifswald for their fast analyses and helpfulness.

To all the past and present members of my working group at the University of Greifswald I would like to thank for their kindly helps, not only in the scientific work but also in my private life. In my whole PhD. time I have been living in a warm and friendly atmosphere of the working group.

- I am thankful to Dr. Matthäus Janczyk and Slawomir Gwiazda for guiding me the operation of the HPLC system.
- Many thanks to Dr. Bettina Appel, Sabine Stingel and Anne Strahl for the synthesis of my oligonucleotides.
- Bei Frau Rita Schroeder and Frau Simone Turski bedanke ich mich für ihre Hilfe sowohl bei der Chemiekalien- und Lösungsmittelvorbereitung als auch bei der Aufreinigung meiner Oligonucleotide. Seit meinen ersten Tagen in Greifswald haben sie,

zusammen mit Dr. Valeska Dombos und Nico Rublack, mich immer ermutigt. Sie waren mir allezeit sehr hilfsbereit und enthusiastisch, nicht nur in der Forschung sondern auch in meinem privaten Leben.

- I am deeply grateful to Dr. Valeska Dombos, Nico Rublack, Dr. Bettina Appel, Danilo Springstube and Thomas Marschall for their scientific discussions and helpful correction of my Thesis. Without their help, I would hardly be able to finish my tedious writing.
- Many thanks to Slawomir Gwiazda, Kristina Salomon, Nico Rublack, Jacui Xu, Dr. Irene Drude and all of my colleagues for their interesting talks and nice times outside the laboratory.

Furthermore, I wish to express my gratefulness to the Vietnamese Ministry of Education and Training, DAAD and DFG for financial supports. Besides, I am thankful to Dr. Jörn Kasbohm, Prof. Dr. Uwe Bornscheuer at the University of Greifswald, Prof. Dr. Le Tran Binh, Dr. Le Thi Lai, Dr. Le Lan Huong and all the members of the Diploma Equivalent program for giving me chance to study in Germany.

Warmly thanks to all of my friends and the members of VietGreif for their encouragement, enthusiasm and support during my Ph. D time, especially to Dr. Dang Thanh Tung, Hung Do and Mrs. Le Thi Anh Tuyet.

Finally, I would like to thank my family for their love, their belief in me and their patient waiting for me for the last three years.

Curriculum vitae

Personal information

Name:	Nguyen Hien
Gender:	male
Date of birth:	07-05-1981
Place of birth:	Phutho, Vietnam
Nationality:	Vietnamese
Marital status:	Single

Education and working experiences

1987-1992:	Nguyen Trai primary school in Hanoi, Vietnam
1992-1996:	Nguyen Trai secondary school in Hanoi, Vietnam
1996-1999:	Marie Curie high school in Hanoi, Vietnam
1999-2003:	Bachelor of Science in Chemistry, Faculty of Chemistry, Hanoi University of Education, Vietnam
2003-2005:	Master of Science in Organic Chemistry, Chemistry Faculty, Hanoi University of Education, Vietnam
2005-2006:	Student of Diploma Equivalent program at the Joint Education and Training Center organized by Hanoi University of Science, Institute of Biotechnology, Vietnam and University of Greifswald, Germany Teaching assistant at the Faculty of Chemistry, Hanoi University of Education
2006-2009:	Ph.D student in the working group of Prof. Dr. Sabine Müller, Institute for Biochemistry, University of Greifswald

List of publications

Papers

1. *Hien Nguyen, Bettina Appel, Danilo Springstube, Sabine Müller*, "Synthesis and application of new amino modified RNA building blocks for post-synthetic RNA labeling". *Close to submission.*
2. *Simon Sindbert, Stanislav Kalinin, Anna Woźniak, Suren Felekyan, Ralf Kühnemuth, Andrea Kienzler, Lilia Clima, Willi Bannwarth, Hien Nguyen, Bettina Appel, Sabine Müller, Claus A. M. Seidel*, "Implications on dye linker length and rigidity on accurate distance determination via FRET of labeled DNA and RNA". *Close to submission.*

Posters

1. **Kich-off meeting: DFG Priority Program - Sensory and regulatory RNAs in prokaryotes**, September 5-6, 2007, Bochum, Germany.
Poster presentation: *Hien Nguyen, Bettina Appel, Sabine Müller*.
"Synthesis of dye-labeled RNAs: preparation of monomer building blocks for post-synthetic labeling".
2. **Thirteenth Annual Meeting of the RNA Society**, July 28 - August 3, 2008, Berlin, Germany.
Poster presentation: *Hien Nguyen, Bettina Appel, Sabine Müller*.
"Synthesis of dye-labeled RNAs: preparation of monomer building blocks for post-synthetic labeling".
3. **Progress meeting: DFG Priority Program - Sensory and regulatory RNAs in prokaryotes**, September 16-18, 2008, Kassel, Germany.
Poster presentation: *Hien Nguyen, Bettina Appel, Sabine Müller*.
"Synthesis of dye-labeled RNAs: preparation of monomer building blocks for post-synthetic labeling".